

THEORETICAL STUDIES OF SILICON SURFACES USING
FINITE CLUSTERS

Thesis by
Antonio Redondo-Muino

In Partial Fulfillment of the Requirements
For the Degree of
Doctor of Philosophy

California Institute of Technology
Pasadena, California

1977

(Submitted December 13, 1976)

Caminante son tus huellas
el camino, y nada más;
caminante, no hay camino,
se hace camino al andar.
Al andar se hace camino,
y al volver la vista atrás
se ve la senda que nunca
se ha de volver a pisar.
Caminante, no hay camino,
sino estelas en la mar.

Antonio Machado

ACKNOWLEDGMENTS

I would like to thank my advisors Bill Goddard and Tom McGill for the many things they have taught me, making it, at the same time, one of the most enjoyable experiences that I have had. In addition, I would like to thank the members of our research group, particularly Barry Olafson and Bill Wadt, for many helpful discussions. I would also like to thank our secretary, Adria McMillan, for her efficiency in getting the job done.

I gratefully acknowledge the support of the California Institute of Technology, the International Business Machines Corporation, the Woodrow Wilson Foundation and the Physics Department of the Universidad de Los Andes, Venezuela.

Finally, I would like to thank my family in Venezuela for their constant support and my wife, Shelby, for her understanding and patience in putting up with the whole thing.

ABSTRACT

The objective of this thesis is to study the electronic structure, geometries and chemical binding characteristics of the surfaces of silicon and of the initial form of oxygenated Si. We examined the (111), (100), and (110) surfaces, relaxation on the (111) and (100) surfaces and reconstruction on the (100) surfaces. In addition we examined steps on the (111) surfaces. In the oxygenated surface we considered the geometry, excited states and ion states of both O and O₂ bonded to the perfect (111) surface.

These studies indicated that surfaces and chemisorption lead to localized electronic states for which explicit inclusion of electronic correlation (many body) effects is essential. These effects are included through use of generalized valence bond (GVB) and configuration interaction (CI) techniques. These techniques require use of a finite collection of Si atoms to represent the surface. We find that very small clusters lead to reliable results if the model system is properly tied off with SiH bonds (to represent internal Si-Si bonds).

In Chapter 1 we report an effective potential for replacing the ten core electrons in calculations involving the Si atom. The potential is obtained directly from ab initio calculations on the states of the Si atom and no empirical data or adjustable parameters are used. The ab initio effective potential is tested by carrying out Hartree-Fock generalized valence bond and configuration interaction calculations on various molecules. We considered Si, Si₂, SiH₃, Si₂H₆ and H₃SiO₂ and calculated excitation energies, ionization potentials, and electron

affinities both using the effective potential and without it (ab initio). In essentially all cases the agreement is to better than 0.1 eV, providing strong evidence that the effective potential adequately represents the Si core. This potential is utilized in all of the calculations reported in subsequent chapters.

In Chapter 2 we consider clean (111), (100) and (110) silicon surfaces. For the (111) surface the relaxation of silicon surface atoms is studied by means of an $\text{Si}(\text{SiH}_3)_3$ cluster. We find that the surface state is accurately described as a dangling bond orbital with 93% p character. We determined the optimum relaxation of the surface layer to be 0.08\AA toward the second layer. For the positive ion we find that the surface atom relaxes toward the second layer by an additional 0.30\AA . Using an Si_3H_6 cluster we find that the interaction between adjacent dangling bond orbitals indicates that they are very weakly coupled (with a splitting of ~ 0.01 eV between the singlet and triplet spin couplings.)

For the (100) surface we used an $\text{Si}(\text{SiH}_3)_2$ cluster. We find a relaxation distance of 0.10\AA toward the vacuum. We also considered the 2×1 reconstruction of such surfaces using the results for Si_2H_4 and $\text{Si}(\text{SiH}_3)_2$ complexes. It is found that adjacent surface atoms form a bond (1.76 eV bond strength), leading to pairing up of adjacent silicons (with an optimum Si-Si bond length of 2.38\AA).

In Chapter 3 we consider the electronic structure of divalent steps on (111) silicon surfaces. We find three localized electronic states separated by less than 0.3 eV. These states have quite

different electronic structure and are expected to be reactive toward a large range of chemical species.

In Chapter 4 we study the chemisorption of oxygen upon Si (111) surfaces. For single oxygen atoms we find an optimum Si-O bond length of 1.63\AA . We also find ionization potentials in the range 11-16 eV. Then we consider a model in which an oxygen molecule chemisorbed onto the silicon surface has an electronic structure corresponding to a peroxy radical. We find ionization potentials in the range 11-18 eV in agreement with experiment. We find an optimum O-O bond length of 1.37\AA and a Si-O-O bond angle of 126° for the chemisorbed peroxy radical.

PREFACE

The subject of this thesis is the theoretical study of silicon surfaces and chemisorption on such surfaces. The electronic structure of surfaces is a problem that has been in the minds of scientists for many years since the pioneering work of Tamm and Shockley in the thirties. However, it has been only in the last few years that theoretical studies have become prominent in the literature.

The primary questions that theory should answer with respect to the study of surfaces concern the nature of the electronic and geometric structure at the surface; the characteristics of chemisorption, such as bond energies, geometrical configurations, excited states. These are questions that are difficult to answer experimentally from a microscopic point of view. They are quite different from the problems generally studied by theoretical methods for the bulk of crystalline solids. In that case the geometrical structure of the solid is usually known from x-ray diffraction studies, and the concentration and characteristics of the electronic states is very different.

In principle, one can obtain all the information required for a complete characterization of the surface from the solutions of the Schrödinger equation

$$H\psi = E\psi .$$

The exact solution of this problem is not known at the present time, and different approximations have to be introduced. For bulk solids the standard approach used in the past has been the introduction of

approximations consistent with the periodicity of crystalline solids, and the band theory of such solids. For surfaces these techniques are not immediately applicable due to the lack of three-dimensional periodicity, the presence of localized states and the lack of explicit electronic correlation for the standard band structure techniques.

We have undertaken the present study with the explicit purpose of including these effects. To do this we have applied quantum chemical techniques developed for studying molecular systems where the states are highly localized and thus require inclusion of electronic correlation for a proper description of the system. Consequently in our studies of surfaces, we have used generalized valence bond (GVB) and configuration interaction (CI) wavefunctions.

At present it is not possible to apply such highly correlated wavefunctions to semi-infinite systems. We have opted, instead, to apply them to finite clusters of atoms designed to include the most important interactions for the particular property being studied. In order to ease these calculations, we have developed an effective potential to replace the ten core electrons of the silicon atom. This potential was obtained from ab initio calculations on the silicon atom without the introduction of any external parameters. The effective potential accurately reproduces the energies and shapes of orbitals in molecular calculations.

To apply these techniques we chose an insulator system of technical importance where a considerable amount of experimental information is available to compare with the theoretical calculations.

In addition, chemical arguments suggest that nonpolar semiconductors, like silicon, have electronic states that are rather localized at the surface, much more, for example, than metals. This has two important consequences: first, it makes for a conceptually ideal situation in the application of the GVB and CI wavefunctions, since these were especially developed for localized systems. Second, microscopic properties such as geometries and excitation energies are expected to converge rapidly as a function of the number of atoms used in the calculation. One can then obtain reliable results with a relatively small number of atoms.

The advantages of the present method are: (i) since total energies are calculated, it is possible to minimize such energies to find the optimum geometry of the system; (ii) due to the inclusion of electronic correlation, reliable results are obtained for ground state and excitation energies and geometries; (iii) low translational symmetry configurations like steps and chemisorbed molecules can be studied without the introduction of ad hoc assumptions as to the geometry of the system; (iv) qualitative interpretation of the results in terms of localized orbitals makes the analysis of such results easily tractable. The disadvantages of the present technique are: (i) because finite clusters must be used, it is not possible to calculate quantities that depend on the presence of large numbers of atoms, like the interaction of surface states with bulk states; (ii) long range effects have to be introduced by additional assumptions, like the dielectric correction for ionization potentials. Our results, however, look very

encouraging because many of the properties arising from localized states do not depend strongly on the size of the system and they agree with experiment.

We have considered the (111), (100) and (110) clean surfaces of silicon. For the (111) surface we studied the relaxation of surface atoms and the interaction of adjacent dangling bonds on the surface. We found an inward relaxation of 0.08\AA for the surface atoms. Adjacent dangling bonds were found to be only weakly coupled. For the (100) surface we found a relaxation of 0.10\AA toward the vacuum. We also considered the 2×1 reconstruction of this surface and found that a strong (1.76 eV) bond is formed between adjacent surface silicon atoms, leading to pairing up of adjacent rows with an optimum Si-Si bond distance of 2.38\AA .

We have also studied the electronic structure of steps on silicon (111) surfaces. Experimentally only steps characterized by divalent atoms (atoms with only two nearest neighbors) are found. For this type of state we found three localized states separated by less than 0.3 eV. The electronic structure at these steps is characterized by the divalent atoms and thus they are quite different from the dangling bonds found on the clean (111) surface. [They are similar to the states found on (100) surfaces, which also have divalent surface atoms.] These states are expected to be reactive toward a large range of chemical species.

As an example of chemisorption we have studied the oxidized perfect (111) surface, with both O atoms and O_2 molecules. For the single oxygen atom bound to the surface we have optimized the silicon-oxygen

bond length, finding an Si-O distance of $1.63\overset{\text{O}}{\text{\AA}}$. This is consistent with experimental values on systems having similar bonding between oxygen and silicon atoms. We have also calculated ionization potentials and excitation energies for this system. We find that the ionization potentials are in the range 11-16 eV. For O_2 molecules we find that on the first stage of chemisorption, the molecule has an electronic structure corresponding to a peroxy radical, that is, only one oxygen atom is bound to a surface silicon. This agrees with recent experimental results in which the two oxygens are found to be inequivalent. For this system we find ionization potentials in the range 11-18 eV. The peak at 18 eV arises from an ionization out of the O-O bond and is not present in the corresponding spectrum of single oxygen atoms chemisorbed onto the surface. For the peroxy radical we find an optimum O-O bond length of $1.37\overset{\text{O}}{\text{\AA}}$ and a Si-O-O angle of 126° .

Summarizing, we have applied correlated wavefunctions to the study of silicon surfaces. We find that the results are very encouraging and agree well with experiment. The methods used in the present work are expected to be applicable to other semiconductors if care is taken, through the choice of clusters, to include all of the important interactions for the problem in question.

The following publications are based on parts of the work described in the present thesis:

W. A. Goddard III, A. Redondo and T. C. McGill, "The Peroxy Radical Model of O_2 Chemisorption onto Silicon Surfaces," Solid State Comm. 28, 981 (1976).

A. Redondo, W. A. Goddard III and T. C. McGill, "Ab initio Effective Potentials for Silicon," Phys. Rev. B 14, Nov. 15, 1976 (in press).

A. Redondo, W. A. Goddard III, T. C. McGill and G. T. Surratt, "Relaxation of (111) Silicon Surface Atoms from Studies on Si_4H_9 Clusters," Solid State Comm. 20, 733 (1976).

TABLE OF CONTENTS

<u>Chapter</u>	<u>Title</u>	<u>Page</u>
1	<u>Ab initio</u> Effective Potentials for Silicon	1
2	The Clean Surfaces of Silicon	38
3	Electronic Structure of Steps on (111) Silicon Surfaces	136
4	Oxygen Chemisorption onto Si (111) Surfaces	177
Appendix A	The Generalized Valence Bond (GVB) Wavefunctions	217
Appendix B	Dielectric Corrections	221
Appendix C	Effect of Correlation, d-Functions and Lattice Constraints on the Si_3H_6 Cluster Model for (100) Si Surfaces	224

Chapter 1

AB INITIO EFFECTIVE POTENTIALS FOR SILICON

I. INTRODUCTION

The idea of using a pseudopotential to replace the core electrons in quantum mechanical calculations of the electronic wavefunctions of atoms, molecules, and solids is now well established. The first attempts consisted of the work of Hellmann and Gombás¹ in the mid-thirties. They realized that these pseudopotentials should incorporate the effects of the Pauli principle in order to avoid the collapse of the valence electrons into the core region. This was put on a sound basis by Phillips and Kleinman² in 1959. This work, together with that of Heine and collaborators,³ initiated a vast series of papers on the applications of pseudopotentials to the electronic structure of solids.⁴ These successes also reawakened the interest in applying this approach to molecules and atoms.⁵

Although the basic idea in the pseudopotential method is to construct an (simple) operator that reproduces the effect of the core electrons of a given atom on the valence electron, there are a number of approaches to determine the specific form of the pseudopotential. The most common procedure (with many variations) is to select a simple functional form for the potential and then to adjust the several parameters in this potential to fit the experimental energy levels of the atom or the band structure of the solid while requiring the pseudopotential to be weak (leading to orbitals with minimal numbers of nodes). The alternate approach is to use only theoretical information

in determining the potential, requiring the core potential to reproduce the results of ab initio calculations. Our approach is of this latter category (the method of Melius and Goddard^{6,7}); we choose the core potential so as to reproduce the shapes and energies of ab initio valence orbitals. The resulting core potential is referred to as the ab initio effective potential, or more simply as the EP. Such effective potentials have been previously developed for Li, Na, and K atoms⁶ and for Fe and Ni atoms⁸ and applied to a number of molecules containing these atoms. Here we report the effective potential for the core electrons of Si, which we have applied to all the calculations to be discussed in the succeeding chapters. We will assess the accuracy of the effective potential by comparing the results of ab initio and effective potential calculations on the ground and excited states of Si_2 , SiH_3 , and SiH_3O_2 .

The interactions of the valence electrons are handled just as in ab initio calculations. Appropriate basis functions are placed on the various centers and the molecular integrals are evaluated. These integrals are then used for self-consistent Hartree-Fock (HF) or generalized valence bond (GVB) calculations and ultimately in configuration interaction (CI) calculations to include various electron-correlation or many-body effects. A special aspect of our approach is that we calculate total energies directly so that we can determine the potential surfaces and geometries for various excited states.

Since the shapes of the valence orbitals are described correctly, we expect the overlap between orbitals on various centers to behave properly and hence for bond energies and geometries to be well described.

Excitation energies, ionization potentials, and electron affinities are obtained by solving directly for the total energies of each state and taking the difference. Consequently, one can distinguish between the different multiplet eigenstates of the molecule (usually not possible in standard solid state pseudopotential methods⁹). Another advantage of the present method is that since we include electron correlation effects explicitly, we can describe processes that involve bond formation or bond breaking.

II. COMPARISON OF THE RESULTS OF EFFECTIVE POTENTIAL AND AB INITIO CALCULATIONS

Before embarking on a description of the calculational details for the Si effective potential, we will summarize some of the results of the comparisons between the EP and ab initio¹⁰ calculations on molecules. This will put into perspective the procedure and what we want to obtain from it. We start with self-consistent ab initio Hartree-Fock calculations of the electronic wavefunctions of Si atoms (both the ground and an excited state). From this ab initio calculation (using the method described in the next section) we obtain an effective potential without the introduction of any experimentally determined parameters. It is this potential that we have used in the calculations below.

As summarized in Table I, we carried out both 28-electron ab initio calculations and 8-electron EP calculations for the electronic states of the Si₂ molecule (at the experimental equilibrium geometry¹¹ for the ground state). The low-lying states considered here have

Table I. Excitation energies for various states of Si_2 ($R = 4.244 a_0$). All energies in eV.

State	GVb ^a		CI ^b	
	<u>Ab Initio</u>	Effective Potential	<u>Ab Initio</u>	Effective Potential
$^3\Sigma_g^-(\pi^2)$	0.0 ^c	0.0 ^d	0.0 ^e	0.0 ^f
$^1\Sigma_g^+(\pi^4)$	0.285	0.218	0.140	0.070
$^1\Delta_g(\pi^2)$	-	-	0.513	0.519
$^3\Sigma_u^+(\pi^4)$	-	-	1.518	1.409
$^1\Sigma_u^-(\pi^2)$	-	-	2.669	2.640
$^3\Delta_u(\pi^4)$	-	-	2.930	2.867
$^1\Delta_u(\pi^4)$	-	-	4.040	3.962
$^3\Delta_g(\pi^4)$	-	-	5.180	5.056
				248
				167
				217
				261
				180
				261
				180
				248

^a The basis sets used were the Si (6s4p) and the Si (4s4p) of Table IV. See the Appendix for a brief summary of the GVB wavefunctions. The $^3\Sigma_g^-$ calculation is GVB(1); that one of the $^1\Sigma_g^+$ state is GVB(3).

^b The CI calculations were based on the SCF valence orbitals from GVB(1) and GVB(3) calculations for the $^3\Sigma_g^-$ state (two electrons in π orbitals or π^2) and the $^1\Sigma_g^+$ state (four electrons in π orbitals or π^4).

cTotal energy calculated is -577.68863 h.

^d Total energy calculated is -7.36094 h.

^e Total energy calculated is -577.74061 h.

^f Total energy calculated is -7.41376 h.

5 This is the number of spin eigenfunctions of proper spatial symmetry.

either two or four electrons in the π orbitals and are denoted as π^2 and π^4 , respectively. The second and third columns show the excitation energies obtained from self-consistent GVB¹² calculations performed on the ground state ($^3\Sigma_g^-$) and the lowest lying excited state ($^1\Sigma_g^+$). The fourth and fifth columns compare the excitation energies obtained from CI calculations on the low lying excited states of Si_2 . In these CI calculations we included all appropriate excitations within the space spanned by the GVB orbitals for the $^3\Sigma_g^-(\pi^2)$ or $^1\Sigma_g^+(\pi^4)$ states, leading to ~ 200 spin eigenfunctions of the proper spatial symmetry for each CI calculation. In all cases the ab initio and effective potential calculations lead to excitation energies agreeing within 0.1 eV for the CI wavefunctions. It is important to note that even for those states that are close in energy, the ordering is not changed in the effective potential calculations. Since there are numerous states of various multiplicities and orbital coupling all within a small range of energy, we consider Si_2 to be a stringent test of the adequacy of our EP.

Next we consider the SiH_3 molecule (using the experimental geometry of silane¹³ but with one hydrogen atom omitted). Here we performed Hartree-Fock self consistent field calculations on both the ground state of the neutral (2A_1) and the ground state of the positive ion (1A_1), leading to the ionization potentials of Table II. The EP calculation leads to an ionization potential within 0.17 eV of the ab initio value. In order to provide an idea of how similar the wavefunctions are, we compare the Mulliken populations¹⁴ in Table II. Also listed in Table II are the ionization potentials (IP) from

Table II. Energies for SiH_3 and SiH_3^+ .^a All Energies in eV.

State ^b	Ionization Potential		Mulliken Population per Atom			
	ab initio	effective potential	ab initio		effective potential	
			Si ^d	H	Si	H
SiH_3 2A_1	0.0 ^b	0.0 ^c	3.50	1.17	3.74	1.09
SiH_3^+ 1A_1	8.637	8.470	2.92	1.03	3.04	0.99
Koopmans Theorem	9.396	9.124				

^a The geometry is the same as in silane but without one hydrogen atom; $R_{\text{Si-H}} = 2.796 a_0$, $\angle \text{HSiH} = 109^\circ 28'$. The basis sets used are the Si (6s4p) and the Si (2s2p) of Table IV, and a (2s) contraction of the three gaussian hydrogen bases of S. Huzinaga, J. Chem. Phys. 42, 1293 (1965).

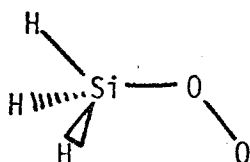
^b Total energy calculated is -290.56390 h.

^c Total energy calculated is -5.38986 h.

^d The ten core electrons have been subtracted from the ab initio Si population.

application of Koopmans theorem. This leads to IP's too high by 0.7 eV for both ab initio and EP.

As a final test, we considered the molecule H_3SiO_2 ,



corresponding to the above SiH_3 unit bound to an oxygen molecule (the new bond lengths are $\text{SiO}: 1.64\text{\AA}$,¹⁵ and $\text{OO}: 1.366\text{\AA}$,¹⁵ while the SiOO bond angle is $125^\circ 53'$ ¹⁵). In these calculations only the Si core is replaced by an EP. Self-consistent GVB calculations (ab initio and EP) were carried out on the ground state ($^2\text{A}''$), and the CI calculations were carried out within the orbital spaces spanned by these GVB orbitals. The range of the excitation energies, as shown in Table III, is from 0 to 19.6 eV, and in all cases the ab initio and effective potential calculations lead to the same ordering of states as in the ab initio calculations.

These results indicate that the excitation energies and ionization potentials obtained with the effective potentials are in excellent agreement with those of the ab initio calculations. Since the systems compared here are reasonably distinct, we consider these results to demonstrate the usefulness of our effective potentials.

C. THE AB INITIO EFFECTIVE POTENTIAL

The general form we use for the EP¹⁶ is

Table III. Energies for Various States SiH_3O_2 and SiH_3O_2^+ .^a All Energies in eV.

State	Excitation Energy		Number of Configurations ^c
	<u>ab initio</u> CI ^b	effective potential CI	
SiH_3O_2			
$^2\text{A}''$	0.0 ^d	0.0 ^e	98
$^2\text{A}'$	0.692	0.662	283
$^2\text{A}'$	6.600	6.617	283
$^2\text{A}''$	7.924	7.850	98
$^2\text{A}'$	8.142	8.116	283
$^2\text{A}''$	15.419	15.453	98
$^2\text{A}'$	16.174	16.172	283
SiH_3O_2^+			
$^3\text{A}''$	11.117	11.173	496
$^1\text{A}''$	12.210	12.263	316
$^1\text{A}'$	12.582	12.613	340
$^1\text{A}'$	13.985	14.031	340
$^1\text{A}''$	15.447	15.459	316
$^3\text{A}'$	15.468	15.493	530
$^3\text{A}''$	15.495	15.520	496
$^3\text{A}'$	15.771	15.790	530
$^3\text{A}''$	17.366	17.415	496
$^1\text{A}''$	18.988	19.048	316
$^1\text{A}'$	19.556	19.620	340
$^3\text{A}'$	19.619	19.638	530

^aThe geometry is as follows: The SiH_3 geometry is the same as in Table II; the O_2 bonded as a peroxy-radical to Si atom, eclipsed with one of the hydrogen atoms; $R_{\text{Si-O}} = 3.099 \text{ a}_0$; $R_{\text{O-O}} = 2.581 \text{ a}_0$; $\angle \text{O-O-Si} = 125^\circ 53'$.

^bThe CI was carried out using the SCF orbitals from GVB(2)-SCF calculations of the $^2\text{A}''$ ground state. All double excitations from ground state configuration into the π orbitals of the O_2 part were included. These calculations were meant as a test of the effective potential as compared with the ab initio results and need not represent the most appropriate way of describing the excitations within this molecule.

^cThis is the number of spin eigenfunctions of proper spatial symmetry.

^dTotal energy calculated is -440.29763 h.

^eTotal energy calculated is -155.15456 h.

$$V^{EP}(r) = \sum_{\ell=0}^{\infty} V_{\ell}(r) |\ell\rangle\langle\ell| \quad (1)$$

centered on each atom whose core is being replaced. Here $V_{\ell}(r)$ is a function of the radius only and

$$|\ell\rangle\langle\ell| \equiv \sum_{m=-\ell}^{\ell} |\ell m\rangle\langle\ell m| \quad (2)$$

is a projection operator onto states of angular momentum ℓ with respect to the center of interest. As described below, the $V_{\ell}(r)$ are obtained from ab initio calculations on various states of the atom; no readjustments are made to fit the molecular systems. Rather, we have in mind that the potential (1) describes the interactions of the atomic core of interest with orbitals on all centers of the system. With this effective potential we then completely eliminate the core orbitals from the system. Consequently, no basis functions for describing the core orbitals are required, considerably simplifying ab initio calculations. We do not require that other orbitals be orthogonal to the core being replaced and hence V_{ℓ} contains components representing the effects of the Pauli principle. As a result, for Si the V_{ℓ} for $\ell = 0$ and $\ell = 1$ are highly repulsive in the core region, as can be seen from Fig. 1.

The $V_{\ell}(r)$ in (1) are fitted to an analytic expansion of the form

$$V_{\ell}(r) = \sum_k C_k r^{n_k} \exp(-\zeta_k r^2) \quad , \quad (3)$$

for ease in evaluating the multicenter integrals required in molecular calculations. Use of two to five such terms allows an excellent fit to

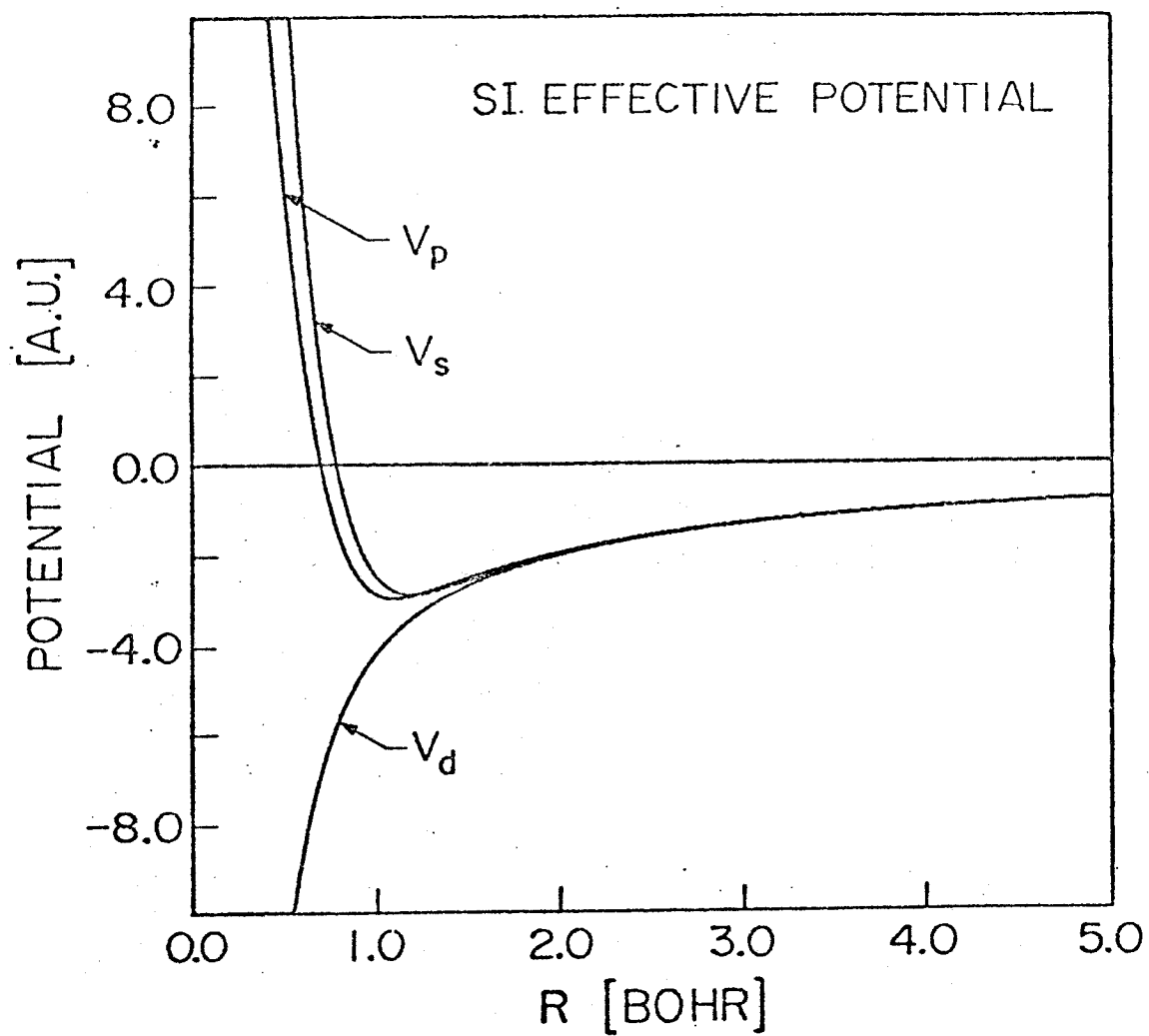


Figure 1. Si Effective Potential (EP) Components $V_l(r)$. Curves plotted include the nuclear attraction term.

the ab initio atomic wavefunctions.

In calculations of the wavefunctions of the molecules (or solids) we must evaluate matrix elements of the form

$$\langle \chi_{\mu A} | V_{\ell}(r_B) | \chi_{\nu C} \rangle ,$$

where the $\chi_{\mu A}$ and $\chi_{\nu C}$ are (Gaussian) basis functions centered on the various nuclei (A,B,C) of the molecule. For terms of the form (3) Melius, Kahn, and Goddard^{6,7} have developed formulae, algorithms, and computer programs allowing rapid evaluation of the various one-, two-, and three-centered integrals.

The EP is obtained as follows. We consider the Hartree-Fock equation for the valence orbital of angular momentum ℓ , $\phi_{n\ell}^{HF}$,

$$(h + \hat{V}_{core}^{HF} + \hat{V}_{val}^{HF}) \phi_{n\ell}^{HF} = \epsilon_{n\ell} \phi_{n\ell}^{HF} , \quad (4)$$

where \hat{V}_{core}^{HF} is the operator (involving Coulomb and exchange operators) describing the interaction of $\phi_{n\ell}^{HF}$ with the core.

The first step consists in replacing the Hartree-Fock orbital $\phi_{n\ell}^{HF}$ by the "coreless Hartree-Fock (CHF)" orbital⁶ $\phi_{n\ell}^{CHF}$ whose amplitude goes smoothly to zero as $r \rightarrow 0$. The reasons for doing this are to avoid singularities in the resulting local potential $V_{\ell}(r)$ and to minimize the number of basis functions required to describe the valence orbitals. The CHF orbital is obtained by simply mixing Hartree-Fock core orbitals of the same ℓ with $\phi_{n\ell}^{HF}$

$$\phi_{n\ell}^{CHF} = \phi_{n\ell}^{HF} - \sum_{c=1}^{n-1} C_c \phi_c^{HF} \quad (5)$$

so that $\phi_{n\ell}^{\text{CHF}}(0) = 0$ and the orbital is smooth.⁶ [This is analogous to the procedure used in OPW formalism where the CHF orbital is replaced by a plane wave.] Once the orbital $\phi_{n\ell}^{\text{CHF}}$ is determined, one obtains a corresponding Hartree-Fock equation. In it the core and valence operators $\hat{V}_{\text{core}}^{\text{HF}}$ and $\hat{V}_{\text{val}}^{\text{HF}}$ are replaced by new operators $\hat{V}_{\text{core}}^{\text{CHF}}$ and $\hat{V}_{\text{val}}^{\text{CHF}}$ which reflect the fact that $\phi_{n\ell}^{\text{CHF}}$ may now overlap the core orbitals. That is, Eq. (4) becomes

$$(h + \hat{V}_{\text{core}}^{\text{CHF}} + \hat{V}_{\text{val}}^{\text{CHF}}) \phi_{n\ell}^{\text{CHF}} = \epsilon_{n\ell} \phi_{n\ell}^{\text{CHF}} \quad (4')$$

Note that the orbital energy is still the same while the operator $\hat{V}_{\text{core}}^{\text{CHF}}$ now contains a repulsive part (arising from the Pauli principle) which serves to prevent the collapse of the valence orbitals into the inner shells.

The CHF orbital in (5) is not normalized. After renormalizing, the amplitude of $\phi_{n\ell}^{\text{CHF}}$ at large r differs from that of $\phi_{n\ell}^{\text{HF}}$ by just the normalization factor. This means that overlaps and other interaction quantities between orbitals on different centers will be modified by this same (small) factor. We want the transformation from HF orbitals to coreless orbitals to leave intermolecular interactions invariant, and hence we have modified the CHF orbital as follows, leading to the coreless valence orbital (CVO). The basis set for the HF orbital is partitioned into the core set (those basis functions important for the 1s and 2s core orbitals of Si) and the valence set,

$$\phi_{nl}^{HF} = \sum_{\mu=1}^{M'} C'_{\mu} \chi'_{\mu l} + \sum_{\mu=M'+1}^M C_{\mu} \chi_{\mu l} \quad , \quad (6)$$

where primes denote the core set. The CVO is taken to have the form

$$\phi_{nl}^{CVO} = \sum_{\mu=1}^{M'} a_{\mu} \chi'_{\mu l} + \sum_{\mu=M'+1}^M C_{\mu} \chi_{\mu l} \quad , \quad (7)$$

where the valence coefficients are exactly the same as in (6). The conditions on the a_{μ} of (7) are: (i) ϕ_{nl}^{CVO} as written in (7) must be normalized and (ii) the CVO goes smoothly to zero as r goes to zero. To determine the $\{a_{\mu}\}$, we set

$$\lim_{r \rightarrow 0} \frac{\phi_{nl}^{CVO}}{r^l} (r) = 0$$

and adjust the other $M'-1$ degrees of freedom so as to minimize the kinetic energy of the orbital. The net result is

$$(h + \hat{V}_{core}^{CVO} + \hat{V}_{val}^{CVO}) \phi_{nl}^{CVO} = \epsilon_{nl} \phi_{nl}^{CVO} \quad . \quad (4'')$$

In Fig. 2 we compare the HF, CHF, and CVO orbitals for the Si atom.

The next step is to replace the operator \hat{V}_{core}^{CVO} in (4'') with an effective potential, $V_l^{EP}(r)$ (that is, a mere function of r), such that the eigenfunction and eigenvalue of (4'') are also the eigenfunction and eigenvalue of (8)

$$(h + V_l^{EP}(r) + \hat{V}_{val}^{CVO}) \phi_{nl}^{CVO} = \epsilon_{nl} \phi_{nl}^{CVO} \quad . \quad (8)$$

The components of the potential $V_l(r)$ are obtained by projecting (8)

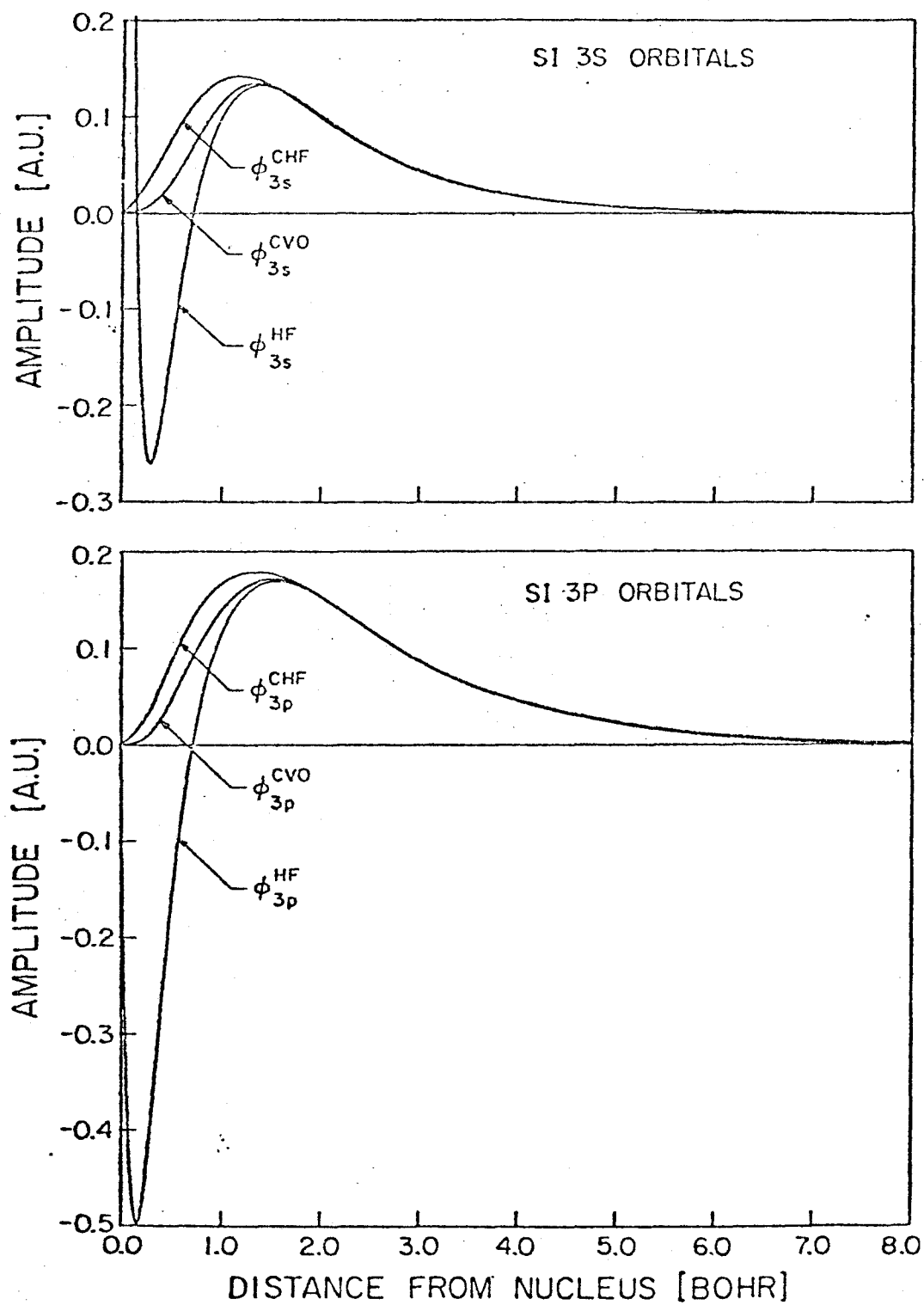


Figure 2. HF, CHF and CVO orbitals for the Si atom.

a) 3s type; b) 3p type.

onto the basis

$$\langle \chi_\mu | (h + V_\ell(r) + \hat{V}_{val} - \epsilon_{n\ell}) | \phi_{n\ell}^{CVO} \rangle \quad (9)$$

and adjusting the parameters in (3) to minimize the deviation of (9) from zero. [More precisely we require that the square of (9) summed over all basis functions is minimized.] In (9) one uses the normal basis functions for an atom plus additional basis functions representing important regions of function space for which $V_\ell(r)$ is significant. In particular, it is important to add diffuse basis functions to the basis in order to ensure that fitting (9) will lead to the correct long-range behavior of $V_\ell(r)$. The basis used to solve (9) is included in Table IV [we solve the HF equations for the new basis so that all basis functions are included in the $\phi_{n\ell}^{CVO}$ of (9)]. After obtaining the effective potential, all basis functions required only for the core can be eliminated (along with the functions added only for fitting the EP).

For those angular momenta ℓ represented in the core, $V_\ell(r)$ contains a large repulsive component representing the effect of the Pauli principle (the orthogonality of the ab initio valence orbital with respect to the core orbital). For ℓ not represented in the core, $V_\ell(r)$ is nearly independent of ℓ . Thus for Si we set

$$V_\ell(r) = V_d(r) \quad \text{for } \ell \geq 2$$

and rewrite (1) as

$$V^{EP}(r) = V_s(r)|s\rangle\langle s| + V_p(r)|p\rangle\langle p| + V_d(r) \sum_{\ell=2}^{\infty} |\ell\rangle\langle \ell|$$

Table IV. Basis Sets^a used in the *ab initio* and effective potential calculations on the Silicon atom.

ℓ	$\zeta_{\mu n}$	Set used to obtain the EP Eq. (8) ^b		Ab initio double zeta (6s4p) basis set ^c		EP (4s4p) _d basis set		EP double zeta (2s2p) basis set ^c	
		μ	$\alpha_{\mu n}$	μ	$\alpha_{\mu n}$	μ	$\alpha_{\mu n}$	μ	$\alpha_{\mu n}$
s	26740.0	1	1.0	1	0.002583				
s	4076.0	2	1.0	1	0.019237				
s	953.3	3	1.0	1	0.093843				
s	274.6	4	1.0	1	0.341235				
s	90.68	5	1.0	1	0.641675				
s	90.68		---	2	0.121439				
s	33.53	6	1.0	2	0.653143				
s	13.46	7	1.0	2	0.277624				
s	4.051	8	1.0	3	1.0	1	1.0	1	0.043662
s	1.484	9	1.0	4	1.0	2	1.0	1	-0.274872
s	0.2704	10	1.0	5	1.0	3	1.0	1	0.653119
s	0.2704		---		---		---	2	-0.200408
s	0.09932	11	1.0	6	1.0	4	1.0	2	0.424753
s	0.03731	12	1.0		---		---		---
s	0.01401	13	1.0		---		---		---
p _x	163.7	14	1.0	7	0.011498		---		---
p _x	38.85	15	1.0	7	0.077726		---		---
p _x	12.02	16	1.0	7	0.263595		---		---
p _x	4.185	17	1.0	7	0.758262	5	1.0	3	-0.004717
p _x	4.185		---	8	-1.173045		---		---
p _x	1.483	18	1.0	8	1.438335	6	1.0	3	-0.036542
p _x	0.3350	19	1.0	9	1.0	7	1.0	3	0.345438
p _x	0.3350		---				---	4	-0.030736
p _x	0.09699	20	1.0	10	1.0	8	1.0	4	0.144725
p _x	0.02766	21	1.0						
p _x	0.007890	22	1.0						
d _{xy}	2.973	23	1.0						
d _{xy}	0.7966	24	1.0						
d _{xy}	0.2863	25	1.0						
d _{xy}	0.1154	26	1.0						
d _{xy}	0.04998	27	1.0						
d _{xy}	0.01789	28	1.0						
d _{xy}	0.007211	29	1.0						

FOOTNOTES FOR TABLE IV

^aThe form of a given basis function, χ_μ , of angular momentum ℓ is

$$\chi_\mu = N_\mu \sum_n \alpha_{\mu n} x^p y^q z^s \exp(-\zeta_{\mu n} r^2)$$

N_μ is the normalization coefficient; $p = q = s = 0$ for an s-type function ($\ell=0$), $p = 1, q = s = 0$ for a p_x -type function ($\ell=1$), etc.

^bThis basis set is essentially the (11s7p) set of S. Huzinaga ("Approximate Atomic Functions. II.", Report from the Department of Chemistry, The University of Alberta, unpublished) with diffuse and d functions added.

^cDunning's double zeta contraction (T. H. Dunning, Jr., private communication) used in all ab initio calculations.

^dThis set was used in the EP calculations on the Si atom and the Si_2 molecule.

^eThis set is equivalent to an ab initio double zeta set. It was used in the EP calculations on SiH_3 and SiH_3O_2 .

or

$$V^{EP} = V_d(r) + V_{s-d}|s\rangle\langle s| + V_{p-d}|p\rangle\langle p| \quad , \quad (10)$$

where

$$V_{s-d}(r) = V_s(r) - V_d(r)$$

$$V_{p-d}(r) = V_p(r) - V_d(r) \quad ,$$

and where s, p, and d indicate $\ell = 0, 1$, and 2.

D. THE EFFECTIVE POTENTIAL FOR SILICON

In Table IV we list the usual basis for ab initio calculations on Si and the additional functions used in (9) for determining the potential.

To determine the d potential, V_d , we considered the

$$(1s)^2(2s)^2(2p)^6(3s)^1(3p)^2(3d)^1$$

quintet state of Si, solving (4) for the ϕ_{3d} orbital. The V_{s-d} and V_{p-d} potentials were obtained from the ϕ_{3s} and ϕ_{3p} orbitals of the triplet ground state of Si

$$(1s)^2(2s)^2(2p)^6(3s)^2(3p)^2 \quad .$$

In doing this we write

$$V_s = V_d + V_{s-d}$$

$$V_p = V_d + V_{p-d}$$

and solve (9) for V_{s-d} and for V_{p-d} .

The resulting potentials are listed in Table V and are plotted in Fig. 1. With just three terms each, we were able to obtain deviations (sums of the squares) of 1.886×10^{-10} , 3.05×10^{-8} , and 8.469×10^{-8} in the least squares fit to (9) for the V_d , V_{s-d} , and V_{p-d} potentials, respectively (for the large basis set of Table IV).

Using the EP, the basis on the Si can be modified to eliminate the functions required for describing the core orbitals. This reduces the double zeta valence basis from 18 to eight functions as indicated in Table IV.

We compare in Table VI the results of EP and ab initio calculations on various states of Si, Si^- , and Si^+ . Here we find errors of the order of 0.01 to 0.06 eV, quite satisfactory for our purposes. Bear in mind that the EP was determined from fitting of the d orbital of a quintet state and of the s and p orbitals to a triplet state. No further adjustments were made and hence the good agreement here is already evidence that the potential adequately represents the core electrons. At the HF and GVB level, the lack of complete electron correlation leads to errors in the excitation energies. Thus the experimental triplet-singlet excitation energy is 0.781 eV¹⁷ and hence 0.275 eV below the GVB value. The experimental IP of Si is 8.149 eV¹⁷ or 0.864 eV higher than the GVB value, and the experimental electron affinity is 1.385 eV¹⁸ or 0.769 eV lower than our value.

For comparison in Fig. 3 we show the 3s and $3p_x$ orbitals of the ground state (s^2p^2) of Si for the ab initio and EP calculations. In Table VII we compare the orbital energies for the EP and the ab initio calculations referred to in Table VI. In most cases the difference

Table V. Parameters for the Si Atom Effective Potentials. See Eq. (3) for the definitions of n , ζ , and C , and Eq.(10) for the form of the total potential. Quantities are in hartree atomic units.^a

	n	ζ	C
V_d	0	0.0991736	-0.01189620
	-1	0.2900090	-0.07889166
	-1	3.2105169	-3.59100110
V_{s-d}	0	3.5641009	30.31756200
	-2	0.1570854	0.24891789
	-2	1.8478285	4.08004340
V_{p-d}	0	4.0620237	36.58557100
	-2	0.2389864	0.45326622
	-2	0.9686443	0.86954814

^a The effective potential for the core electrons also includes a long-range term of $+10/r$. There is also a $-14/r$ term in the h of (4), corresponding to the nuclear attraction. We have deleted the $+10/r$ term from the table with the understanding that the nuclear attraction term in h will be $-4/r$.

Table VI. Energies for Various States of Si, Si⁺, and Si⁻ (Energies in eV).

Electronic State	Type of Wavefunction ^a	Excitation Energy		
		Ab Initio SCF	Effective Potential	Simplified Effective Potential
Si ⁻ quartet (s ² p ³)	HF	-0.616	-0.623	-0.030
Si triplet (s ² p ²)	GVB(1)	0.0 ^c	0.0 ^d	0.0 ^e
Si ⁻ doublet (s ² p ³) ^b	GVB(1)	0.684	0.696	1.532
Si singlet (s ² p ²)	GVB(1)	1.056	1.078	1.107
Si quintet (sp ³)	HF	2.893	2.836	2.476
Si ⁺ doublet (s ² p ¹)	GVB(1/3)	7.285	7.276	7.192

^aThe basis sets used were the Si (6s4p) and the Si (4s4p) sets of Table IV. Both of them were complemented with one diffuse function for each angular momentum type ($\zeta_{un} = 0.03731$ for s and $\zeta_{un} = 0.2766$ for p type). See Ref. 12 and the appendix to the present chapter for an explanation of the terms used in this column.

^bFor each state we considered the wavefunction using real orbitals and orbital symmetry restrictions. Thus this state is not an eigenstate of \hat{L}^2 .

^cTotal energy calculated is -288.84378 h.

^dTotal energy calculated using the effective potential is -3.67668 h.

^eTotal energy calculated using the simplified effective potential is -3.81514 h.

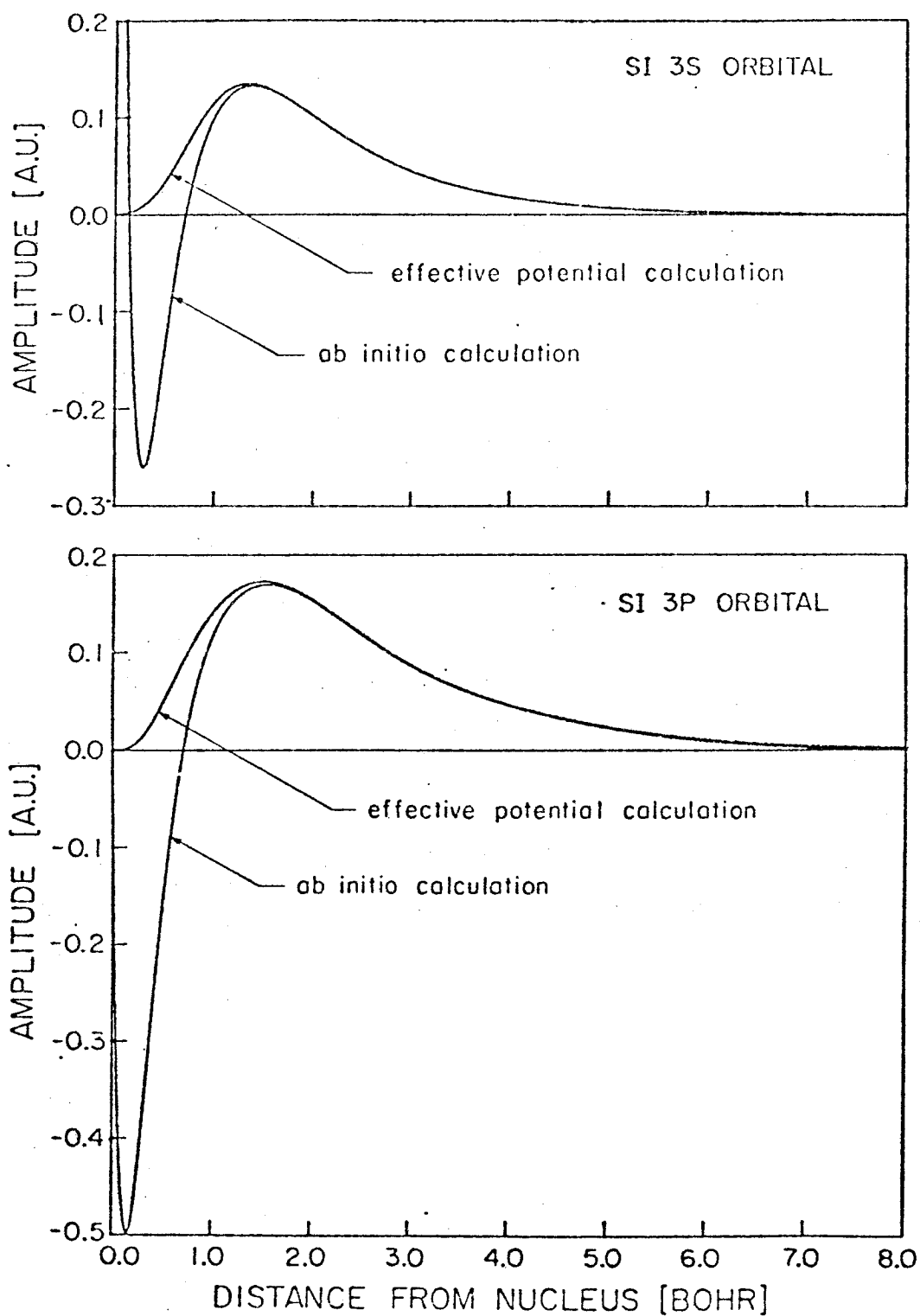


Figure 3. HF orbitals of Si (3P) as calculated ab initio and using the EP.
a) 3s; b) 3p.

Table VII. Comparison of Orbital Energies for Ab Initio (AI) and Effective Potential (EP) Calculations for Various States of Si, Si⁺, and Si⁻. All Energies in hartree atomic units.

State		Orbital		
		3s	3p _x	3p _y
Si ⁻ quartet (s ² p ³)	AI	-0.3020	-0.0615	-0.0615
	EP	-0.3028	-0.0620	-0.0620
Si triplet (s ² p ²)	AI	-0.5544	-0.2958	-0.8671
		(0.9904) ^b		(-0.1380)
	EP	-0.5551	-0.2956	-0.8725
		(0.9900)		(-0.1409)
Si ⁻ doublet (s ² p ³) ^a	AI	-0.3187	-0.0586	-0.0272
				(0.7071) ^c
	EP	-0.3199	-0.0593	-0.0275
Si singlet (s ² p ²)	AI	-0.5617	-0.2597	-0.8747
		(0.9904)		(-0.1382)
	EP	-0.5629	-0.2590	-0.8804
		(0.9900)		(-0.1412)
Si quintet (sp ³)	AI	-0.7247	-0.3487	-0.3487
	EP	-0.7298	-0.3489	-0.3489
Si ⁺ doublet (s ² p ¹)	AI	-0.8661	-0.5817	-1.185
		(0.9819)		(-0.1341) ^d
	EP	-0.8664	-0.5801	-1.189
		(0.9811)		(-0.1370)

FOOTNOTES FOR TABLE VII

^aSee footnote b of Table VI.

^bNumbers in parentheses indicate CI coefficients of GVB correlated pairs. The wavefunctions of these pairs have the form $C_1\phi_1^2 + C_2\phi_2^2 + C_3\phi_3^2$, where the C_i (CI coefficients) satisfy $\sum_i C_i^2 = 1$. See Ref. 12 and the appendix to the present chapter.

^cThis orbital is correlated with a $3p_z$ orbital having also $C_i = 0.7071$.

^dThis orbital and a $3p_z$ orbital like it correlate the $3s$ orbital in a GVB(1/3) wavefunction.

between the ab initio and EP orbital energies was about 0.001 hartree \approx 0.037 eV. This difference is as high as 0.005 hartree only for some of the GVB correlated pairs. In Tables VIII, IX, and X we show the orbital energies for the Si_2 , SiH_3 , and SiH_3O_2 SCF calculations, respectively. Here we note that the differences between the ab initio and EP values are larger than they were in the atomic case. This is to be expected since the effective potential was constructed from the atomic SCF calculations. In the molecular orbital energies most of the differences between the ab initio and EP values are below 0.020 hartree \approx 0.3 eV except for some of the GVB correlated pairs in which it is as high as 0.030 hartree. We note, however, that the correlation energies for most of those same GVB pairs (given in Tables VIII-X) agree to better than 0.005 hartree \approx 0.015 eV.

We have also performed calculations on disilane, $\text{H}_3\text{Si-SiH}_3$. The double zeta (2s2p) basis set of Table IV was used for silicon and a Si-H bond length¹³ of 1.48\AA with tetrahedral H-Si-H angles were employed. A Si-Si bond potential energy curve was calculated by doing HF and GVB calculations at four different points (2.22, 2.32, 2.43 and 2.53\AA , respectively) for the $^1\text{A}_g$ ground state of the system. From the HF calculations we find an equilibrium bond length of 2.35\AA . The experimental value is¹⁹ 2.331\AA . We therefore predict a bond length which is 0.02\AA too long. By using a Numerov numerical integration of the HF potential curve we find that the first vibrational level for the Si-Si stretch is at 0.055 eV, whereas the experimental value is²⁰ 0.054 eV. From the GVB calculations on this molecule and those on

Table VIII. Comparison of Orbital Energies for Ab Initio and Effective Potential Calculations for the $^3\Sigma_g^-$ and the $^1\Sigma_g^+$ states of Si_2 ($R = 4.244 a_0$). All Energies in hartree atomic units.

	$^3\Sigma_g^-$		$^1\Sigma_g^+$	
	<u>ab initio</u>	effective potential	<u>ab initio</u>	effective potential
A. Orbital energies				
ϵ_{σ_g}	-0.6613	-0.6678	-0.6829	-0.6843
ϵ_{σ_g}	-0.3374 ^a	-0.3303	-0.6648 ^a	-0.6675
ϵ_{σ_u}	-0.4728	-0.4732	-0.4749 ^a	-0.4761
$\epsilon_{\pi_{ux}}$	-0.3104	-0.3116	-0.2972 ^a	-0.2976 ^c
B. GVB pair quantities ^b				
	bond pair		π bonds (π_x and π_y)	π bonds (π_x and π_y)
C_2	-0.1118	-0.1147	-0.2983	-0.2990
S_{ab}	0.7977	0.7931	0.5239	0.5228
ΔE	0.0094	0.0095	0.0278	0.0278
			σ nonbonding pair	σ nonbonding pair
			-0.9774	-0.9773
			0.6445	0.6434
			0.0424	0.0202

^aThis orbital is the first natural orbital of a correlated pair. See Refs. 12 and 22.

^bThe wavefunction for a correlated pair has the form $C_1\phi_1^2 + C_2\phi_2^2$; C_2 is the CI coefficient for the second natural orbital ($C_1^2 + C_2^2 = 1$); ΔE is the correlation energy of the pair; S_{ab} is the overlap of the GVB orbitals of the pair. See Ref. 12 and the appendix to the present chapter.

Table IX. Orbital Energies for SiH_3 and SiH_3^+ . All Energies in hartree atomic units.

orbital energies	$\text{SiH}_3 \ ^2\text{A}_1$		$\text{SiH}_3^+ \ ^1\text{A}_1$	
	<u>ab initio</u>	effective potential	<u>ab initio</u>	effective potential
$\epsilon_{a'}^a$	-0.7137	-0.7110	-0.9981	-0.9965
$\epsilon_{a'}^a$	-0.4823	-0.4802	-0.7559	-0.7548
$\epsilon_{a'}^b$	-0.3453	-0.3353	--	--
$\epsilon_{a''}^a$	-0.4822	-0.4801	-0.7559	-0.7548

^a Doubly-occupied orbital.

^b Singly-occupied orbital.

Table X. Orbital Energies for the $^2A''$ Ground State of SiH_3O_2 .^a

All Energies in hartree atomic units.

	<u>ab initio</u>	<u>effective potential</u>
A. Orbital Energies		
$\epsilon_{a'}$	-20.6740	-20.6777
$\epsilon_{a'}$	-20.6181	-20.6148
$\epsilon_{a'}$	-1.3737	-1.3771
$\epsilon_{a'}$	-1.0588	-1.0638
$\epsilon_{a'}$	-0.7313	-0.7293
$\epsilon_{a'}$	-0.5940	-0.5972
$\epsilon_{a'}$	-0.5099	-0.5084
$\epsilon_{a''}$	-0.6345	-0.6367
$\epsilon_{a''}$	-0.4910	-0.4911
$\epsilon_{a''}^b$	-0.6172	-0.6207
B. For GVB Pairs^c		
a. Si-O bond		
$\epsilon_{1\text{NO}}$	-0.7721	-0.7691
C_2	-0.0852	-0.0881
S_{ab}	0.8424	0.8376
ΔE	-0.0142	-0.0147
b. O-O bond		
$\epsilon_{1\text{NO}}$	-0.7871	-0.7909
C_2	-0.1639	-0.1637
S_{ab}	0.7151	0.7154
ΔE	-0.0397	-0.0396

FOOTNOTES FOR TABLE X

^aThe basis sets used are the Si (6s4p) and the Si (2s2p) of Table IV and the H (2s) and O (4s2p) of T. H. Dunning, Jr., J. Chem. Phys. 53, 2823 (1970) and S. Huzinaga, ibid. 42, 1293 (1965).

^bThis orbital is singly occupied.

^c₁ NO and 2 NO indicate the natural orbitals of the correlated pair, $C_1 \phi_1^2 \text{ NO} + C_2 \phi_2^2 \text{ NO}$; C_2 is the CI coefficient ($C_1^2 + C_2^2 = 1$); ΔE is the correlation energy of the pair; S_{ab} is the overlap of the GVB orbitals of the pair. See Ref. 12 and the appendix to the present chapter.

SiH_3 of Table II we find a bond energy of 3.08 eV or 71.1 kcal. Experimentally it is found²¹ that this bond strength is 82 ± 4 kcal.

For reference in future chapters we have listed in Table XI all the different basis sets used in the calculations to be described in them. Two basic types of basis sets have been used: first a minimum basis set (MBS) which consists of the same number of functions per symmetry type as there are orbitals in the atom in question. This basis set is the one that has the least amount of flexibility of all of the types described here. A second type of basis set is the double zeta (DZ) in which the number of functions is twice that of orbitals in the atom. We have also used in some of the calculations basis sets which consist of modifications of the two mentioned above. One such type of basis set is what we have termed as a mixed basis set (MXS1 and MXS2) which for some parts of the molecule consists of a MBS set while the "surface" part has DZ character. The set MXS1 has only been used in calculations on the Si_3H_6 cluster of Chapter 2. The set MXS2 has been used in the silicon part of the $\text{Si}_3\text{H}_6\text{O}_2$ calculations of Chapter 4. Two other types of sets have been used; one is a double zeta set with additional d-functions (denoted DZd) which has been used in various calculations in Chapters 2 and 3. The last set consists of a double zeta part with diffuse s and p functions (denoted DZR). This set was used in the Si_4H_9 calculations of Chapter 2.

We find that the EP obtained using the above ideas leads to excellent agreement with ab initio calculations while eliminating

Table XI. Si Atom Basis Sets^a Used in Calculations Discussed in Chapters 2 to 4

ℓ	$\zeta_{\mu n}$	Minimum Basis Set (MBS) ^b		Double Zeta (DZ) ^c	
		μ		μ	$\alpha_{\mu n}$
s	4.051	1	0.043662	1	0.043662
s	1.484	1	-0.274872	1	-0.274872
s	0.2704	1	0.452711	1	0.653119
s	0.2704	-		2	-0.200408
s	0.09932	1	0.424753	2	0.424753
p _x	4.185	2	-0.004717	3	-0.004717
p _x	1.483	2	-0.036542	3	-0.036542
p _x	0.3350	2	0.314702	3	0.345438
p _x	0.3350	-		4	-0.030736
p _x	0.09699	2	0.144725	4	0.144725

^aThe form of a given function is given in footnote a to Table IV, together with a meaning of the symbols used in this table.

^bTwo mixed basis sets, MXS1 and MXS2 are obtained from this MBS set by adding the function with $\mu = 4$ of the DZ set (for MXS1) and functions with $\mu = 2$ and $\mu = 4$ of the DZ set (for MXS2). In all calculations in which hydrogen atoms are present the 3-gaussian basis of S. Huzinaga [J. Chem. Phys. 42, 1293 (1965)] was used.

^cThis set is the same as the (2s2p) set of Table IV. For the DZR set two diffuse functions are added to DZ, of s and p_x type, with $\zeta_{\mu n} = 0.03648$ and $\zeta_n = 0.02808$, respectively. For the DZd basis set, a set of d-functions with $\zeta_{\mu n} = 0.3247$ was added to the DZ basis set. In all calculations in which hydrogen atoms are present a DZ contraction of the 3-gaussian basis of S. Huzinaga [J. Chem. Phys. 42, 1293 (1965)] was used.

core orbitals and core basis functions. However, although this EP leads to great computational gains, it still requires four basis functions of each type (s , p_x , p_y , p_z) on each Si. For use in our studies of large clusters we have also developed a much cruder, simplified EP (SEP) adjusted so as to require only two basis functions per type per center. In this case we eliminated all core functions from (7) leading to a smooth valence orbital with finite amplitude at the nucleus. The parameters for the SEP are listed in Table XII. Since the orbital is finite at the nucleus, the SEP is much less repulsive at small r than the EP. A plot of this potential is shown in Fig. 4. Table VI compares values of energies obtained with this SEP and ab initio calculations for the Si atom.

We have also tested the SEP as compared to the EP in calculations in Si_4H_9 complexes. Here the complex models a Si(111) surface with one Si surface atom bound to three "second layer" Si atoms. These in turn are bound to nine hydrogens, used to decouple what otherwise would be "second layer dangling bonds". These second layer electrons are then localized in Si-H bonds and do not couple with the surface dangling bond. In the calculations (described in more detail in Chapter 2) the surface atom is allowed to move along the [111] direction, keeping all other atoms fixed. When we use the EP to substitute the core electrons of all four Si atoms the minimum energy is found at 0.152 bohr from the tetrahedral geometry, toward the bulk. When in the three second layer silicons we use the SEP, with the EP only on the surface atom, the minimum occurs at 0.153 bohr. Thus the SEP gives a good description of the environment of the core electrons when one

Table XII. Parameters for the Si Atom Simplified Effective Potentials.
Quantities are in hartree atomic units. ^a

	n	ζ	c
V_d	0	0.0991736	-0.01189620
	-1	0.2900090	-0.07889166
	-1	3.2105169	-3.59100110
V_{s-d}	0	1.90165	14.7148
	0	0.25328	0.195044
V_{p-d}	0	1.31007	5.87041
	0	0.19252	-0.0595822

^aSee Footnote a to Table V.

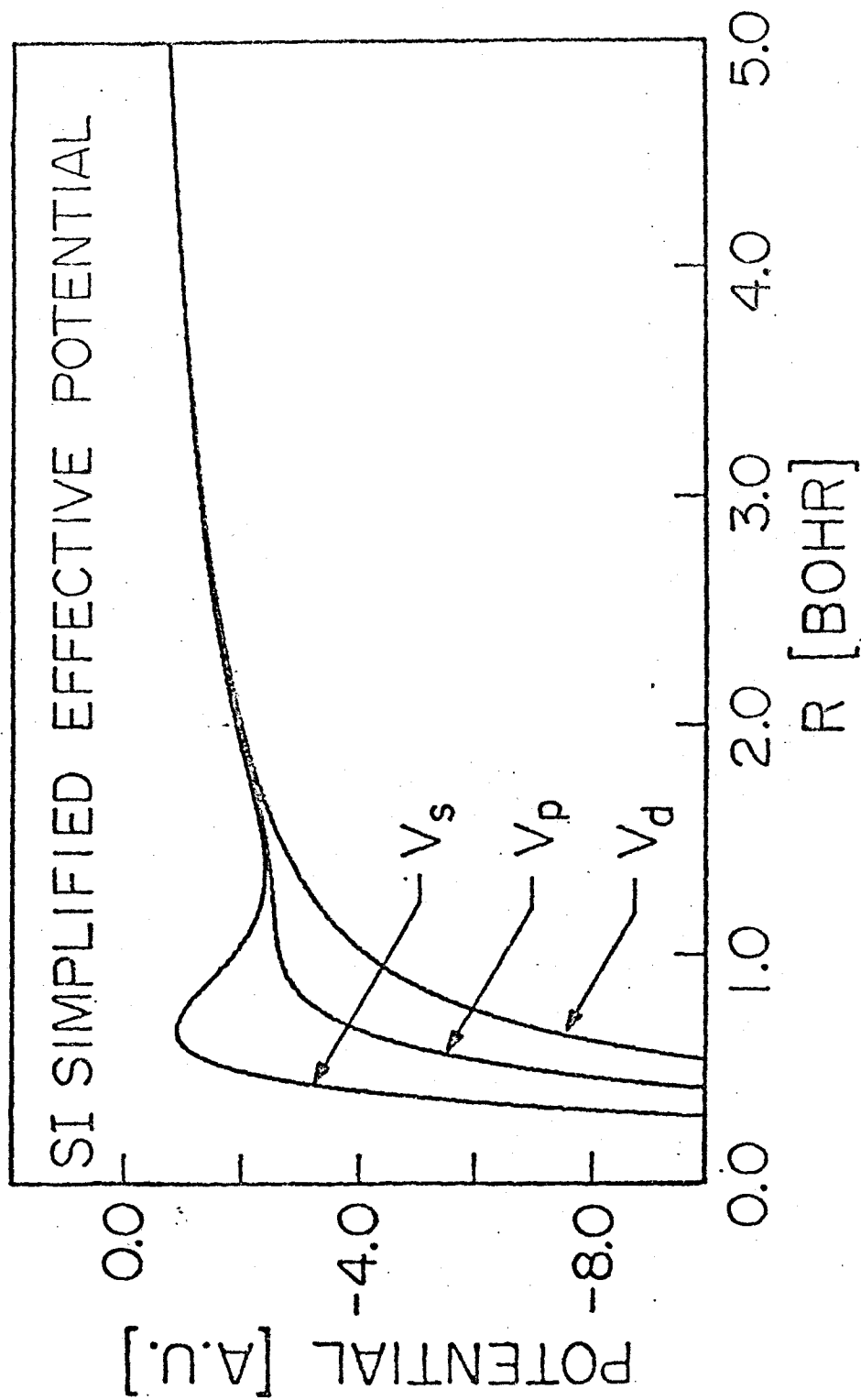


Figure 4. Si Simplified Effective Potential (SEP) Components $V_i(r)$.
Curves plotted include the nuclear attraction term.

uses it in atoms which do not determine the principal characteristics of the electronic states of the cluster.

For band calculations on solids using plane wave expansions, an overriding consideration is the reduction of the number of plane wave components. Thus, for such studies the SEP is likely to be more useful than the EP.

E. CONCLUSIONS

These results are very encouraging. The effective potential produces wavefunctions of ab initio quality, as well as very good agreement in the energy quantities of molecular and atomic systems. It must also be noted that since the wavefunctions obtained with the effective potential are smooth at the core, we can reduce considerably the number of primitive functions on the basis sets employed. This produces an appreciable reduction of cost in the calculation of the integrals. A further reduction in cost (for large complexes) is obtained when one uses the simplified effective potential for atoms that are not actively involved in the calculation (e.g., "bulk" atoms) when calculating surface properties. Besides this, one gets the corresponding reduction in the SCF costs due to the smaller number of electrons involved.

REFERENCES FOR CHAPTER 1

1. (a) H. Hellmann, J. Chem. Phys. 3, 61 (1935); (b) P. Gombás, Z. Phys. 94, 473 (1935).
2. J. C. Phillips and L. Kleinman, Phys. Rev. 116, 287 (1959).
3. (a) M. H. Cohen and V. Heine, *ibid.* 122, 1821 (1961); (b) B. J. Austin, V. Heine, and L. J. Sham, *ibid.* 127, 276 (1961).
4. For a review, see the following (and the references cited therein): (a) W. A. Harrison, Pseudopotentials in the Theory of Metals (Benjamin, New York, 1966); (b) M. L. Cohen and V. Heine, in Solid State Physics, ed. by H. Ehrenreich, F. Seitz, and D. Turnbull (Academic Press, New York, 1970), Vol. 24, p. 37.
5. For a review, see (a) J. D. Weeks, A. Hazi, and S. A. Rice, Adv. Chem. Phys. 16, 283 (1969); (b) J. N. Bardsley, Case Studies in Atomic Physics 4, 299 (1974).
6. C. F. Melius and W. A. Goddard III, Phys. Rev. A 10, 1528 (1974).
7. Earlier work on related approaches is summarized in (a) L. R. Kahn and W. A. Goddard III, J. Chem. Phys. 56, 2685 (1972); (b) *idem*, Chem. Phys. Lett. 2, 667 (1968); (c) L. R. Kahn, Ph.D. Thesis, California Institute of Technology, 1971.
8. C. F. Melius, B. D. Olafson, and W. A. Goddard III, Chem. Phys. Lett. 28, 457 (1974).
9. See, for example, M. L. Cohen, M. Schluter, J. R. Chelikowsky, and S. G. Louie, Phys. Rev. B 12, 5375 (1975).
10. By ab initio we mean a calculation in which all the electrons of the system are taken into account and all energy quantities are calculated exactly.

11. B. Rosen, Selected Constants--Spectroscopic Data Relative to Diatomic Molecules (Pergamon Press, Oxford, 1970).
12. a) W. J. Hunt, P. J. Hay, and W. A. Goddard III, J. Chem. Phys. 57, 738 (1972); b) W. A. Goddard III, T. H. Dunning, Jr., W. J. Hunt, and P. J. Hay, Accts. Chem. Res. 6, 368 (1973).
13. D. R. Boyd, J. Chem. Phys. 23, 922 (1955).
14. R. S. Mulliken, J. Chem. Phys. 23, 1833, 1841 (1955).
15. W. A. Goddard III, A. Redondo, and T. C. McGill, Solid State Comm. 18, 981 (1976); see also Chapter 4.
16. A similar form for the effective potential was used by V. Heine and I. Abarenkov [Phil. Mag. 9, 451 (1964)]. They used

$$V_{\ell}(r) = \begin{cases} -A_{\ell}(E) & r < R_M \\ -Z/r & r \geq R_M \end{cases},$$
 where $A_{\ell}(E)$ is a constant that depends on the orbital energy E of the eigenstates of the ion core of charge Z . R_M is the core radius.
17. C. Moore, Atomic Energy Levels (NBS Circular 467, Vol. I, 1949).
18. H. Hotop and W. C. Lineberger, J. Phys. Chem. Ref. Data 4, 439 (1975).
19. B. Beagley, A. R. Conrad, J. M. Freeman, J. J. Monaghan, B. G. Norton and G. C. Holywell, J. Mol. Structure 11, 371 (1972).
20. G. Bethke and M. K. Wilson, J. Chem. Phys. 26, 1107 (1957).
21. R. Walsh, private communication to W. A. Goddard III.
22. W. J. Hunt, T. H. Dunning, Jr. and W. A. Goddard III, Chem. Phys. Lett. 3, 606 (1969).

Chapter 2

THE CLEAN SURFACES OF SILICON

I. INTRODUCTION

In this chapter we will consider the (111), (100), and (110) surfaces of silicon. In particular, we will be concerned with the electronic structures for clean surfaces (i.e., in the absence of impurities) and some of the consequences the electronic structure has on the geometrical configurations of such surfaces.

The presence of a surface on a semiconductor can modify the electronic structure in two ways:¹ (i) The interruption of the long range periodicity will modify the properties and characteristics of the bulk states; such effects should not be very sensitive to the specific surface; (ii) there will generally also be localized electronic states associated with the unsaturated valences of the surface atoms and hence quite sensitive to the specific atomic arrangement at the surface. Case (i) can be studied using the techniques of bulk band structure calculations to treat the two-dimensional region parallel to the surface and matching layers in the direction perpendicular to the surface using appropriate boundary conditions.

It is the localized states, case (ii), we will be concerned with herein. For such localized states it is essential to account properly for electronic correlation or many body effects, and hence the usual band techniques are inadequate. Consequently we will apply the generalized valence bond²(GVB) and configuration interaction³ (CI) methods to the study of the wavefunctions characteristic of these

localized states.

Of particular interest in the study of the localized surface states is the determination of the displacement of the surface atoms from their respective locations in the bulk. We will distinguish two such distortions: (i) relaxation, which we define as a uniform motion of the surface atoms along the direction perpendicular to the surface, either toward or away from the free surface; (ii) reconstruction, that is, nonuniform displacement of atoms, either laterally or perpendicularly to the surface, or movement of the atoms to entirely new positions. Here we will consider both relaxation and some types of reconstruction.

The major difficulty in applying the GVB and CI methods to surfaces is that we do not yet know how to include such correlation effects for infinite systems. As a result we must use a finite cluster of silicon atoms. In order to obtain rapid convergence of the surface states as a function of cluster size, it is very important to ensure that all Si atoms included in the cluster have the same coordination as in the semi-infinite system. Thus visualizing the formation of a cluster by cutting it away from the semi-infinite solid, we maintain the proper coordination numbers by replacing any broken Si-Si bond with a Si-H bond. This procedure has been applied to the clusters discussed herein.

Unless otherwise stated, all calculations described in the present chapter have the following characteristics in common: (i) The Si effective potential (EP) described in Chapter 1 was employed to

replace the core electrons of each silicon atom in the cluster;
(ii) a Si-Si bond length of 2.35\AA (from the Si crystal structure⁴)
and a Si-H bond length of 1.48\AA (from silane⁵ SiH_4) were used. In
studies of relaxation and rearrangement effects involving motion of
a Si atom attached to a hydrogen, the H atom was moved so that all
bond angles were the same as for the semi-infinite system. That is,
the virtual position of the (stationary) Si represented by the H de-
termines the motion of the H atom so that the Si-H bonds move as if
they were the original Si-Si bonds.

II. THE (111) SURFACE OF SILICON

A. Introduction

The cleavage faces of silicon crystals are (111) surfaces.⁶ On
this plane each surface Si atom is bonded to three Si atoms on the
plane below (this is sketched in Fig. 1) and one electron is left in
a nonbonding or dangling bond orbital, pointing away from the surface.
Retaining the full symmetry of the surface (1x1 unit cell), we find
(vide infra) that the surface Si atoms relax 0.08\AA toward the bulk
positions (this is 10% of the bulk interlayer spacing of 0.78\AA).

Experimentally, freshly cleaved Si (111) surfaces exhibit a
 2×1 unit cell⁶ in the low energy electron diffraction⁷ (LEED) pat-
terns, indicating some degree of reconstruction. Further treatment
(usually thermal) leads to additional rearrangement and a more stable
 7×7 unit cell.⁶ This suggests that considerable motion of the surface
atoms might be involved in the 7×7 structure. Although the real
cleaved surfaces suffer reconstruction, it is of considerable

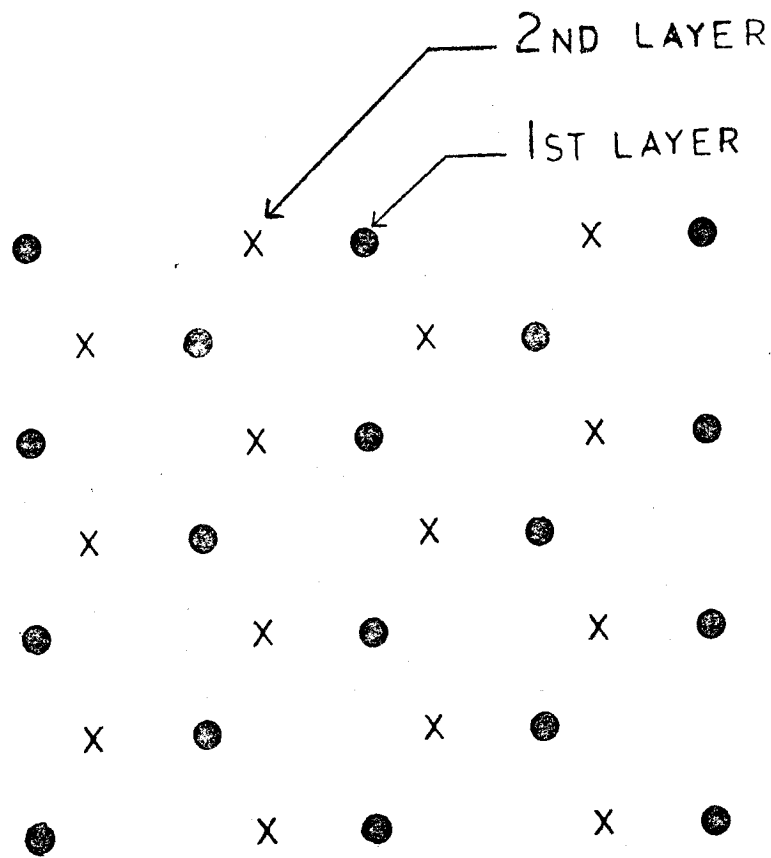


Fig. 1. Sketch of (111) Surface of Silicon. Surface atoms are indicated by filled circles. Second layer atoms are indicated by crosses.

theoretical value to investigate the electronic structures of ideal (tetrahedral geometry) and relaxed surfaces.

For the clean (111) surface we were interested in investigating two basic problems: (i) the relaxation of the surface Si atoms; and (ii) the interaction between dangling bond orbitals on different neighboring surface atoms. Two different types of clusters (described below) were employed for these studies.

B. Surface Relaxation

General Description

In order to study the relaxation of the surface atoms, we used a cluster consisting of one surface Si atom, its three Si neighbors on the next layer plus three H atoms bonded to each of these second layer Si's, leading to a Si_4H_9 complex as shown in Fig. 2. To investigate the effect of relaxation we allowed the surface silicon to move along the [111] direction. Similar studies were also carried out for the positive and negative ion systems in order to determine the ionization potential (IP) and electron affinity (EA) for this complex.

Calculational Details

The calculations described in the present section were performed using the double zeta (DZ) basis set of Table XI, Chapter 1 (p.31). (Double zeta means that two basis functions are included for each orbital present in the atom). Since a negative ion generally leads to more diffuse orbitals the DZR basis set (Table XI, Chapter 1) was used for the case in which a second electron had been added to the dangling bond orbital (negative ion). This set contains diffuse s and p basis

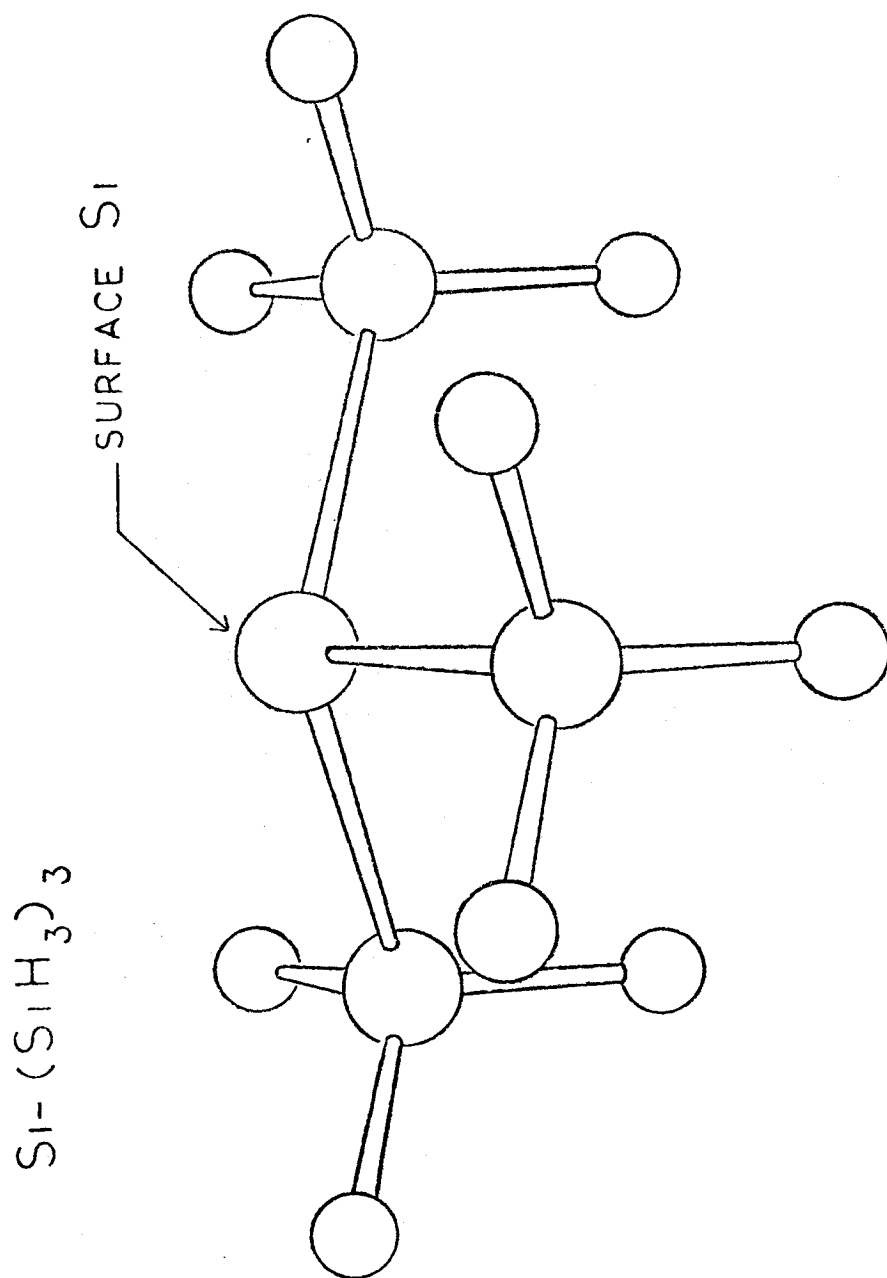


Fig. 2. Geometrical Configuration for the Si_4H_9 Cluster. Silicon atoms are shown by large spheres, hydrogens by small spheres.

functions on the surface Si to allow a greater flexibility in the variational calculation of such an orbital.

The geometry chosen is that of a tetrahedral bulk configuration except that the position of the surface atom was varied along the [111] direction (threefold axis). The range of the variation was from -0.8 to 0.6 bohr. (Positive displacement implies motion away from the surface.)

An important consideration is the form of the wavefunctions used. The neutral complex is a doublet state and we carried out fully self-consistent open-shell Hartree-Fock (HF) calculations for this state. The wavefunction has the form

$$\begin{aligned} & \mathcal{A} [(\phi_1\phi_1^{\alpha\beta})(\phi_2\phi_2^{\alpha\beta}) \cdots (\phi_{12}\phi_{12}^{\alpha\beta})(\phi_{13}^{\alpha})] \\ & = \mathcal{A} \{ \Phi_{\text{bulk}}(1, \dots, 24) [\phi_{13}(25) \alpha(25)] \} \quad , \end{aligned} \quad (1)$$

where \mathcal{A} is the antisymmetrizer or determinant operator; ϕ_i is a spatial orbital, α and β are the up and down one-electron spin functions. (Note, spatial and spin functions are always ordered with sequence of increasing electron number unless directed otherwise.) On the right hand side $\Phi_{\text{bulk}}(1, \dots, 24)$ denotes the wavefunction of the 24 nondangling-bond electrons. (Recall that the Si 1s, 2s, and 2p electrons are included in the EP). $\phi_{13}(25)$ and $\alpha(25)$ correspond to the spatial and spin functions of the dangling bond electron. We thus have a total of 12 doubly-occupied bonding valence orbitals plus the dangling bond orbital, ϕ_{13} . In our calculations all 13 orbitals are solved

self-consistently, allowing each orbital to delocalize and distort to whatever extent it wishes.

The positive ion is a closed-shell singlet and the corresponding closed-shell HF calculations were performed. In this case the wavefunction is

$$a [\Phi'_{\text{bulk}}(1, \dots, 24)] ,$$

where the prime indicates that the optimum orbitals ϕ_1 to ϕ_{12} are not the same as (although very similar to) those of (1).

For the negative ion state the HF description is to place the new electron in ϕ_{13} with spin β ,

$$a [\Phi_{\text{bulk}}(1, \dots, 24) \phi_{13}(25) \phi_{13}(26) \alpha(25) \beta(26)] ,$$

solving consistently for the 13 orbitals.

Since two electrons are moving, uncorrelated, in one orbital, this description of the negative ion should lead to too low an electron affinity. To be consistent with (1) we allowed these two electrons to be correlated. In the GVB wavefunction such correlation is introduced by replacing a doubly-occupied orbital with a pair of overlapping orbitals

$$\phi_i(1)\phi_i(2) \longrightarrow \phi_{ia}(1)\phi_{ib}(2) + \phi_{ib}(1)\phi_{ia}(2) .$$

In the Si surface, ϕ_{ia} and ϕ_{ib} are lobe orbitals localized on the surface atom but ϕ_{ia} is more compact while ϕ_{ib} is more diffuse, thereby allowing for radial correlation of the motion of the electrons (this is referred to as in-out correlation). An alternate way of writing the

GVB pair, as described in Appendix A is

$$\phi_{ia}(1)\phi_{ib}(2) + \phi_{ib}(1)\phi_{ia}(2) = C_g \bar{\phi}_{ig}(1)\bar{\phi}_{ig}(2) + C_u \bar{\phi}_{iu}(1)\bar{\phi}_{iu}(2) \quad (2)$$

where

$$\bar{\phi}_{ig} = (\phi_{ia} + \phi_{ib})/D_1$$

$$\bar{\phi}_{iu} = (\phi_{ia} - \phi_{ib})/D_2$$

$$\frac{C_g}{C_u} = \frac{1 - S^2}{1 + S^2}$$

$$S = \langle \phi_{ia} | \phi_{ib} \rangle$$

(D_1 and D_2 are appropriate normalization constants). The orthogonal orbitals $\bar{\phi}_{ig}$ and $\bar{\phi}_{iu}$ are referred to as natural orbitals, $\bar{\phi}_{ig}$ resembles a localized Hartree-Fock orbital (see Fig. 3); $\bar{\phi}_{iu}$ is denoted as the correlating orbital; generally $C_g \approx 1.0$ and $C_u \approx 0.1$.

Although the GVB wavefunction includes the dominant correlation term, there are smaller terms that are important in properly describing negative ions. In general, the most significant correlating orbitals are those that have one more nodal surface than the orbital being correlated. Thus the two important correlations in addition to those in (2) involve correlating orbitals whose nodal plane bisects ϕ_{13} and passes perpendicular to the surface (see Fig. 3). We refer to

Si_4H_9^- NEGATIVE ION NATURAL ORBITALS

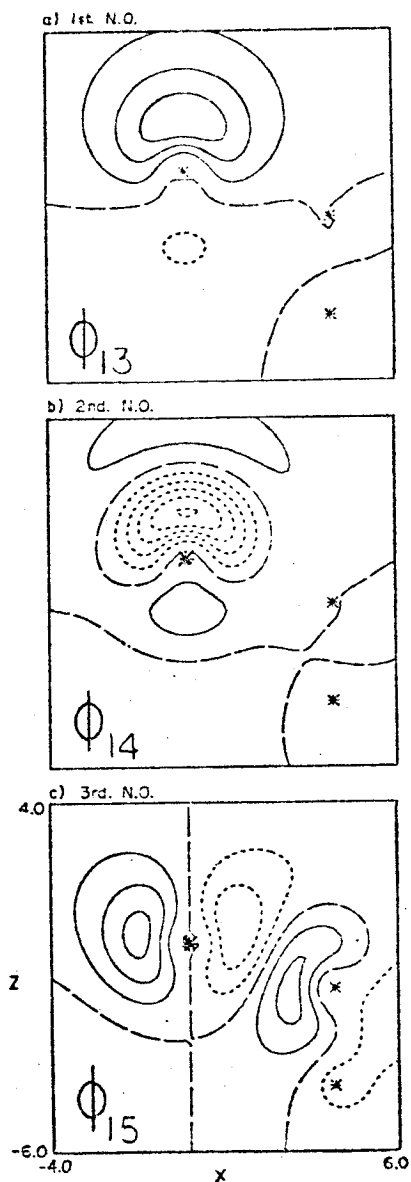


Fig. 3. Amplitudes for the natural orbitals of the negative ion GVB ($1/4$) Si_4H_9^- Calculation. a) First Natural Orbital, ϕ_{13} ; b) Second Natural Orbital, ϕ_{14} (in-out correlating orbital); c) Third Natural Orbital, ϕ_{15} (angular correlating orbital). Solid lines indicate positive amplitude values, short dashes indicate negative amplitudes, long dashes indicate nodal surfaces. Contours are drawn every 0.05 atomic units. Atoms are denoted by an asterisk. Distances are in atomic units.

these as π orbitals ($m_l = \pm 1$ with respect to the [111] axis) while the orbitals of (2) are referred to as σ orbitals ($m_l = 0$ with respect to the [111] axis). The correlations effected by π orbitals are called angular correlations. Including all these correlations together the dangling bond pairs of the negative ion are described as

$$\Phi_{\text{surf}}(25,26) = [C_{13}\phi_{13}(25)\phi_{13}(26) + \dots + C_{16}\phi_{16}(25)\phi_{16}(26)][\alpha(25)\beta(26)]$$

and the total wavefunction is

$$a [\Phi_{\text{bulk}}''(1, \dots, 24) \Phi_{\text{surf}}(25,26)] . \quad (3)$$

All 16 orbitals and the coefficients C_{13} to C_{16} are solved self-consistently. In the present case,^{8,9} the coefficients C_{14} to C_{16} have values between 0.04 and 0.08, whereas C_{13} has a value of 0.995. The energy obtained with the wavefunction (3) is 0.35 eV lower than that of the corresponding HF wavefunction.

Results

Our results for the Si_4H_9 complex are summarized in Table I. For the neutral system we find that the surface atom moves towards the bulk 0.08\AA (10% of the interplanar distance), leading to a new Si-Si bond length of 2.33\AA (compared to 2.35\AA in the bulk). The resulting dangling bond orbital, ϕ_{13} , is shown in Fig. 4. It is localized in the region of the surface atom (93.1%) and is mainly p-like (92.9%).

For the positive ion the surface atom moves toward the bulk by an additional 0.30\AA (a total relaxation of 48% of the interplanar distance). The new Si-Si bond length is 2.25\AA . The resulting vertical

Table I. Summary of Quantities Relating to the Si_4H_9 Cluster Model of the Si(111) Surfaces

	Neutral	With dielectric corrections		Without dielectric corrections	
		Positive Ion	Negative Ion	Positive Ion	Negative Ion
Relaxation(\AA) ^a	-0.08	-0.38	0.17	-0.36	0.23
$R_{\text{Si-Si}}$ (\AA)	2.33	2.25	2.41	2.26	2.44
Excitation Energy (eV)					
Adiabatic	0.0 ^{b,d}	5.435	-3.062	7.358	-0.667
Vertical	0.0	5.778	-2.745	7.661	-0.862
$\hbar\omega$ (eV) ^c	0.036	0.030	0.030		

^aThe relaxation is with respect to the undistorted positions of the surface Si, the positive direction is away from the bulk.

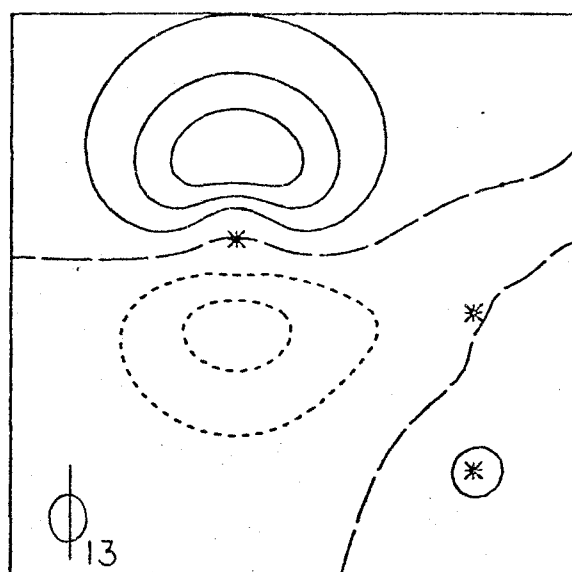
^bThe total energy is -20.04811 hartree

^cEnergy necessary to excite the first symmetric C_{3v} vibrational state. This was calculated by solving numerically for the lowest two vibrational wavefunctions. The use of the harmonic force constant leads to vibrational frequencies of 0.033, 0.030, 0.028 eV, respectively.

^dThe energy at the minimum is 0.024 eV lower than the energy at the tetrahedral undistorted geometry.

Si_4H_9 DANGLING BOND ORBITALS

a) NEUTRAL



b) NEGATIVE ION, 1st N.O.

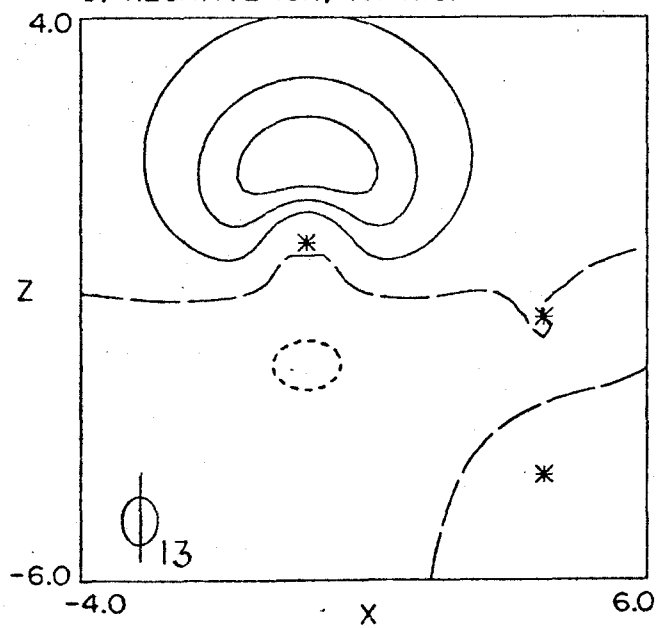


Fig. 4. Dangling Bond Orbitals for the Neutral and Negative Ion for the Si_4H_9 Cluster. (a) Dangling Bond Orbital for the Neutral Complex. (b) Dominant Natural Orbital for the Dangling-Bond Electron Pair of the Negative Ion.

ionization potential is 5.78 eV which is to be compared with experimental values¹⁰ of 5.6 eV to 5.9 eV. Allowing the ion to relax to its new equilibrium position leads to an energy decrease of 0.34 eV giving an adiabatic ionization potential of 5.44 eV.

For the negative ion we find that the surface atom moves away from the surface by 0.25\AA (from the location of the optimum neutral surface), leading to a new Si-Si bond length of 2.41\AA . The adiabatic electronic affinity is 3.06 eV.

Discussion

The relaxation distance of 0.08\AA reported above was obtained by optimizing the total energy of the system. This is, to our knowledge, the first time this has been done for a silicon surface. In the past, a formula due to Pauling¹¹ relating bond order to bond length was used to estimate relaxation distances.³⁴⁻⁴⁰ This leads to a relaxation distance that is 4 times as large as our calculated value.

Recently Shih et al.¹² have used LEED to analyze an impurity stabilized Si(111) 1×1 structure. They find excellent agreement between the observed and calculated spectra when the first layer relaxes 0.12\AA toward the bulk (15% of the interlayer spacing). This is in very good agreement with our results.

In the above calculations the initial (undistorted) geometry was based on the experimental geometry of the solid⁴ ($R_{\text{Si-Si}} = 2.35\text{\AA}$). As shown in Chapter 1, the results on $\text{H}_3\text{Si-SiH}_3$ demonstrate that similar calculations overestimate the Si-Si bond length by 0.02\AA . Assuming such an overestimate for $\text{Si-(SiH}_3)_3$ we would expect the optimum Si-Si

bond at the surface to be at 2.31\AA leading to a relaxation of 0.13\AA rather than 0.08\AA . On the other hand, in our relaxation calculations we allowed only the one surface Si to relax. Repeating the calculations and letting the six hydrogen atoms representing other Si surface atoms also relax a proportional amount, produces a calculated Si-Si bond length of 2.34\AA and the surface relaxation changes from 0.08\AA to 0.03\AA . Combining both corrections leads to a corrected Si-Si bond length of 2.33\AA and hence a surface relaxation of 0.08\AA , that is, the two corrections cancel out.

Size of Complex: Neutral System

To test the convergence of our results with the size of the complex, we also carried out calculations on SiH_3 , certainly an extremely small complex for modelling the surface. The orbital coefficients for the dangling bond orbital for SiH_3 and $\text{Si}-(\text{SiH}_3)_3$ are compared in Table II. Here we see that the dangling bond orbitals are very similar. In addition, the orbital energy (which by Koopmans' theorem is the ionization potential for the case where the other orbitals are not allowed to readjust) for the dangling bond orbital changes only by 0.5% between these two cases.

Our conclusion is that the $\text{Si}-(\text{SiH}_3)_3$ complex provides an excellent model for the dangling bond state and its interactions with the bulk bonds. The remaining question concerning the interaction of surface Si atoms with each other (through their dangling bonds) is addressed in Section C of the present chapter.

Table II. Comparison of Quantities Relative to the Dangling Bond
Orbitals of SiH_3 and Si_4H_9 .^a

	$\text{Si}-(\text{SiH}_3)_3$		SiH_3	
orbital energy (hartrees)	-0.3340		-0.3356	
	s-functions	p_z -functions	s-functions	p_z -functions
coefficients ^b	0.2315	0.5197	0.2585	0.5313
	0.0992	0.5558	0.1239	0.5263

^aAt the undistorted geometry

^bThese are the expansion coefficients for the appropriate basis functions on the "surface" Si atom.

Size of the System: Ion Systems

For the neutral surface state, the effects of the bulk bonds on the surface orbital are basically related to the overlap of the localized bond pairs with the localized dangling bond orbital. Hence the effects should decrease exponentially with the distance and satisfactory results are expected with a small complex. On the other hand for states with a net charge at the surface long range effects are expected. Thus, upon ionizing the electron from the dangling bond orbital, the resulting positive charge leads to effects that fall off as r^{-1} . In the semi-infinite system this results in polarizations extending over a large region of the crystal surrounding the surface charge. For example, in Table III we see that although the Koopmans' ionization potential is nearly the same, 9.13 eV and 9.09 eV, for SiH_3 and $\text{Si}-(\text{SiH}_3)_3$ respectively, the self-consistent calculations yield smaller and much different values, 8.47 eV and 7.81 eV, respectively. These differences are due to polarization of the bonds in the complex in response to the positive charge at the surface. Our estimate is that it would require a complex having a radius of $\sim 65\text{\AA}$ to treat correctly all polarization effects to within 0.1 eV ($\sim 20\text{\AA}$ for 0.3 eV). Such large size complexes are not currently practicable, and we have instead developed an approximate procedure as explained in the following subsection.

The Dielectric Continuum Correction

Consider a semi-infinite solid with dielectric constant ϵ , and a positive charge at a height h above the surface as in part a of the

Table III. Comparison of Ionization Potentials for SiH_3 and Si_4H_9 .^a All energies are in eV.

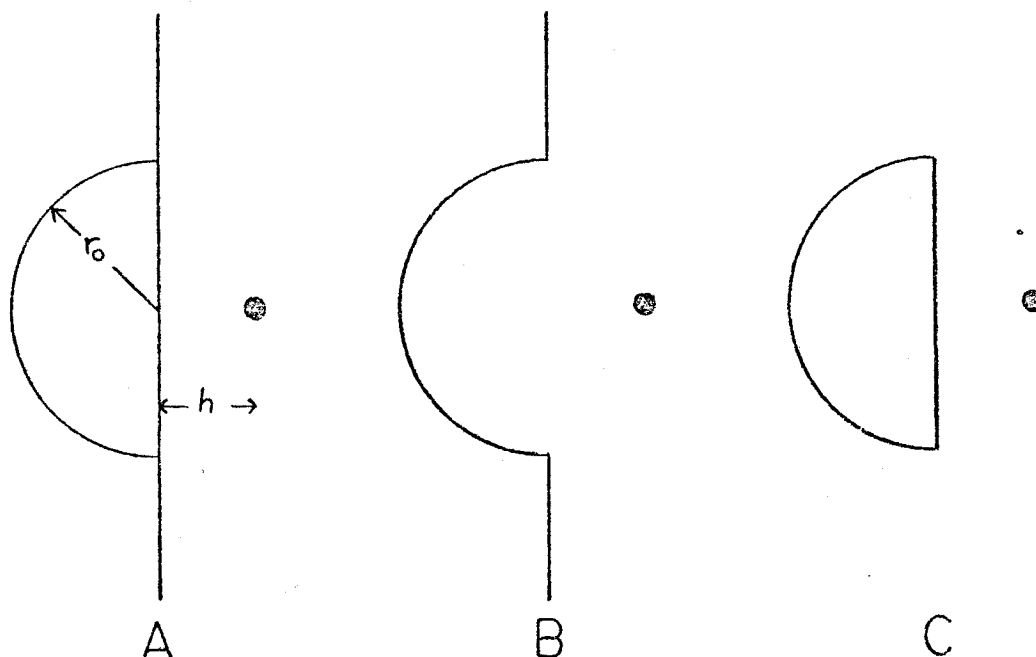
	SiH_3	$\text{Si}-(\text{SiH}_3)_3$
Koopmans' theorem ^b	9.13	9.09
Self-consistent ionization potential ^c	8.47	7.81

^aAt the undistorted geometry

^bObtained from the orbital energy of the appropriate dangling bond orbital

^cObtained by taking the difference between the energies of the positive ion and the ground state self-consistent calculations

diagram below.



The total interaction energy of the charge with the surface is

$$\Delta E = -\frac{1}{4} \left(\frac{\epsilon - 1}{\epsilon + 1} \right) \frac{1}{h}$$

resulting from the polarization induced on the dielectric medium.

Considering our finite complex as a hemisphere of radius r_0 , as in part c of the diagram above, we include the polarizations within this hemisphere but ignore the polarization effects in the balance of the semi-infinite system (part b in the diagram). We have estimated this additional correction as follows. From the wavefunctions of the $\text{Si}-(\text{SiH}_3)_3$ complex we evaluated the average position h of the dangling bond orbital from the surface,^{13a} obtaining $h = 0.805 \text{ \AA}$. Using this value of h , the self-consistent energies for the Si_4H_9 complex were corrected using the polarization energy of the semi-infinite slab minus the hemisphere of radius r_0 , due to a positive charge at h (part b of

the diagram above). This correction energy is^{13b}

$$\Delta E = -\frac{1}{4} \left(\frac{\epsilon - 1}{\epsilon + 1} \right) \frac{1}{h} \left\{ \frac{h}{r_0 + h} - \log \left[\frac{(r_0^2 + h^2)^{1/2}}{r_0 + h} \right] \right\} ,$$

which for the undisturbed complex becomes

$$\Delta E = -1.87 \text{ eV} .$$

Similar corrections were made for each position of the surface Si leading to the results in Tables I and IV.

An ambiguity in our model is the value to use for r_0 . Is it the radius to the nearest Si atom ($r_0 = 2.35\text{\AA}$), or to the midpoint of the SiH bonds ($r_0 = 3.09\text{\AA}$), or to the H atoms ($r_0 = 3.83\text{\AA}$)? (The numbers used in parentheses are for the undisturbed complex.) Since the Si-H bond is much less polarizable than the Si-Si bond, the value of r_0 should be smaller than the value to the midpoint of the Si-H bond but not smaller than the Si-Si bond length. In our calculations we took r_0 to be the distance to the nearest Si atom ($r_0 = 2.35\text{\AA}$ for the undisturbed geometry). Changing r_0 by $\pm 0.1\text{\AA}$ leads to a change of 0.1 eV in the correction energy. Similarly changing h by $\pm 0.3\text{\AA}$ changes the correction energy by 0.3 eV. Thus we estimate that our corrections are probably good to ± 0.4 eV.

The procedure is approximate, of course. One would like to carry out such corrections self-consistently, replacing the charge at h with a charge density spread over the complex.

Table IV. Total Energies for the Relaxation of the Surface Atom in the Si_4H_9 Cluster Model of the Si (111) Surface. All energies are in hartrees.

Distortion ^a (bohr)	$R_{\text{Si-Si}}$ (Å)	Neutral ^b	Without dielectric corrections		With dielectric corrections	
			Positive ^b Ion	Negative ^c Ion	Positive Ion	Negative Ion
0.6	2.476			-20.09123		-20.15749
0.442	2.440			-20.09155 ^d		-20.15851 ^d
0.312	2.412			-		-20.15890 ^d
0.2	2.389	-20.04333	-19.74962	-20.08981	-19.81757	-20.15849
0.0	2.352	-20.04724	-19.76032	-	-19.82899	-
-0.152	2.326	-20.04811	-19.76657	-20.07978	-19.83577	-20.14898
-0.2	2.319	-20.04802	-19.76822		-19.83757	
-0.4	2.290	-20.04591	-19.77335		-19.84333	
-0.6	2.266	-20.04129	-19.77574		-19.84619	
-0.683	2.257		-19.77596 ^d		-19.84659 ^d	
-0.718	2.254		-		-19.84663 ^d	
-0.8	2.246		-19.77553		-19.84642	
Optimum dis- tortion(bohr)		-0.152	-0.683	0.442	- 0.718	0.312

FOOTNOTES FOR TABLE IV

^aDistance along the [111] direction. Zero corresponds to the unrelaxed geometry; positive values indicate motion toward the vacuum.

^bHartree-Fock calculations [eqs. (1) and (2)] using DZ basis of Table XI of Chapter 1 (p. 31).

^cGeneralized Valence Bond calculations [eq. (3)] using the DZR basis of Table XI of Chapter 1. From G. T. Surratt, Ph.D. Thesis, California Institute of Technology, 1975, Table VI.4.

^dInterpolated energy from a cubic splines fit.

C. Interaction of the Surface Dangling Bonds

General Description

In order to study the interaction between adjacent dangling bond orbitals on the unrelaxed-unreconstructed surface, we used the Si_3H_6 cluster illustrated in Fig. 5, the smallest complex suitable for this study. It consists of three silicon atoms, two of which are on the surface, and the third is bonded to both surface Si atoms. The six hydrogen atoms replace the bulk Si-Si bonds broken in cutting the complex from the semi-infinite solid.

Self-consistent solutions of the wavefunctions of this complex lead to a ground state possessing a singly occupied dangling bond orbital on the end of the two surface Si atoms. These two orbitals will be denoted as ϕ_ℓ and ϕ_r . Coupling these orbitals together leads to both a singlet state and a triplet state. Treating all Si-H and Si-Si bond pairs as doubly-occupied (as in the Hartree-Fock description) but allowing the dangling bond orbitals, ϕ_ℓ and ϕ_r , to each be singly-occupied, leads to the two wavefunctions (for valence electrons only)

$${}^1A'(\ell r) \equiv \Phi^{\text{singlet}} = a\{\phi_{\text{bulk}}[\phi_\ell(1)\phi_r(2) + \phi_r(1)\phi_\ell(2)] \\ \times [\alpha(1)\beta(2) - \beta(1)\alpha(2)]\} , \quad (4)$$

and

$${}^3A''(\ell r) \equiv \Phi^{\text{triplet}} = a\{\phi_{\text{bulk}}[\phi_\ell(1)\phi_r(2) - \phi_r(1)\phi_\ell(2)] \\ \times [\alpha(1)\beta(2) + \beta(1)\alpha(2)]\} , \quad (5)$$

where

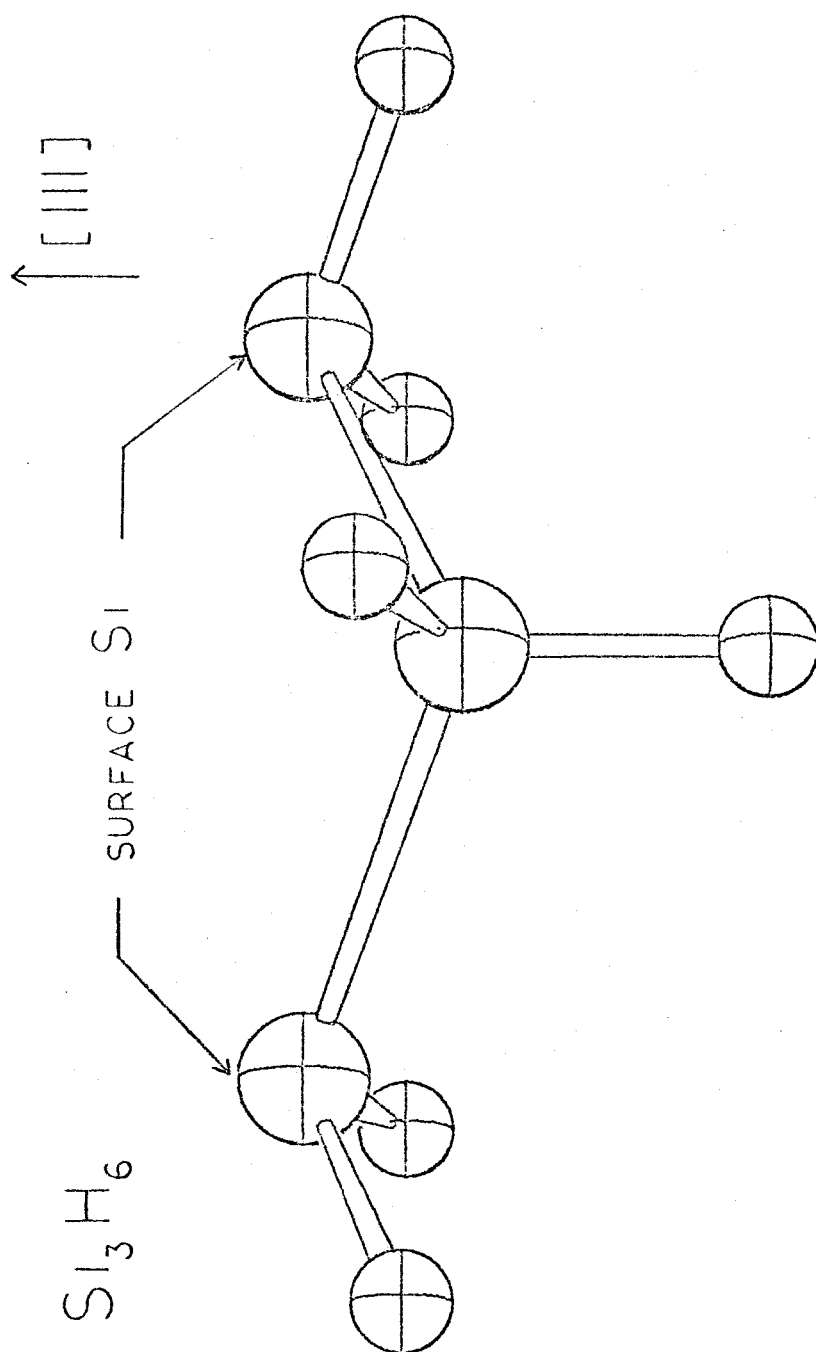


Fig. 5. Geometrical Configuration for the Si_3H_6 Cluster Modeling the (111) Surface. Silicons are represented by large spheres, hydrogens by small spheres.

$$\Phi_{\text{bulk}} = [\phi_1(3)\alpha(3)][\phi_1(4)\beta(4)]\cdots[\phi_8(17)\alpha(17)][\phi_8(18)\beta(18)] \quad (6)$$

contains all bond pairs. Solving for these wavefunctions self-consistently leads to the results in Table V. Here we see that the triplet state is consistently 0.01 eV below the singlet. Although both states were solved self-consistently, the orbitals of wavefunctions (4) and (5) are nearly identical so that use of the Φ^{singlet} orbitals in the Φ^{triplet} wavefunction increases the energy by only 0.002 eV. The dangling bond orbitals of (4) are shown in Fig. 6.

Using the same orbitals for both states the energies of (4) and (5) can be written as¹⁴

$$E^{\text{singlet}} = \frac{E_0 + E_x}{1 + S^2},$$

$$E^{\text{triplet}} = \frac{E_0 - E_x}{1 - S^2},$$

where S is the overlap, $\langle\phi_\ell|\phi_r\rangle$ of the two orbitals,¹⁵

$$E_0 = \langle\phi_\ell|h|\phi_\ell\rangle + \langle\phi_r|h|\phi_r\rangle + J_{\ell r}$$

is the energy of the product wavefunction, $\phi_\ell\phi_r$, and¹⁵

$$E_x = 2S\langle\phi_\ell|h|\phi_r\rangle + K_{\ell r}$$

is the exchange term. Here $J_{\ell r}$ and $K_{\ell r}$ are the usual two-electron Coulomb and exchange interactions.

In the case that $S = 0$, we see that $E_x = K_{\ell r} \geq 0$, and hence that the triplet state is the ground state (just as in Hund's rule). The

Table V. Quantities Related to the Interaction of Adjacent Dangling Bonds in the Si_3H_6 Cluster Model of the Si(111) Surface. All energies are in eV.

State ^a	Unrelaxed			Relaxed ^b
	MBS ^c	MXS1 ^c	DZ ^c	DZ
$^3A''(\ell r)$	0.0 ^d	0.0 ^d	0.0 ^d	0.0 ^d
$^1A'(\ell r)$	0.009	0.014	0.013	0.015
Overlap ^e	0.004	0.006	0.013	0.006

^aThe states are defined by the local symmetry, C_s , of the Si_3H_6 complex, see (4) and (5) for the wavefunctions.

^bThe relaxation distance of the surface Si atoms was 0.08\AA . The "surface" hydrogens were relaxed as if the Si-H bonds were Si-Si bonds.

^cThe basis sets are defined in Table XI of Chapter 1; DZ is the most flexible.

^dTotal energies calculated were -14.12125, -14.47428, -14.54304 and -14.54255 hartrees, respectively.

^eOverlap of the two dangling bond orbitals, ϕ_ℓ and ϕ_r , from the $^1A'(\ell r)$ GVB calculation.

Si_3H_6 $^1\text{A}'$ ORBITALS

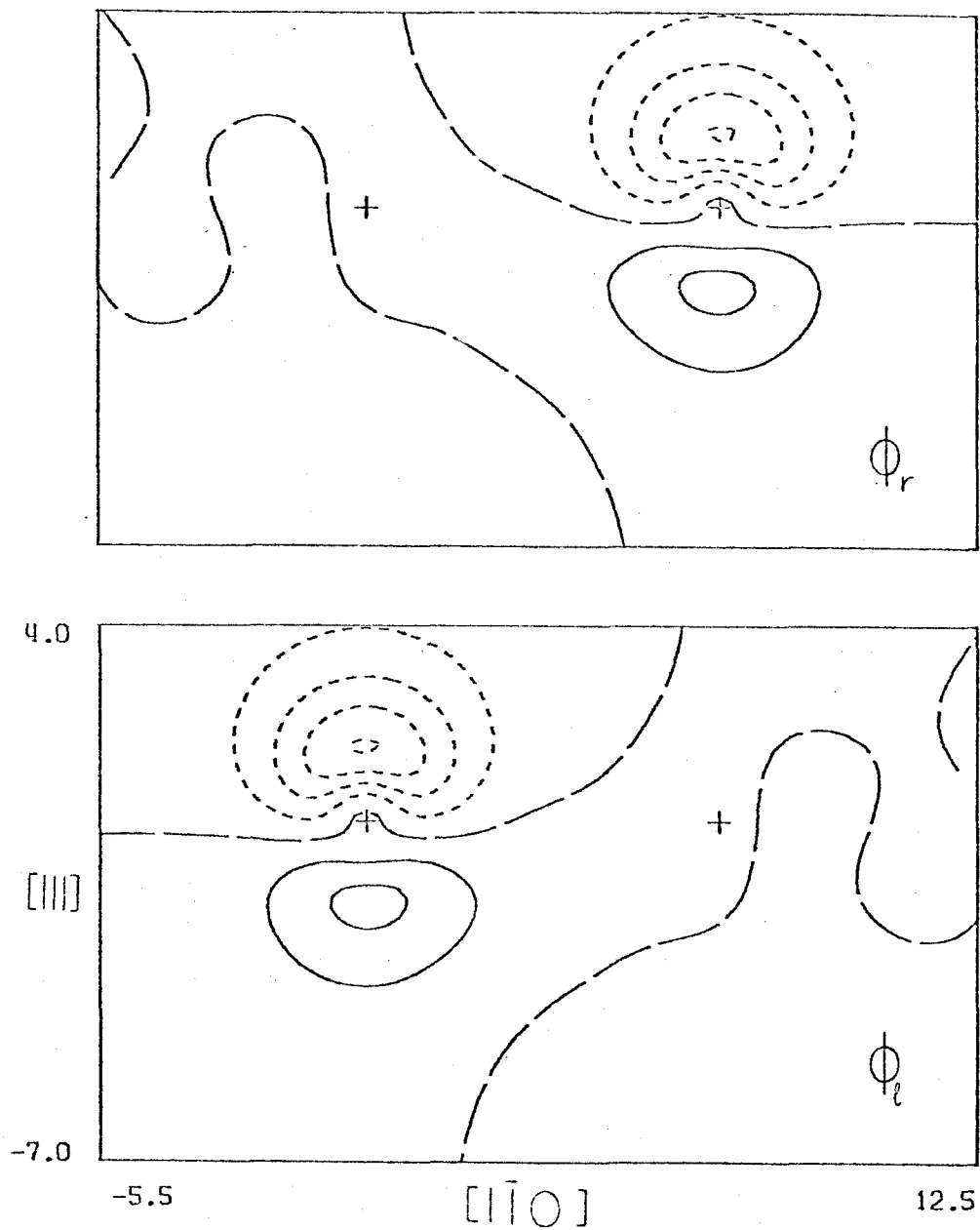


Fig. 6. Dangling Bond Orbitals for the $^1\text{A}'(\ell r)$ GVB(1) Calculation of Si_3H_6 . Positive amplitudes are denoted by solid lines, negative amplitudes by short dashes. Long dashes indicate nodal planes. Amplitude contours are drawn every 0.05 atomic units.

one-electron term in E_x is negative and, for larger S (e.g., $S > 0.1$), this term dominates over K_{lr} , leading to $E_x \leq 0$ and hence a singlet ground state.

Thus, depending upon the sign of E_x and the relative magnitude of E_x and kT (thermal energy) the surface could be diamagnetic, paramagnetic or ferromagnetic.

Computational Details

Initially we chose the Si_3H_6 complex to have a tetrahedral geometry, as in an unrelaxed-unreconstructed (111) Si surface. A second calculation was performed at the relaxed geometry, obtained from the calculations reported in Section B. [The surface silicons were relaxed by 0.08\AA towards the bulk along the [111] direction, keeping the other silicon fixed and rotating the Si-H bonds as if they were Si-Si bonds with the (virtual) second layer silicons fixed.]

In order to study the effect of basis sets on the wavefunctions, we carried out similar calculations using three different basis sets: MBS (Minimum Basis Sets, one basis function per atomic orbital), MXS1 (Mixed Set) and DZ (Double Zeta, two basis functions per atomic orbital), as described in Table XI, Chapter 1 (p. 31). The MXS1 deviates from the MBS only by the presence of an extra p_z basis function on each surface center.

Excited States

The states (4) and (5) are referred to as covalent states since each atom is bonded as expected from its neutral atomic configuration. Other excited states of this cluster are as follows:

(i) Neutral ionic states: Keeping two electrons distributed over the two dangling bond orbitals, we can construct two states in addition to (4) and (5), namely

$$^1A''(\ell^2-r^2) \equiv a\{\phi_{\text{bulk}}[\phi_{\ell}(1)\phi_{\ell}(2) - \phi_r(1)\phi_r(2)][\alpha(1)\beta(2)]\}, \quad (7)$$

$$^1A'(\ell^2+r^2) \equiv a\{\phi_{\text{bulk}}[\phi_{\ell}(1)\phi_{\ell}(2) + \phi_r(1)\phi_r(2) - \lambda(\phi_{\ell}(1)\phi_r(2) + \phi_r(1)\phi_{\ell}(2))][\alpha(1)\beta(2)]\}. \quad (8)$$

These states correspond to the ionic or charge transfer states in which an electron is moved from one dangling bond orbital to the other, leading to a positive ion on one surface Si and a negative ion on the other. For the actual calculation it is computationally more expedient to recombine these states to yield symmetry functions (with respect to the local symmetry of the cluster, in this case C_s).

The $^1A''(\ell^2-r^2)$ state is straightforward to obtain from a self-consistent calculation; however, the $^1A'(\ell^2+r^2)$ state is more complex (due to a lower state of the same symmetry; note the orthogonalization parameter λ). Both states were studied with CI calculations, as described below.

A simple estimate for such charge transfer excitation energies is

$$\Delta E = IP - EA - \frac{1}{R}$$

where R is the separation distance of the centers; IP is the ionization potential and EA is the electron affinity. Using the values of Table I

for the Si_4H_9 complex, and assuming no geometrical relaxation, this leads to

$$\begin{aligned} E &= 7.66 \text{ eV} - (-0.86 \text{ eV}) - \left(\frac{1}{7.25a_0}\right)(27.21 \text{ eV/hartree}) \\ &= 4.77 \text{ eV} \end{aligned}$$

which is in very good agreement with the value of 4.82 eV obtained from self-consistent calculations (Table VI).

Such states may be significantly stabilized by polarization effects around each charge center and hence the use of a finite complex may lead to an excessively large excitation energy.

(ii) Band to surface states: Since the dangling bond orbitals are only partially occupied, one expects low-lying transitions in which an electron is excited out of a "bulk" orbital, say ϕ_b , into a dangling bond orbital (ϕ_ℓ or ϕ_r). The simplest description of such states is

$$^3(b \rightarrow s) = a[\Phi'_{\text{bulk}}(\phi_\ell \phi_\ell \phi_r \phi_b \pm \phi_r \phi_r \phi_\ell \phi_b)_{\alpha\beta\alpha\alpha}] \quad , \quad (9)$$

and

$$^1(b \rightarrow s) = a[\Phi'_{\text{bulk}}(\phi_\ell \phi_\ell \phi_r \phi_b \pm \phi_r \phi_r \phi_\ell \phi_b)_{\alpha\beta\alpha\beta}] \quad ; \quad (10)$$

[here Φ'_{bulk} denotes the wavefunction corresponding to (6) but with the ϕ_b terms deleted], leading to A' and A'' symmetries for both spins. Although certain of these states can be solved self-consistently, a consistent level of description of all states requires a configuration interaction wavefunction.

Of course, the use of a finite cluster with an abbreviated description of the bulk states should have a great effect in the excitation energies as compared with the semi-infinite system.

(iii) Surface to bulk states: Other transitions involving the surface orbitals consist of excitations into the empty bulk states. Such transitions should require a more complete basis (diffuse s- and p-functions in addition to d-functions) as well as a large complex. Typical excitations have the form

$$^3(s \rightarrow b^*) = a[\phi_{\text{bulk}}(\phi_l \pm \phi_r)\phi_{b^* \alpha \alpha}] \quad (11)$$

and

$$^1(s \rightarrow b^*) = a[\phi_{\text{bulk}}(\phi_l \pm \phi_r)\phi_{b^*}(\alpha\beta - \beta\alpha)] \quad , \quad (12)$$

leading to A' and A'' symmetries for both spins.

Configuration Interaction Studies

In order to explore the effects of electronic correlation in the bulk orbitals upon the covalent states and to obtain a consistent description of the other excited states, we carried out configuration interaction calculations as follows.

Starting out with the self-consistent wavefunction for the $^3A''$ ground state and using the MXS1 basis we allowed all double excitations within the space spanned by the four orbitals describing the dangling bond region (for the $^3A''$ state two of them are occupied and two unoccupied) simultaneous with all single excitations out of the "bulk" orbitals (denoted as CI). CI should lead to a good description of

the covalent and neutral ionic states and to a fairly good description of the $b \rightarrow s$ and $s \rightarrow b^*$ transitions (within the restrictions of our basis).

Hartree-Fock Wavefunctions

Combining the ϕ_ℓ and ϕ_r orbitals as

$$\phi_g = (\phi_\ell + \phi_r) / \sqrt{2(1+S)}$$

$$\phi_u = (\phi_\ell - \phi_r) / \sqrt{2(1-S)}$$

leads to two orthogonal orbitals which are symmetry functions for this particular complex. Since

$$\phi_u \phi_g - \phi_g \phi_u = (\phi_\ell \phi_r - \phi_r \phi_\ell) / \sqrt{1-S^2}$$

we see that wavefunction (5) can be equally well written in the Hartree-Fock form,

$$\Phi^{\text{triplet}} = \mathcal{A} \{ \Phi_{\text{bulk}} [\phi_u(1)\phi_g(2) - \phi_g(1)\phi_u(2)] [\alpha(1)\beta(2) + \beta(1)\alpha(2)] \} . \quad (5')$$

On the other hand,

$$\phi_\ell \phi_r + \phi_r \phi_\ell = c_1 \phi_g \phi_g - c_2 \phi_u \phi_u$$

where $c_1 \approx c_2$ for $S \sim 0$. Thus the GVB wavefunction for the singlet cannot be expressed as a simple molecular orbital (MO) wavefunction.

Indeed, the best closed-shell MO calculation

$$\Phi(g^2) = \mathcal{A} \{ \Phi_{\text{bulk}} [\phi_g(1)\phi_g(2)\alpha(1)\beta(2)] \}$$

leads to energies¹⁶ ~ 3 eV above the GVB wavefunction (4). Thus, the

HF wavefunction does particularly poorly for singlet coupled orbitals having a small overlap. Since most band structure techniques are based on the closed-shell HF formalism we expect such approaches to yield erroneous results for such surface states despite the use of a large complex or a semi-infinite system.

Since

$$\phi_g \phi_u + \phi_u \phi_g = (\phi_\ell \phi_\ell - \phi_r \phi_r) / \sqrt{1-S^2}$$

Hartree-Fock calculations on the $^1A''(\ell^2-r^2)$ state should be quite adequate, however, the $^1A'(\ell^2+r^2)$ state cannot be well described. Some of the $b \rightarrow s$ and $s \rightarrow b^*$ transitions can also be adequately described with a HF wavefunction.

Results

(i) Covalent states - In Table V we show some of the quantities relating to the two covalent states for the Si_3H_6 cluster model of Si (111) surfaces. For both the unrelaxed and relaxed calculations the overlap $S = \langle \phi_\ell | \phi_r \rangle$ is very small ($S \approx 0.01$). This means that there is only a relatively small amount of interaction between adjacent dangling bonds. This leads to a 0.01 eV splitting between the triplet ground state and the singlet state.

Including the surface atoms of the whole surface these results suggest the use of a Heisenberg Hamiltonian

$$H = E_0 - \sum_{i,j} J_{ij} \hat{S}_i \cdot \hat{S}_j$$

with an exchange term between adjacent surface atoms of

$$J_{ij} = 0.01 \text{ eV}$$

For kT (thermal energy) large compared to J_{ij} , the surface dangling bonds would act as individual paramagnets, but for kT small compared with J_{ij} we could expect cooperative magnetic behavior. The calculated J_{ij} would seem to indicate a ferromagnetic surface for $kT \ll 0.01 \text{ eV}$. However, slight displacements of the surface atoms can cause energy effects much larger than 0.01 eV and indeed could stabilize singlet pairing of adjacent dangling bonds. Because of the Pauli principle, distortions leading to stabilization of singlet pairing would be expected to produce a lowering of the surface symmetry to at least a 2×1 unit cell (since the singlet paired orbitals would not be translationally equivalent).

(ii) Excited states - Table VI shows self-consistent field results for some of the excited states discussed above. We also compare the effect of the basis set on the energies. The ionization potential of 8.63 eV is about 3 eV higher than the experimental value.¹⁰ This discrepancy is due mainly to polarization of the solid, as discussed in Section B. The wavefunctions for the positive ion states have the form

$$^2A'(s \rightarrow \text{vacuum}) = \mathcal{A}[\Phi_{\text{bulk}}(\phi_{\ell} + \phi_r)\alpha] \quad ,$$

and

$$^4A'(b \rightarrow \text{vacuum}) = \mathcal{A}[\Phi'_{\text{bulk}}(\phi_{\ell}\phi_r - \phi_{\ell}\phi_r)\phi_b\alpha\alpha\alpha] \quad ,$$

where Φ'_{bulk} is similar to (6) but with the ϕ_b terms omitted. $^2A'(s \rightarrow \text{vacuum})$ represents an ionization out of one of the dangling bond orbitals while $^4A'(b \rightarrow \text{vacuum})$ is the wavefunction for an ionization from one of the bulk orbitals.

Table VI . Comparison of Calculations for the Si_3H_6 Cluster Model of (111) Si surfaces using the MBS, MXSI and DZ Basis Sets.^a All energies are in eV.

State	DZ Basis Set	MXSI Basis Set	MBS Basis Set
$^3\text{A}''(\ell\text{r})$	0.0 ^b	0.0 ^b	0.0 ^b
$^1\text{A}'(\ell\text{r})$	0.013	0.014	0.009
$^1\text{A}''(\ell^2-\text{r}^2)$	4.816	5.064	6.793
$^3\text{A}'(\text{b} \rightarrow \text{s})$	4.856	4.824	6.415
$^3\text{A}'(\text{s} \rightarrow \text{b}^*)$	7.252	11.172	10.871
$^2\text{A}'(\text{s} \rightarrow \text{vacuum})$	8.630	8.440	7.830
$^4\text{A}'(\text{b} \rightarrow \text{vacuum})$	9.496	9.236	8.711

^aThe unrelaxed geometry was used.

^bTotal energies calculated were -14.54304, -14.47428, and -14.12125 hartree, respectively.

It is interesting to note that for the DZ basis the $^1A''(\ell^2-r^2)$ state is lower in energy than the $^3A'(b \rightarrow s)$ state. For the MSX1 basis the $^3A'(b \rightarrow s)$ state is relatively well described because the surface part of the basis has the same flexibility as the DZ set (for the p_z -functions). On the other hand, MSX1 is the same as the MBS set for the "bulk" part of the complex. This is reflected in a poor description of the ℓ^2-r^2 state, where the ϕ_g and ϕ_u orbitals are more delocalized over this region.

The results of the CI calculations are illustrated in Table VII. The separation between the singlet and triplet covalent states is still very small (~ 0.02 eV) but the total energy of the ground state is 0.26 eV lower than the corresponding SCF value. The order of the $^1A''(\ell^2-r^2)$ and $^3A'(b \rightarrow s)$ is reversed with respect to the SCF value for the same basis set. The reason for this is that the CI description for the ℓ^2-r^2 state is better than that of the $b \rightarrow s$ state (some configurations important for the $b \rightarrow s$ state are not present in CI).

In Table VIII we compare the CI results of calculations of the positive ion, $Si_3H_6^+$, with Koopmans' theorem values for the ionization potentials. The CI configurations were obtained by doing all single excitations out of a basic set of 10 configurations formed by omitting one electron at a time from each occupied orbital. This latter set of basic configuration was used for the Koopmans' theorem calculation. In Table VIII we also show the values obtained from the orbital energies of the $^3A''(\ell r)$ SCF calculation.

Table VII. Results of CI Calculations for the Si_3H_6 Cluster Model of the Si (111) Surface.^{a,b} All energies are in eV.

State ^c	Energy	No. of Spin Eigenfunctions	No. of Determinants
$^3\text{A}''(\ell r)$	0.0 ^d	824	1036
$^1\text{A}'(\ell r)$	0.019	614	1632
$^1\text{A}''(\ell^2 - r^2)$	4.286	612	-
$^3\text{A}'(b \rightarrow s)$	4.293	814	1018
$^3\text{A}''(b \rightarrow s)$	4.482	824	1036
$^1\text{A}'(\ell^2 + r^2)$	4.561	614	1632
$^1\text{A}''(b' \rightarrow s)$	4.607	612	-
$^1\text{A}'(b \rightarrow s)$	4.629	614	1632
$^3\text{A}''(b' \rightarrow s)$	6.392	824	1036
$^3\text{A}'(b' \rightarrow s)$	6.407	814	1018
$^1\text{A}''(b'' \rightarrow s)$	6.487	612	-
$^1\text{A}'(b' \rightarrow s)$	6.492	614	1632
$^3\text{A}'(b'' \rightarrow s)$	7.407	814	1018

^aThe MXSI basis set was used with a tetrahedral (unrelaxed) geometry.

^bIn the CI calculations double excitations were allowed within the two occupied and two virtual orbitals corresponding to the dangling bond. Simultaneously, all single excitations were allowed from all "bulk" orbitals to all virtual orbitals of the basis.

^cSuccessive primes on the b's indicate different "bulk" orbitals.

^dThe total energy calculated is -14.48445 hartree.

Table VIII. Comparison of CI and Koopmans' Theorem Ionization Potentials for the Si_3H_6 Cluster Model of Si (111) Surfaces.^a All energies are in eV.

CI Ionization Potentials ^b	Koopmans' Theorem from 10 Configuration CI ^c	Koopmans' Theorem from $^3A''(\lambda r)$ SCF	Koopmans' Theorem from Closed Shell HF
$^2A''(g \rightarrow \text{vacuum})$	7.603	8.780	5.966
$^2A'(u \rightarrow \text{vacuum})$	7.774	8.828	5.966
$^4A'(b_u \rightarrow \text{vacuum})$	8.891	10.014	10.462
$^2A'(b_u \rightarrow \text{vacuum})$	9.591	10.014	10.462
$^2A''(b_g \rightarrow \text{vacuum})$	9.838	11.354	11.743
$^4A''(b_g \rightarrow \text{vacuum})$	10.155	11.354	11.743
$^2A''(b'_g \rightarrow \text{vacuum})$	10.822	12.976	13.140
$^2A'(b'_u \rightarrow \text{vacuum})$	11.377	13.038	13.382
$^4A''(b'_g \rightarrow \text{vacuum})$	11.607	12.976	13.140
$^4A'(b'_u \rightarrow \text{vacuum})$	11.840	13.038	13.382
$^4A''(b''_g \rightarrow \text{vacuum})$	12.218	13.488	13.775

^aFor the MXS1 basis set and at the tetrahedral (unrelaxed) geometry.

^bThe wavefunctions consist of 851 to 1882 determinants. The energies are referred to the ground state of the CI calculation of the neutral.

^cReferred to the energy of the $^3A''(\lambda r)$ self-consistent field calculation.

D. Review of Experimental Data

One of the most important experimental characteristics of the (111) surface of silicon single crystals is that it is the cleavage face of the diamond structure.⁶ This has very important consequences on the experimental determination and study of silicon surfaces. Any other surface has to be cut or prepared and annealed⁶ before one can study it. This can modify the ideal environment of the surfaces in ways that are difficult to predict. On the other hand, a freshly cleaved surface corresponds more closely to the idea that one has of what an undisturbed surface is. The cleaving can be performed under conditions of ultra-high vacuum, so that for good cleaves the surface, besides being undisturbed, is not contaminated by other atomic or molecular species.

The basic experimental tool in the structural study of surfaces is Low Energy Electron Diffraction.⁷ It is based on principles similar to those of X-ray diffraction techniques for crystalline solids. In LEED, the probe consists of electrons ejected by a gun at energies ranging from 10 eV to 1000 eV. This means that their de Broglie wavelengths lie between 3.87\AA and 0.39\AA , that is, of the same order of magnitude as the typical interatomic dimensions in a solid. On the other hand, low energy (10 to 500 eV) electrons exhibit inelastic mean free paths^{7b} of 2 to 10\AA , thus the electrons collected by the LEED apparatus come from the first few layers of the surface.

A freshly cleaved silicon (111) surface leads to a structure showing a 2×1 pattern,¹⁷ indicating that the unit cell is twice as

large in one direction (compared to the ideal or 1×1 surface). Upon heating this 2×1 structure changes irreversibly into a 7×7 structure.¹⁷ The transition occurs¹⁸ between 350°C and 390°C (depending on the surface roughness).

Clearly, some sort of rearrangement has occurred for both structures. The temperature behavior indicates that the degree of rearrangement involves greater motion for the 7×7 structure than for the 2×1 structure. Since the 7×7 structure cannot be transformed back into the 2×1 structure, the 7×7 pattern most likely is the more stable one.

Other LEED patterns have been observed in Si (111) surfaces.^{6,17} However, since they are not easily reproduced and since some of them seem to be due to the presence of small amounts of impurities^{17a}, we will ignore these cases.

In the early sixties it was speculated that the low energy tail in the total electron yield vs photon energy in photoemission experiments was due to surface states.¹⁹ This view was supported later by further photoemission experiments.²⁰ More recently, photoemission experiments by Eastman and Grobman^{10a} and by Wagner and Spicer^{10b} have shown the presence of surface states on silicon and germanium (111) surfaces. They used synchrotron radiation with photon energies in the range 7 to 30 eV. The energy distribution curves of the emitted electrons were measured for fixed incident photon energies. The emitted electrons contain contributions from both the bulk solid and the surface. The surface contribution was separated by making a second measurement when the surface was contaminated with oxygen (presumably

removing the surface states by bonding to oxygen atoms or molecules.) The photoemission curves of the oxidized surface would then only have the bulk contribution, together with photoemission from the oxygen-surface complex. By studying the difference spectra between the clean and contaminated surfaces, one can observe peaks assumed to be produced by the surface states. Eastman and Grobman^{10a} find, for silicon (111) surfaces, a band of states centered at 0.75 eV below the Fermi energy, or 0.43 eV below the valence band edge. Wagner and Spicer^{10b} obtained similar results, with a peak at 1.1 eV and a shoulder at 0.5 eV below the Fermi level. From these measurements and from the known width of the valence band, and assuming that the matrix elements for surface and bulk transitions are the same, it was concluded^{10b} that the surface state density is 8×10^{14} electrons-cm⁻². Assuming one electron per each surface silicon atom leads to a surface state density of 7.85×10^{14} electrons-cm⁻². Since there is a band bending of 0.6 eV, Poisson's equation requires^{10b} 0.3×10^{14} surface states per cm², leading to a total of 8.1×10^{14} occupied surface states per cm², in good agreement with the photoemission estimate. Additional photoemission experiments by Rowe^{21a} and Rowe and Ibach^{21b} also lend support to the idea of characteristic surface states.

Other experimental techniques have also successfully identified the presence of surface states on silicon (111) surfaces. An example is shown by the field emission experiments of Lewis and Fischer.²² Their results are in qualitative agreement with the photoemission measurements discussed above. Hagstrum and Becker²³ have also reported

ion-neutralization spectroscopy experiments in which the presence of surface states is made evident.

It is now possible to detect transitions between surface states. One of the methods used in this context is total internal optical reflection spectroscopy. Chiarotti et al.²⁴ have measured a transition peaked at 0.5 eV, which occurs in 2×1 structures of Si(111) surfaces but disappears when the surface is exposed to oxygen or when heated to obtain the 7×7 structure.²⁴ Another way of detecting surface state transitions is by photoconductance measurements; Müller and Mönch²⁵ have shown that a surface sensitive shoulder appears in the bulk photoconductance curves for cleaved Si(111) surfaces. The shoulder disappears when the surface is exposed to oxygen. Further experimental evidence for surface state transitions is obtained from ellipsometry experiments²⁶ and energy-loss experiments.²⁷

We now return to a more detailed analysis of the LEED patterns for (111) Si surfaces and their interpretations in terms of theoretical models. Two basic patterns are found: a 2×1 and a 7×7 . We will consider the 2×1 pattern first. This structure is found when cleaving silicon single crystals at room temperature under ultra-high vacuum¹⁷. It is believed⁶ that the rearrangement suffered by the surface does not involve large migrations of surface atoms. This is confirmed by mating experiments⁶ in which two surfaces are created by brittle cracking in ultra-high vacuum. They are then replaced on top of each other, thereby healing the crack. The experiment is only applicable to materials that show no plastic flow at the temperature at which the

experiment is performed. This applies to silicon at room temperature under mild fracture stress. Evidence has been obtained⁶ that almost perfect atom-on-atom replacement occurs when the two surfaces are mechanically fused together. One of the important aspects of this experiment is that the two surfaces are not allowed to fully separate; this insures that precise replacement is possible. Large atomic rearrangements are practically ruled out by this experiment, suggesting that the 2×1 structure is originated by small displacements of the surface atoms (possibly more than one layer) about the positions that they occupied on the solid. (Note that LEED cannot be used in this technique to determine what pattern is present in the crack; the assumption is that the 2×1 pattern is present since the experiment is performed in ultra-high vacuum and at room temperature.) Unfortunately, these experiments cannot be performed at high temperatures (to observe the transition to the 7×7 pattern) because the necessary electrical contacts to the Si crystal are lost upon heating.

Haneman²⁸ has proposed a model to account for the observed 2×1 structure on Si (111) cleaved surfaces. This widely discussed model assumes that the surface undergoes buckling, so that alternate rows of surface atoms are raised and lowered, producing the observed LEED pattern. The mechanism for the buckling is based on the following.^{6,28} The lowered rows have dangling bonds with sp^2 hybridization (tending to produce a planar configuration, hence the lowering of the row), while the raised rows have pure s character for the dangling bonds (producing 90° angles for the bonds to the second layer, thereby raising the atoms). This model was designed to explain the

salient experimental features known at the time; namely, the 2×1 structure observed in LEED experiments and the Electron Paramagnetic Resonance (EPR) experiments by Haneman and coworkers²⁹ in which a spin density of 0.8 to 2×10^{14} spins per cm^2 was found (that is, roughly one spin per four to ten surface atoms). It is now known that single crystal (111) surfaces of silicon have no detectable EPR signal³⁰ that can be ascribed to a surface spin density.

Our calculations on the Si_3H_6 cluster (see Section C) indicate that the coupling between adjacent dangling bond orbitals is too small to produce the distortions proposed by Haneman.²⁸ Of course, slight motions might account for such reconstruction, but it is our opinion that the mechanism proposed by Haneman²⁸ and Haneman and Heron³¹ is not entirely correct (i.e., we do not find the hybridization schemes proposed in Ref. 31). It is possible that charge transfer states might account for such a reconstruction. This is suggested by our calculations on Si_4H_9 clusters (see Table I), where we found that the positive ion state relaxes inward (toward the bulk) whereas the negative ion state relaxes outward (toward the vacuum). Further calculations, using larger clusters, to test this model are warranted.

When a cleaved (111) surface of silicon is heated to at least 400°C , the 7×7 LEED pattern appears. All the fractional order spots are present in this pattern, indicating that the basic structure of the surface has a truly 7×7 unit cell and it is not the result of a smaller unit cell with an overall 7×7 pattern. Also, since the formation of such patterns requires high temperatures, it is believed⁶ that there is considerable motion of the atoms on the surface. A model for this

structure has been proposed by Lander and Morrison,³² based on a series of vacancies of the surface atoms so that benzene-type rings are formed, presumably stabilizing the surface structure. Up to the present no strong evidence has been found to favor this proposed structure. Our studies of Si-Si bonds indicate that the π bond is very weak, suggesting that benzene-like structures are not particularly favored.

E. Review of Other Theoretical Calculations

Theoretical calculations of surface states have been performed since the early work of Tamm^{33a} and Shockley^{33b} in the thirties. One can partition the techniques into those utilizing finite clusters and those utilizing semi-infinite systems.

Cluster calculations on silicon surfaces have been performed by Batra and Ciraci.³⁴ They used the $X\alpha$ method,³⁵ which uses a molecular orbital (doubly-occupied orbital) wavefunction. Their results seem to be in general accordance with those obtained using semi-infinite systems. They find a dangling bond orbital with a high degree of p_z character whose orbital energy is in the neighborhood of 7 to 8 eV.

Most of the theoretical calculations in the literature use a semi-infinite solid. These calculations can be divided into two classes: (i) calculations utilizing an effective hamiltonian (non-self-consistent); and (ii) calculations involving some sort of self-consistent procedure. Non-self-consistent calculations have used the tight-binding formalism,³⁶ the bond orbital method³⁷ or pseudo-potential methods.³⁸ The self-consistent calculations use self-consistent

pseudo-potentials and a local approximation to the exchange energy.^{39,40} Basically, the same conclusions are reached by both Appelbaum and Hamann³⁹ and Schlüter et al.⁴⁰

The method of Appelbaum and Hamann^{39a} assumes a potential of the form

$$V_T(\vec{r}) = V_{es}(\vec{r}) + V_{xc}(\vec{r}) + V_{ion}(\vec{r}) ,$$

where V_{es} and V_{xc} are the electrostatic (found by solving Poisson's equation) and exchange potentials. $V_{xc}(\vec{r})$ is a local approximation to the exchange energy which uses the Wigner interpolation form⁴¹ for the correlation energy of the jellium model. $V_{ion}(\vec{r})$ represents the non-electrostatic electron-ion core interactions and was obtained⁴² by fitting to bulk band structure calculations. The potential $V_T(r)$ is then introduced into the one-electron Schrödinger equation

$$-\frac{1}{2} \nabla^2 \psi(\vec{r}) + V_T(\vec{r}) \psi(\vec{r}) = E \psi(\vec{r}) . \quad (11)$$

Equation (11) is then expanded in the Laue representation⁴³ which assumes two-dimensional periodicity parallel to the surface. This results in a one-dimensional set of coupled differential equations that have to be solved numerically.^{39a}

Appelbaum and Hamann³⁹ find an ionization potential of 5.3 eV for the ideal (111) surface, which is insensitive to small normal displacements. For all geometries a dangling bond state is found which is highly localized on the surface atoms. This band is partially occupied, lying close to the top of the valence band. When relaxation

is allowed this band splits into two peaks and additional bands appear.

Schluter et al.⁴⁰ used a standard solid band structure calculation technique with a slab geometry which is repeated in a direction normal to the slab. They find an ionization potential of ~ 4.0 eV. They find a surface band structure near the top of the valence band which is similar to that found in Ref. 39.

One characteristic common to all these methods is that for geometry variations all these methods use a priori chosen values of the relaxation distances. The reason for this is that the techniques cannot be used to calculate total energies, and therefore cannot optimize geometries. One of the methods used to estimate relaxation distances³⁷⁻⁴⁰ uses a formula due to Pauling¹¹ in which bond lengths are related to bond order. In the case of the unreconstructed Si (111) surface this predicts a relaxation of 0.34\AA . This is four times as large as the value we have calculated using the $\text{Si}-(\text{SiH}_3)_3$ cluster (see Table I) and about three times as large as the experimental value of Shih et al.¹² For this reason, since the electronic structures calculated using these techniques are highly dependent on what relaxation distances are used,^{37,39,40} a careful comparison between experiment and theoretical calculations for different geometries would clarify the situation.

The techniques discussed in this section use doubly occupied orbitals (i.e., explicit electronic correlation is not included), leading to systematic errors which can be of great importance in obtaining the correct electronic structure of the systems in consideration.⁴⁴

II. THE (100) SURFACE OF SILICON

A. Introduction

The (100) surface of diamond structure (as of crystalline silicon) presents a completely different geometry from that of the (111) surface. Whereas the surface atoms of the (111) surface form a hexagonal pattern, with nearest (surface) neighbor distances of 3.83\AA , the (100) surface presents a square lattice structure (shown in Fig. 7), also with nearest neighbor distances of 3.83\AA .

In the unreconstructed (111) surface each surface atom is bonded to three second layer nearest neighbors. This leads to one dangling bond electron per surface atom. In the (100) surface each surface atom is bonded to two second layer nearest neighbors (for the ideal unreconstructed surface). This leaves two nonbonding electrons per surface atom.

An important experimental difference between the (100) and the (111) surfaces is the fact that a (100) surface cannot be cleaved. Instead one has to prepare the crystals by first cutting and then submitting them to extensive treatment to clean and heal the disruption caused by the cutting process. This may eliminate simple metastable structures similar to the 2×1 pattern of the (111) surface. The treatment to which the crystal faces are subjected is capable of producing the most stable structure, even if this means very considerable rearrangement of the surface atoms. It is not surprising then, to find LEED patterns indicating reconstruction of the surface.

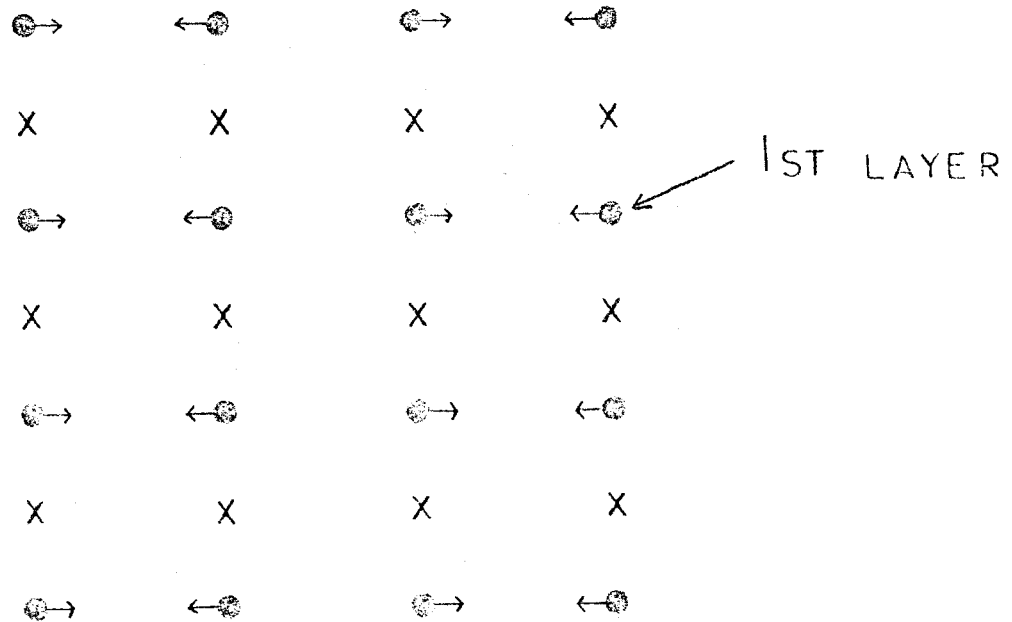


Fig. 7. Sketch of (100) Surface of Silicon. Surface atoms are denoted by filled circles. Second layer atoms are denoted by crosses. Arrows indicate the motion of atoms for one of the reconstruction models (discussed in Section C).

In our approach we again use a finite cluster of atoms. In the present case we were interested in investigating two types of problems: (i) the basic electronic structure of an ideal surface, as well as the relaxation distances for the different states; and (ii) the feasibility of one of the proposed reconstruction mechanisms for the (100) surface.

Our results can be summarized as follows. For the ideal (100) surface we find that the electronic structure is determined by the divalent character of the surface silicons. There are two "surface" electrons per surface silicon atom with two basic low-lying states. For the ground state the relaxation distance is 0.10\AA towards the vacuum, while for the first excited state the surface relaxes inward by 0.05\AA . We also find that bond pairing of adjacent surface atoms leads to a bond whose strength is 1.74 eV. (Each Si atom moves so that the Si-Si bond length is 2.38\AA). This makes plausible the reconstruction of the surface by the mechanism proposed by Levine⁴⁵ in which two adjacent rows rotate towards each other producing a 2×1 unit cell.

B. Basic Electronic Structure

General Description

For the basic model of the (100) Si surface we have chosen an Si_3H_6 cluster (quite different from the Si_3H_6 complex used in the (111) surface), in which only one silicon atom is a surface atom, bound to two nearest neighbors corresponding to second layer atoms in the ideal unreconstructed surface. These, in turn, should each be bound to three other silicon atoms but we have substituted them by hydrogen atoms. Here, as before, the hydrogens have the function of decoupling the

"back-side-of-the-cluster" electrons from the "surface" electrons.

This complex is shown in Fig. 8 for the tetrahedral (ideal) geometry.

Since each surface Si is bound to two other silicons, two nonbonded electrons are left. Thus the complex can be schematically represented as $\text{H}_3\text{Si-Si-SiH}_3$, where the "bulk" (second layer) Si are fixed at the normal tetrahedral positions, but the surface Si (divalent) are allowed to relax. Two basic low-lying states result from this particular configuration (shown schematically in Fig. 9):

$(\sigma\pi)$: Of the two nonbonded electrons one is in a p-like orbital perpendicular to the Si-Si-Si plane (this is denoted by π and indicated in Fig. 9 by a circle; visualize an orbital sticking out of the paper) and the other is in an sp-hybrid orbital located mainly in the plane of the three silicons (this is denoted as σ and indicated in Fig. 9 by a lobe). Two different spin couplings are possible, a triplet and a singlet. Since the two orbitals are orthogonal, a favorable exchange integral predicts the triplet to be the lowest of the two (as in Hund's rule). The triplet and singlet states are denoted in Fig. 9 by $^3(\sigma\pi)$ and $^1(\sigma\pi)$ respectively.

(σ^2) : The other state can be thought of as having both nonbonded valence electrons in a σ orbital. In our GVB calculations this σ pair is correlated, leading to one orbital pointing above the Si-Si-Si plane with a shape of the form⁴⁶ $\sigma + \lambda\pi$ and the other electron is in an orbital pointing below the Si-Si-Si plane, of the form $\sigma - \lambda\pi$. These orbitals are spin-paired into a singlet state denoted $^1(\sigma^2)$.

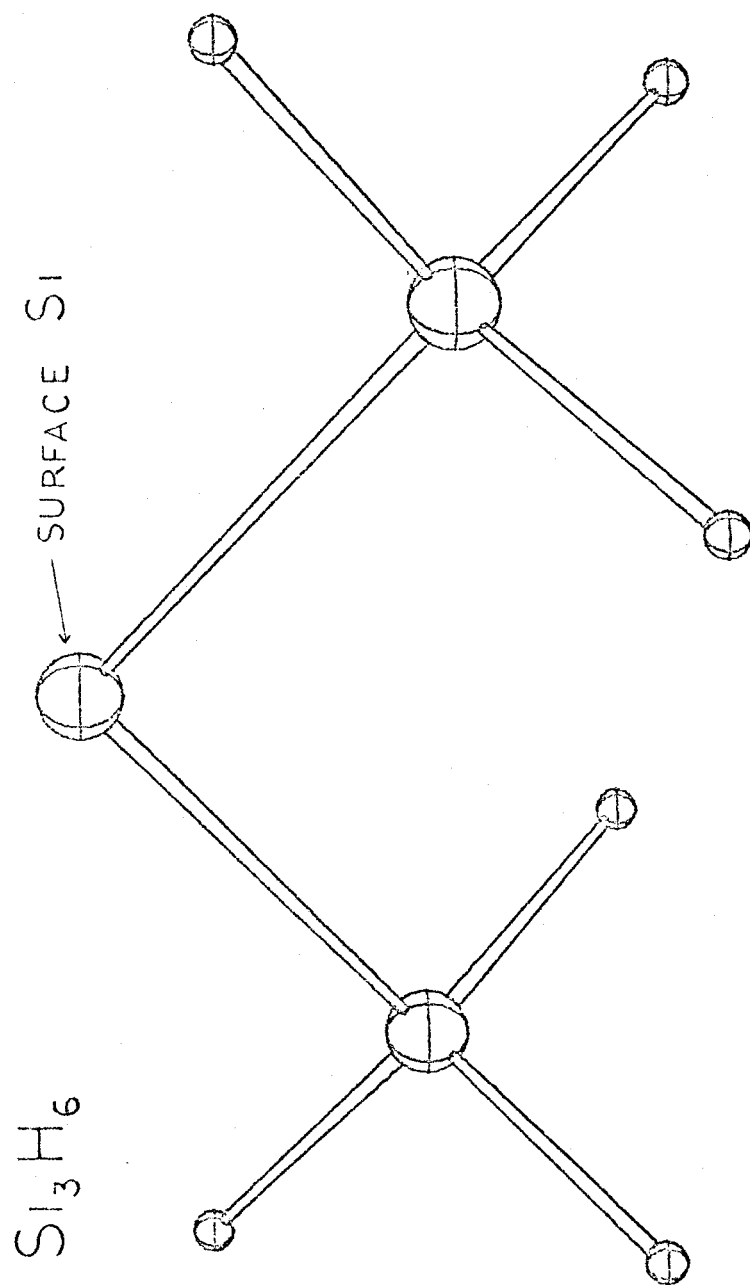


Fig. 8. Si_3H_6 Complex Used in the (100) Surface Calculations.

DIVALENT SURFACE Si

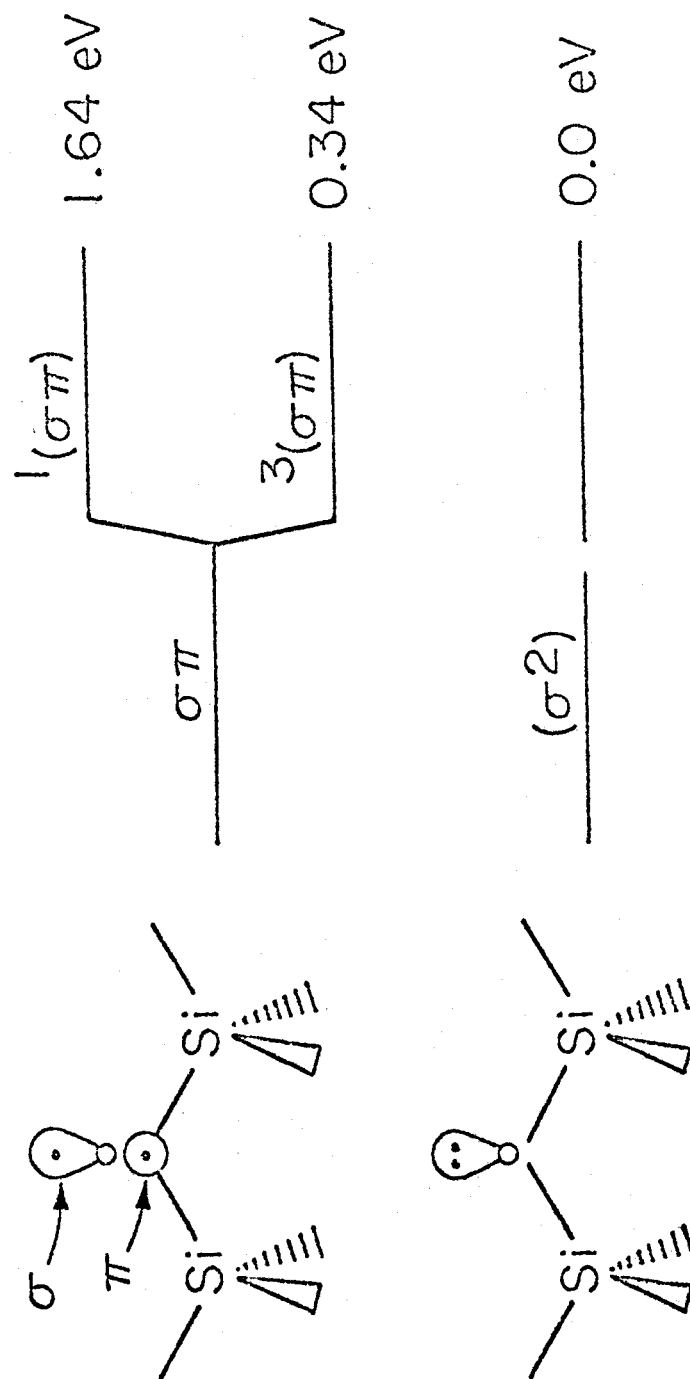


Fig. 9. Schematic of the states of the Si_3H_6 Cluster Modeling the (100) Surface. A circle represents a p-like orbital coming out of the plane of the paper; a lobe, \odot , represents a σ orbital in the plane of the paper; dots denote the number of electrons for each orbital.

For the ($\sigma\pi$) states electron correlation effects are not of major importance because each orbital is singly occupied. For the (σ^2) configuration a Hartree-Fock description leads to large correlation errors and as a result obtains the wrong ordering of the states. Introducing normal correlation (GVB wavefunction), we find the $^3(\sigma\pi)$ and $^1(\sigma^2)$ states to be very close to each other with $^1(\sigma^2)$ lower.

These states are analogous to the states of the methylene molecule⁴⁷ (CH_2) and its derivatives. Few such systems are known for silicon; an example is SiH_2 , which has a singlet $^1(\sigma^2)$ ground state⁴⁸ (with an optimum angle of 92°). For the carbon systems the ground state is generally the $^3(\sigma\pi)$ state.⁴⁷

Computational Details

The geometry variations performed in this system consisted of keeping the "second layer" silicons fixed at the tetrahedral positions and letting the "surface" Si relax along the [100] direction. The actual calculations were performed for four different values of the Si-Si-Si angle; namely 95° , 105° , $109^\circ 28'$ (tetrahedral geometry) and 115° , corresponding to 0.402, 0.116, 0.0 and -0.135\AA , respectively, for the relaxation distance along the [100] direction (positive values indicate motion away from the bulk, toward the vacuum). For each of these points the $^1(\sigma^2)$, $^3(\sigma\pi)$ and $^1(\sigma\pi)$ states were each solved self-consistently.

The calculations for the $^3(\sigma\pi)$ and $^1(\sigma\pi)$ states consisted of open-shell Hartree-Fock wavefunctions, in which the σ and π orbitals

were singly-occupied. Thus the wavefunctions have the form

$$^3(\sigma\pi) = \mathcal{A}\{\Phi_{\text{bulk}}[\phi_{\sigma}(1)\phi_{\pi}(2) - \phi_{\pi}(1)\phi_{\sigma}(2)][\alpha(1)\beta(2) + \beta(1)\alpha(2)]\}$$

and

$$^1(\sigma\pi) = \mathcal{A}\{\Phi_{\text{bulk}}[\phi_{\sigma}(1)\phi_{\pi}(2) + \phi_{\pi}(1)\phi_{\sigma}(2)][\alpha(1)\beta(2) - \beta(1)\alpha(2)]\} ,$$

where Φ_{bulk} represents the wavefunction of all bond pairs.

For the $^1(\sigma^2)$ state a GVB(1) wavefunction was utilized (see Appendix A) in which each nonbonded electron is allowed to have its own orbital. The wavefunction has the form

$$^1(\sigma^2) = \mathcal{A}\{\Phi_{\text{bulk}}[\phi_{\sigma+\lambda\pi}(1)\phi_{\sigma-\lambda\pi}(2) + \phi_{\sigma-\lambda\pi}(1)\phi_{\sigma+\lambda\pi}(2)] \\ \times [\alpha(1)\beta(2) - \beta(1)\alpha(2)]\} .$$

As shown in Appendix C, the closed-shell Hartree-Fock wavefunction for this state

$$^1(\sigma^2)^{\text{HF}} = \mathcal{A}\{\Phi_{\text{bulk}}[\phi_{\sigma}(1)\phi_{\sigma}(2)][\alpha(1)\beta(2)]\} ,$$

gives an energy which is approximately 0.54 eV higher than the GVB(1) result, therefore predicting the wrong ground state.

The basis set used in these calculations consists of the double zeta (DZ) basis on the bulk Si and H atoms (see Table XI of Chapter 1). However, from studies of methylene systems, it is known that d-functions are essential for a consistent description of (σ^2) and $(\sigma\pi)$ states. We have tested this for the present system and have confirmed the need for

d-functions on the central (divalent) Si of the cluster (the comparison between basis sets with and without d-functions is discussed in Appendix C). Hence, all calculations include d-functions on the central Si atom of the Si_3H_6 complex. (This basis is described as DZd in Table XI of Chapter 1.)

Results

The results for the relaxation calculations are summarized in Table IX and in Fig. 9. As is found⁴⁸ in SiH_2 , the ground state of the system is the $^1(\sigma^2)$ state. The optimum Si-Si-Si angle is 105.4° , corresponding to a displacement (along the [100] direction) of 0.10\AA toward the vacuum (with respect to the unreconstructed, unrelaxed tetrahedral geometry). The first excited state is $^3(\sigma\pi)$, with a vertical excitation energy of 0.34 eV. The optimum bond angle for this state is 111.5° , corresponding to a displacement of the surface atom by 0.05\AA toward the bulk from the unrelaxed tetrahedral geometry. The $^1(\sigma\pi)$ state, as expected, is higher in energy, with a vertical excitation energy of 1.64 eV. The optimum angle for this state is 111.7° , also corresponding to a displacement of 0.05\AA toward the bulk. Geometric relaxation effects account for a further drop of 0.16 eV in the energy of these states, giving 0.18 and 1.48 eV for the adiabatic excitation energies of the $^3(\sigma\pi)$ and $^1(\sigma\pi)$ states, respectively.

Since the $^3(\sigma\pi)$ and $^1(\sigma\pi)$ states have the same electronic configuration, their geometries are very similar. They both lead to larger central angles because there is only one electron in the nonbonding σ orbital. For the $^1(\sigma^2)$ state the geometry is quite different. Now two

Table IX. Results for the Si_3H_6 Cluster Modes of the (100) Si Surface

State and Wavefunction ^a	Optimum Energy ^b (hartrees)	Optimum Angle (°)	Relaxation Distance ^c (Å)	Vertical Excitation Energy (eV)	Adiabatic Excitation Energy (eV)
$1(\sigma^2)\text{GVB}(1)$	-14.594092	105.43	0.104	0.0	0.0
$3(\sigma\pi)\text{HF}$	-14.587655	111.49	-0.050	0.34	0.18
$1(\sigma\pi)\text{HF}$	-14.539713	111.67	-0.055	1.64	1.48

^aSee the text for an explanation of the symbols.

^bObtained by a cubic splines fit to the calculated points (see Appendix C).

^cPositive values indicate motion toward the vacuum. Zero corresponds to the tetrahedral (unrelaxed) geometry.

electrons occupy overlapping σ -like orbitals leading to repulsive interactions (because of the Pauli principle) with the adjacent Si-Si bonds. This leads to the surface Si moving toward the vacuum and hence smaller angles at the central Si. These effects are more drastic for a system in which the constraints of the lattice are absent (see Appendix B).

In that case we find optimum angles of 95.2° and 119.9° for the (σ^2) and $^3(\sigma\pi)$ states respectively. Here the vertical and adiabatic excitation energies for the $^3(\sigma\pi)$ state are 0.49 eV and 0.18 eV respectively.

For the $^1(\sigma^2)$ state, the two σ -orbitals point away from each other, one above the Si-Si-Si plane and the other below. The final hybridizations for these orbitals⁴⁹ is $s^{0.44}p^{0.53}$, where the shape of the orbitals is $\sigma \pm \lambda\pi$. These orbitals are plotted in Fig. 10. For the $^3(\sigma\pi)$ state the two (triplet coupled) electrons occupy a π -like orbital, localized at the central Si, and a σ -like orbital, also localized at the central Si, whose hybridization⁴⁹ is $s^{0.20}p^{0.68}d^{0.01}$. These orbitals are plotted in Fig. 11.

C. Surface Reconstruction

Introduction

The (100) surface is sketched in Fig. 7. Each surface Si (denoted by a filled circle) is bonded to two bulk Si (denoted by x) leaving two non-bonded surface electrons. It has been suggested (by Schlier and Farnsworth⁵⁰ and modified by Levine⁴⁵) that these surface Si pair up by moving alternate rows towards each other (as shown by the arrows in Fig.

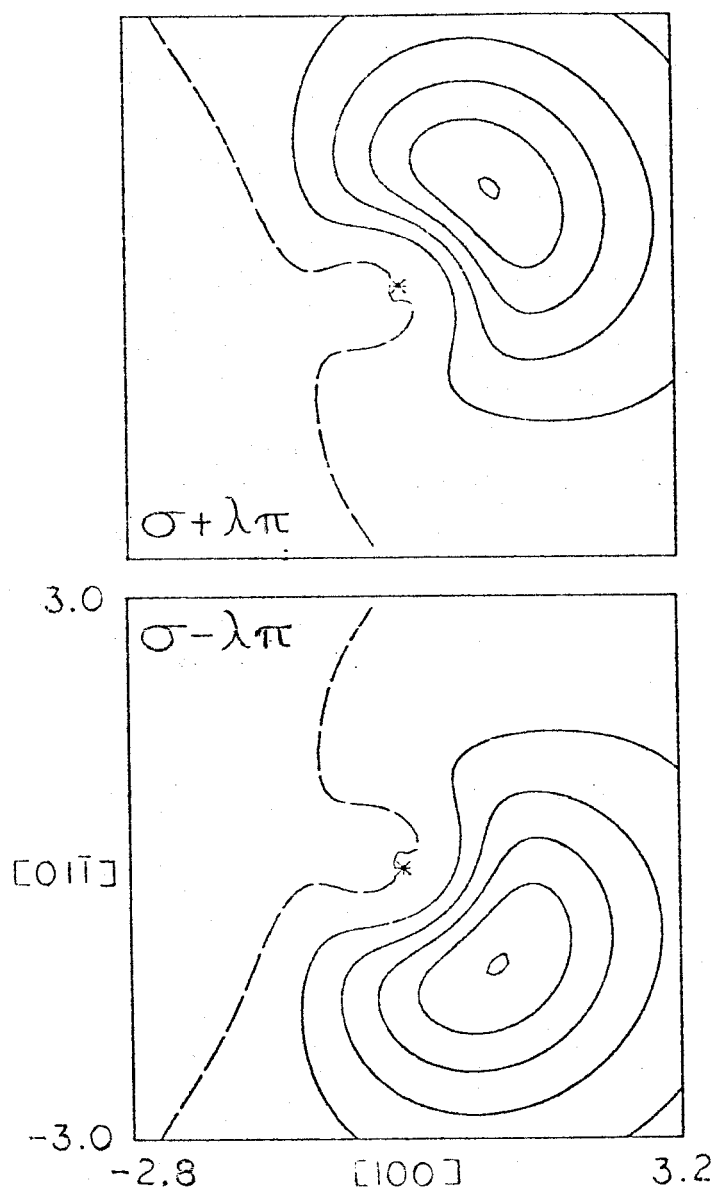
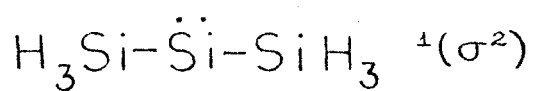


Fig. 10. $\sigma + \lambda\pi$ and $\sigma - \lambda\pi$ GVB Orbitals for the Non-Bonded Electrons of the ${}^1(\sigma^2)$ State of the Si_3H_6 Cluster Model of (100) Surfaces.

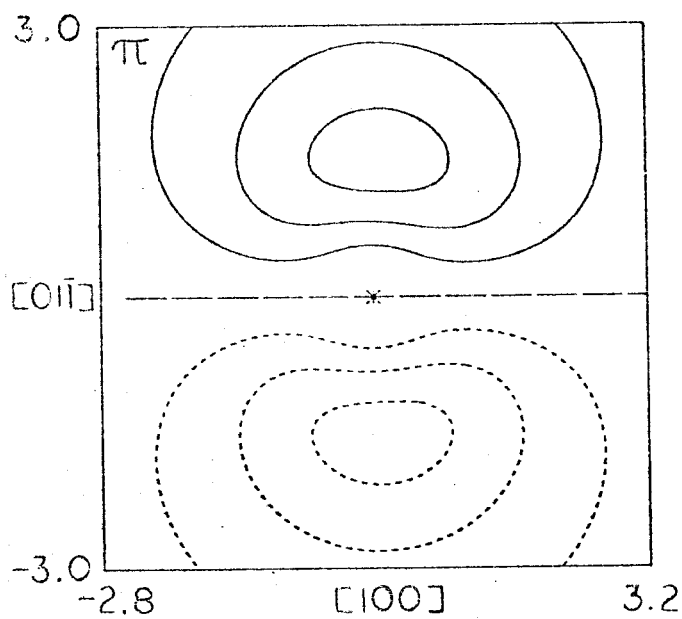
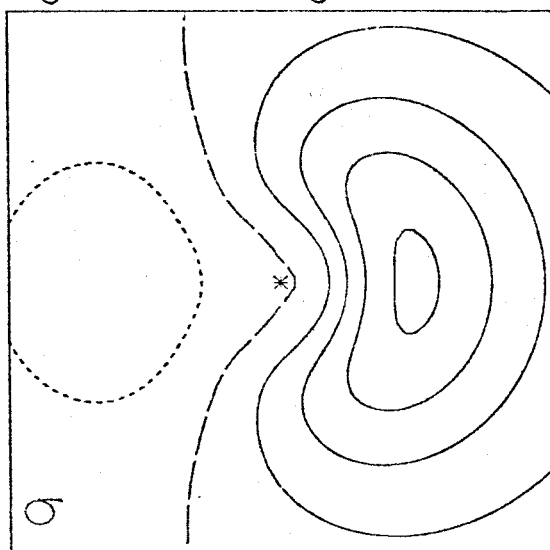
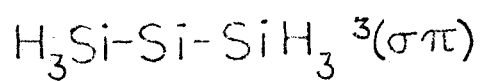


Fig. 11. σ and π Orbitals for the Non-Bonded Electrons of the ${}^3(\sigma\pi)$ State of the Si_3H_6 Cluster Model of (100) Surfaces.

7) leading to formation of single or double bonds. In the latter case it is assumed that the optimum dimer distance should then be very close to the optimum distance observed in the gas spectra⁵¹ of the molecule Si_2 of 2.25\AA . If single bonds are more appropriate, it is expected⁴⁵ that the dimer distance is very similar to the Si-Si distance in the bulk, namely 2.35\AA .

To test this model we have performed calculations utilizing an Si_2H_4 cluster consisting of two separate SiH_2 units.

Let us now consider how the states of this system can be described. Starting with the (σ^2) , $^3(\sigma\pi)$ and $^1(\sigma\pi)$ states of two SiH_2 units at an infinite $R_{\text{Si-Si}}$ distance we can construct the states by considering the different combinations as sketched in Fig. 12. Four different singlets ($S = 0$), four triplets ($S = 1$) and one quintet are possible. At $R_{\text{Si-Si}} = \infty$ the ground state should consist of two $^1(\sigma^2)$. The next state should have the form $^3[{}^1(\sigma_\ell^2){}^3(\sigma_r\pi_r)] \pm {}^3[(\sigma_\ell\pi_\ell){}^1(\sigma_r^2)]$. [Recall that for SiH_2 the order of the states is $^1(\sigma^2)$, $^3(\sigma\pi)$ and $^1(\sigma\pi)$]. Since the difference^{48b} between the $^3(\sigma\pi)$ and $^1(\sigma\pi)$ of SiH_2 is about 1.4 eV, one expects that two $^3(\sigma\pi)$ is lower in energy than a $^1(\sigma^2)$ and a $^1(\sigma\pi)$, thus the next state should have the form $^5[{}^3(\sigma_\ell\pi_\ell){}^3(\sigma_r\pi_r)]$. Next a state with $^1(\sigma\pi)$ must be considered, namely $^1[{}^1(\sigma^2){}^1(\sigma_r\pi_r)] \pm {}^1[{}^1(\sigma_\ell\pi_\ell){}^1(\sigma_r^2)]$. Similarly for higher states. As the two SiH_2 units are brought together to the unreconstructed Si (100) nearest surface neighbor distance, we expect the shapes and spin couplings of the orbitals to remain basically the same with only small changes in the energy.

For our calculations we started with the two Si atoms at the positions they would have in an unreconstructed (100) surface. We then allowed them to rotate as if the SiH bonds were Si-Si bonds, letting the two Si atoms get closer. In Fig. 12 we show the geometry for this complex for two different Si-Si distances (at the unreconstructed (100) surface and the bulk Si-Si distances for the two silicons).

As the two silicons move towards each other we expect to find more drastic changes in the nature of the orbitals and the spin couplings. The total energies also change noticeably as sketched in Fig. 13 (for that figure we have used the calculated shapes of the lowest singlet, lowest triplet and the quintet states; all other curves constitute guesses). In Fig. 14 we show how the orbitals change as a function of distance for the singlet ground state and the lowest triplet state. We notice that for the orbitals of the singlet state for the unreconstructed (100) surface geometry, the ground state can be accurately described as $^1[{}^1(\sigma_\ell^2){}^1(\sigma_r^2)]$. This is no longer true at the bulk Si, silicon-silicon distance. Here we would have to describe this state as $^1[{}^1(\pi_\ell\pi_r){}^1(\sigma_\ell\sigma_r)]$. Similarly, the triplet state can be well described by $^3[{}^1(\sigma_\ell^2){}^3(\sigma_r\pi_r)] \pm ^3[{}^3(\sigma_\ell\pi_\ell){}^1(\sigma_r^2)]$ for the unreconstructed geometry. At the bulk silicon distance, that state is better described by $^3[{}^1(\pi_\ell\pi_r){}^3(\sigma_\ell\sigma_r)]$. We thus see that forming a π - π bond between adjacent silicons produces a considerable lowering in the energy, particularly as the silicons get closer to each other. For states that do not form a π - π bond we expect the

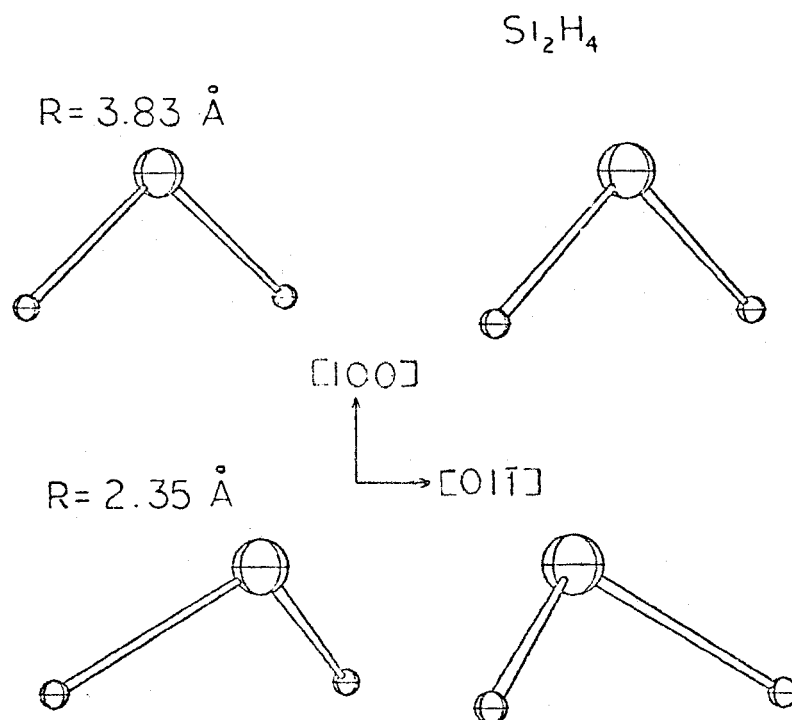


Fig. 12. Geometry for the Si_2H_4 Cluster Model of Reconstruction on the (100) Surface. (a) $R_{\text{Si-Si}} = 3.83 \text{ \AA}$ (unreconstructed geometry). (b) $R_{\text{Si-Si}} = 2.35 \text{ \AA}$ (bulk Si-Si bond length).

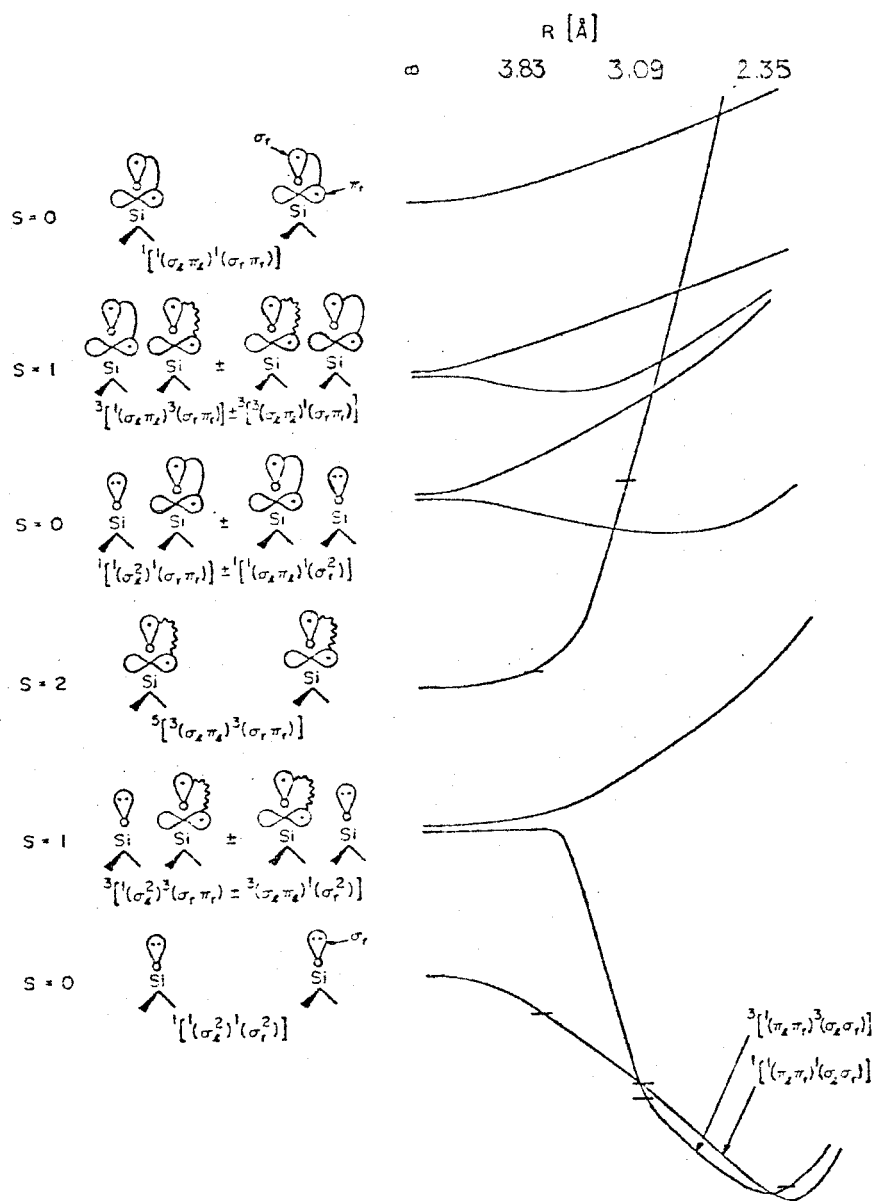


Fig. 13. Schematic of the Different States for the Si_2H_4 Model of Reconstruction for (100) Surfaces. Small horizontal lines denote values obtained from actual calculations. Values at infinity are estimates based on Ref. 48b. All other features are approximate. Orbitals connected by a solid line are singlet coupled; orbitals connected by a wavy line are triplet coupled.

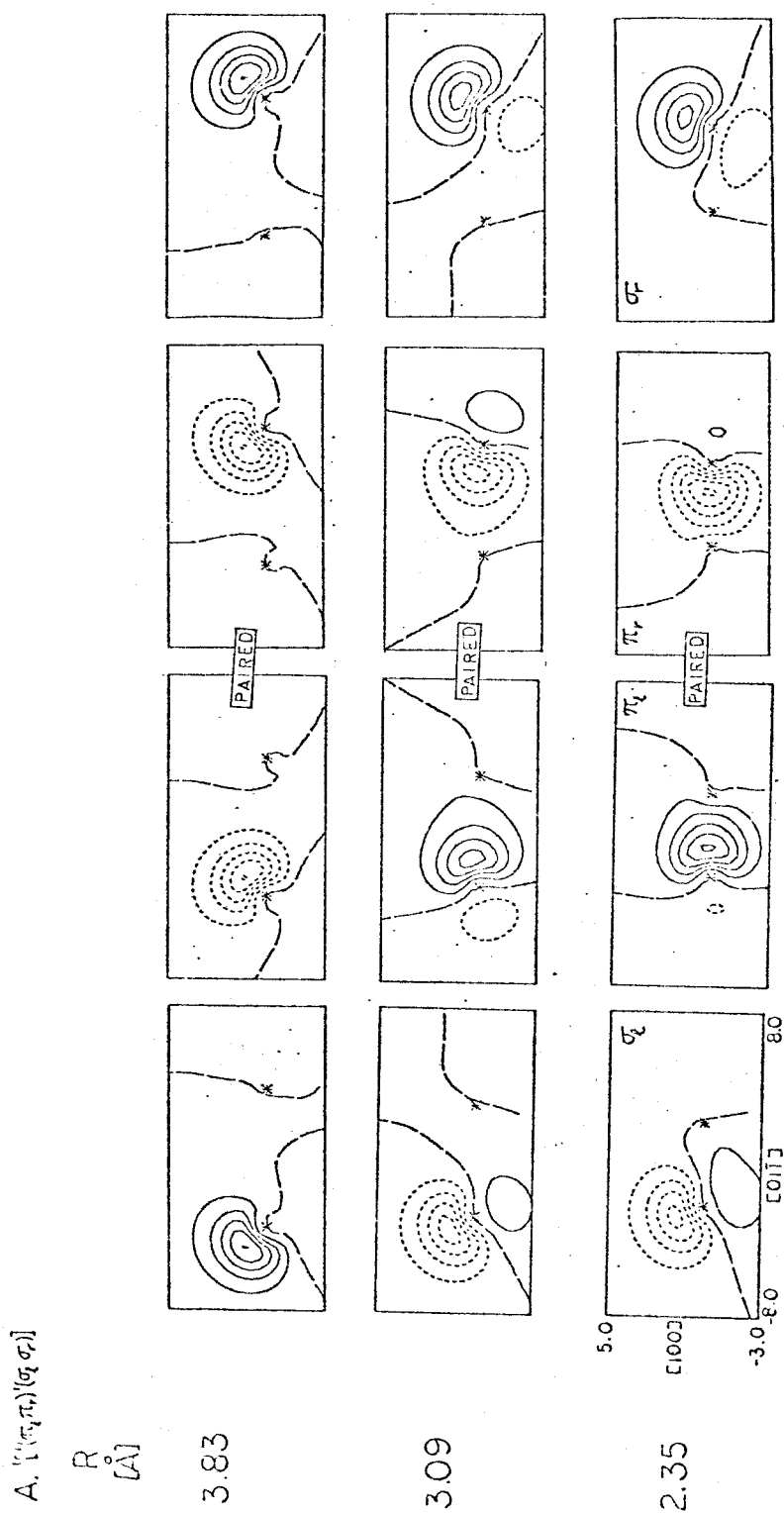


Fig. 14. Orbital Changes as a Function of Distance for the Si_2H_4 Cluster Model of Reconstruction on $\text{Si}(100)$ Surfaces. (a) 1A_1 SOGVB Calculation, $[(\pi_r \pi_r)(\sigma_r \sigma_r)]$. For $R_{\text{Si-Si}} = 3.09 \text{ \AA}$ and for $R_{\text{Si-Si}} = 2.35 \text{ \AA}$ the orbitals on the ends are paired into a singlet.

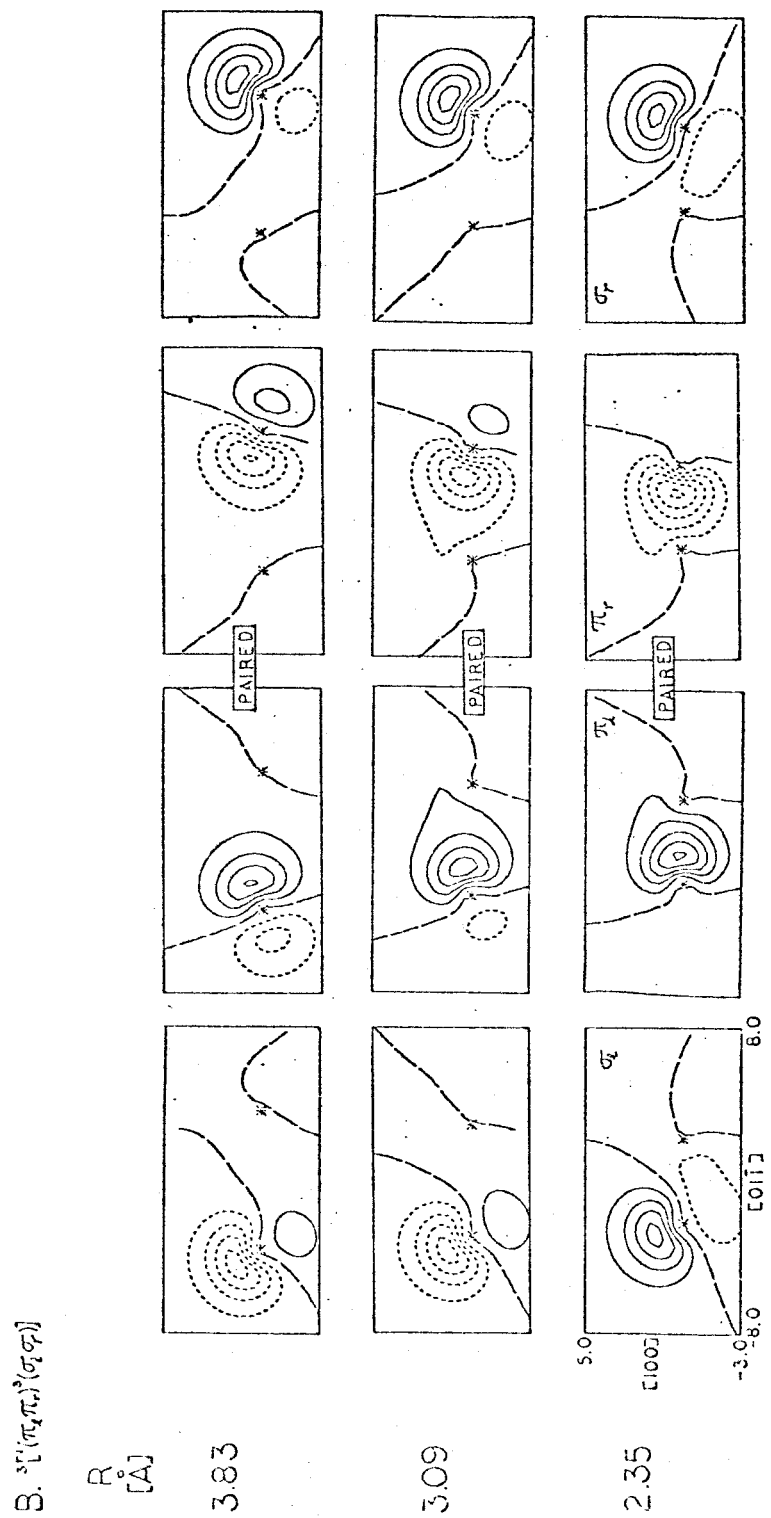


Fig. 14. (b) $3B_2$ SOGVB calculation, $3[(\pi_d \pi_r)^3(\sigma_d \sigma_r)]$.

potential energy surface to be repulsive or to have a very shallow minimum.

Results

The results of the Si_2H_4 calculations are summarized in Table X. Figure 15 shows the potential curves obtained for the $^3[{}^1(\pi_\ell\pi_r){}^3(\sigma_\ell\sigma_r)]$, ${}^1[{}^1(\pi_\ell\pi_r){}^1(\sigma_\ell\sigma_r)]$ and ${}^5[{}^3(\pi_\ell\sigma_\ell){}^3(\pi_r\sigma_r)]$ states. The ground state, at the unreconstructed geometry, is the ${}^1[{}^1(\sigma_\ell^2){}^1(\sigma_r^2)]$. This corresponds to two, noninteracting ${}^1(\sigma^2)$ states localized on each of the surface Si atoms. Both the ${}^3[{}^1(\pi_\ell\pi_r){}^3(\sigma_\ell\sigma_r)]$ and ${}^1[{}^1(\pi_\ell\pi_r){}^1(\sigma_\ell\sigma_r)]$ states are very close in energy, with the singlet state being lower (by 0.13 eV). The bond energy (energy difference between the ${}^1[{}^1(\pi_\ell\pi_r){}^1(\sigma_\ell\sigma_r)]$ at its minimum and the ${}^1[{}^1(\sigma_\ell^2){}^1(\sigma_r^2)]$ at the unreconstructed geometry) is 2.41 eV.

The Si_2H_4 cluster does not include the energy due to the bending of the Si-Si bonds at the second layer (i.e., the Si-H bonds of the Si_2H_4 cluster do not account for hybridization changes). We have accounted for the change in the hybridization at the second layer Si atoms by doing a calculation on the $\text{H}_3\text{Si}-\dot{\text{Si}}-\text{SiH}_3$ cluster. Here we bend the central silicon off the plane formed by the two second layer Si atoms and the divalent silicon (at the tetrahedral geometry) as shown in Fig. 16. Here one expects the energy due to the change in hybridization increases as the bending angle departs from the tetrahedral geometry.

Table X Results of the Calculations on the Si_2H_4 Cluster Model of Si (100) Surface Reconstruction.^a
All energies are in hartrees.

State ^b	$R_{\text{Si-Si}}$ (bohr)						Optimum $R_{\text{Si-Si}}$ Distance (bohr)	Minimum Energy ^c
	7.257	5.851	4.644	4.444	4.244	3.038		
$1[{}^1(\sigma_x^2)({}^1(\sigma_r^2))]$	-9.653631 (-9.653631)	-9.679895 (-9.675008)	-9.735305 (-9.716203)	-9.740428 (-9.717530)	-9.742333 (-9.715378)	-9.481533 (-9.412466)	4.269 (4.458)	-9.742384 ^d (-9.717539) ^e
$3[{}^1(\sigma_x^2)({}^3(\sigma_r\pi_r))]$	-9.631230	-9.681478	-9.735847	-9.737643	-9.734225]	-	4.463	-9.737667
$-3[{}^3(\sigma_x\pi_x)({}^1(\sigma_r^2))]$	-9.631230)	(-9.676591)	(-9.716745)	(-9.714745)	(-9.707270)		(4.642)	(-9.716745)
$5[{}^3(\sigma_x\pi_x)({}^3(\sigma_r\pi_r))]$	-9.617458 (-9.617458)	-9.582699 (-9.577812)	-9.470576 (-9.451474)	-9.438297 (-9.415399)	-9.400452 (-9.373497)	-	7.028 7.036	-9.618829 (-9.618891)

^aValues in parentheses are corrected for bending of second layer silicon.

^bSee Fig. 13 and text for an explanation of the symbols used in this column.

^cObtained by cubic splines fits to the calculated points.

^dThis corresponds to a well depth of 2.41 eV as compared to the value at 7.257 bohr.

^eThis corresponds to a well depth of 1.74 eV.

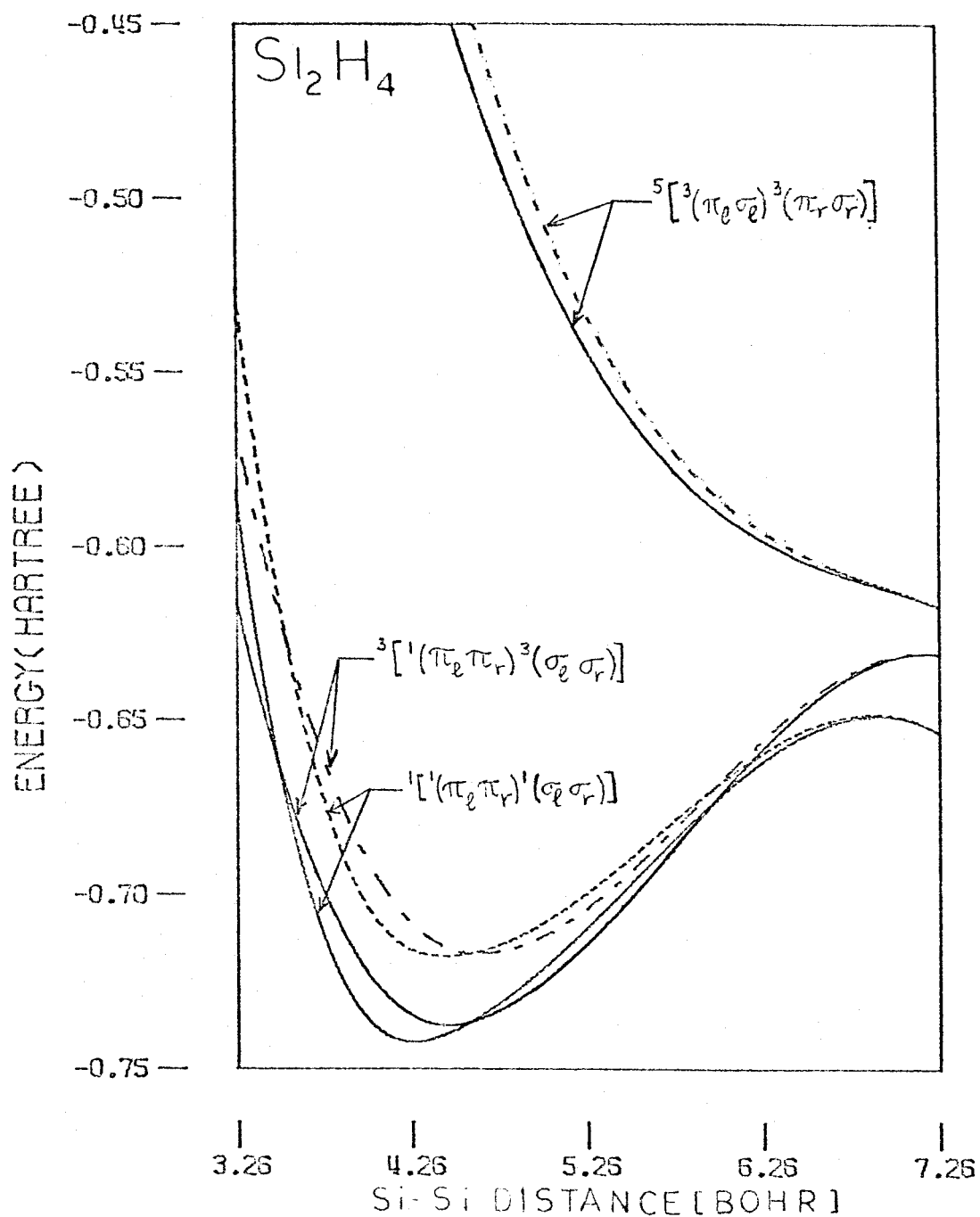


Fig. 15 Potential Curves for the Si_2H_4 Cluster Model of Reconstruction on Si (100) Surfaces. Solid lines indicate uncorrected energies, dashed lines indicate energies corrected for the bending of second layer silicons.

To account for the increase in energy due to the change in hybridization of the second layer atoms, we must add to the Si_2H_4 results the potential curve obtained from the Si_3H_6 bending calculations. The energies obtained in the Si_3H_6 calculations are shown in Table XI. Since the Si_3H_6 calculations were performed by bending the two "surface" hydrogens as well as the central silicon, they already include the potential barrier that we should add for both sides of the dimer (Si_2H_4). The corrected potential curves for the dimer are also shown in Fig. 15. When these corrections are included we obtain a bond energy of 1.74 eV with an optimum Si-Si distance of 2.38\AA .

From these calculations one concludes that the Schlier-Farnsworth-Levine model is energetically feasible. Of course, these calculations do not rule out other models.

Calculational Details

(i) Si_2H_4 cluster

For the Si_2H_4 cluster the geometry was varied by allowing the two SiH_2 groups to rotate as if the Si-H bonds were Si-Si bonds (as if the second layer Si atoms were fixed at the tetrahedral unreconstituted geometry). The actual calculations were performed for Si-Si distances of 3.84, 3.09, 2.46, 2.35 and 2.25\AA (corresponding to bending angles of 0.0, 15.91, 33.24 and 55.31 degrees). The basis set consisted of a double zeta basis with d-functions added to each silicon (DZd set of Table XI, Chapter 1, p. 31). We have shown in Appendix C that this is necessary for a proper description of the σ^2 and states. As in the $\text{H}_3\text{Si}-\ddot{\text{Si}}-\text{SiH}_3$ calculations, correlation effects are

Table XI. Potential Curve for the Bending of the Central Si Atom in the $\text{H}_3\text{Si}-\ddot{\text{Si}}-\text{SiH}_3$ Complex.

Angle ^a	Energy (hartrees)
0.0	-14.594074
15.0	-14.589742
30.0	-14.575700
45.0	-14.549754

^aThis is the angle between the plane formed by the three Si atoms and the vertical plane that contains the Si atoms and the two "surface" hydrogens for the tetrahedral geometry.

crucial for the $^1[{}^1(\sigma_\ell^2){}^1(\sigma_r^2)]$ state. For this state we have used a SOGVB wavefunction,⁵⁷ in which both pairs of "surface" electrons are correlated. The wavefunction has the form

$$^1[{}^1(\sigma_\ell^2){}^1(\sigma_r^2)] = \mathcal{A}\{\Phi_{\text{Si-H}}(1, \dots, 8) \Phi_{\text{surface}}(9, \dots, 12)\} , \quad (12)$$

where $\Phi_{\text{Si-H}}$ represents the wavefunction for the Si-H bond pairs (having the standard closed-shell Hartree-Fock form); and where

$$\begin{aligned} \Phi_{\text{surface}}(9, \dots, 12) = & \phi_{(\sigma+\lambda\pi)_\ell}^{(9)} \phi_{(\sigma+\lambda\pi)_\ell}^{(10)} \phi_{(\sigma+\lambda\pi)_r}^{(11)} \phi_{(\sigma-\lambda\pi)_r}^{(12)} \\ & \times \{c_1[\alpha(9)\beta(10)\alpha(11)\beta(12) - \alpha(9)\beta(10)\beta(11)\alpha(12) \\ & - \beta(9)\alpha(10)\alpha(11)\beta(12) + \beta(9)\alpha(10)\beta(11)\alpha(12)] \\ & + c_2[2\alpha(9)\alpha(10)\beta(11)\beta(12) - \beta(9)\alpha(10)\beta(11)\alpha(12) \\ & - \alpha(9)\beta(10)\beta(11)\alpha(12) - \alpha(9)\beta(10)\alpha(11)\beta(12) \\ & + 2\beta(9)\beta(10)\alpha(11)\alpha(12) - \beta(9)\alpha(10)\alpha(11)\beta(12)]\} \end{aligned}$$

Correlation is also necessary to properly describe the $^3[{}^1(\pi_\ell\pi_r){}^3(\sigma_\ell\sigma_r)]$ state. The wavefunction has the form of (12), with

$$\begin{aligned}
 \Phi_{\text{surface}}(9, \dots, 12) &= [\phi_{\pi_\ell}(9)\phi_{\pi_r}(10)\phi_{\sigma_\ell}(11)\phi_{\sigma_r}(12)] \\
 &\times \{c_1[\alpha(9)\beta(10)\alpha(11)\alpha(12) - \beta(9)\alpha(10)\alpha(11)\alpha(12)] \\
 &+ c_2[2\alpha(9)\alpha(10)\beta(11)\alpha(12) - \alpha(9)\beta(10)\alpha(11)\alpha(12) - \beta(9)\alpha(10)\alpha(11)\alpha(12)] \\
 &+ c_3[3\alpha(9)\alpha(10)\alpha(11)\beta(12) - \beta(9)\alpha(10)\alpha(11)\alpha(12) \\
 &\quad - \alpha(9)\beta(10)\alpha(11)\alpha(12) - \alpha(9)\alpha(10)\beta(11)\alpha(12)]\}
 \end{aligned}$$

For the quintet $^5[{}^3(\sigma_\ell\pi_\ell){}^3(\sigma_r\pi_r)]$ the wavefunction is also of the form (12) with

$$\begin{aligned}
 \Phi_{\text{surface}}(9, \dots, 12) &= [\phi_{\pi_\ell}(9)\phi_{\sigma_\ell}(10)\phi_{\pi_r}(11)\phi_{\sigma_r}(12)] \\
 &\times [\alpha(9)\alpha(10)\alpha(11)\alpha(12)] .
 \end{aligned}$$

(ii) Si₃H₆ cluster

For this cluster the geometry variation consisted of "bending" the central Si atom off the vertical plane, indicated in Fig.16 . All the calculations were performed for an Si-Si-Si angle of 105°. The bending angles (determined by the three silicon atoms and the vertical plane; $\alpha = 0$ for an unreconstructed surface) for which the calculations were performed were 0, 15, 30 and 45 degrees. At each of these geometries, only the $^1(\sigma^2)$ state was solved at the GVB(1) level.

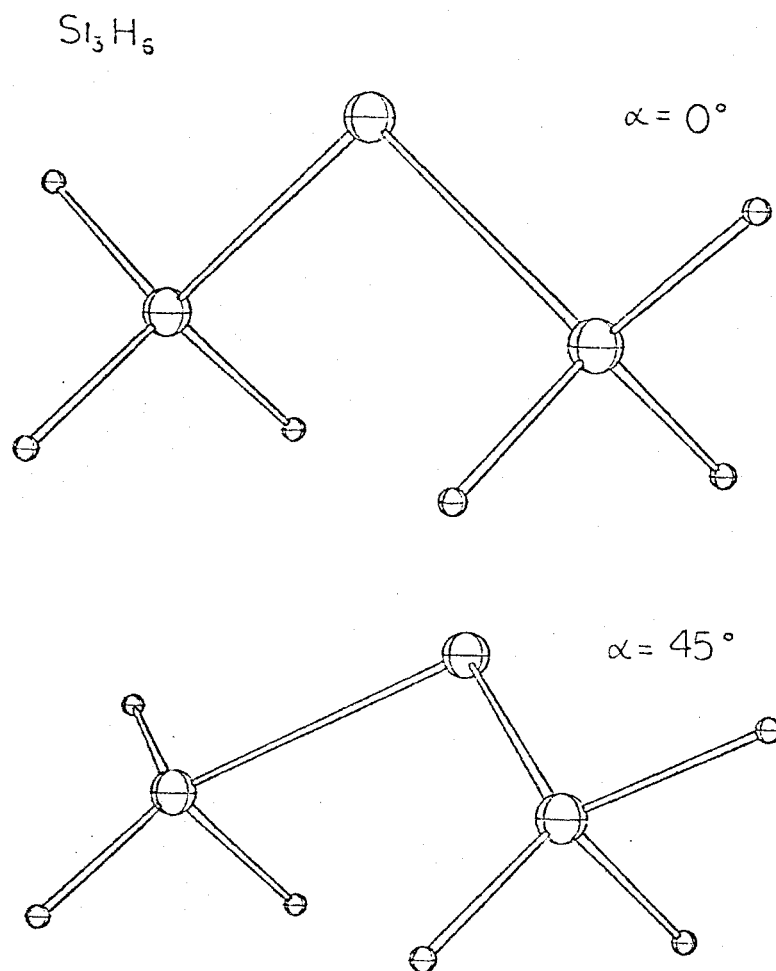


Fig. 16 Geometry for Si_3H_6 Calculations in which the Central Silicon is bent off the tetrahedral geometry. (a) No bending (tetrahedral geometry). (b) Bending angle equal to 45° (the angle between the plane of the 3 silicons and the vertical plane is 45°).

D. Review of Experimental Data

The experimental situation for the Si (100) surface is, by far, much less clear than that of the (111) surface. The reason for this is that these surfaces are cleaned usually by ion bombardment followed by annealing.⁶ Several LEED patterns have been observed, but differences among them suggest that impurities might be of crucial importance in obtaining such patterns.⁶ The involvement of impurities has not been exhaustively studied⁶ and no conclusive results are as yet available. The most commonly known structure is a 2x2 pattern.^{50,52} A 4x4 structure has also been observed.⁵³ The 2x2 and 4x4 LEED patterns can be explained by 2x1 and 4x2 structures (unit cells with basis vectors that are twice or four times as long as those of the unreconstructed tetrahedral geometry). The observed LEED patterns are obtained from the 2x1 and 4x2 structures by orienting these in orthogonal directions in different domains of the surface of the crystal.

Two basic models have been proposed for the reconstruction of Si (100) surfaces. Lander and Morrison^{53a} have proposed a model for the 4x2 structure in which atoms in the first two layers are drawn together in pairs, leading to the appropriate reconstruction. The other model is for the 2x1 reconstruction, initially proposed by Schlier and Farnsworth⁵⁰ and modified by Levine.⁴⁵ In this model adjacent rows of Si surface atoms form bonds via their dangling bonds, producing double rows. The surface atoms are constrained to move in such a way that they keep the same bond length as in the bulk, but variable bond angles.

If only single bonds are formed between adjacent surface atoms, it is expected that the dimer distance is approximately that of the bulk interatomic spacing, 2.35\AA . This leads to a displacement of $\pm 0.75\text{\AA}$ in the horizontal plane (for the surface Si atoms), and a vertical displacement of 0.23\AA in such a way that the surface silicons are still at 2.35\AA from their nearest neighbors in the second layer. This is equivalent to a rotation of $\pm 34^\circ$ of the surface atoms as measured from the [100] direction to the [010] direction. This model leads to a unit cell with a rectangular shape with sides $a/\sqrt{2}$ and $2a/\sqrt{2}$, where a is the bulk unit cell side, 5.4173\AA . The atoms are arranged in "caves" (grooves) and "pedestals" (formed by the two rows drawn together).

We have previously discussed some of the features of this model in relation to our calculations on Si_2H_4 complexes. At that time we concluded that this is a feasible model.⁵⁴ Recently, experimental evidence has been obtained that suggests that the 2×2 LEED pattern is due to the 2×1 pairing (dimer) model. The experiments⁵⁵ consist of a study of the chemisorption of hydrogen on Si (100) surfaces. Two different phases have been found, one with a 2×2 LEED pattern, the other with a 1×1 LEED pattern. Each phase can be obtained from the other one by controlling the temperature and the time of exposure to atomic hydrogen. This suggests that the reconstruction is produced by motion of the surface atoms rather than by vacancies. Furthermore, using the pairing model of Schlier-Farnsworth-Levine^{45,50} one can explain the experimental results of Sakurai and Hagstrum.⁵⁵ The two stages of H

chemisorption are explained as follows. Starting with the pairing model, two adjacent atoms are close to each other due to the $\pi_{\ell}\pi_r$ bond (i.e., we start out with either the $^3[{}^1(\pi_{\ell}\pi_r){}^3(\pi_{\ell}\pi_r)]$ or ${}^1[{}^1(\pi_{\ell}\pi_r){}^1(\sigma_{\ell}\sigma_r)]$ states of Si_2H_4). This leaves two dangling bonds, σ_{ℓ} and σ_r , which can be coupled into singlet and triplet spin states with very similar energies. In the first stage of the chemisorption, hydrogen atoms can bind to each of these dangling bonds still producing a 2×2 LEED pattern. This phase has been called by Sakurai and Hagstrum⁵⁵ the monohydride phase, since at saturation there is one H atom per surface Si. In the second stage of the chemisorption process additional hydrogen atoms attack the dimer breaking the $\pi_{\ell}\pi_r$ bonds, with the result that two hydrogens bind to one surface silicon. This leads to a 1×1 LEED pattern, since the lateral bonds which produced the displacement of adjacent surface rows are no longer present. Sakurai and Hagstrum⁵⁵ have termed this phase the dihydride phase.

III. THE (110) SURFACE OF SILICON

A. Introduction

Looking at an unreconstructed (110) surface of the diamond structure from above, the surface atoms appear arranged in bands with a rectangular unit cell. Each band consists of atoms in a zig-zag fashion, lying on the (110) plane and with tetrahedral bond angles of $109^{\circ}28'$ (see Fig.17). The nearest neighbor distance for the atoms within one of these zig-zag bands is 2.35\AA (for the unreconstructed geometry). The length of the short side of the rectangular unit cell is 3.83\AA , while the distance between two adjacent zig-zag bands is equal to the side of the cubic unit cell of the bulk, namely 5.41\AA . Each surface atom is trivalent, i.e., it is bound to three nearest neighbors, two of which are surface atoms in the same zig-zag band, and the third is a second layer atom. This means that each surface atom has one electron in a dangling bond. For the tetrahedral geometry this orbital makes an angle of about 36° with the normal to the plane of the surface.

As in the case of the (100) surface, the (110) surface cannot be cleaved, and therefore has to be prepared by other methods, usually cutting and cleaning with ion bombardment followed by annealing at high temperature. This means that considerable rearrangement of the surface atoms is possible, so that the surface attains its most stable structure before any kind of experiment can be performed on it. This allows rather complicated LEED structures to form.

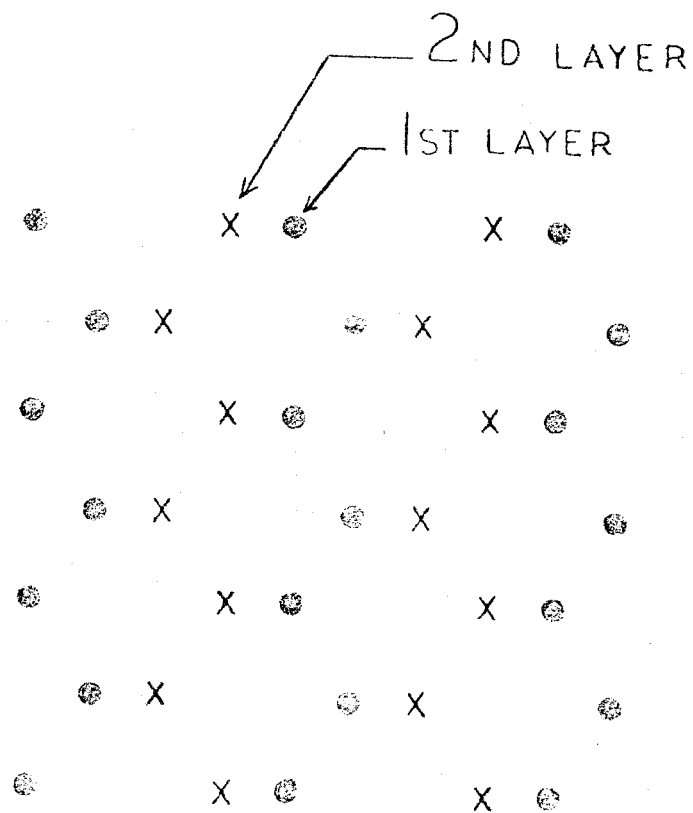


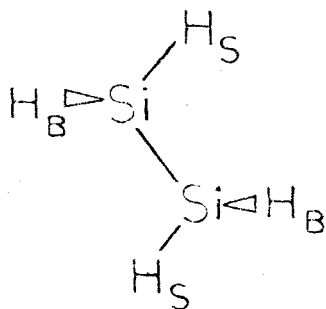
Fig. 17 Sketch of the (110) Surface of Silicon. Surface atoms are denoted by filled circles, second layer atoms are denoted by crosses.

The basic characteristic we wanted to investigate was the interaction between dangling bond orbitals on adjacent atoms. In particular we wanted to determine the basic spin states when a number of Si atoms are present in the zig-zag configuration. Since the orbitals initially point towards opposite sides of the zig-zag band and at an angle of approximately 36° (for the tetrahedral unrelaxed geometry) from the normal to the surface, triplet and singlet pairing of these orbitals are nearly equivalent.

To study the basic spin couplings we have chosen three clusters consisting of two, three and four silicons, namely Si_2H_4 , Si_3H_5 and Si_4H_6 . From these calculations the most important conclusion is that for the undistorted geometry the ground state has high spin coupling (all dangling bonds having the same spin). Of course distortions might stabilize the singlet spin coupling of adjacent dangling bonds.

B. Summary

In order to establish the basic nature of the coupling of adjacent Si dangling bond orbitals we considered the Si_2H_4 model shown in the diagram below.

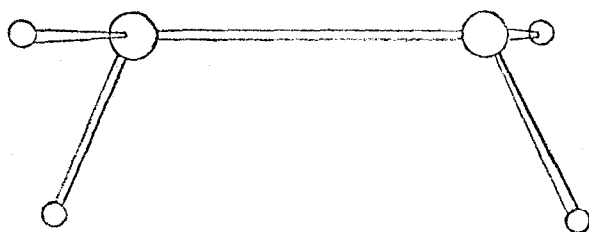


Here both Si represent surface Si, while both H_s replace surface Si and both H_b replace bulk Si. There are two important electronic states $^3(\sigma_1\sigma_2)$ and $^1(\sigma_1\sigma_2)$, depending upon the coupling of the dangling bond orbitals.

In the undistorted geometry we find that the triplet state is the ground state, with the singlet state 0.1 eV higher. This is a small excitation energy, one that might be removed upon relaxation of the surface Si atoms. In order to examine the effect of such distortions we allowed the hydrogens to rotate about the Si-Si bond, so that the two pairs of hydrogens end up in front of each other (eclipsed geometry) as shown in Fig.18. In this case the two dangling bonds are almost parallel to each other. (This would be the optimum configuration for pairing). For this system we also expect two low lying states: a singlet, $^1(\sigma_1\sigma_2)$, and a triplet, $^3(\sigma_1\sigma_2)$. For the real reconstructed Si (110) surface one would not expect the eclipsed geometry to be a very strong possibility, since this would introduce strains in the lattice, raising the energy. An intermediate geometry is more likely in which the Si atoms would rotate slightly so that the dangling bonds point in directions that are closer to being parallel than the directions in which they point at the unreconstructed tetrahedral geometry.

The results of these calculations are shown in Table XII. For the tetrahedral geometry the ground state is the triplet. The singlet state is up by 0.10 eV. For the eclipsed geometry the ground state is the singlet, $^1(\sigma_1\sigma_2)$ by 0.19 eV. We also note that the

A.



B.

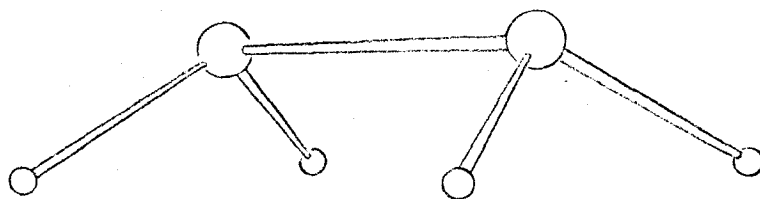


Fig. 18 Geometry for the Si₂H₄ Cluster Model of (110) Surfaces.
(a) Unreconstructed geometry. (b) Eclipsed geometry.

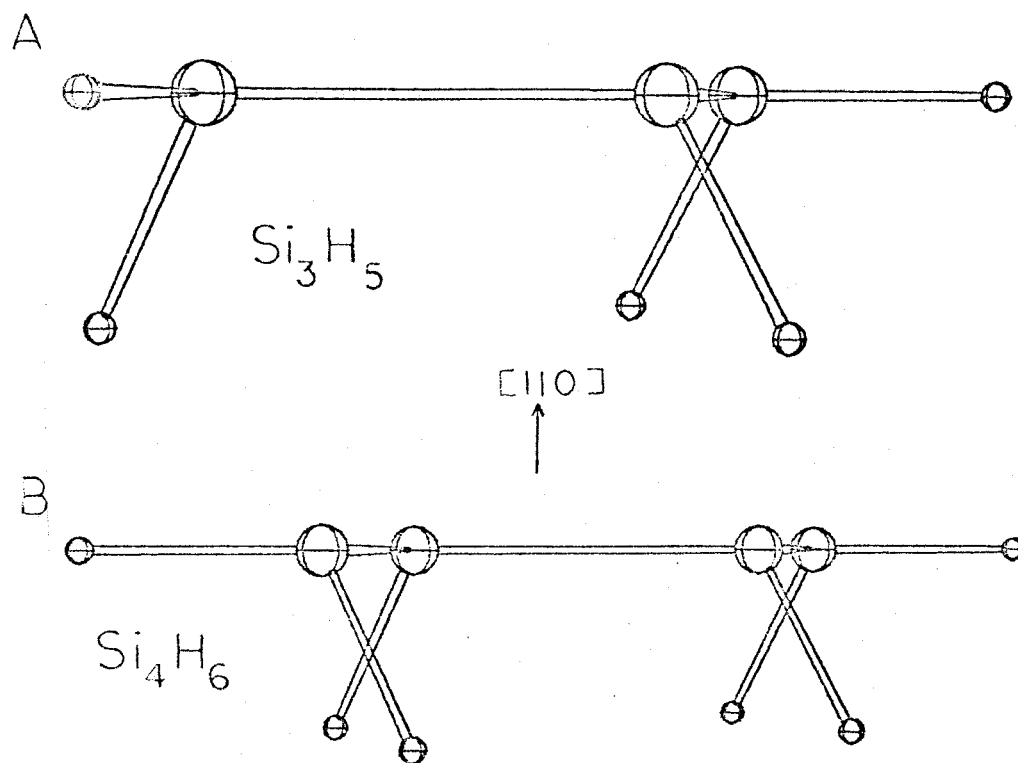


Fig. 19 Geometry for Three and Four Silicon Clusters Modeling the (110) Surface. (a) Si_3H_5 . (b) Si_4H_6 .

Table XII Comparison of Energies for the Si_2H_4 Cluster Model of (110) Surfaces.^a Energies are in hartrees.

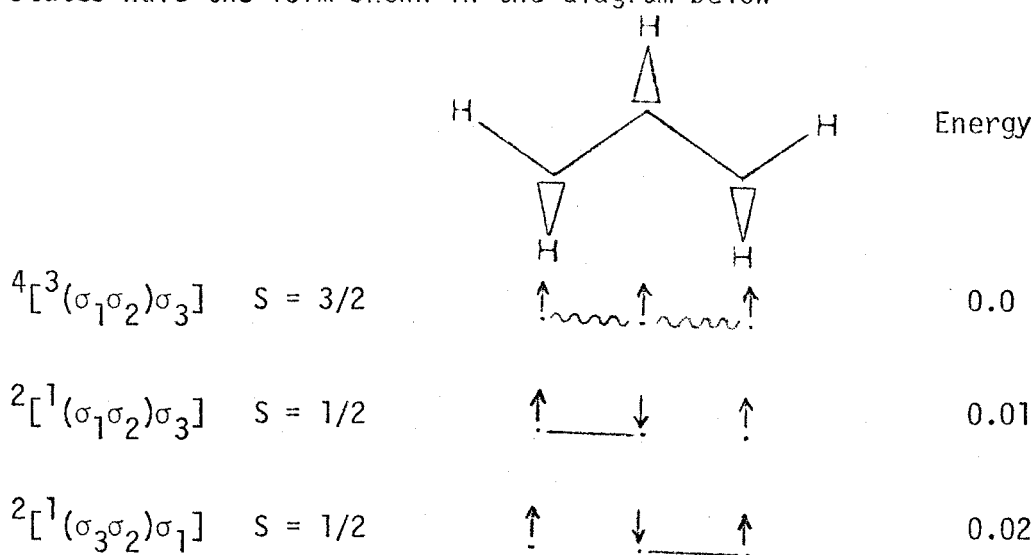
State and Wavefunction	Geometry	
	Dangling Bands Point- ing in Opposite Directions (tetrahedral)	Dangling Bands Point- ing in Parallel Directions (eclipsed)
$^1(\sigma_1\sigma_2)\text{GVB}(1)$	-9.659599 (0.23)	-9.668258 (0.0)
$^3(\sigma_1\sigma_2)\text{HF}$	-9.663312 (0.13)	-9.661324 (0.19)

^aValues in parentheses are the energies in eV measured with respect to the ground state $^1(\sigma_1\sigma_2)$ of the eclipsed geometry.

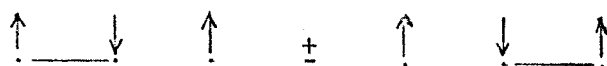
ground state singlet of the eclipsed geometry is lower than the triplet $^3(\sigma_1\sigma_2)$ of the tetrahedral geometry by 0.13 eV. This means that singlet coupling of adjacent dangling bonds on the Si (110) surface is at least possible for a non-tetrahedral geometry. This can be a cause for some of the rearrangement that the surface suffers.

In the (110) surface there are infinite chains of such atoms and in order to study the effects of coupling more than two together, we considered complexes with three and four silicons.

With three Si (Si_3H_5 complex shown in Fig. 19) the low lying states have the form shown in the diagram below



Here a $\uparrow \text{---} \downarrow$ indicates singlet pairing of two orbitals, while a $\uparrow \text{~~~~} \uparrow$ indicates triplet pairing. Note that two different doublet states can be obtained from three electron systems, which can be described as the resonant and anti-resonant states

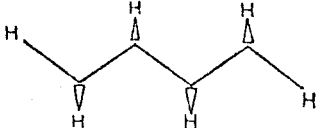
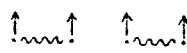
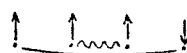
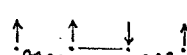
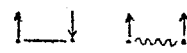
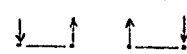
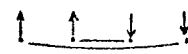


or in terms of wavefunctions, as

$$\{[\sigma_1(1)\sigma_2(2)\sigma_3(3) \pm \sigma_3(1)\sigma_2(2)\sigma_1(3)][\alpha(1)\beta(2) - \beta(1)\alpha(2)]\alpha(3)\}.$$

As expected from the Si_2H_4 results, the undisturbed surface leads to a high spin ground state.

For four Si (Si_4H_6 complex shown in Fig. 19) the low lying states (for the undisturbed surface) have the form

		Energy	Average
			
$^5[{}^3(\sigma_1\sigma_2){}^3(\sigma_3\sigma_4)] \quad S = 2$		0.0	0.0
$^3[{}^1(\sigma_1\sigma_4){}^3(\sigma_2\sigma_3)] \quad S = 1$		0.05	
$^3[{}^1(\sigma_1\sigma_2){}^1(\sigma_3\sigma_4)] \quad S = 1$		0.14	0.13
$^3[{}^3(\sigma_1\sigma_4){}^1(\sigma_2\sigma_3)] \quad S = 1$		0.21	
$^1[{}^1(\sigma_1\sigma_2){}^1(\sigma_3\sigma_4)] \quad S = 0$		0.10	
$^1[{}^1(\sigma_1\sigma_4){}^1(\sigma_2\sigma_3)] \quad S = 0$		0.10	0.10

Note that one electron in each of the four orbitals leads to one quintet ($S = 2$), three triplet ($S = 1$) and two singlet ($S = 0$) states. Again, the ground state is the high spin state, but the excitation energies are smaller than for the 3 and 2 silicon cases. These results are also shown in Table XIII.

For both the Si_3H_5 and Si_4H_6 clusters, correlation effects are important for all states that have at least one pair of dangling bond orbitals coupled into a singlet. In this case a closed-shell Hartree-Fock wavefunction would put both electrons in the same orbital spread over both centers which, even for adjacent centers, leads to considerable error.⁵⁶ The effect is more pronounced in the case in which two pairs of electrons are singlet coupled, as in $^1[{}^1(\sigma_1\sigma_2){}^1(\sigma_3\sigma_4)]$.

Computational Details

Only self-consistent field calculations were performed at the GVB level for the Si_2H_4 complex. The two geometries chosen are shown in Fig. 18. The double zeta (DZ) basis of Table XI of Chapter I was used. The general form of the wavefunction is that of (13) with

$$^1(\sigma_1\sigma_2): \quad \Phi_{\text{surf}} = [\phi_1(1)\phi_2(2) + \phi_2(1)\phi_1(2)][\alpha(1)\beta(2) - \beta(1)\alpha(2)]$$

$$^3(\sigma_1\sigma_2): \quad \Phi_{\text{surf}} = [\phi_1(1)\phi_2(2) - \phi_2(1)\phi_1(2)][\alpha(1)\beta(2) + \beta(1)\alpha(2)] .$$

For Si_3H_5 and Si_4H_6 the geometry used in all the calculations was the unreconstructed tetrahedral one. Two types of calculations were

Table XIII. Energies Relating to the Si_3H_5 and Si_4H_6 Cluster Model of (110) Si Surfaces.

All energies are in hartrees; the tetrahedral unrelaxed geometry was used.

Si_3H_5			Si_4H_6		
State and SCF Wavefunction ^a	Energy		State and SCF Wavefunction ^a	Energy	
	SCF	CI		SCF	CI
$4[{}^3(\sigma_1\sigma_2)\sigma_3]\text{HF}$	-13.938200	-13.938264	$5[{}^3(\sigma_1\sigma_2)^3(\sigma_3\sigma_4)]\text{HF}$	-18.213504	-18.213581
$2[{}^1(\sigma_1\sigma_2)\sigma_3]\text{SOGVB}^b$	-13.932513	-13.931669	$3[{}^1(\sigma_1\sigma_4)^3(\sigma_2\sigma_3)]$ GVB(1)	-18.210690	-18.211828
$2[{}^1(\sigma_1\sigma_2)\sigma_3]\text{GVB}(1)$	-13.875002	-	$3[{}^3(\sigma_1\sigma_4)^1(\sigma_2\sigma_3)]$ GVB(1)	-18.207477	-18.208491
$2[{}^1(\sigma_1\sigma_2)\sigma_3]\text{HF}$	-13.834889	-	$1[{}^1(\sigma_1\sigma_4)^1(\sigma_2\sigma_3)]$ GVB(2)	-18.207472	-18.209890
			$1[{}^1(\sigma_1\sigma_2)^1(\sigma_3\sigma_4)]$ GVB(2)	-18.205048	-18.202889

^aSee text for an explanation of the symbols in this column.

^bThis is an SOGVB wavefunction in which spin coupling optimization is incorporated to the self-consistent-field equations [see F. Bobrowicz, Ph.D. Thesis, California Institute of Technology, 1973 (unpublished)].

performed on both clusters. In the first case self-consistent GVB level wavefunctions were utilized. The second kind was a CI wavefunction in which a full CI was performed over the dangling bond space of the high spin state of each cluster ($^4[{}^3(\sigma_1\sigma_2)\sigma_3]$ for Si_3H_5 and $^5[{}^3(\sigma_1\sigma_2)^3(\sigma_3\sigma_4)]$ for Si_4H_6) augmented by the dangling bond space of the lowest energy low spin state ($^2[{}^1(\sigma_1\sigma_2)\sigma_3]$ for Si_3H_5 and $^1[{}^1(\sigma_1\sigma_2)^1(\sigma_3\sigma_4)]$ for Si_4H_6). The general form of the wavefunctions for the states of the Si_3H_5 cluster at the GVB level is

$$\Phi = \mathcal{A}\{\Phi_{\text{bulk}} \Phi_{\text{surf}}\} \quad , \quad (13)$$

where Φ_{bulk} is the wavefunction for the Si-H and Si-Si bond pairs; Φ_{surf} is the wavefunction for the dangling bond electrons with the form shown below

$$\begin{aligned} {}^4[{}^3(\sigma_1\sigma_2)\sigma_3]: \quad \Phi_{\text{surf}} &= \phi_1(1)\phi_2(2)\phi_3(3) \alpha(1)\alpha(2)\alpha(3) \\ {}^2[{}^1(\sigma_1\sigma_2)\sigma_3]: \quad \Phi_{\text{surf}} &= [\phi_1(1)\phi_2(2) + \phi_2(1)\phi_1(2)][\alpha(1)\beta(2) \\ &\quad - \beta(2)\alpha(1)] \phi_3(3)\alpha(3) \end{aligned}$$

For the Si_4H_6 cluster the GVB level wavefunction has the form (13), with Φ_{surf} having the form shown below for the different states:

$$\begin{aligned} {}^5[{}^3(\sigma_1\sigma_2)^3(\sigma_3\sigma_4)]: \quad \Phi_{\text{surf}} &= \phi_1(1)\phi_2(2)\phi_3(3)\phi_4(4)\alpha(1)\alpha(2)\alpha(3)\alpha(4) \\ {}^3[{}^1(\sigma_1\sigma_4)^3(\sigma_2\sigma_3)]: \quad \Phi_{\text{surf}} &= [\phi_1(1)\phi_4(2) - \phi_4(1)\phi_1(2)][\alpha(1)\beta(2) \\ &\quad - \beta(1)\alpha(2)] \phi_2(3)\phi_3(4)\alpha(3)\alpha(4) \end{aligned}$$

$$^3[{}^1(\sigma_1\sigma_2){}^3(\sigma_3\sigma_4)]: \Phi_{\text{surf}} = [\phi_1(1)\phi_2(2) + \phi_2(1)\phi_1(2)][\alpha(1)\beta(2) - \beta(1)\alpha(2)]\phi_3(3)\phi_4(4)\alpha(3)\alpha(4)$$

$$^1[{}^1(\sigma_1\sigma_2){}^1(\sigma_3\sigma_4)]: \Phi_{\text{surf}} = [\phi_1(1)\phi_2(2) + \phi_2(1)\phi_1(2)][\alpha(1)\beta(2) - \beta(1)\alpha(2)] \times [\phi_3(3)\phi_4(4) + \phi_4(3)\phi_3(4)][\alpha(3)\beta(4) - \beta(3)\alpha(4)]$$

$$^1[{}^1(\sigma_1\sigma_4){}^1(\sigma_2\sigma_3)]: \Phi_{\text{surf}} = [\phi_1(1)\phi_4(2) + \phi_4(1)\phi_1(2)][\alpha(1)\beta(2) - \beta(1)\alpha(2)] \times [\phi_2(3)\phi_3(4) + \phi_3(3)\phi_2(4)][\alpha(3)\beta(4) - \beta(3)\alpha(4)]$$

The basis set used was the double zeta (DZ) set of Table XI of Chapter 1.

For the $^2[{}^1(\sigma_1\sigma_2)\sigma_3]$ we have also performed SOGVB calculations⁵⁷ in which the spin coupling is optimized concurrently with the self-consistent solution of the orbitals. The wavefunction has the form (13) with

$$\Phi_{\text{surf}} = \phi_1(1)\phi_2(2)\phi_3(3) \{c_1[\alpha(1)\beta(2) - \beta(1)\alpha(2)]\alpha(3) + c_2[2\alpha(1)\alpha(2)\beta(3) - [\alpha(1)\beta(2) + \beta(1)\alpha(2)]\alpha(3)]\}$$

where $c_1^2 + c_2^2 = 1$.

D. Review of Experimental Data

Several LEED structures have been observed, in general it is agreed that this surface also suffers reconstruction. The different LEED structures include^{52a,58} 2x1, 5x1, 7(or 9)x1, 4x5 and 5x2 depending on the annealing process. Jona^{52a} could not find a recipe for the

preparation of the above structures in a reproducible way. The only general statement that could be made was that the 5×1 structure was likely to appear at high temperatures ($T > 1000^\circ\text{C}$). The high temperatures used in the cleaning and annealing process introduce the possibility of impurities at the surface. These can possibly come⁶ from the bulk by diffusion or from the ambient. Sakurai and Hagstrum⁵⁹ have recently determined by hydrogen chemisorption, that the 5×1 reconstruction is likely to be due to relaxation or slight motion of the surface Si atoms, rather than due to surface vacancies. (They concluded this from the observation that when the 5×1 structure is exposed to H atoms at 350°C the pattern is replaced by a 1×1 pattern).

The experimental situation for this surface, other than what was mentioned above, is in a relatively poor status, as compared with the (111) surface and even with the (100) surface. Due to the experimental uncertainty, no models for the reconstruction have been put forth in the literature.

REFERENCES FOR CHAPTER 2

1. See, for example, S. G. Davison and J. D. Levine, *Solid State Phys.* 25, 1 (1970).
2. (a) W. J. Hunt, P. J. Hay and W. A. Goddard III, *J. Chem. Phys.* 57, 738 (1972); (b) W. A. Goddard III, T. H. Dunning, Jr., W. J. Hunt and P. J. Hay, *Accts. Chem. Res.* 6, 368 (1973); see also Appendix A.
3. B. J. Moss and W. A. Goddard III, *J. Chem. Phys.* 63, 3523 (1975).
4. M. E. Straumanis and E. Z. Aka, *J. Appl. Phys.* 23, 330 (1952).
5. D. R. Boyd, *J. Chem. Phys.* 23, 922 (1955).
6. D. Haneman in Surface Physics of Phosphors and Semiconductors, C. G. Scott and C. E. Reed, eds. (Academic Press, New York, 1975), p. 1, and references cited therein.
7. Many excellent reviews on LEED are available, we only list a few; (a) J. B. Pendry, Low Energy Electron Diffraction (Academic Press, New York, 1974); (b) C. B. Duke, *Adv. Chem. Phys.* 27, 1 (1974); (c) J. A. Strotzier, Jr., D. W. Jepsen and F. Jona, in Surface Physics of Materials, J. M. Blakeley, ed. (Academic Press, New York, 1975), Vol. I, p. 1.
8. A. Redondo, W. A. Goddard III, T. C. McGill and G. T. Surratt, *Solid State Comm.*, in press.
9. G. T. Surratt, Ph.D. Thesis, California Institute of Technology, 1975 (unpublished).
10. (a) D. E. Eastman and W. D. Grobman, *Phys. Rev. Lett.* 28, 1378 (1972); (b) L. F. Wagner and W. E. Spicer, *Phys. Rev. Lett.* 28, 1381 (1972); (c) F. G. Allen and W. Gobeli, *Phys. Rev.* 127, 150 (1962).

11. L. Pauling, The Nature of the Chemical Bond (Cornell Univ. Press, Ithaca, New York, 1960), p. 239.
12. H. D. Shih, F. Jona, D. W. Jepsen and P. Marcus, to be published.
13. (a) To find h we evaluated $\langle z \rangle$ and $\langle z^2 \rangle$ for the dangling bond orbital.
(b) See, for example, L. D. Landau and E. M. Lifshitz, Electrodynamics of Continuous Media (Addison-Wesley, Reading, Mass., 1960), p. 52. The results for the present case are derived in Appendix B; see also Ref. 9, p. 169.
14. This point is explained in detail in W. A. Goddard III, Lecture Notes for Chem. 120, California Institute of Technology, 1975 (unpublished).
15. In the expression for E_0 , h is the one-electron part of the Hamiltonian, including the kinetic and potential energy terms. $J_{\ell r}$ is the Coulomb energy integral, given by

$$J_{\ell r} = \langle \phi_{\ell}(1) \phi_r(2) | \frac{1}{r_{12}} | \phi_{\ell}(1) \phi_r(2) \rangle .$$

In the expression for E_x , $K_{\ell r}$ is the exchange energy integral,

$$K_{\ell r} = \langle \phi_{\ell}(1) \phi_r(2) | \frac{1}{r_{12}} | \phi_r(1) \phi_{\ell}(2) \rangle .$$

16. Using the DZ basis for the unrelaxed geometry, this value is 2.948 eV, while for the relaxed geometry it is 2.978 eV.
17. (a) F. Meyer and M. J. Sparnaay, in Surface Physics of Phosphors and Semiconductors, C. G. Scott and C. E. Reed, eds. (Academic Press, New York, 1975), p. 321; (b) J. A. Strozier, Jr., D. W. Jepsen and F. Jona, in Surface Physics of Materials, J. M. Blakeley,

- ed. (Academic Press, New York, 1975), Vol. 1, p. 1, and references cited therein.
18. (a) F. Bauerle, W. Monch and M. Henzler, J. Appl. Phys. 43, 3917 (1972); (b) M. Erbudak and T. E. Fischer, Phys. Rev. Lett. 29, 732 (1972).
 19. J. J. Scheer and J. van Laar, Solid State Comm. 3, 189 (1965).
 20. R. C. Eden, Proc. 10th Int. Conf. on Semiconductors, Cambridge, Mass. p. 22 (1970), quoted in Ref. 6.
 21. (a) J. E. Rowe, Phys. Lett. A46, 400 (1974); (b) J. E. Rowe and H. Ibach, Phys. Rev. Lett. 32, 421 (1974).
 22. B. F. Lewis and T. E. Fischer, Surf. Sci. 40, 371 (1974).
 23. H. D. Hagstrum and G. E. Becker, Phys. Rev. B 8, 1580, 1592 (1973).
 24. (a) G. Chiarotti, G. Del Signore and S. Nannarone, Phys. Rev. B 4, 3398 (1971); (b) G. Chiarotti, P. Chiaradia and S. Nannarone, Surf. Sci. 49, 315 (1975); (c) G. Chiarotti, G. Del Signore and S. Nannarone, Phys. Rev. Lett. 21, 1170 (1968); (d) P. Chiaradia and S. Nannarone, Surf. Sci. 54, 547 (1976).
 25. W. Müller and W. Mönch, Phys. Rev. Lett. 27, 250 (1971).
 26. F. Meyer, Phys. Rev. B 9, 3622 (1974); see also Ref. 17a, where further references are quoted.
 27. J. E. Rowe and H. Ibach, Phys. Rev. Lett. 31, 102 (1973).
 28. D. Haneman, Phys. Rev. 121, 1093 (1961); see also Ref. 6.
 29. (a) D. Haneman, Phys. Rev. 170, 705 (1968); (b) M. F. Chung and D. Haneman, J. Appl. Phys. 37, 1879 (1966); (c) D. Haneman, Jap. J. Appl. Phys., Suppl. 2, Pt. 2, 371 (1974) and references cited therein.

30. (a) D. Kaplan, D. Lepine, Y. Petroff and P. Thirry, Phys. Rev. Lett. 35, 1376 (1975); (b) B. P. Lemke and D. Haneman, ibid 35, 1379 (1975); (c) D. Haneman, talk presented at the American Chemical Society Centennial Meeting, San Francisco, California, August 30, 1976.
31. D. Haneman and D. L. Heron in The Structure and Chemistry of Solid Surfaces, G. Somorjai, ed. (Wiley, New York, 1969), p. 24.
32. J. J. Lander and J. Morrison, J. Appl. Phys. 34, 1403, 3517 (1963).
33. (a) I. Tamm, Phys. Z. Sowj. Un. 1, 733 (1932); (b) W. Shockley, Phys. Rev. 56, 317 (1939).
34. I. P. Batra and S. Ciraci, Phys. Rev. Lett. 34, 1337 (1975).
35. (a) K. H. Johnson, J. Chem. Phys. 45, 3085 (1966); (b) J. C. Slater and K. H. Johnson, Phys. Rev. B 5, 844 (1972); (c) K. H. Johnson and F. C. Smith, Jr., Phys. Rev. B 5, 831 (1972); (d) J. C. Slater, Adv. Quantum Chem. 6, 1 (1972).
36. (a) K. C. Pandey and J. C. Phillips, Phys. Rev. Lett. 32, 1433 (1974); (b) V. Bortolani, C. Calandra and M. J. Kelly, J. Phys. C 6, L349 (1973).
37. (a) W. A. Harrison, Surf. Sci. 55, 1 (1976); (b) S. Ciraci, I. P. Batra and W. A. Tiller, Phys. Rev. B 12, 5811 (1975); (c) S. Ciraci and I. P. Batra, Solid State Comm. 18, 1149 (1976).
38. (a) R. O. Jones, J. Phys. C 5, 1615 (1972); (b) J. A. Appelbaum and D. R. Hamann, Phys. Rev. Lett. 31, 106 (1973); (c) R. O. Jones in Surface Physics of Phosphors and Semiconductors, C. G. Scott and C. E. Reed, eds. (Academic Press, New York, 1975) p. 95 and references cited therein.

39. (a) J. A. Appelbaum and D. R. Hamann, Phys. Rev. B 6, 2166 (1972); (b) idem, Phys. Rev. Lett. 32, 225 (1974); (c) idem, Phys. Rev. B 12, 1410 (1975); (d) idem, Rev. Mod. Phys. 48, 479 (1976).
40. (a) M. Schluter, J. R. Chelikowsky, S. G. Louie and M. L. Cohen, Phys. Rev. Lett. 34, 1385 (1975); (b) idem, Phys. Rev. B 12, 4200 (1975).
41. E. P. Wigner, Phys. Rev. 46, 1002 (1934).
42. J. A. Appelbaum and D. R. Hamann, Phys. Rev. B 8, 1777 (1973).
43. M. von Laue, Phys. Rev. 37, 53 (1931).
44. This is well known for molecular systems and is well documented in the literature (see Refs. 2 and 3, for example). For infinite or semi-infinite systems there are few examples in which proper account of electron correlation has been taken. One such system is the jellium model of electrons in a metal (a free electron gas which is assumed to move in the potential created by a uniform background of positive charge, adjusted so that the system has zero net charge). Wigner has shown (Ref. 41) that the effect of correlation can have a magnitude of several eV in this system. This is large enough to considerably affect the resulting theoretical electronic structures; this is particularly acute in the case of wavefunctions using double occupancy of the orbitals [see for example, R. P. Messmer and D. R. Salahub, J. Chem. Phys. 65, 779 (1976)].
45. J. D. Levine, Surf. Sci. 34, 90 (1973).

46. Here σ and π represent orbitals that are symmetric and anti-symmetric, respectively, relative to the Si-Si-Si plane.
47. G. Herzberg, Electronic Spectra and Electronic Structure of Polyatomic Molecules (Van Nostrand-Reinhold, New York, 1966), Table 62, p. 584.
48. (a) I. Dubois, G. Herzberg and R. D. Verma, J. Chem. Phys. 47, 4262 (1967); (b) B. Wirsam, Chem. Phys. Lett. 14, 214 (1972); (c) H. Burger and R. Eujen, Topics in Current Chem. (Silicon Chemistry I) 50, 1 (1974).
49. Hybridizations are obtained from Mulliken population analysis [R. S. Mulliken, J. Chem. Phys. 23, 1833, 1841 (1955)]. We did not renormalize and hence the sum of the $s^x p^y d^z$ exponent ($x+y+z$) indicates the percentage character on the surface atom.
50. R. E. Schlier and H. E. Farnsworth, J. Chem. Phys. 30, 917 (1959).
51. R. D. Verma and P. A. Warsop, Can. J. Phys. 41, 152 (1963).
52. (a) F. Jona, IBM J. Res. Dev. 9, 375 (1965); (b) B. Goldstein, Surf. Sci. 35, 227 (1973).
53. (a) J. J. Lander and J. Morrison, J. Appl. Phys. 34, 1403, 3517 (1963); (b) R. E. Weber and W. T. Peria, Surf. Sci. 14, 13 (1969).
54. LEED calculations for this model do not seem to agree with the experimental spectra; M. van Hove, private communication.
55. T. Sakurai and H. D. Hagstrum, Phys. Rev. B 14, 1593 (1976).
56. See parts I and II of this chapter for a more complete discussion of these effects.
57. F. Bobrowicz, Ph.D. Thesis, California Institute of Technology, 1973 (unpublished).

58. G. O. Krause, Phys. Stat. Sol. 35, K59 (1969).
59. T. Sakurai and H. D. Hagstrum, J. Vac. Sci. Technol. 13, 807 (1976).

Chapter 3

ELECTRONIC STRUCTURE OF STEPS ON (111) SILICON SURFACES

A. Introduction

An important aspect of real cleaved semiconductor surfaces is the presence of steps. Such steps lead to significant modifications of the electronic and mechanical properties and the chemical reactivity¹, as compared with the behavior expected of an ideal cleaved surface. Unfortunately, due to significant experimental and theoretical difficulties, little is known about the microscopic structure at steps. Experimentally, major difficulties are reproducibility in forming the steps and in separating the properties due to the steps from those of the perfect surface and the bulk. Major theoretical problems are: (i) lack of symmetry (even lower than that of a perfect surface) and (ii) the importance of electron correlation effects in the resulting localized electronic states. As in the calculations described in the previous chapter, our approach has been to include the electronic correlation explicitly but to replace the semi-infinite solid with a finite cluster of atoms.

As described in Chapter 2, the cleavage face of silicon crystals is the (111) surface. For (111) surfaces two types of steps are possible: those in which the edges consist of atoms with three nearest neighbors (trivalent) and those whose edges consist of atoms with two nearest neighbors (divalent). The edges toward the three $[1\bar{1}2]$ directions consist of trivalent atoms, whereas the edges toward the $[\bar{1}\bar{1}2]$ directions are divalent. Both sets of directions have been

distinguished experimentally^{1a} by X-ray diffraction. Henzler^{1a} has determined that, upon cleaving, only one of these types is preferred. This type has been found to have edges toward the $[\bar{1}\bar{1}2]$ direction. In other words, experimentally only the steps with divalent Si atoms at the edges are observed (this is shown in Fig. 1). For this reason we have concentrated our efforts on calculations that model steps with divalent silicon atoms.

The calculations to be described in the present chapter were performed on Si_3H_5 and Si_3H_4 clusters. The Si_3H_5 cluster models the basic divalent step in which the edge atom is divalent (central atom of the complex). It is bound to a "bulk" atom and to a trivalent, upper terrace atom with a dangling bond. This complex can then be denoted by $\text{H}_2\dot{\text{Si}}-\ddot{\text{Si}}-\text{SiH}_3$, where $\text{H}_2\dot{\text{Si}}$ represents the upper terrace atoms (the hydrogens substitute other silicons as in previous chapters), and $-\text{SiH}_3$ represents the "bulk" atoms on the lower terrace (again hydrogens replace silicons as before). This complex is indicated in Fig. 1 by a cross hatching of the appropriate atoms. By binding other silicon atoms between two adjacent divalent edge atoms in a step we can also produce "kinks" on the steps. These are modelled by $\text{H}_2\text{Si}-\dot{\text{Si}}-\dot{\text{Si}}\text{H}_2$ clusters as shown in Fig. 2. A similar structure to that of the (100) surface can be constructed on the edges of the divalent steps. These are shown in Fig. 3. We will use the results on Si_3H_6 clusters discussed in Chapter 2 to describe the electronic structure of such atomic configurations. Finally, we will briefly consider the trivalent silicon atom steps (those toward the $[1\bar{1}2]$ directions), by

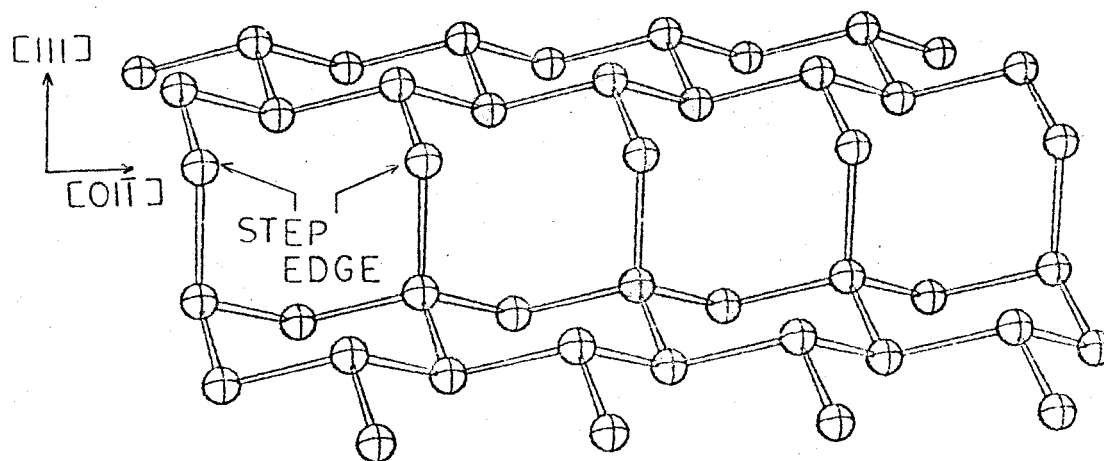


Fig. 1 Divalent Step Geometry. Shaded atoms are those represented in the Si_3H_5 cluster.

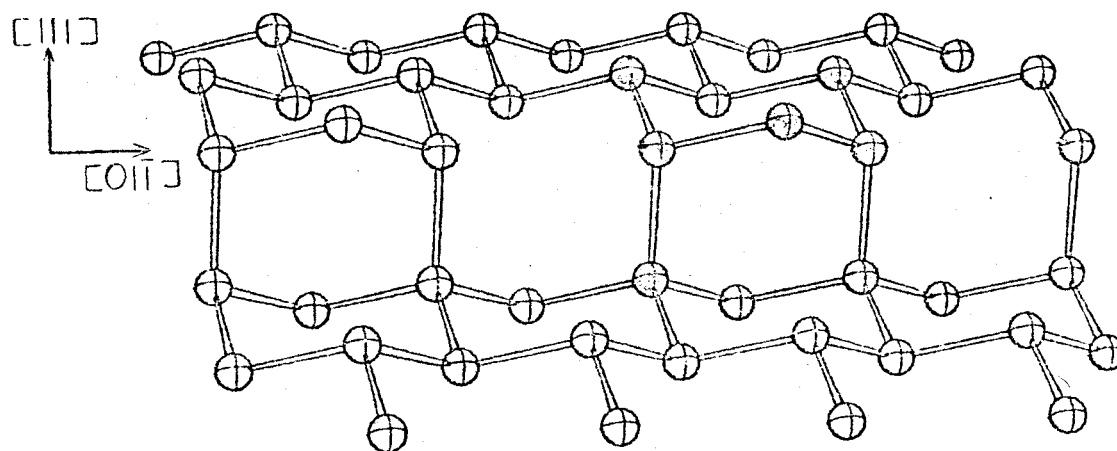


Fig. 2 Additional Configuration Possibly Present at Divalent Steps on Si (111) Surfaces. Shaded atoms are those represented in the Si_3H_4 Cluster.

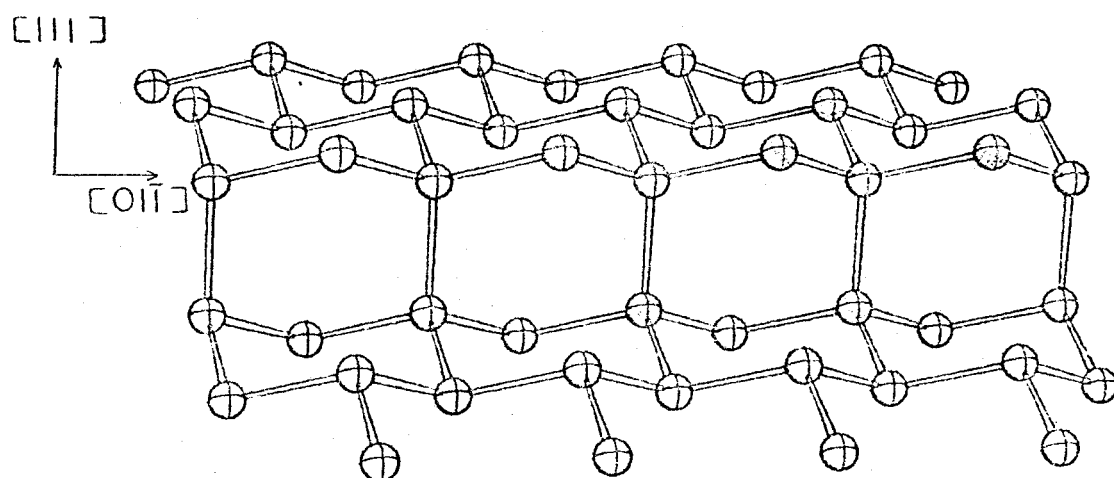


Fig. 3 Divalent Step Configuration Similar to that in Si (100) Surfaces. Shaded atoms are those represented in the Si_3H_6 Cluster.

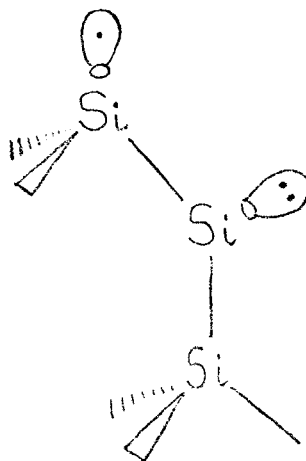
recalling the results of our calculations that model the (110) surface. (The steps with trivalent edge atoms have the same configuration as atoms on (110) surfaces.)

B. Divalent Steps on Si (111) Surfaces: Basic Step Configuration

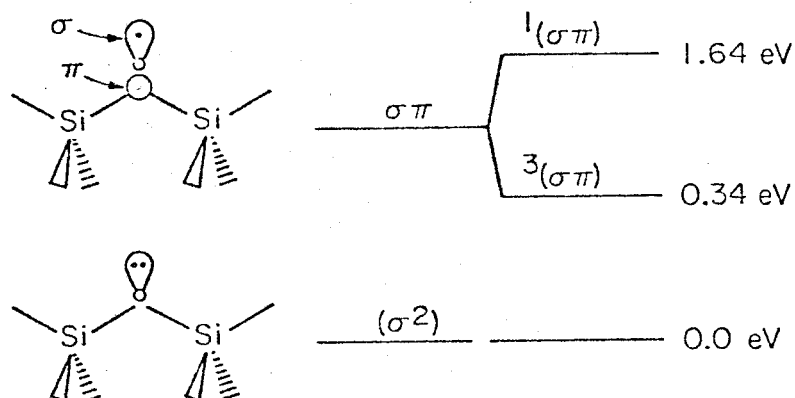
Summary

All the configurations for the step with divalent edge atoms or any of the combinations obtained by binding new Si atoms bridging two divalent step atoms have an electronic structure dominated by the divalent atom. As discussed in Chapter 2, a divalent Si on (100) surfaces (the same basic configuration as in the present case) leads to two low lying electronic configurations (see Fig. 4a): a $^1(\sigma^2)$ ground state (optimum bond angle of 105.4°) and a $^3(\sigma\pi)$ excited state with 0.34 eV vertical excitation energy and 0.18 eV adiabatic excitation energy (optimum bond angle of 111.5°).

In the (111) divalent step (geometry sketched in Fig. 1) each divalent atom is bonded to a trivalent surface atom leading to a structure of the form



A. DIVALENT SURFACE Si



B. DIVALENT STEP Si AT (111) SURFACE

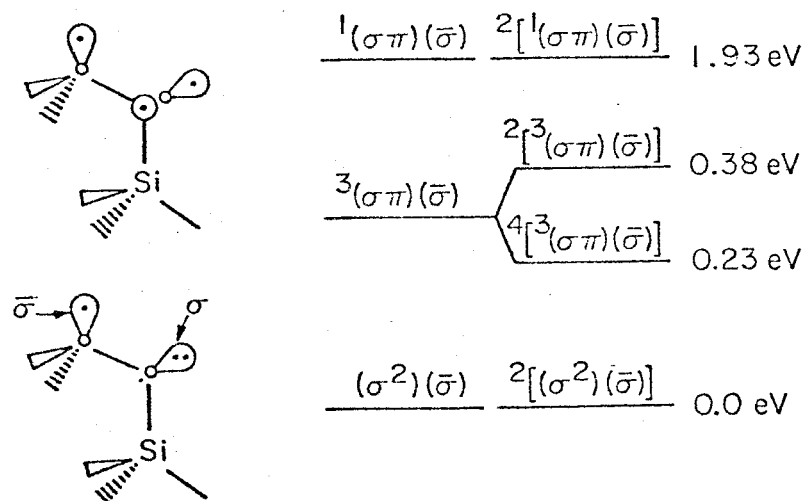


Fig. 4 Schematic of the Electronic States at Divalent Steps on Si (111) Surfaces. (a) Basic divalent configuration, Si_3H_6 cluster. (b) Divalent step, Si_3H_5 cluster. A circle represents a p-like orbital coming out of the paper; a lobe represents a σ orbital in the plane of the paper; dots represent the number of electrons for each orbital. Energies are not drawn to scale.

The electronic states expected for this complex are outlined in Fig.

4b. Three low lying states result:

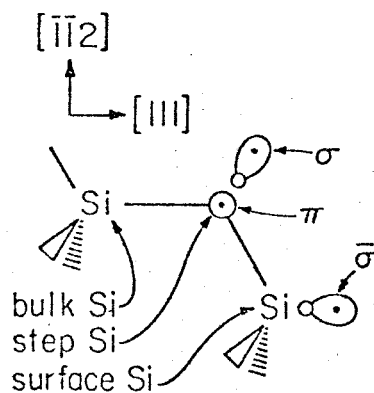
$^3_{(\sigma\pi)(\bar{\sigma})}$: Starting with the $^3_{(\sigma\pi)}$ state of the divalent Si, we couple the $\bar{\sigma}$ dangling bond orbital of the upper terrace surface Si in two different ways, leading to quartet ($S = 3/2$) and doublet ($S = 1/2$) states, denoted $^4[{}^3_{(\sigma\pi)(\bar{\sigma})}]$ and $^2[{}^3_{(\sigma\pi)(\bar{\sigma})}]$, respectively. If the overlap between the σ and $\bar{\sigma}$ orbitals is small, the quartet is expected to be lower in energy.

$^1_{(\sigma\pi)(\bar{\sigma})}$: There is one additional $(\sigma\pi)(\bar{\sigma})$ state, corresponding to the $^1_{(\sigma\pi)}$ states of the divalent silicon. The new dangling bond, $\bar{\sigma}$, necessarily couples as a doublet with the $^1_{(\sigma\pi)}$ electrons leading to an overall doublet spin coupling ($S = 1/2$). This state is denoted $^2[{}^1_{(\sigma\pi)(\bar{\sigma})}]$.

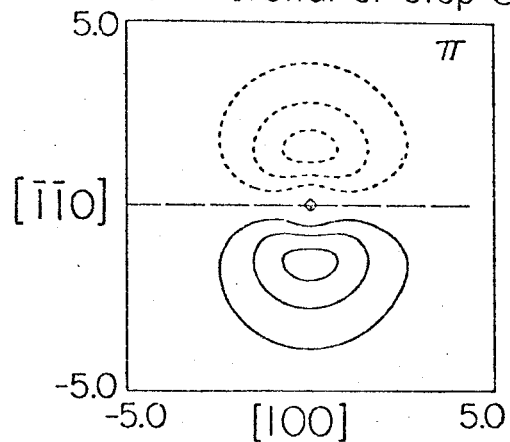
$^1_{(\sigma^2)(\bar{\sigma})}$: The $^1_{(\sigma^2)}$ ground state of the divalent Si is coupled to the dangling bond orbital, $\bar{\sigma}$, of the surface with an overall doublet spin ($S = 1/2$). This state is denoted $^2[{}^1_{(\sigma^2)(\bar{\sigma})}]$.

The results of self consistent field and configuration interaction (CI) calculations are shown in Tables I and II. In Fig. 5 we plotted the σ, π and $\bar{\sigma}$ orbitals of the $^4[{}^3_{(\sigma\pi)(\bar{\sigma})}]$ state. We see that the ground state of the system is the $^2[{}^1_{(\sigma^2)(\bar{\sigma})}]$ (which is to be expected since $^1_{(\sigma^2)}$ is the ground state of the divalent Si). For the $^3_{(\sigma\pi)(\bar{\sigma})}$ states the overlap of the σ and $\bar{\sigma}$ orbitals on the step and surface atoms is quite small ($\langle\sigma|\bar{\sigma}\rangle = 0.12$) and hence, of the two overall spin couplings, the quartet is the lowest with a vertical excitation

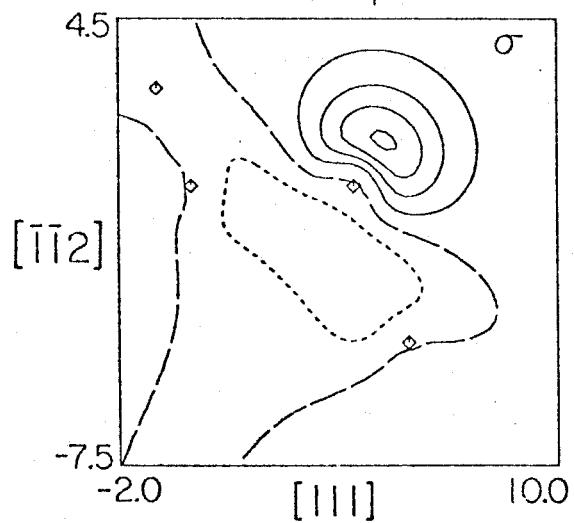
A. $\text{H}_3\text{Si}-\ddot{\text{Si}}-\ddot{\text{Si}}\text{H}_2$ Schematic



B. π orbital of step Si



C. σ orbital of step Si



D. $\bar{\sigma}$ orbital of surface Si

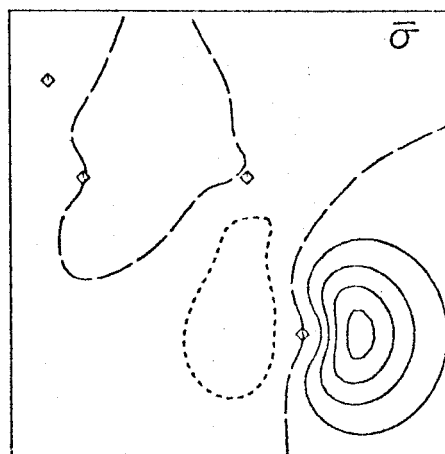


Fig. 5

Nodal surfaces are indicated by long dashes, solid lines indicate positive amplitude values, short dashes indicate negative amplitude values. Contours are drawn every 0.05 atomic unit. Atoms are denoted by an asterisk.

Table I. Quantities Relating to the $\text{H}_2\text{Si-Si-SiH}_3$ Cluster Model of Divalent Steps.
Consistent-Field Calculations. All energies are in hartrees unless otherwise stated.

	Total Energies			Optimum Energy ^a	Optimum Angle (°)	Vertical Excitation Energy(eV)	Adiabatic Excitation Energy(eV)
	100°	105°	109°28'	115°			
$2[(\sigma^2)(\bar{\sigma})]$ GVB(1) ^b	-14.014613	-14.014743	-14.012044	-14.005206	102.68	0.0	0.0
$4[{}^3(\sigma\pi)(\bar{\sigma})]$ HF	-14.003247	-14.009605	-14.012464	-14.012377	112.11	0.218	0.060
$2[{}^3(\sigma\pi)(\bar{\sigma})]$ GVB(1) ^c	-13.986270	-13.989345	-13.991456	-13.991486	112.41	0.739	0.630

^aObtained by a cubic splines fit to the calculated points

^bThe HF energy for this state at 109°28' is 0.54 eV higher than the GVB(1) value at the same point.

^cThe HF energy for this state at 109°28' is 1.64 eV higher than the corresponding GVB(1) value at the same point.

Table II. Quantities Relating to the $\text{H}\ddot{\text{Si}}\text{-Si-SiH}_3$ Cluster Model of Divalent Steps. GVB CI Calculations. All energies are in hartrees unless otherwise stated.

	Total Energies			Optimum Energy ^a	Optimum Angle (°)	Vertical Excitation Energy(eV)	Adiabatic Excitation Energy(eV)
	100°	105°	109°28'	115°			
$2[(\sigma^2)(\bar{\sigma})]$	-14.01499	-14.01510	-14.01241	-14.00563	102.65	0.0	0.0
$4[{}^3(\sigma\pi)(\bar{\sigma})]$	-14.00331	-14.00966	-14.01252	-14.01244	112.12	0.226	0.068
$2[{}^3(\sigma\pi)(\bar{\sigma})]$	-13.99859	-14.00334	-14.00559	-14.00526	111.78	0.382	0.260
$2[{}^1(\sigma\pi)(\bar{\sigma})]$	-13.94081	-13.94704	-13.95071	-13.95195	113.90	1.934	1.726

^aObtained from a cubic splines fit to the calculated points.

energy of 0.23 eV and an adiabatic excitation energy of 0.07 eV. The $^2[{}^3(\sigma\pi)(\bar{\sigma})]$ state is only 0.15 eV higher than the $^4[{}^3(\sigma\pi)(\bar{\sigma})]$ and thus its vertical excitation energy is 0.38 eV with 0.26 eV adiabatic excitation energy. Finally, $^2[{}^1(\sigma\pi)(\bar{\sigma})]$, as expected, is higher in energy with 1.93 eV vertical excitation energy and 1.73 eV adiabatic excitation energy.

The optimum Si-Si-Si angles for the $^4[{}^3(\sigma\pi)(\bar{\sigma})]$ and $^2[{}^3(\sigma\pi)(\bar{\sigma})]$ states are very close, 112.1° and 111.8° respectively, corresponding to the step Si moving 0.09 Å toward the bulk position. The hybridizations² of the σ and $\bar{\sigma}$ orbitals are $s^{0.16}p^{0.74}d^{-0.01}$ and $s^{0.08}p^{0.85}d^{0.03}$ respectively; the π orbital has pure p-character. For the ground state the presence of the less rigid surface atom allows the divalent Si to distort so as to decrease its bond angle to 102.7, while allowing the surface atom to attain its preferred, less-pyramidal configuration (the step Si moves 0.25 Å away from the bulk position).

The electronic structure found here for the divalent step suggests that this step site is particularly reactive for a range of chemical species. In the σ^2 state the σ pair can act as a donor (for molecules with an appropriate acceptor site), while the empty π orbital can act as an acceptor (for molecules with a donor pair). On the other hand, the presence of the two low lying ${}^3(\sigma\pi)(\bar{\sigma})$ states provides two radical orbitals for effective coupling with molecules having radical sites (singly-occupied orbitals). Having both σ^2 and $\sigma\pi$ states within 0.2 eV of each other, these step sites should be considerably more reactive than the sites of the perfect (111) surface. As would be

expected for such a reactive site, few molecules have been detected containing divalent silicons; an example is SiH_2 which leads to a singlet (σ^2) ground state³ (with an optimum angle of 92°).

Correlation effects

As in the $^3(\sigma\pi)$ state of Si_3H_6 (Chapter 2) correlation effects are of minor importance for $^4[{}^3(\sigma\pi)(\bar{\sigma})]$. For the $^2[{}^3(\sigma\pi)(\bar{\sigma})]$ state, correlation between the σ and $\bar{\sigma}$ orbitals is very important since these orbitals are localized on different centers. From Table I (footnote c) we see that in this case the Hartree-Fock (HF) wavefunction,

$$^2[{}^3(\sigma\pi)(\bar{\sigma})]_{\text{HF}} = \mathcal{A}\{\phi_{\text{bulk}}[\phi_{\sigma}(1)\phi_{\sigma}(2)][\alpha(1)\beta(2) - \beta(1)\alpha(1)]\phi_{\pi}(3)\alpha(3)\} , \quad (1)$$

leads to an energy 1.64 eV higher than the Generalized Valence Bond⁴ (GVB) wavefunction,

$$\begin{aligned} ^2[{}^3(\sigma\pi)(\bar{\sigma})]_{\text{GVB}} = \mathcal{A}\{\phi_{\text{bulk}}[\phi_{\sigma}(1)\phi_{\bar{\sigma}}(2) + \phi_{\bar{\sigma}}(1)\phi_{\sigma}(2)] \\ \times [\alpha(1)\beta(2) - \beta(1)\alpha(2)]\phi_{\pi}(3)\alpha(3)\} , \quad (2) \end{aligned}$$

where ϕ_{bulk} represents the wavefunction of the Si-Si and Si-H bond pairs.

Electron correlation effects are also crucial for the $^2[{}^1(\sigma^2)(\bar{\sigma})]$ state, as they were in the σ^2 state of the divalent Si. From Table I (footnote b) we see that the HF wavefunction,

$${}^2[{}^1(\sigma^2)(\bar{\sigma})]_{\text{HF}} = \mathcal{A}\{\phi_{\text{bulk}}[\phi_{\sigma}(1)\phi_{\sigma}(2)][\alpha(1)\beta(2) - \beta(1)\alpha(2)]\phi_{\bar{\sigma}}(3)\alpha(3)\}, \quad (3)$$

leads to an energy which is 0.54 eV higher than that of the corresponding GVB wavefunction,

$${}^2[{}^1(\sigma^2)(\bar{\sigma})]_{\text{GVB}} = \mathcal{A}\{\phi_{\text{bulk}}[\phi_{\sigma+\lambda\pi}(1)\phi_{\sigma-\lambda\pi}(2) + \phi_{\sigma-\lambda\pi}(1)\phi_{\sigma+\lambda\pi}(2)] \\ \times [\alpha(1)\beta(2) - \beta(1)\alpha(1)]\phi_{\bar{\sigma}}(3)\alpha(3)\} . \quad (4)$$

The HF and GVB wavefunctions for the ${}^4[{}^2(\sigma\pi)(\bar{\sigma})]$ state are identical, e.g.,

$${}^4[{}^3(\sigma\pi)(\bar{\sigma})]_{\text{HF}} = {}^4[{}^3(\sigma\pi)(\bar{\sigma})]_{\text{GVB}} \\ = \mathcal{A}\{\phi_{\text{bulk}}[\phi_{\sigma}(1)\phi_{\pi}(2) - \phi_{\pi}(1)\phi_{\sigma}(2)][\alpha(1)\beta(2) + \beta(1)\alpha(2)]\phi_{\bar{\sigma}}(3)\alpha(3)\} . \quad (5)$$

Therefore, had we performed our calculations using HF wavefunctions only, we would have found the ground state to be ${}^4[{}^3(\sigma\pi)(\bar{\sigma})]$ with the ${}^2[{}^1(\sigma^2)(\bar{\sigma})]$ state at ~ 0.32 eV and the ${}^2[{}^3(\sigma\pi)(\bar{\sigma})]$ state at ~ 2.16 eV, giving the wrong ground state.

Comparing Tables I and II we see that for the GVB CI calculation there is almost no lowering of the total energy for the quartet state. This is also true for the ${}^2[{}^1(\sigma^2)(\bar{\sigma})]$ state. The reason for this is that the basis space used for the CI calculation involved valence orbitals of the corresponding state only (with no virtuals added), thus the basic correlations are already included at the GVB level. The largest change occurs for the ${}^2[{}^3(\sigma\pi)(\bar{\sigma})]$ state, where

at the GVB level only one of the important spin configurations for this state is included, namely that of eq. (2), e.g.,

$$X_1 = [\alpha(1)\beta(2) - \beta(1)\alpha(2)]\alpha(3) \quad . \quad (6)$$

The other important spin coupling is

$$X_2 = 2\alpha(1)\alpha(2)\beta(3) - [\alpha(1)\beta(2) + \beta(1)\alpha(2)]\alpha(3) \quad . \quad (7)$$

Because no spin optimization is included at the GVB level, only the solution with spin coupling (6) is solved. The potential curves for the SCF and CI calculations are shown in Figs. 6 and 7, respectively.

Computational details

As we have seen in Chapter 2, to obtain a consistent description of the σ^2 and $\sigma\pi$ states it is necessary to include d-functions. We have done so for the step and surface Si atoms (i.e., these atoms have the DZd basis of Table XI of Chapter 1, p. 31). For the "bulk" Si the DZ basis of Table XI, Chapter 1 was used; for the hydrogens a double zeta contraction of the three gaussian hydrogen bases of Huzinaga⁵ was used.

For the GVB CI calculations we used the valence spaces of both the $4[{}^3(\sigma\pi)(\bar{\sigma})]$ and $2[{}^1(\sigma^2)(\bar{\sigma})]$ states. In both cases a total of 10 valence orbitals was used, allowing double excitations out of the 10 orbitals, with the restriction that all initially doubly-occupied orbitals (not involving the correlated GVB pair) were not allowed to

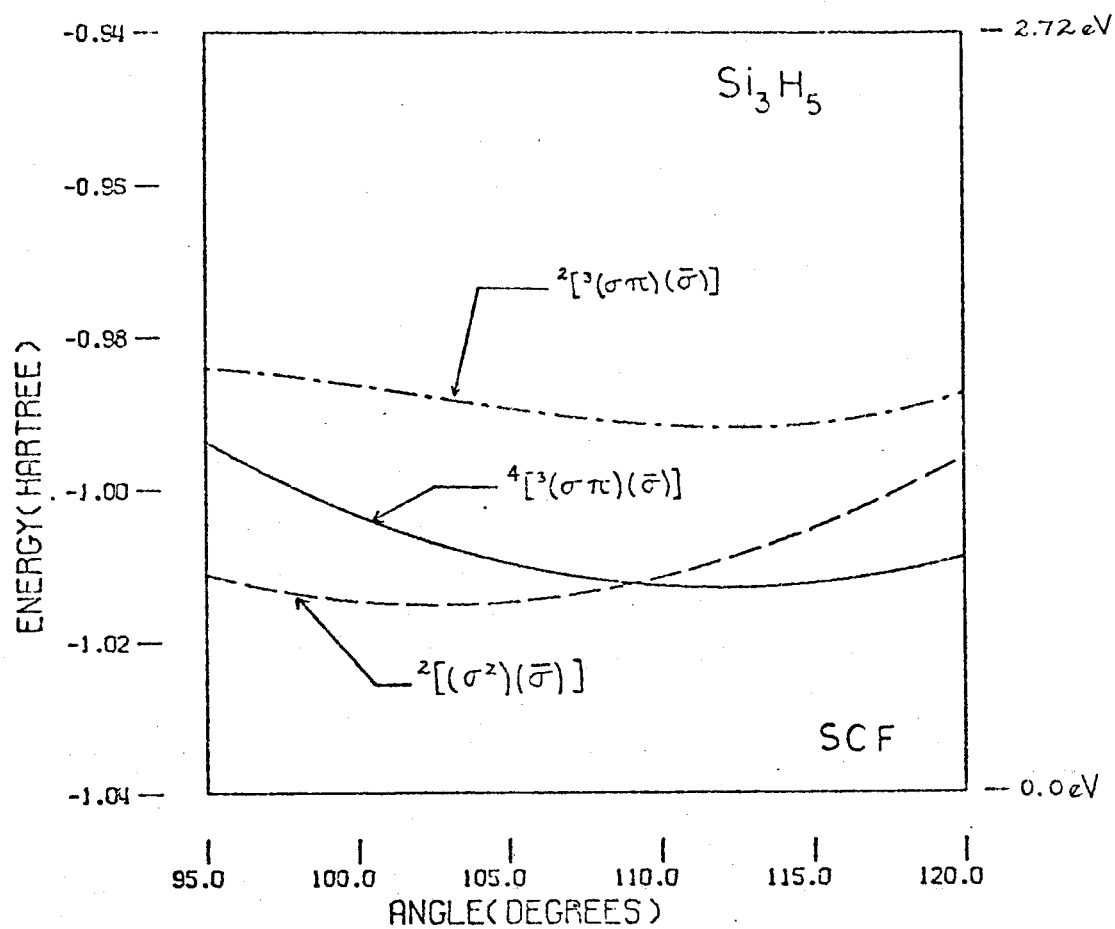


Fig. 6 Potential Surfaces for the SCF Calculations on the Si_3H_5 Cluster

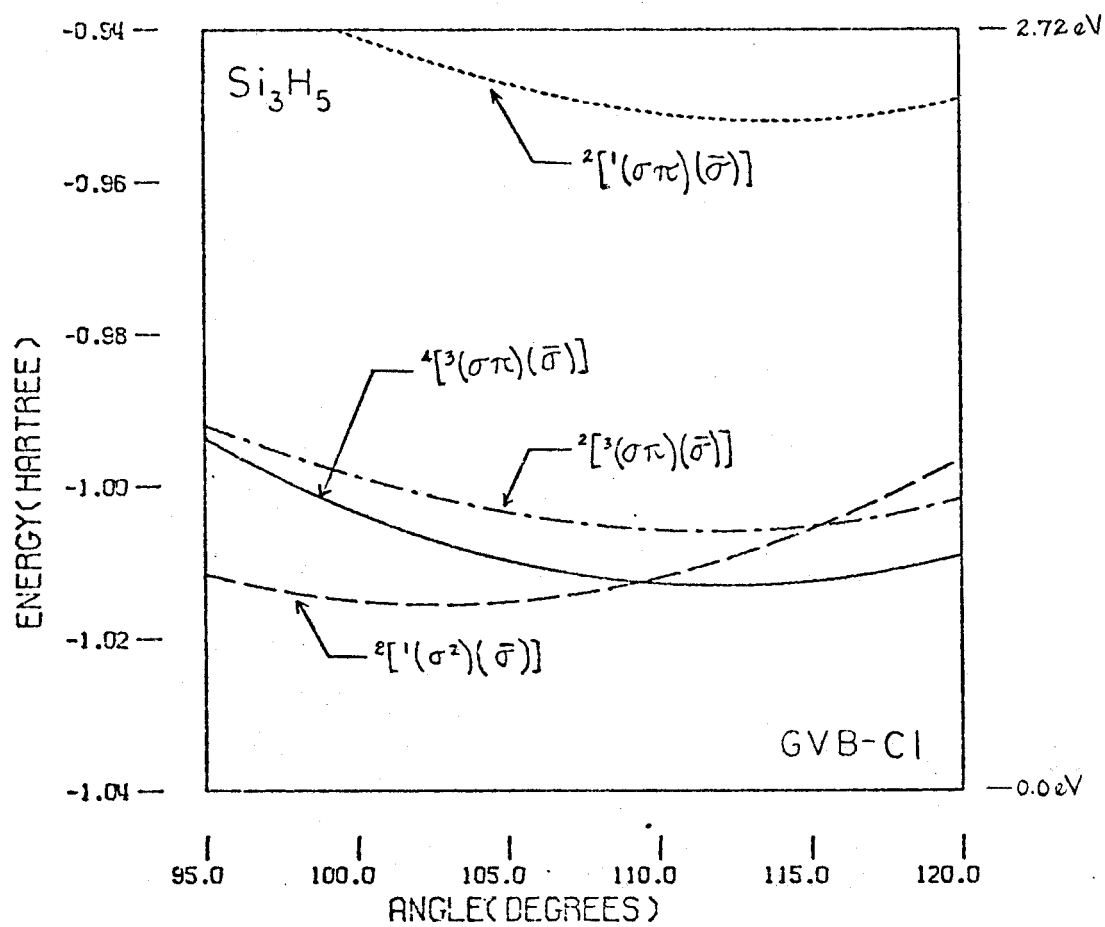


Fig. 7 Potential Surfaces for the GVB-CI Calculation on the Si_3H_5 Cluster

have zero occupation number. This leads to wavefunctions having from 44 to 142 determinants. We have compared this (at the tetrahedral geometry only) with the same calculation doing all double excitations with no restrictions, with the result that all corresponding energies agreed within 0.03 eV. Thus, we believe that the restriction imposed on the selection of configurations leads to a good description of states within the valence orbital space (no virtuals added).

C. Divalent Steps on Si (111) Surfaces: Additional Atomic Arrangements

General description

A particularly interesting divalent state for a step configuration is obtained by binding a silicon atom to two adjacent Si atoms of the row of divalent Si's. The geometry for this system is shown in Fig. 2. Note that completing a whole row in this way leads to the configuration observed in a (100) surface and described in Fig. 3. This has been previously described in Chapter 2 using an $\text{H}_3\ddot{\text{Si}}-\ddot{\text{Si}}-\ddot{\text{SiH}}_3$ complex. For the present case the appropriate complex to use (see Fig. 2) results in a divalent Si atom at the center, bonded to two trivalent silicons, leading to an $\text{H}_2\ddot{\text{Si}}-\ddot{\text{Si}}-\ddot{\text{SiH}}_2$ complex. One can think of this system as describing kinks on the step edge.

The central silicon is again a divalent silicon atom with two dangling bonds, σ_ℓ and σ_r , on the adjacent silicons. The low lying states of the system are dominated by the (σ^2) and $(\sigma\pi)$ configurations of the central Si (these are outlined in Fig. 8):

STEP KINK $\text{H}_2\dot{\text{Si}}-\dot{\text{Si}}-\dot{\text{Si}}\text{H}_2$

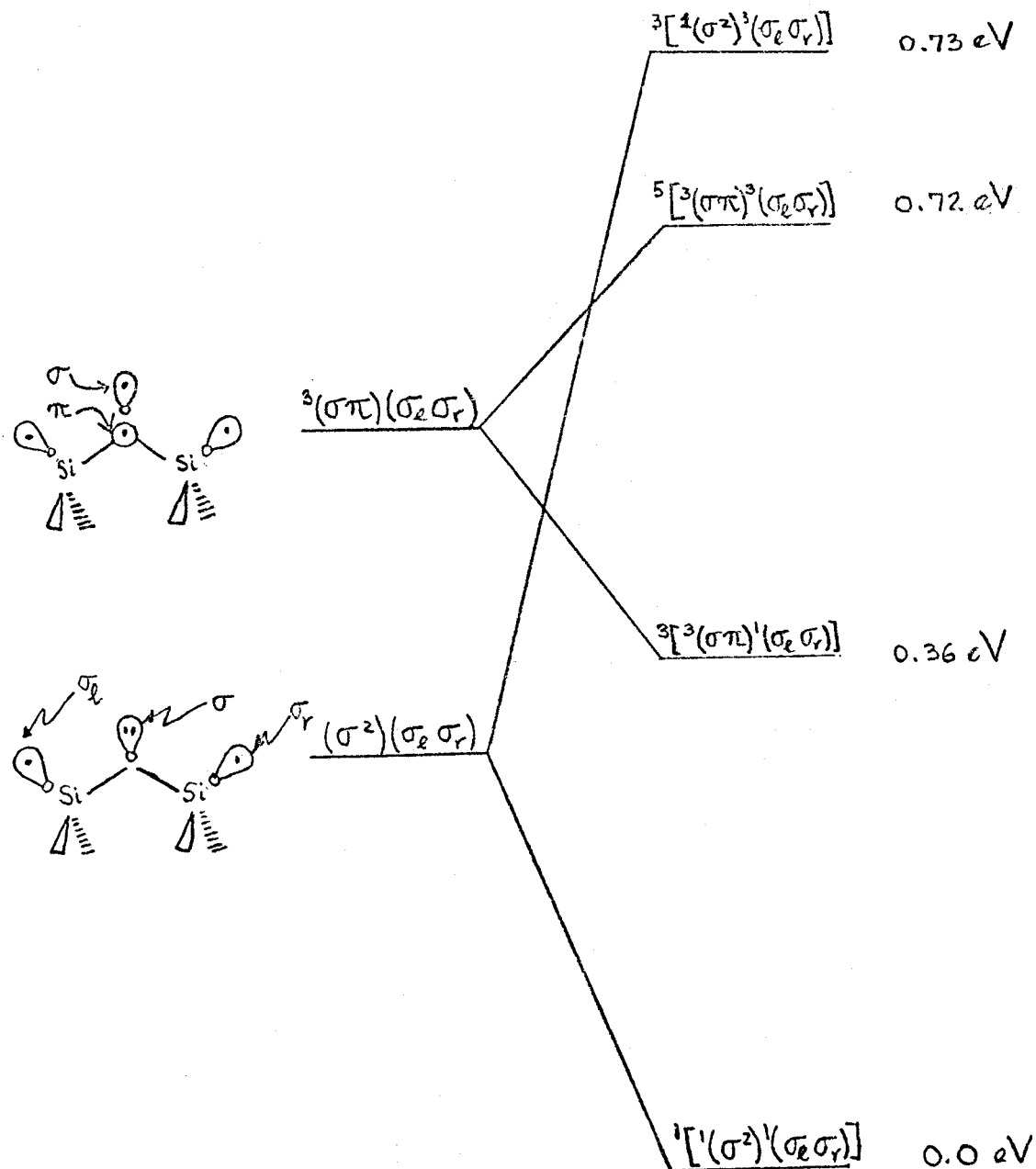


Fig. 8 Schematic of the Electronic Structure for the Si_3H_4 Cluster.

$^3(\sigma\pi)(\sigma_\ell)(\sigma_r)$: Starting out with the $^3(\sigma\pi)$ state of the divalent Si we can construct several states according to how we couple the other dangling bonds. Coupling σ_ℓ and σ_r into a singlet leads to an overall triplet ($S = 1$), denoted $^3[{}^3(\sigma\pi)^1(\sigma_\ell\sigma_r)]$. When we couple the σ_ℓ and σ_r orbitals into a triplet, an overall quintet ($S = 2$) state results, which we denote $^5[{}^3(\sigma\pi)^2(\sigma_\ell\sigma_r)]$. The quintet will be lower in energy if the overlap between the σ_ℓ and σ_r orbitals is small.

$^1(\sigma\pi)(\sigma_\ell)(\sigma_r)$: We now start with the $^1(\sigma\pi)$ state of the divalent Si. Two states are possible: if we couple σ_ℓ and σ_r into a singlet, an overall singlet ($S = 0$) state results, denoted $^1[{}^1(\sigma\pi)^1(\sigma_\ell\sigma_r)]$. For the triplet coupling of σ_ℓ and σ_r an overall triplet ($S = 1$) is obtained, $^3[{}^1(\sigma\pi)^3(\sigma_\ell\sigma_r)]$. The lowest of the two will be determined by the overlap between the two dangling bond orbitals, σ_ℓ and σ_r .

$^1(\sigma^2)(\sigma_\ell)(\sigma_r)$: Starting with the $^1(\sigma^2)$ ground state of the divalent silicon we can obtain an overall singlet ($S = 0$), $^1[{}^1(\sigma^2)^1(\sigma_\ell\sigma_r)]$, and an overall triplet ($S = 1$), $^3[{}^1(\sigma^2)^3(\sigma_\ell\sigma_r)]$. One can compare these states with those with $(\sigma\pi)$ configurations and estimate (before any calculations are done) some of the relative energy orderings. For example, knowing that the σ^2 state is lower in energy than the $\sigma\pi$ states for the divalent Si, one estimates that the $^1[{}^1(\sigma^2)^1(\sigma_\ell\sigma_r)]$ should be lower in energy than the $^3[{}^3(\sigma\pi)^1(\sigma_\ell\sigma_r)]$ or the $^1[{}^1(\sigma\pi)^1(\sigma_\ell\sigma_r)]$. Similarly, one expects

$^3[(\sigma^2)^3(\sigma_\ell\sigma_r)]$ to be lower in energy than $^5[{}^3(\sigma\pi)^3(\sigma_\ell\sigma_r)]$ or $^3[{}^1(\sigma\pi)^3(\sigma_\ell\sigma_r)]$.

${}^1(\sigma\sigma_\ell){}^3(\pi\sigma_r)$: Finally, we consider a state in which one of the dangling bonds (σ_ℓ or σ_r) couples into a singlet with σ of the divalent Si, whereas the other dangling bond (σ_r or σ_ℓ) couples into a triplet with π . The overall spin state is a triplet ($S = 1$), denoted ${}^3[{}^1(\sigma\sigma_\ell){}^3(\pi\sigma_r)]$. (The true wavefunction of this state will be a combination of this and ${}^3[{}^1(\sigma\sigma_r){}^3(\pi\sigma_\ell)]$).

Results

The results for self-consistent field and CI calculations are shown in Tables III and IV. The σ , π , σ_ℓ and σ_r orbitals of the ${}^3[{}^3(\sigma\pi)^1(\sigma_\ell\sigma_r)]$ state are shown in Fig. 9. Figures 10 and 11 show the appropriate orbitals for ${}^5[{}^3(\sigma\pi)^3(\sigma_\ell\sigma_r)]$ and ${}^1[{}^1(\sigma^2)^1(\sigma_\ell\sigma_r)]$, respectively. Note that for ${}^5[{}^3(\sigma\pi)^3(\sigma_\ell\sigma_r)]$ instead of σ_ℓ and σ_r we show the corresponding symmetry orbitals σ_g and σ_u , where

$$\sigma_g \sim \sigma_\ell + \sigma_r,$$

$$\sigma_u \sim \sigma_\ell - \sigma_r.$$

The ground state of the system is ${}^1[{}^1(\sigma^2)^1(\sigma_\ell\sigma_r)]$, with an optimum angle of 61.0° . Here the three Si atoms are almost in an equilateral triangle position. This is due to the fact that σ_ℓ and σ_r can form a relatively strong bond as the two trivalent Si atoms move together. This can be represented by the following diagram

Table III. Quantities Relation to the $H_2\dot{S}i-\dot{S}i-H_2$ Cluster Model of Divalent Steps. Self-Consistent-Field Calculations.
All energies are in hartrees unless otherwise stated.

	Total Energies							Optimum Angle (°)	Optimum Energy ^a	Adiabatic Excitation Energy (ev)
	55°	65°	75°	85°	95°	105°	109°28'	115°		
$1[(\sigma^2)^1(\sigma_x\sigma_r)]$ GVB(2) ^b	-13.407866	-13.409370	-13.401659	-13.399110	-13.396000	-13.387146	-13.380653	-13.370285	-13.410751	0.0
$3[(\sigma\pi)^1(\sigma_x\sigma_r)]$ GVB(1)	-	-	-	-	-13.379402	-13.381026	-13.379626	-13.375716	-13.381195	0.80
$3[(\sigma^2)^3(\sigma_x\sigma_r)]$ GVB(1) ^c	-	-	-	-	-13.370485	-13.370787	-13.367304	-13.360162	-13.372091	1.05
$5[(\sigma\pi)^3(\sigma_x\sigma_r)]$ HF	-	-	-	-	-13.356135	-13.368520	-13.370370	-13.369704	-13.370506	1.10
$3[(\sigma\sigma)^3(\pi\sigma_r)]$ SOGVB	-	-	-	-	-	-13.359903	-13.361353	-13.360479	-13.361414	1.34
$1[(\sigma\pi)^1(\sigma_x\sigma_r)]$ GVB(1)	-	-	-	-	-13.329276	-13.331650	-13.330731	-13.327412	-13.331668	2.15

^aObtained from a cubic splines fit to the calculated points.

^bThe HF energy for this state at 109°28' is 2.03 eV higher than the corresponding GVB(2) value.

^cThe HF energy for this state at 109°28' is 0.53 eV higher than the corresponding GVB(1) value.

Table IV. Quantities Relating to the $H_2\dot{S}i-\dot{S}i-H_2$ Cluster Model of Divalent Steps. GVB CI Calculations.
All energies are in hartrees unless otherwise stated.

	Total Energies							Optimum Energy	Optimum Angle (°)	Adiabatic Excitation Energy(eV)
	55°	65°	75°	85°	95°	105°	109°28'	115°		
$1[(\sigma^2)^1(\sigma_g\sigma_r)]$	-13.409009	-13.41225	-13.403451	-13.400582	-13.397225	-13.388245	-13.381741	-13.371408	-13.412432	0.0
$3[{}^3(\sigma\pi)^1(\sigma_g\sigma_r)]$	-	-	-	-	-13.383786	-13.383827	-13.382081	-13.377937	-13.384388	0.76
$5[{}^3(\sigma\pi)^3(\sigma_g\sigma_r)]$	-	-	-	-	-13.356370	-13.368742	-13.370589	-13.369920	-13.370724	1.13
$3[(\sigma^2)^3(\sigma_g\sigma_r)]^b$	-	-	-	-	-13.368529	-13.369630	-13.366512	-13.359865	-13.370583	1.14
$3[{}^1(\sigma\sigma_g)^3(\pi\sigma_r)]$	-	-	-	-	-	-13.361230	-13.362621	-13.361735	-13.362674	1.35
$1[{}^1(\sigma\sigma_g)^1(\pi\sigma_r)]$	-	-	-	-	-13.347999	-13.357229	-13.358400	-13.357419	-13.358423	1.47
$1[{}^1(\sigma\pi)^1(\sigma_g\sigma_r)]^b$	-	-	-	-	-13.322110	-13.320162	-13.318920	-13.315867	-	-

^aObtained from a cubic splines fit.

^bThese energies are higher than the corresponding SCF value because the orbital spaces used for the GVB CI calculation do not contain the virtual orbitals necessary to describe this state correctly. In the case of the $1[{}^1(\sigma\pi)^1(\sigma_g\sigma_r)]$ this is so pronounced that the SCF values are more trustworthy.

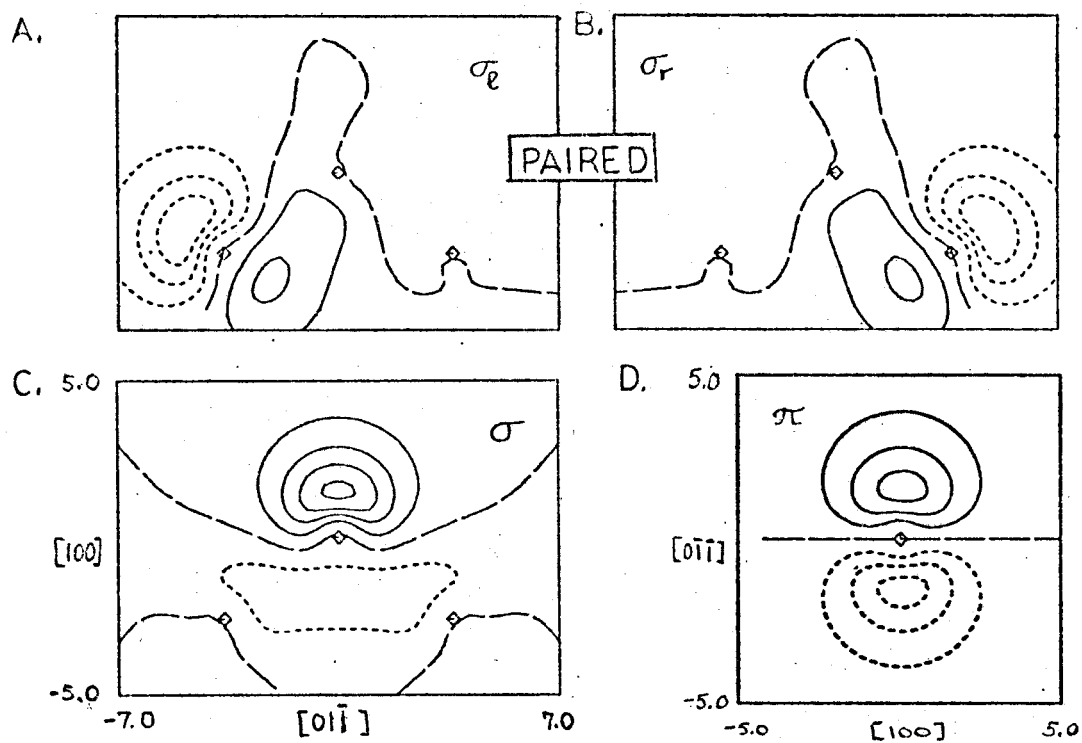


Fig. 9 Orbitals for the $3[{}^3(\sigma\pi)1(\sigma_\ell\sigma_r)]$ State of Si_3H_4 . (a) σ_ℓ orbital; (b) σ_r orbital; (c) σ orbital (d) π orbital.

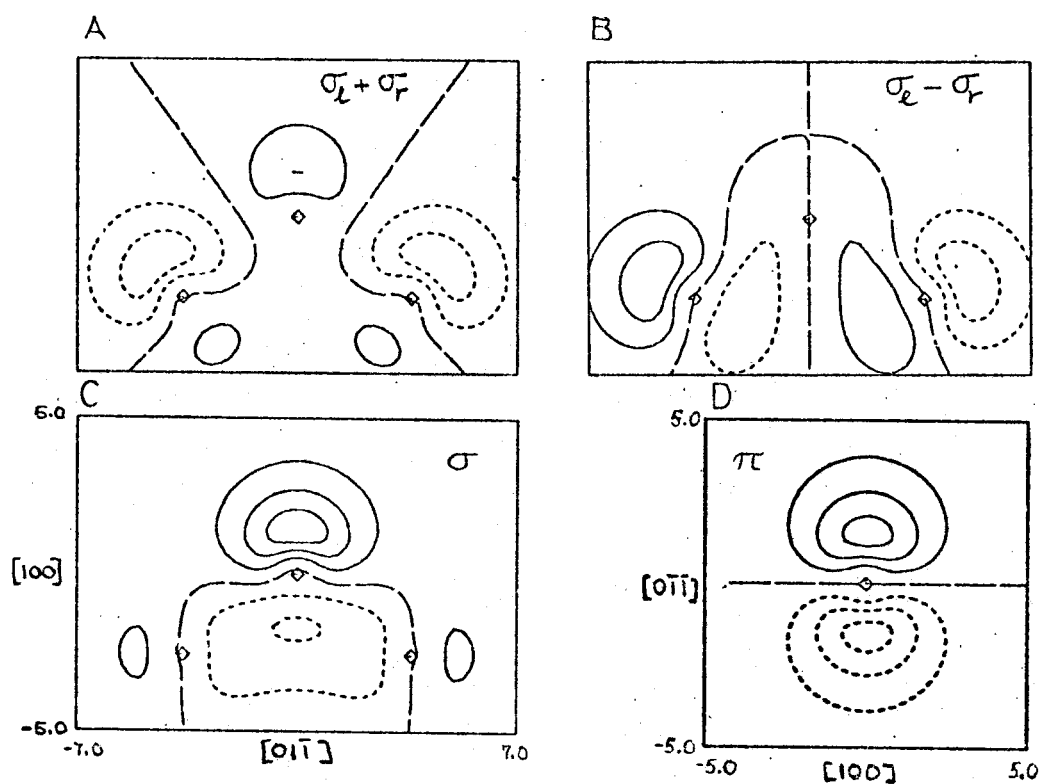


Fig. 10 Orbitals for the $5[{}^3(\sigma\pi)^3(\sigma_g\sigma_r)]$ State of Si_3H_4 . (a) σ_g orbital; (b) σ_u orbital; (c) σ orbital; (d) π orbital.

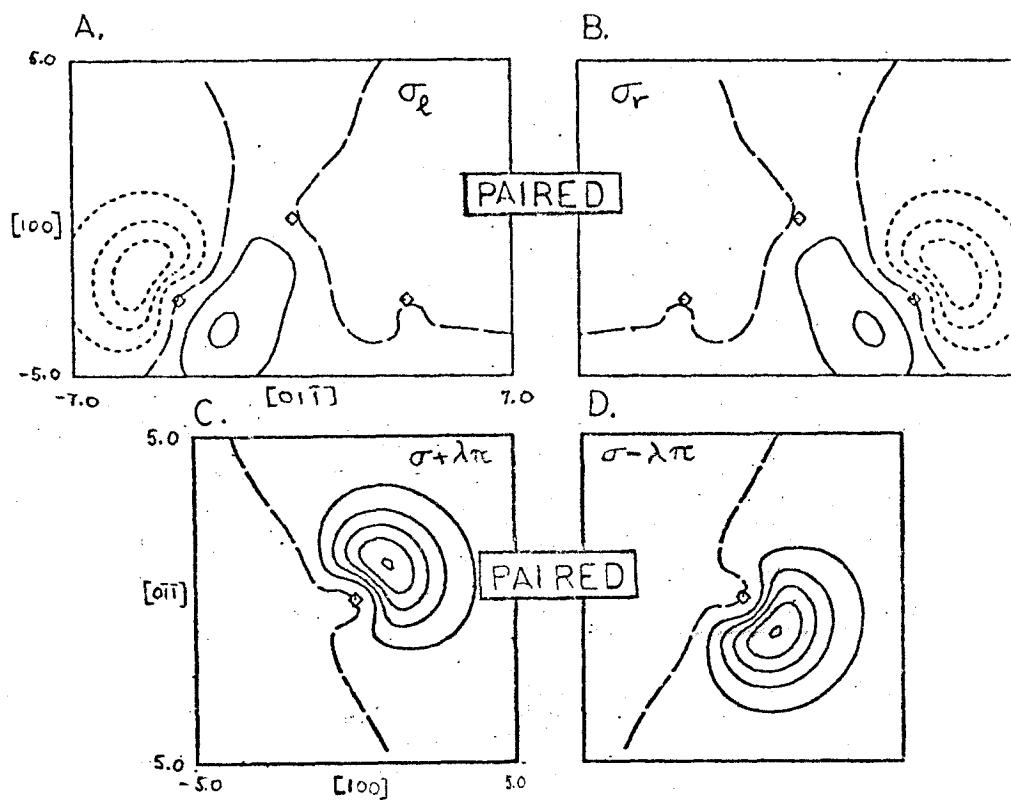
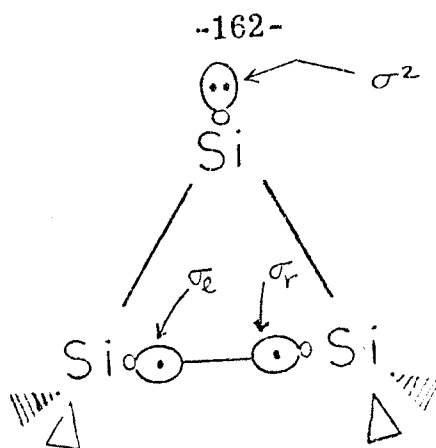


Fig. 11. Orbitals for the $1[(\sigma^2)^1(\sigma_x\sigma_r)]$ state of Si_3H_4 . (a) σ_x orbital, (b) σ_r orbital, (c) $\sigma + \lambda\pi$ orbital, (d) $\sigma - \lambda\pi$ orbital.



Note also that the σ^2 electrons get out of the way of the Si-Si bonds by buckling out. All the other states have geometries with Si-Si-Si angles more in accord with those of the Si_3H_5 complex. For this reason we only quote adiabatic excitation energies. The first excited state is the $^3[{}^3(\sigma\pi)^1(\sigma_\ell\sigma_r)]$ at 0.76 eV. The $^5[{}^3(\sigma\pi)^3(\sigma_\ell\sigma_r)]$ and $^3[{}^1(\sigma^2)^3(\sigma_\ell\sigma_r)]$ are quite close in energy at 1.13 and 1.14 eV. (The vertical excitation energy of the quintet is larger). We then find the $^3[{}^1(\sigma\sigma_\ell)^3(\pi\sigma_r)]$ state at 1.35 eV. The $^1[{}^1(\sigma\sigma_\ell)^1(\pi\sigma_r)]$ state is only 0.12 eV higher at 1.47 eV adiabatic excitation energy.

The optimum Si-Si-Si angle for the ground state, as discussed above, is 61.0° . For the $^3[{}^3(\sigma\pi)^1(\sigma_\ell\sigma_r)]$ state there are two competing tendencies: the $(\sigma\pi)$ configuration at the divalent silicon favors large central angles, the ${}^1(\sigma_\ell\sigma_r)$ spin coupling favors small angles (by trying to form a bond as in the ground state). The resulting optimum angle is 100.3° . The $^3[{}^1(\sigma^2)^3(\sigma_\ell\sigma_r)]$ is dominated by the ${}^1(\sigma^2)$ configuration, leading to an optimum angle of 100.9° . The $^5[{}^3(\sigma\pi)^3(\sigma_\ell\sigma_r)]$ state is dominated by the ${}^3(\sigma\pi)$ configuration, leading to an optimum angle of 111.1° . The optimum angles for the $^3[{}^1(\sigma\sigma_\ell)^3(\pi\sigma_r)]$ and $^1[{}^1(\sigma\sigma_\ell)^1(\pi\sigma_r)]$ states are very similar at 110.5° and 110.2° .

Potential curves are plotted in Figs. 12 (SCF results) and 13 (GVB CI results).

Correlation effects

As in the systems previously discussed, correlation effects are of minor importance in the $^5[{}^3(\sigma\pi){}^3(\sigma_\ell\sigma_r)]$ state, where the Hartree-Fock and GVB wavefunctions are identical, e.g.,

$$\begin{aligned} {}^5[{}^3(\sigma\pi){}^3(\sigma_\ell\sigma_r)]_{\text{HF}} &= {}^5[{}^3(\sigma\pi){}^3(\sigma_\ell\sigma_r)]_{\text{GVB}} \\ &= \mathcal{A}\{\Phi_{\text{bulk}}[\phi_\sigma(1)\phi_\pi(2) - \phi_\pi(1)\phi_\sigma(2)][\phi_{\sigma_\ell}(3)\phi_{\sigma_r}(4) - \phi_{\sigma_r}(3)\phi_{\sigma_\ell}(4)] \\ &\quad \times \alpha(1)\alpha(2)\alpha(3)\alpha(4)\} \end{aligned} \quad (8)$$

For the $^1[{}^1(\sigma^2){}^1(\sigma_\ell\sigma_r)]$ state correlation is important for both pairs of electrons. As shown in Table III (footnote b) the HF wavefunction

$$\begin{aligned} {}^1[{}^1(\sigma^2){}^1(\sigma_\ell\sigma_r)]_{\text{HF}} &= \mathcal{A}\{\Phi_{\text{bulk}}[\phi_\sigma(1)\phi_\sigma(2)][\alpha(1)\beta(2) - \beta(1)\alpha(2)] \\ &\quad \times [\phi_{\sigma_g}(3)\phi_{\sigma_g}(4)][\alpha(1)\beta(2) - \beta(1)\alpha(2)]\} \end{aligned} \quad (9)$$

(where $\phi_{\sigma_g} \sim \phi_{\sigma_\ell} + \phi_{\sigma_r}$ is an appropriate symmetric orbital), leads to an energy 2.03 eV higher than that of the corresponding GVB wavefunction,

$$\begin{aligned} {}^1[{}^1(\sigma^2){}^1(\sigma_\ell\sigma_r)]_{\text{GVB}} &= \mathcal{A}\{\Phi_{\text{bulk}}[\phi_{\sigma+\lambda\pi}(1)\phi_{\sigma-\lambda\pi}(2) + \phi_{\sigma-\lambda\pi}(1)\phi_{\sigma+\lambda\pi}(2)] \\ &\quad \times [\alpha(1)\beta(2) - \beta(1)\alpha(2)][\phi_{\sigma_\ell}(3)\phi_{\sigma_r}(4) + \phi_{\sigma_r}(3)\phi_{\sigma_\ell}(4)][\alpha(3)\beta(4) - \beta(3)\alpha(4)]\}. \end{aligned} \quad (10)$$

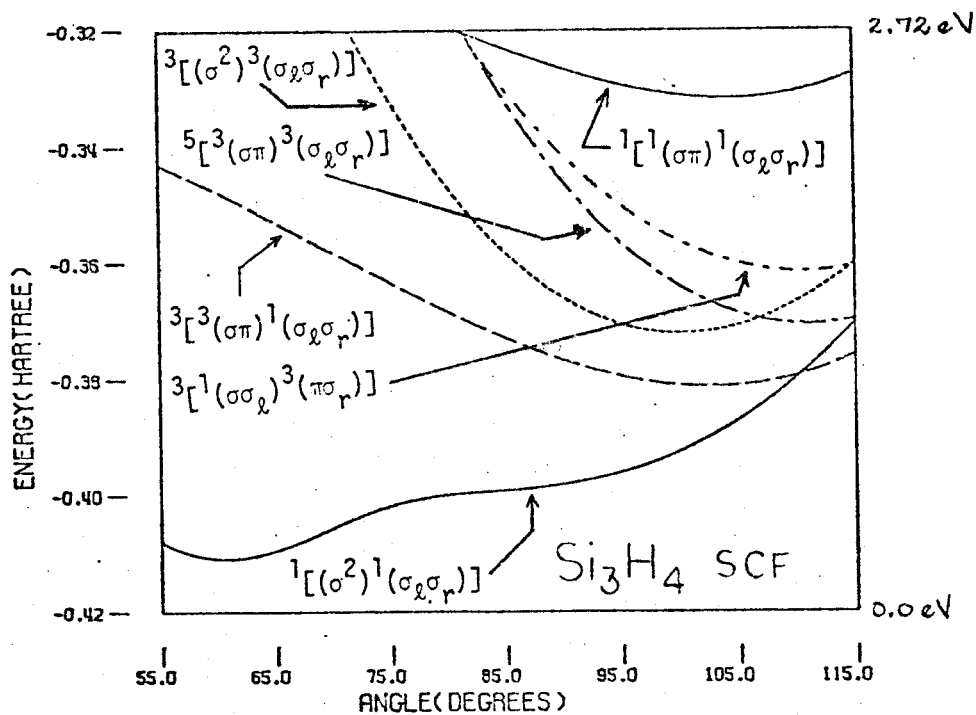


Fig. 12. Potential surfaces for the SCF calculations on the Si_3H_4 cluster.

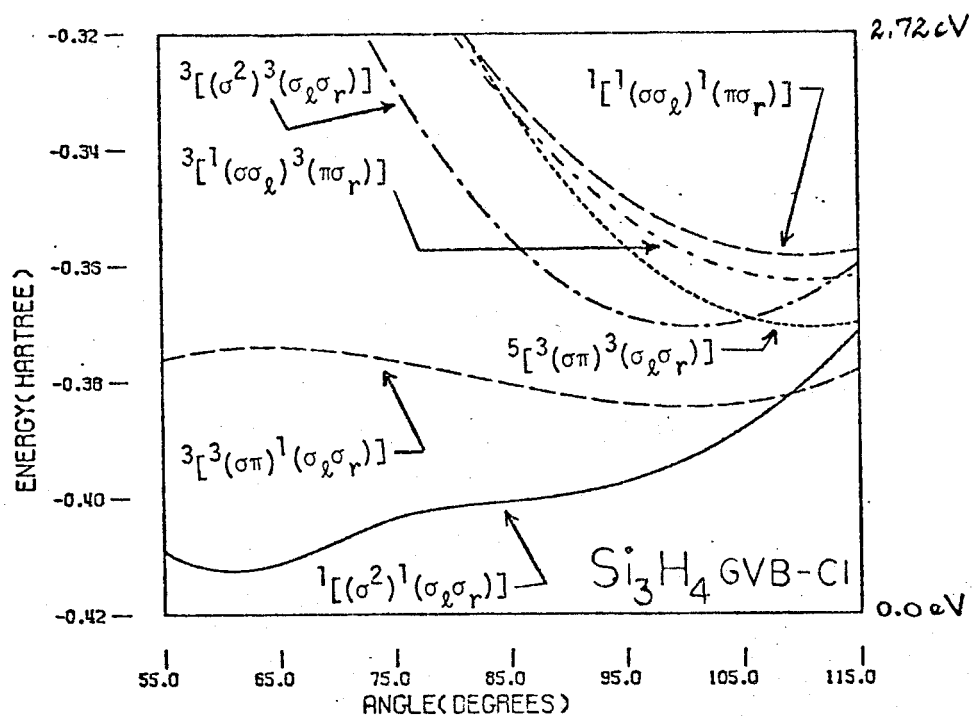


Fig. 13. Potential surfaces for the GVB-CI calculations on the Si_3H_4 cluster.

Similarly, for the $^3[{}^1(\sigma^2){}^3(\sigma_\ell\sigma_r)]$ state the HF wavefunction

$$\begin{aligned} {}^3[{}^1(\sigma^2){}^3(\sigma_\ell\sigma_r)]_{\text{HF}} = & \mathcal{A}\{\Phi_{\text{bulk}}[\phi_\sigma(1)\phi_\sigma(2)][\alpha(1)\beta(2) - \beta(1)\alpha(2)] \\ & \times [\phi_{\sigma_\ell}(3)\phi_{\sigma_r}(4) - \phi_{\sigma_r}(3)\phi_{\sigma_\ell}(4)][\alpha(3)\beta(4) + \beta(3)\alpha(4)]\} \quad \text{..} \quad (11) \end{aligned}$$

leads to an energy 0.53 eV higher than that of the GVB wavefunction

$$\begin{aligned} {}^3[{}^1(\sigma^2){}^3(\sigma_\ell\sigma_r)]_{\text{GVB}} = & \mathcal{A}\{\Phi_{\text{bulk}}[\phi_{\sigma+\lambda\pi}(1)\phi_{\sigma-\lambda\pi}(2) + \phi_{\sigma-\lambda\pi}(1)\phi_{\sigma+\lambda\pi}(2)] \\ & \times [\alpha(1)\beta(2) - \beta(1)\alpha(2)][\phi_{\sigma_\ell}(3)\phi_{\sigma_r}(4) - \phi_{\sigma_r}(3)\phi_{\sigma_\ell}(4)] \\ & \times [\alpha(3)\beta(4) + \beta(3)\alpha(4)]\} \quad \text{.} \quad (12) \end{aligned}$$

For the $^3[{}^1(\sigma\sigma_\ell){}^3(\pi\sigma_r)]$ state appropriate correlation is introduced by considering a wavefunction in which the spin coupling is optimized concurrently with the spatial orbitals. We have chosen a strongly orthogonal Generalized Valence Bond⁶ (SOGVB) wavefunction of the form

$${}^3[{}^1(\sigma\sigma_\ell){}^3(\pi\sigma_r)]_{\text{SOGVB}} = \mathcal{A}\{\Phi_{\text{bulk}}\phi_\sigma(1)\phi_{\sigma_g}(2)\phi_\pi(3)\phi_{\sigma_u}(4)\chi_{\text{spin}}(1,\dots,4)\} \quad (13)$$

where $\phi_{\sigma_g} \sim \phi_{\sigma_\ell} + \phi_{\sigma_r}$ and $\phi_{\sigma_u} \sim \phi_{\sigma_\ell} - \phi_{\sigma_r}$ are symmetry orbitals. Here the spin function χ_{spin} is defined by

$$\begin{aligned} \chi_{\text{spin}}(1,\dots,4) = & C_1[\alpha(1)\beta(2) - \beta(1)\alpha(2)]\alpha(3)\alpha(4) + C_2 \\ & + C_2[2\alpha(1)\alpha(2)\beta(3)\alpha(4) - \alpha(1)\beta(2)\alpha(3)\alpha(4) - \alpha(1)\alpha(2)\alpha(3)\alpha(4)] + \\ & + C_3[3\alpha(1)\alpha(2)\alpha(3)\beta(4) - \beta(1)\alpha(2)\alpha(3)\alpha(4) - \alpha(1)\beta(2)\alpha(3)\alpha(4) - \alpha(1)\alpha(2)\beta(3)\alpha(4)] \end{aligned}$$

From these results we see that, had we used the standard HF wavefunction, we would have obtained the wrong ground state again.

Corrections due to changes in the hybridization of the trivalent Si atoms

If the system we are treating by means of the Si_3H_4 complex were part of a real crystal (i.e., when the semi-infinite solid is included), one expects that the bending of the trivalent silicons at the ends of the $\text{H}_2\ddot{\text{Si}}\text{-Si-SiH}_2$ complex would increase the total energy of the system because of changes in the hybridization. In the present case we have substituted Si-Si bonds by Si-H bonds; thus this change is not taken into account. We can include this effect by adding to the energies of Table IV the results of the Si_3H_6 calculations of Section II-B of Chapter 2, where we calculated the effect of the bending of the central Si off the plane formed by the three atoms (see Fig.16 of Chapter 2, p.111).

The potential curves obtained in this way are shown in Fig. 14. Table V summarizes the results when this correction is included. We notice that except for a change in the optimum angle of the ground state no significant changes are produced by this correction. (The total optimum energy of the ground state is raised so all adiabatic excitation energies are decreased by approximately the same amount.)

Calculational details

For the central Si atom, as discussed in Chapter 2 and in Appendix C, we have used the DZd basis set of Table XI, Chapter 1 (p. 31). Here, as before, the reason is that the σ^2 and $\sigma\pi$ states

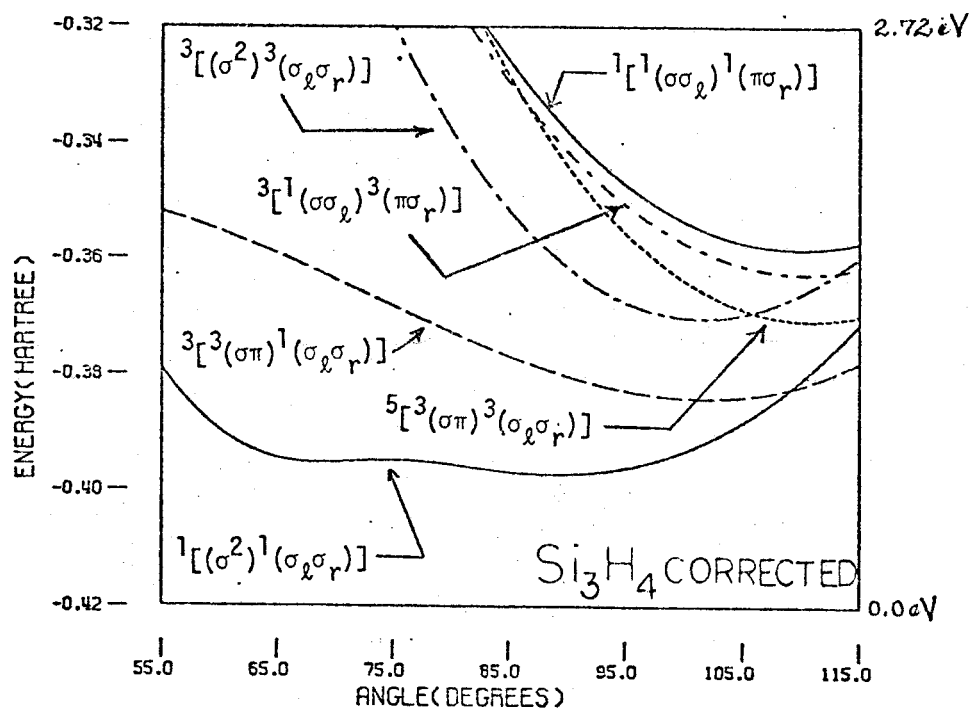


Fig. 14. Potential surfaces for the GVB-CI calculations on the Si_3H_4 cluster corrected for the hybridization changes due to the bending on "bulk atoms".

Table V. Summary of Results Relating to the Si_3H_4 Cluster Model of Divalent Steps when Bending Corrections for Si_3H_6 Are Taken into Account.^a

State	Adiabatic Excitation Energy (eV)	Optimum Angle (°)
$^1[(\sigma^2)^1(\sigma_\ell\sigma_r)]$	0.0 ^b	89.01
$^3[{}^3(\sigma\pi)^1(\sigma_\ell\sigma_r)]$	0.36	101.96
$^3[(\sigma^2)^3(\sigma_\ell\sigma_r)]$	0.73	101.63
$^3[{}^1(\sigma\sigma_\ell)^3(\pi\sigma_r)]$	0.94	110.46
$^5[{}^3(\sigma\pi)^3(\sigma_\ell\sigma_r)]$	0.72	110.94
$^1[{}^1(\sigma\sigma_\ell)^1(\pi\sigma_r)]$	1.05	110.12

^aSee Chapter 2 for the Si_3H_6 calculation.

^bTotal energy is -13.397155 hartree.

are not correctly described unless d-functions are present at the divalent atom.

For the geometry optimizations all silicon atoms were allowed to rotate so that they would allow the system to reach its minimum in energy. The Si-H bonds rotated as if they were Si-Si bonds with the "bulk" (virtual) Si atoms kept fixed.

In the GVB CI calculations we used the valence spaces of the $1[1(\sigma^2)1(\sigma_\ell\sigma_r)]$, $3[3(\sigma\pi)1(\sigma_\ell\sigma_r)]$ and $5[3(\sigma\pi)3(\sigma_\ell\sigma_t)]$ states. In all three cases, the total valence space was used (10 orbitals). All double excitations were allowed between the 10 valence orbitals leading to wavefunctions consisting of 32 to 278 determinants.

D. Trivalent Steps on (111) Si Surfaces

Although the trivalent edge atoms in steps on Si (111) surfaces are not observed experimentally^{1a}, they should exist in at least one edge. This can be seen from the fact that although most of the observed steps have edges toward the $[\bar{1}\bar{1}2]$ directions, since the actual crystals used are finite in size, some edge must point toward the $[11\bar{2}]$ direction. This means that toward those directions trivalent edge atoms exist (or atoms in configurations that result from the rearrangement of such trivalent steps). It is, therefore, useful to consider the possible electronic states arising from such configurations.

By looking at a model of trivalent steps⁷ one quickly realizes that the geometry for such steps is the same as that of the

unreconstructed (110) surface. Each step atom has then one dangling bond and each surface atom in the upper terrace also has one dangling bond. We can use the results on our calculations on the Si_2H_4 , Si_3H_5 and Si_4H_6 clusters of Chapter 2, modelling the (110) surface to draw conclusions about the trivalent steps. We first note that, at the tetrahedral geometry, the overlap between adjacent dangling bonds (about 0.07) is too small to allow singlet pairing as compared to the high spin coupling states. Thus, for this geometry one expects the high spin states to be the lower energy states. However, as we have seen for the Si_2H_4 calculations, small rotations might produce a ground state in which some or all of the adjacent pairs of dangling bonds are paired up into singlets. This would produce a relaxation of the tetrahedral geometry leading to a new ground state at a relaxed geometry.

E. Review of Experimental Evidence

As mentioned in the introduction to this chapter, some experimental difficulties exist that preclude the complete and unique determination of effects due to steps. However, some properties can be experimentally investigated. Henzler^{1a,8} has studied the prevalence of steps on silicon and germanium. The presence of steps in the surface, even in small concentrations, can lead to considerable effects in the electronic and chemical properties of the surface.⁹ Ibach et al.^{9a} have provided evidence that step sites on Si lead to an increase of O_2 sticking probabilities by $\sim 10^3$; this is consistent with the

electronic structure at the divalent states we have found. For either the σ^2 or $\sigma\pi$ states, the presence of the $\bar{\sigma}$ radical orbital on the surface Si adjacent to the step Si provides even greater flexibility for scission of molecular bonds. Comprehensive studies of the increased reactivity of Pt due to steps have been provided by Somorjai et al.^{1c,10}.

For Si steps on (111) surfaces, it has been already mentioned that the preferred steps are those that have divalent edge atoms. The work of Rowe et al.^{9b} has indicated that surface states characteristic of steps have a different nature from those of the clean surface dangling bonds. They made a study in which Ultraviolet Photoelectron Spectroscopy (UPS) was used, together with Low Energy Electron Diffraction (LEED) to establish the relationship between the spectra and the surface structure as the step density was increased. Their main conclusions are that the Fermi level shifted by 0.25 eV toward the top of the valence band for a high density of steps surface. The one-half-order LEED features of the 2×1 structure were not present on the highest step-density surfaces [$\sim (16\pm 3)\%$]. These spots were observed only for step densities of less than $(12\pm 2)\%$. This means that the 2×1 reconstruction occurs only on terraces which have widths larger than $40\text{--}50\text{\AA}$. Similar results have been found by Henzler⁸ in germanium.

Other theoretical methods¹¹ have included a semi-infinite or a slab geometry in which an infinite number of atoms are present in an a priori chosen geometrical configuration. These methods use

wavefunctions in which the orbitals are doubly-occupied. As shown previously, this leads to the wrong ground state for the localized states present at the step configuration. We believe that such states require a proper account of correlation in order to be correctly described.

REFERENCES FOR CHAPTER 3

1. (a) M. Henzler, Surf. Sci. 36, 109 (1973); (b) H. P. Bonzel, in Surface Physics of Materials, J. M. Blakely, ed. (Academic Press, New York, 1975), Vol. II, p. 279; (c) G. A. Somorjai, R. W. Joyner and B. Lang, Proc. Roy. Soc. (London) A331, 335 (1972).
2. Hybridizations are obtained from Mulliken population analysis [R. S. Mulliken, J. Chem. Phys. 23, 1833, 1841 (1955)]. We did not renormalize and thus the sum of the $s^x p^y d^z$ exponents ($x+y+z$) represents the percentage character on the appropriate atom.
3. (a) I. Dubois, G. Herzberg and R. D. Verma, J. Chem. Phys. 47, 4262 (1967); (b) B. Wirsam, Chem. Phys. Lett. 14, 214 (1972); (c) H. Bürger and R. Eujen, Topics in Current Chem. 50 (Silicon Chemistry I), 1 (1974).
4. (a) W. A. Goddard III, T. H. Dunning, Jr., W. J. Hunt and P. J. Hay, Accts. Chem. Res. 6, 368 (1973); (b) W. J. Hunt, P. J. Hay and W. A. Goddard III, J. Chem. Phys. 57, 738 (1972).
5. S. Huzinaga, J. Chem. Phys. 42, 1293 (1965).
6. F. Bobrowicz, Ph.D. Thesis, California Institute of Technology, 1973 (unpublished).
7. See, for example, Fig. 6 of Ref. 1a.
8. (a) M. Henzler, Surf. Sci. 19, 159 (1970); (b) ibid, 22, 12 (1970).
9. (a) H. Ibach, K. Horn, R. Dorn and H. Luth, Surf. Sci. 38, 433 (1973); (b) J. E. Rowe, S.B. Christman and H. Ibach, Phys. Rev. Lett. 34, 874 (1975).

10. (a) K. Baron, D. W. Blakely, G. A. Somorjai, Surf. Sci. 41, 45 (1974); (b) M. A. Chester and G. A. Somorjai, Surf. Sci. 52, 21 (1975).
11. (a) V. T. Rajan and L. M. Falicov, J. Phys. C: Solid State Phys. 9, 2533 (1976); (b) M. Schlüter, K. M. Ho and M. L. Cohen, Phys. Rev. B 14, 550 (1976); see also J. A. Appelbaum, G. A. Baraff and D. R. Hamann, Phys. Rev. B 11, 3822 (1976).

Chapter 4

OXYGEN CHEMISORPTION ONTO SILICON (111) SURFACES

A. Introduction

In this chapter we will describe the results of calculations in which oxygen is chemisorbed onto the (111) surface of silicon.

Experimentally, when a clean Si (111) surface is exposed to oxygen, the chemisorption process occurs in two phases¹: First there is rapid adsorption until a saturation level is reached (at 10^{-4} - 10^{-2} torr-sec oxygen exposures); this is followed by a slow formation of an oxide layer. We will consider here only the early stages of the first phase. We conclude that in the initial chemisorption of O_2 on (111) silicon surfaces the O_2 is bound as a peroxy radical, in which the oxygen molecule binds to only one dangling bond on the surface. This model is consistent with all current experimental data^{1,15,23-32} (much of which was obtained subsequent to the proposal of the peroxy radical model⁵).

As in previous chapters we have used finite clusters in which the core electrons of all the silicon atoms have been replaced by the effective potential (EP) of Chapter 1. Hydrogen atoms have been utilized in a manner similar to that of Chapters 1 to 3, with a Si-H bond length of 1.48\AA (from silane²). The Si-Si bond length is taken from crystalline silicon³, i.e., $R_{\text{Si-Si}} = 2.35\text{\AA}$.

The motivation for these studies arises from the considerable amount of controversy existing in the literature⁴ as to the actual

manner in which oxygen chemisorbs on silicon. Two basic mechanisms have been postulated: in one the oxygen fissions as it chemisorbs; in the other the O_2 stays basically intact and bridges between two surface Si. By performing calculations with both single oxygen atoms and O_2 molecules chemisorbed on the surface and comparing them with the experimental data, we expect to shed some light on the actual mechanism of chemisorption. This, of course, is a problem of considerable technical interest. Also, an understanding of chemisorption in silicon can be of considerable value in the understanding of oxidation of other systems.

We start our discussion by considering the chemisorption of atomic oxygen on the surface. In Section C we consider the peroxy radical model.⁵

B. Atomic Oxygen Chemisorption

General Description

We will start by considering the chemisorption of single oxygen atoms on the clean (111) surface of silicon. This surface has been described in Chapter 2, where we found that its basic electronic structure consists of one dangling bond electron per surface Si.

The ground state of the oxygen atom 3P , has the configuration $(1s)^2(2s)^2(2p)^4$. From various studies of oxygen containing molecules^{6,7} it is found that the 1s and 2s electrons do not participate actively in bonding. Thus the active part of the O atom can be described schematically as shown in Fig. 1a. We have four electrons to

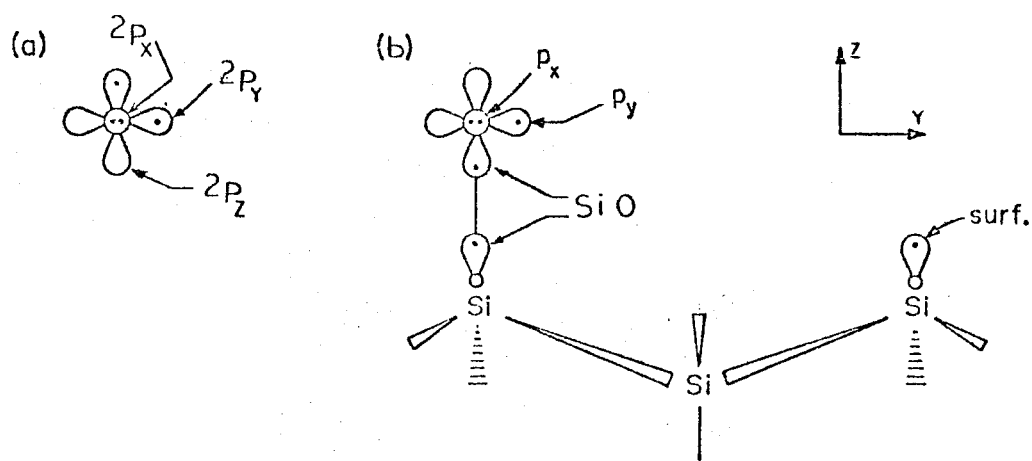


Fig. 1 Schematic diagrams for (a) oxygen atom (3P); (b) ground state of chemisorbed oxygen atom. $1s$ and $2s$ orbitals have been ignored and p orbitals parallel and perpendicular to the plane of the paper are indicated by ∞ and \circ , respectively. Dots indicate how many electrons are in each orbital.

be distributed between the three 2p orbitals, leading to one doubly occupied orbital ($2p_x$ in Fig. 1a, denoted by two dots), and two singly-occupied orbitals ($2p_y$ and $2p_z$ in Fig. 1a).

Now consider bonding this O atom to a dangling bond orbital of the (111) surface, as in Fig. 1b. A strong Si-O bond is formed by pairing one of the oxygen singly-occupied orbitals, say $2p_z$, with the singly-occupied dangling bond of the surface. This leaves one singly-occupied orbital ($2p_y$) and a doubly-occupied orbital ($2p_x$) on the oxygen, a configuration we will denote as

$$(p_y)^1 (p_x)^2 \quad (1a)$$

The state

$$(p_y)^2 (p_x)^1 \quad (1b)$$

also has the same energy so that the ground state of the chemisorbed O atom is a doubly degenerate doublet state. Classifying the states in terms of the Si-O axis⁹ the ground state becomes $^2\Pi$. Low lying excitations will involve

$$\begin{array}{lcl} \text{band} & \rightarrow & 0p_y \\ \text{Si-O} & \rightarrow & 0p_y \end{array} \quad (2)$$

Considering now the positive ion states associated with the O, direct ionizations from the ground state lead to configurations of the form⁹

$$^3\Sigma^-, ^1\Delta^- : (\text{SiO})^2 (0p_y)^1 (0p_x)^1 \quad (3)$$

$$1_{\Delta}^+, 1_{\Sigma}^+ \quad \begin{array}{c} (\text{SiO})^2 (\text{Op}_y)^2 \\ (\text{SiO})^2 (\text{Op}_x)^2 \end{array} \quad (4)$$

$$3_{\Pi}, 1_{\Pi} \quad \begin{array}{c} (\text{SiO})^1 (\text{Op}_y)^2 (\text{Op}_x)^1 \\ (\text{SiO})^1 (\text{Op}_y)^1 (\text{Op}_x)^2 \end{array} \quad (5)$$

where in each case the symmetry designation is in terms of the SiO axis only. (SiO) represents the orbital localized mainly in the region of the silicon-oxygen bond, (Op_y) and (Op_x) represent p-like orbitals.

For our calculations we have used two clusters, one having only one Si atom, O-SiH_3 , and the other having four silicons, $\text{O-Si}(\text{SiH}_3)_3$, with the additional silicons corresponding to second layer atoms.

Results

The results of Hartree-Fock (HF) calculations on OSiH_3 are shown in Table I. The HF wavefunction [eq. (6) below] was utilized to solve for the $(p_y)^1(p_x)^2$ ground state. The optimum bond length for the Si-O bond is 1.63\AA which compares well to the values 1.63\AA to 1.64\AA found experimentally in systems with SiO single bonds.¹⁰

In Table II we show the excitation energies for the GVB-CI calculation for the neutral OSiH_3 and $\text{O-Si}(\text{SiH}_3)_3$ complexes. Note that the two components of the $^2\Pi$ state, (1), are separated by 0.1 to 0.2 eV. This result obtains because we solved for one component, (1a), self-consistently and then carried CI calculations based on these orbitals.

Table I. Hartree-Fock Energies for the Ground State of the O-SiH₃ Cluster.^a All energies are in hartrees.

Si-O Distance [Å]	Energy
1.528	-80.355637
1.617	-80.364242
1.634	-80.364254
1.740	-80.359823
Minimum ^b	
1.626 ^c	-80.364295

^aThe geometry is that of silane for the SiH₃ part. The DZd basis set of Table XI, Chapter 1, was used for Si.

^bObtained from a cubic splines fit to the calculated points.

^cExperimental values of SiO bond lengths are: $R_{\text{SiO}} = 1.633\text{\AA}$ from (SiH₃)₂O, $R_{\text{SiO}} = 1.64\text{\AA}$ from (SiCl₃)₂O, $R_{\text{SiO}} = 1.63\text{\AA}$ from (CH₃)₃Si-O-Si(CH₃)₃ and $R_{\text{SiO}} = 1.63\text{\AA}$ from Si[OSi(CH₃)₃]₄ (see Ref. 10). The calculated force constant for O-SiH₃ is 0.362 atomic units, corresponding to a vibrational energy of 0.096 eV.

Table II GVB-CI Calculations for the Neutral States of O-SiH_3 and $\text{O-Si(SiH}_3)_3$ Clusters.^a

All energies are in eV.

Excitations	Configuration			Spin	O-SiH_3	$\text{O-Si(SiH}_3)_3$	0 atom	
	SiO	0_{p_x}	0_{p_y}				Calculated ^f	Experimental ^e
Ground state	2	2	1	doublet	0.0 ^c	0.0 ^d	0.0	0.0
$02p_x \rightarrow 02p_y$	2	1	2	doublet	0.11	0.20	-	0.0
$\text{SiO} \rightarrow 02p_y$	1	2	2	doublet	2.29	2.48	2.19	1.97

^aSee the text for a description of the level of CI employed. The Si-O distance was 1.63Å.

^bSee Fig. 1 for a schematic of the orbitals referred to in this column.

^cTotal energy calculated was -80.33873 hartree.

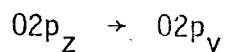
^dTotal energy calculated was -94.98157 hartree.

^eRef. 11

^fRef. 12

This leads to a slight bias, 0.1 to 0.2 eV, in favor of (1a) with respect to (1b).

Comparing the $\text{SiO} \rightarrow 02p_y$ excited state to the experimental¹¹ and calculated¹² spectra for the free oxygen atom, we see that the excitation energy of 2.3-2.5 eV indicates that this transition is very much like the



transition of the free oxygen atom (see also Fig. 1a). This transition is characteristic of the oxygen atom and is not present in the O_2 molecule¹³. It should be mentioned that a peak in the range 2.9-3.9 eV is found in the energy loss spectra of oxygen chemisorbed on Si (111) surfaces,¹⁴ but the interpretation of these spectra is made very difficult because of the presence of many peaks due to bulk and surface phenomena not associated with the oxygen. Ibach and Rowe¹⁵ observe a similar peak at 2.0 eV, but they associate it with the intrinsic states of the surface because its intensity decreases as the coverage of oxygen increases.

In Table III we compare the (Koopmans' theorem) ionization potentials for corresponding orbitals using the OSiH_3 and $\text{OSi}(\text{SiH}_3)_3$ clusters. The oxygen 1s orbitals do not change, as expected from chemical arguments. The ionization potential of the 02s orbitals increases by 0.9%, indicating a slight effect due to charge readjustment for the larger cluster. The largest changes occur in the p-like valence orbitals, and here the most sizable change is only 4.1%. This shows that these ionization potentials (from Koopmans' theorem) are not very sensitive to the size of the cluster.

Table III Comparison of Ionization Potentials for the O-SiH_3
and $\text{O-Si(SiH}_3)_3$ Cluster Calculations.^a

Orbital	Koopmans' Theorem Ionization Potential [eV]		% Change
	O-SiH_3	$\text{O-Si(SiH}_3)_3$	
01s	560.53	560.38	0.027
02s	318.36	321.09	0.85
02p _y	17.50	16.81	4.1
02p _x	15.86	15.48	2.5
Si-O ^b	20.18	19.41	4.0

^aUsing a GVB(1) wavefunction of the form (2). The Si-O bond length is 1.63Å.

^bOrbital energy of the first natural orbital of the GVB pair. This energy does not correspond to the Koopmans' Theorem energy, but should be close to it.

In Table IV we show the ionization potentials obtained from GVB-CI calculations for the O-SiH_3 and $\text{O-Si}(\text{SiH}_3)_3$ clusters. We first notice that even though these are not Koopmans' theorem ionization potentials (since each system is allowed to readjust its charge density) the comparison between the two clusters shows that the ionization potentials are not very sensitive to the size of the complex.

The comparison with the experimental values for a free oxygen atom¹¹ follows the same lines as that made for the neutral. As in the atom, it is easiest to ionize out of the doubly occupied ($02p_x$) orbital. We are then left with two singly occupied orthogonal orbitals ($02p_y$ and $02p_x$). This leads to two states: a triplet and a singlet. The triplet is lower due to a favorable exchange interaction. These two states have been referred to

$$^3\Sigma^- \text{ and } ^1\Delta^-: (\text{SiO})^2(0p_y)^1(0p_x)^1.$$

Ionizing out of the Si-O bond (or $02p_z$ for the free O atom) we are left with two singly-occupied orbitals again (the Si-O and $02p_y$). Since Si-O has σ symmetry and $02p_y$ has π symmetry with respect to the Si-O axis, we obtain two states again,

$$^3\Pi \text{ and } ^1\Pi (\text{SiO})^1(02p_y)^1(02p_x)^2$$

Ionizations out of the singly-occupied $02p_y$ orbital leave all orbitals doubly occupied. Two possibilities exist,

$$^1\Delta^+ \text{ and } ^1\Sigma^+ (\text{SiO})^2(02p_x)^2$$

Table IV GVB-CI Calculations for the Ion States of O-SiH_3 and $\text{O-Si(SiH}_3)_3$ Clusters.^a All energies are in eV.

State ^b		Spin	Ionization Potential ^c		
Ionizations ^d			O-SiH_3	$\text{O-Si(SiH}_3)_3$	O atom Experimental ^e
$02p_x$	vacuum	triplet	12.27	11.91	13.62
Si0	vacuum	triplet	13.87	13.52	16.94
$02p_y$	vacuum	singlet	14.60	14.07	16.94
$02p_x$	vacuum	singlet	14.63	14.24	-
Si0	vacuum	singlet	16.30	15.88	18.64

^aSee the text for a description of the level of CI employed. The Si-O distance was 1.63Å. Ionization potentials are calculated by solving for the appropriate state and subtracting the energy from that of the ground state.

^bSee Fig. 1 for a schematic of the orbitals referred to in this column

^cReferred to the corresponding energy of the neutral ground state.

^dIonizations involving simultaneous excitation of an electron are omitted as are ionizations involving Si-Si and Si-H bonds. Polarization corrections are estimated to be between 0.2 and 0.4 eV.

^eRef. 11.

of which Table IV shows only the lowest one.

These ionization potentials range between 11.9 and 16.3 eV. In comparing these values with the experimental data of Ibach and Rowe¹⁵ we see that they find peaks at 11.9, 15.1 and 18.4 eV (see Table VII and Fig. 4). Although the first two are within the range of values shown in Table IV, the 18.4 eV peak is not. We shall see later that this peak can be tentatively assigned to an ionization out of the O-O bond and thus one does not expect to see this peak in the spectrum of chemisorbed single oxygen atoms.

Two types of errors are present in these calculations: (i) a positive charge on the surface leads to long range polarization effects that cannot be treated by a small finite cluster. Using the dielectric corrections discussed in Chapter 2 and Appendix B, we have estimated¹⁶ these errors to be between 0.2 and 0.4 eV. (ii) Because of the use of Koopmans' theorem in Table III, the positive ion states are described in terms of orbitals suitable for the ground state. This prevents the orbitals from contracting about the charged centers resulting in too large an ionization potential. A compensating error is that through the use of a HF ground state, the extra correlation error tends to lead to too small an ionization potential.

Computational Details

For the OSiH_3 system we have carried out calculations to optimize the SiO bond distance. This is done by letting the O atom move in a direction perpendicular to the surface (along the [111] direction). The ground state was solved self-consistently, using the DZd basis of

Table XI, Chapter 1 (p. 31) for the Si atom and the double zeta (4s2p) contraction of Dunning¹² for the O atom.

A Hartree-Fock wavefunction of the form

$$\begin{aligned} \Phi_{\text{HF}} = & \{ \Phi_{\text{bulk}} \phi_{\text{SiO}}(1) \phi_{\text{SiO}}(2) \alpha(1) \beta(2) \phi_{02p_x}(3) \phi_{02p_x}(4) \\ & \times \alpha(3) \beta(4) \phi_{02p_y}(5) \alpha(5) \} \end{aligned} \quad (6)$$

was used. Here Φ_{bulk} represents the wavefunction of the SiH bond pairs.

Once the optimum Si-O distance was determined we performed GVB and GVB-CI calculations on both the OSiH_3 and $\text{OSi}(\text{SiH}_3)_3$ clusters. The basis set in this case was the DZ basis of Table XI, Chapter 1 for the Si atoms, and Dunning's DZ basis for oxygen.¹² The GVB(2) wavefunction has the form

$$\begin{aligned} \Phi_{\text{GVB}} = & \{ \Phi_{\text{bulk}} [\phi_{\text{SiO}}(1) \overline{\phi_{\text{SiO}}}(2) + \overline{\phi_{\text{SiO}}}(1) \phi_{\text{SiO}}(2)] [\alpha(1) \beta(2) - \beta(1) \alpha(2)] \\ & \times [\phi_{02p_x}(3) \overline{\phi_{02p_x}}(4) + \overline{\phi_{02p_x}}(3) \phi_{02p_x}(4)] [\alpha(3) \beta(4) - \beta(3) \alpha(4)] \phi_{02p_y}(5) \alpha(5) \} \end{aligned} \quad (7)$$

Φ_{bulk} represents the SiH bond pairs for OSiH_3 and the SiH and SiSi bond pairs for $\text{O-Si}(\text{SiH}_3)_3$. Here both the Si-O bond pair and the $02p_x$ doubly occupied orbital are correlated.

For the CI calculations we used the space spanned by the orbitals of (7) plus one additional (virtual) orbital in the p_y direction (denoted $\overline{02p_y}$). For the neutral system the configurations were generated

by doing all single excitations from the basic configurations shown in Table V. All orbitals corresponding to ϕ_{bulk} were kept doubly occupied and no excitations were allowed out of them (thus we do not include them in Table V). In Table V, under each orbital we show the occupation number of that orbital for a particular configuration. Thus, if we write the CI wavefunction as

$$\Psi_{\text{CI}} = \sum_i c_i \Phi_i \quad (8)$$

(Φ_i is called a configuration, c_i is the CI coefficient), then for configuration 1 of Table V, Φ_1 has the form

$$\Phi_1 = \phi_{\text{bulk}} \phi_{02s}^{(1)} \phi_{02s}^{(2)} \phi_{\text{Si}0}^{(3)} \phi_{\text{Si}0}^{(4)} \phi_{02p_x}^{(5)} \phi_{02p_x}^{(6)} \phi_{02p_y}^{(7)} \chi_1 \quad (9)$$

(where χ_1 is an appropriate spin function). Note that when the occupation number is 2 the orbital appears twice (two electrons in that orbital), when it is 1 the orbital appears once and when the occupation is zero the orbital is omitted.

For the ionic system, all single excitations were performed from the basic configurations shown in Table VI. Again all orbitals represented by ϕ_{bulk} were kept doubly occupied.

C. Molecular Oxygen Chemisorption

General Description

We shall now consider the chemisorption of oxygen molecules to Si (111) surfaces. Due to the greater complexity of the electronic structure, new features appear in the spectrum. Also because

Table IV Basic Configurations for CI on the Neutral Systems of OSiH_3 and $\text{OSi}(\text{SiH}_3)_3$. All SiH and SiSi bond orbitals were kept doubly occupied.

Configuration	Orbital ^a						
	02s	Si0	$\overline{\text{Si0}}$	02p _x	$\overline{02p_x}$	02p _y	$\overline{02p_y}^b$
1	2	2	0	2	0	1	0
2	2	1	1	2	0	1	0
3	2	0	2	2	0	1	0
4	2	2	0	1	0	2	0
5	2	1	1	1	0	2	0
6	2	0	2	1	0	2	0
7	2	1	0	2	0	2	0
8	2	0	1	2	0	2	0
9	1	2	0	2	0	2	0
10	1	1	1	2	0	2	0
11	1	0	2	2	0	2	0

^aNumber shown represents the occupation of the orbital.

^bThis is a virtual orbital constructed by the orthogonalization to all other orbitals of (2).

Table VI Basic Configurations for CI on the Ion Systems of OSiH_3 and $\text{OSi}(\text{SiH}_3)_3$. All SiH and SiSi bond orbitals were kept doubly occupied.

Configuration	Orbital ^a						
	02s	Si0	$\overline{\text{Si0}}$	02p _x	$\overline{02p_x}$	02p _y	$\overline{02p_y}^b$
1	2	2	0	2	0	0	0
2	2	1	1	2	0	0	0
3	2	0	2	2	0	0	0
4	2	2	0	1	0	1	0
5	2	1	1	1	0	1	0
6	2	0	2	1	0	1	0
7	2	2	0	0	0	2	0
8	2	1	1	0	0	2	0
9	2	0	2	0	0	2	0
10	2	1	0	2	0	1	0
11	2	0	1	2	0	1	0
12	2	1	0	1	0	2	0
13	2	0	1	1	0	2	0
14	1	2	0	2	0	1	0
15	1	1	1	2	0	1	0
16	1	0	2	2	0	1	0
17	1	2	0	1	0	2	0
18	1	1	1	1	0	2	0
19	1	0	2	1	0	2	0

^aNumber shown represents the occupation of the orbital.

^bThis is a virtual orbital constructed by orthogonalization to all other orbitals of (2).

of the added degrees of freedom, more than one vibrational frequency is possible.

First we consider the electronic structure of an isolated oxygen molecule. We will start with a qualitative description of the system. The oxygen atom can be pictured as in Fig. 2a (or 1a) as discussed in Section B. Pairing two such oxygen atoms to form the O_2 molecule leads to Fig. 3b as the ground state^{6,7}. Here two singly-occupied 2p orbitals are paired up into a singlet to form the O-O bond. This leaves two other singly-occupied orthogonal orbitals leading to triplet ($^3\Sigma_g^-$) and singlet ($^1\Delta_g$) states of which the triplet is lower (due to a favorable exchange interaction). The other way of pairing these orbitals^{6,7}, Fig. 2c, leads to excited singlet states ($^1\Sigma_g^+$ and the other component of $^1\Delta_g$). Solving self-consistently for the orbitals of O_2 leads to significant delocalization of the orbitals but the qualitative picture still applies. The basic reason why the configuration of Fig. 2b is better than that of Fig. 2c is that the doubly-occupied p π orbitals¹⁷ can delocalize onto the other center for Fig. 2b (where there is a singly-occupied orbital on this center) but not for Fig. 2c (where there is another doubly-occupied orbital on this center).

Consider now bonding the O_2 to a dangling bond orbital of the (111) surface, as in Fig. 2d. After bonding one end of the O_2 to a surface silicon atom, there is a remaining unpaired orbital on the O_2 . However, this orbital is perpendicular to the SiO₂ plane and hence parallel to the surface so that it cannot (for the perfect surface)

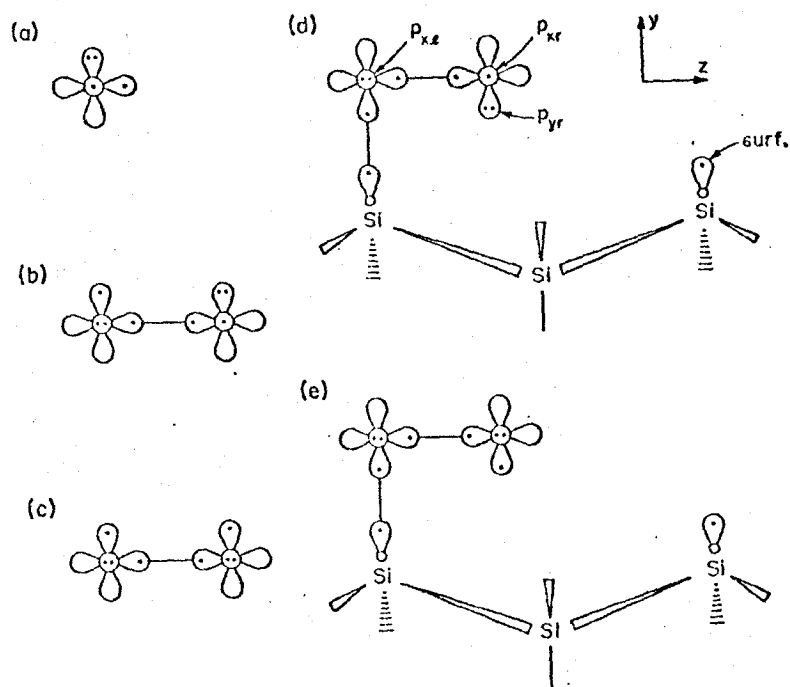


Fig. 2 Orbital diagrams for (a) oxygen atom (3P), (b) ground state O_2 , (c) excited state O_2 , (d) ground state of chemisorbed O_2 , (e) excited state of chemisorbed O_2 . 1s and 2s orbitals have been ignored and p orbitals parallel and perpendicular to the plane of the paper are denoted by ∞ and o , respectively. Dots indicate how many electrons are in each orbital. Orbitals combined into a singlet pair are indicated by a connecting line.

bond to another surface atom to form a bridged structure. That is, the chemisorbed O_2 is a peroxy radical.

On the other hand, the excited state of O_2 , Fig. 2c, leads to Fig. 2e upon bonding to the surface. In this case it is possible for the unpaired orbital of the silicon to form a bridged O_2 bond. The vertical excitation energy from the ground (Fig. 2d) to the excited (Fig. 2e) states of the bound O_2 should be similar to that found in the free molecule for the corresponding excitation, about 1eV.

The basic ionizations in this system occur out of the p_{y_r} orbital (refer to Fig. 2d), which is a doubly occupied orbital; the p_{x_r} singly-occupied orbital; the p_{x_l} doubly-occupied orbital the SiO; and OO bonds.

Results

To test the ideas discussed above and to allow detailed comparison with experiment, we carried out theoretical calculations on O_2SiH_3 and $O_2Si_3H_6$ clusters. For the O_2 -SiH₃ complex we have optimized the O-O bond length and the SiO-O angle, leading to $R_{O-O} = 1.366\text{\AA}$ and an Si-O-O angle of 125.9° . These compare with O-O bond lengths of 1.21\AA for the oxygen molecule¹⁰, 1.28\AA in ozone¹⁰ (O_3), 1.23 and 1.26\AA for iron dioxygen complexes¹⁸ (FeO_2); 1.28 to 1.48\AA for various cobalt dioxygen compounds²⁰ (CoO_2) and 1.34 for hydroperoxyl radical¹⁹ (HO_2). The bond angles range from 102° to 105° for hydroperoxyl radical¹⁹, to 110° to 120° for CoO_2 compounds²⁰, to 135° - 137° for FeO_2 complexes.¹⁸ We thus see that the geometry we have obtained for this peroxy radical falls within the values observed in other systems in

which the oxygen molecule has the same type of bonding with other ligands. Our results are shown in Tables VII and VIII. Table VII shows the GVB-CI energies for the different geometries of some of the relevant states of the O_2 -Si-H₃ complex. These are indicated by the most important excitations (refer to Fig. 2 for the meaning of the orbitals). In Table VIII we show the optimum values for the O-O bond length and the Si-O-O angle obtained by fitting a parabola to the appropriate points of Table VII.

In Fig. 3 we show the orbitals for the ground state of $O_2Si_3H_6$, at the optimum geometry of the O_2SiH_3 ground state (i.e., for $R_{O_2} = 1.366 \text{ \AA}$ and $\theta_{Si-O-O} = 125.9^\circ$). The band orbitals and the O1s-like orbitals are not shown. Just as assumed in the previous discussion (and found for other oxygen systems^{6,7}), the O2s orbitals are only slightly changed (Fig. 3c). The other orbitals are much as pictured in Fig. 2d, supporting the peroxy radical model.

Table IX summarizes the results for the peroxy radical. The calculated states are also shown in Table X where more information is given. Here we see that the neutral states of the peroxy radical can be interpreted on the basis of the excitations observed in the oxygen molecule. Thus the transition at 0.92-0.95 eV, in which an electron is excited from the doubly-occupied p_{y_r} orbital to the singly-occupied p_{x_r} orbital, follows the pattern of the 0.98 eV transition of O_2 , and in fact can be interpreted in exactly the same way. The transition at 6.2 eV ($p_{x_\ell} \rightarrow p_{x_r}$) is characteristic of peroxy radicals. It has a strong (oscillator strength ~ 0.1) broad (~ 2 eV)

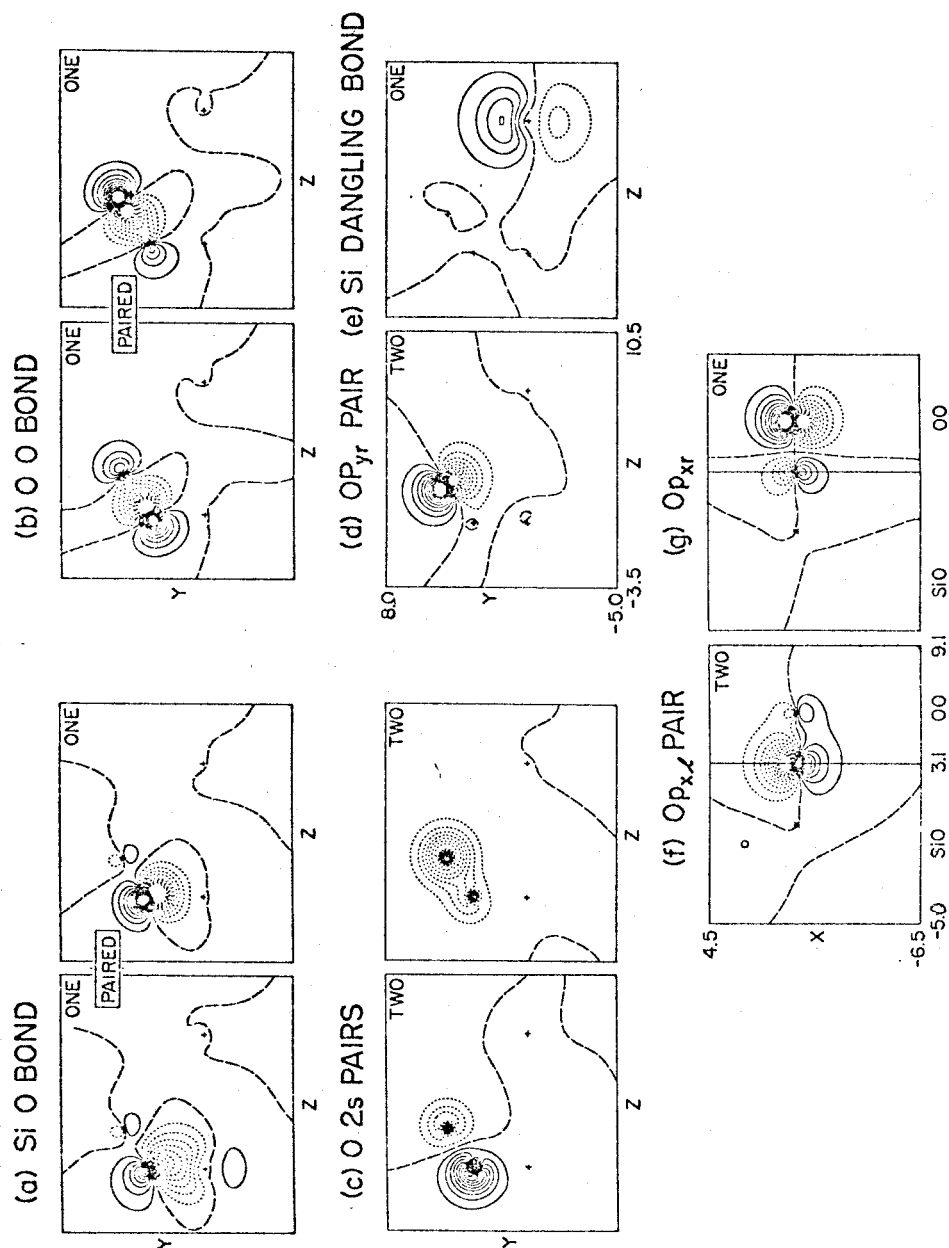


Fig. 3. The GVB orbitals of the $Si_3H_6O_2$ complex, where the O_2 is in the plane passing through two surface atoms and perpendicular to the surface (the atom positions are indicated by +). Bond orbitals and $O1s$ -like orbitals are not shown. Long dashes indicate nodal planes; the separation between contours is 0.05 a.u. Parts (a)–(e) are plotted in the SiO plane; (f) and (g) are each composite plots in planes perpendicular to the SiO plane and passing through the SiO and OO bonds, respectively.

Table VII GVB-CI Energies Relative to the Geometry Optimization for the O_2-SiH_3 Cluster.^a All energies are in hartrees.

State ^a	$R_{00} = 1.23\text{\AA}$ $\theta = 130^\circ$	$R_{00} = 1.34\text{\AA}$ $\theta = 130^\circ$	$R_{00} = 1.45\text{\AA}$ $\theta = 130^\circ$	$R_{00} = 1.34\text{\AA}$ $\theta = 115^\circ$	$R_{00} = 1.34\text{\AA}$ $\theta = 145^\circ$
Excitations					
$2A''$ ground state	-155.12918	-155.15160	-155.15284	-155.15304	-155.14344
$2A'$ $p_{y_r} \rightarrow p_{x_r}$	-155.09351	-155.12366	-155.13132	-155.09636	-155.12898
$2A'$ $SiO \rightarrow p_{x_r}$	-154.82007	-154.88348	-154.92629	-154.88693	-154.87167
$2A'$ $O-O \rightarrow p_{x_r}$	-154.77014	-154.83680	-154.86849	-154.84091	-154.82758
$2A''$ $p_{x_2} \rightarrow p_{x_r}$	-154.75924	-154.82982	-154.86670	-154.82593	-154.82632
Ionizations					
$3A''$ $p_{y_r} \rightarrow$ vacuum	-154.73603	-154.73701	-154.72281	-154.71767	-154.73991
$1A''$ $p_{y_r} \rightarrow$ vacuum	-154.69660	-154.69882	-154.68608	-154.67991	-154.70245
$1A'$ $p_{x_r} \rightarrow$ vacuum	-154.69377	-154.69091	-154.67329	-154.68798	-154.68630
$3A'$ $p_{x_r} \rightarrow$ vacuum	-154.53002	-154.57858	-154.59711	-154.57402	-154.57607
$3A''$ $Si-O \rightarrow$ vacuum	-154.49558	-154.55737	-154.58859	-154.54469	-154.55907
$1A''$ $Si-O \rightarrow$ vacuum	-154.49558	-154.55737	-154.58859	-154.54469	-154.55907
$3A''$ $O-O \rightarrow$ vacuum	-154.43011	-154.47403	-	-154.47859	-154.46274

^aThe local C_s symmetry of the cluster is used so the states have A' or A'' symmetry. See Fig. 2 for an explanation of symbols used in this column.

Table VIII Optimum Geometries for the GVB-CI Calculations on the O_2-SiH_3 Cluster. All bond lengths are in angstroms and all angles are in degrees

State ^a	R_{00}	θ_{SiO}
Excitations		
$^2A''$ ground state	1.366	125.88
$^2A'$ $p_{y_r} \rightarrow p_{x_r}$	1.381	135.54
$^2A'$ $SiO \rightarrow p_{x_r}$	1.459	124.78
$^2A'$ $O-O \rightarrow p_{x_r}$	1.495	110.45
$^2A''$ $p_{x_\ell} \rightarrow p_{x_r}$	1.410	123.35
Ionizations		
$^3A''$ $p_{y_r} \rightarrow$ vacuum	1.303	135.22
$^1A''$ $p_{y_r} \rightarrow$ vacuum	1.306	135.64
$^1A'$ $p_{x_r} \rightarrow$ vacuum	1.279	129.73
$^3A'$ $p_{x_r} \rightarrow$ vacuum	1.392	130.11
$^3A''$ $SiO \rightarrow$ vacuum	1.407	136.00
$^1A''$ $SiO \rightarrow$ vacuum	1.402	136.45
$^3A''$ $O-O \rightarrow$ vacuum	1.756	128.04

^aThe local C_s symmetry of the cluster is used so the states have A' or A'' symmetry. See Fig. 2 for an explanation of symbols used in this column.

Table IX. Excitation Energies and Ionization Potentials for the Peroxy-Radical Model. Ionizations involving simultaneous excitation of an electron are omitted, as are ionizations involving the SiH bonds. All energies are in eV.

State	Calculated Energy (GVB-Cl) ^a		Experi- mental Results ^d	Corresponding values for O ₂ ^e for HO ₂ ^e	
Excitation	SiH ₃ O ₂	Si ₃ H ₆ O ₂	O ₂ on Si		
Ground State	0.00	0.00, 0.007	0.00	0.00	0.00
$p_{yr} \rightarrow p_{xr}$	0.84	0.92, 0.95		0.98	0.93
$p_{xl} \rightarrow p_{xr}$	6.65	6.19, 6.19		8.6	6.40
$OO\sigma \rightarrow p_{xr}$	6.51	6.54, 6.55		—	7.54
SURF ^b $\rightarrow p_{xr}$	—	7.68		—	
SiO $\rightarrow p_{xr}$	7.96	7.90, 8.17		—	
$p_{yr} \rightarrow \text{SURF}^b$	—	9.98		—	
Ionization					
$p_{yr} \rightarrow \text{vac}$	10.81, 11.82	11.00, 11.08, 11.99	} 11.9	16.7	
$p_{xr} \rightarrow \text{vac}$	11.51	11.37		12.3	
$p_{xl} \rightarrow \text{vac}$	14.4	14.23, 14.23	} 15.1	16.7	
SiO $\sigma \rightarrow \text{vac}$	14.73, 14.78	15.00, 15.04, 15.28		—	
$OO\sigma \rightarrow \text{vac}$	17.42	17.54, 18.02, 18.06	18.4	18.2	

^aFor the states of the neutral system, the two entries correspond to the triplet and singlet states resulting from the coupling of the surface orbital with the singly-occupied orbital of the O₂. For the infinite solid, one expects a narrow band of states corresponding to each of these pairs of states. For the ion states there are generally two doublet states and one quartet for each configuration.

^bHere SURF indicates the surface dangling bond orbital.

^cRef. 19c

^dRef. 15, assignments are tentative.

^eRef. 13

Table X. Excitation Energies and Ionization Potentials for the GVB-CI Calculations of the $O_2-Si_3H_6$ Cluster.^a All energies are in eV.

State	Energy	Spin
Excitations		
ground state	0.0 ^b	triplet
	0.007	singlet
$p_{y_r} \rightarrow p_{x_r}$	0.922	singlet
	0.951	triplet
$p_{x_\ell} \rightarrow p_{x_r}$	6.191	triplet
	6.193	singlet
$0-0 \rightarrow p_{x_r}$	6.542	triplet
	6.548	singlet
surf $\rightarrow p_{x_r}$	7.684	singlet
SiO $\rightarrow p_{x_r}$	7.904	triplet
	8.171	singlet
$p_{y_r} \rightarrow \text{surf}$	9.978	triplet
Ionizations		
surf \rightarrow vacuum	8.712	doublet
surf \rightarrow vacuum + $p_{y_r} \rightarrow p_{x_r}$	10.265	doublet
$p_{y_r} \rightarrow$ vacuum	11.004	quartet
	11.084	doublet
	11.990	doublet
$p_{x_r} \rightarrow$ vacuum	11.366	doublet
$p_{y_r} \rightarrow$ vacuum + $p_{y_r} \rightarrow p_{x_r}$	13.378	doublet
$p_{x_\ell} \rightarrow$ vacuum	14.225	quartet
	14.231	doublet
surf \rightarrow vacuum + $p_x \rightarrow p_{x_r}$	14.684	doublet

Table X - Continued

State	Energy	Spin
SiO → vacuum	15.001	doublet
	15.039	quartet
	15.280	doublet
	15.874	doublet
SiO → vacuum + $p_{y_r} \rightarrow p_{x_r}$	15.975	quartet
	16.605	doublet
	17.543	doublet
O-O → vacuum	18.021	quartet
	18.062	doublet
O-O → vacuum + $p_{y_r} \rightarrow p_{x_r}$	18.707	doublet
	18.857	quartet

^aAt the optimum geometry for the O₂-Si-H₃ cluster. The orbital space used was obtained from a GVB(3) calculation for the ²A¹ ground state. The basis was the MXS2 set of Table XI, Chapter 1 for the two surface silicons, and the double zeta contraction of Dunning (Ref. 12) for the oxygen atoms.

^bTotal energy calculated was -164.25595 hartree.

absorption. This transition has the same origin as the $3\Sigma_u^- \leftarrow 3\Sigma_g^-$ absorption band of oxygen¹³ at 8.6 eV and should result in dissociation of the O_2 bond, leading to a chemisorbed atom plus a free oxygen atom, with a significant probability of the O atom being in the singlet state.

As indicated in Table IX and shown in Fig. 4 we find ionization potentials in very good agreement with the experimental values of Ibach and Rowe.¹⁵ The calculated excitation energies and ionization potentials are close to what would be predicted using our model and the known values for O_2 or HO_2 . The main changes occur in (i) the singly-occupied oxygen orbital (p_{x_r}) whose ionization potential increases from 12.3 eV (for O_2) to 15 eV upon bonding to the Si and (ii) the doubly-occupied orbital (p_{y_r}), which is a bonding orbital in O_2 (with an ionization potential of 16.7 eV) but which must delocalize onto the oxygen on the right, thereby decreasing its ionization potential to ~11.5 eV.

Replacing the Si_3H_6 unit with an SiH_3 unit leads to small changes, indicating that these excitation energies and ionization potentials are not greatly affected by changes in the size of the cluster. Corrections due to the polarizability of the semi-infinite solid can be estimated in the manner discussed in Chapter 2 and Appendix B. For the present system we estimate²¹ them to be of the order of 0.2-0.4 eV.

Combining excitation energies from calculations with experimental thermochemical data²² for silicon compounds with bonding

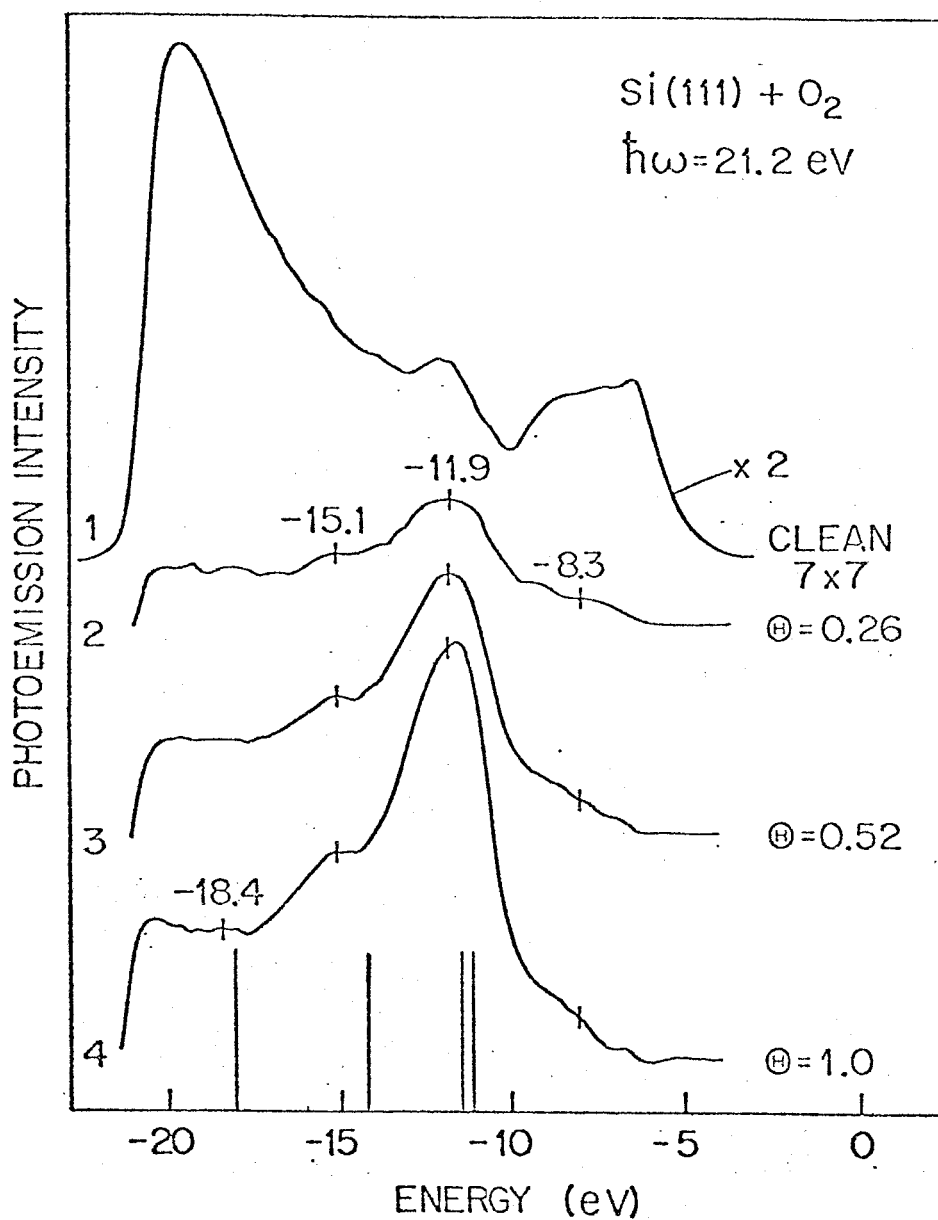


Fig. 1 Comparison of the calculated ionization potentials for the peroxy radical model and the experimental spectrum (after Ref. 15). Calculated values are indicated by vertical lines. Θ is the fractional O₂ coverage. Curves 2-4 are difference spectra between the surface exposed to O₂ and the clean surface.

configurations similar to those found in oxygen chemisorption, our best estimates of the energetics in this case are as follows: referencing all the bond energies to an O_2 molecule and a free silicon surface, the O_2 bonded to the silicon surface (in the peroxy radical form) is at -2.2 to -2.5 eV; the dissociative adsorption of the O_2 , leaving a single oxygen bonded to the surface and the other oxygen free, is at +0.5 to +0.3 eV. The state with the O_2 bond broken and the two oxygen atoms independently bonded to two separate sites on the silicon surface is at -4.1 to -4.5 eV; however, the barrier separating this state from the ground state of the peroxy radical is expected to be large. The excited state of the O_2 is at +1.0 eV. The state with the O_2 in an excited state and bonded to the silicon surface in the peroxy radical form is at -1.3 to -1.5 eV. The barrier between this state and that with two oxygen atoms separately bonded to the surface should be rather much smaller than the comparable barrier for the ground state of the O_2 bonded to the surface.

In Table XI we show some of the energies for GVB and GVB-CI calculations on complexes related to O_2 chemisorption. Referencing all the bond energies to an O_2 molecule and a free silicon surface, we estimate the energetics (based on the GVB calculations) as follows: The O_2 bonded to the silicon surface (in the peroxy radical form) is at -3.87 eV; the dissociative chemisorption of the O_2 leaving a single oxygen bonded to the surface and the other oxygen free is at -3.23 eV. The state with the O_2 bond broken and the two oxygen atoms independently bonded to two separate sites on the silicon surface is at -6.56 eV.

Table XI Total Energies Relative to the Energetics Involved on the Peroxy Radical Model.^a

Complex	GVB Total Energy (hartree)	GVB-CI
O-SiH ₃	-80.31098	-80.33873
O ₂ -SiH ₃	-155.13326	-155.17888
SiH ₃	-5.38986	-
O	-74.79884	-
O ₂	-149.60125	-149.68480

^aValues obtained from SCF GVB calculations.

Computational Details

The geometry of the clusters used in these calculations is as follows: for O_2-SiH_3 an oxygen molecule is placed on top of an SiH_3 unit with one of the oxygen atoms bonded to the Si atom, as in Fig. 2. For $O_2-Si_3H_6$, an O_2 molecule is placed on top of one of the surface silicons of a (111) Si surface modelled by an Si_3H_6 cluster as in Chapter 2. Here the three silicon atoms are placed at the positions of a silicon lattice, as in Fig. 2. Hydrogens replace broken Si-Si bonds. The Si-O bond length used was 1.63\AA for all cases considered.

For O_2-SiH_3 we optimized the O-O bond length and the Si-O-O angle (see Tables VII and VIII). This was done by (i) choosing a fixed angle ($\theta_{Si-O-O} = 130^\circ$) and minimizing the energy for in the O-O bond length and (ii) choosing a fixed O-O bond length ($R_{OO} = 1.34\text{\AA}$) and minimizing the energy for variations of the Si-O-O angle. These calculations were performed for GVB and CI wavefunctions. The choice of wavefunction in this case is important because the HF method is not adequate for these studies. (For O_2 the HF wavefunction only accounts⁷ for 0.9 eV of the 5.2 eV experimental bond energy. Including a configuration interaction over just the GVB orbitals (GVB-CI) accounts⁷ for 4.9 eV of the 5.2 eV bond energy of O_2 .)

The basis set used was the double zeta basis of Table XI, Chapter 1, for the Si part in O_2-SiH_3 . The oxygen double zeta contraction of Dunning¹² was used. In $O_2-Si_3H_6$ we used the MXS2 basis

of Table XI, Chapter 1 with the Dunning¹² double zeta basis for oxygen.

For the GVB-CI calculations on $O_2-Si_3H_6$ the space spanned by the GVB orbitals was used. Two virtual orbitals were added, localized mainly in the p_{x_l} and p_{x_r} directions. The orbitals were divided into two sets. These localized on Si-Si and Si-H bonds were kept doubly-occupied for all configurations. The other orbitals consist of two O_2s orbitals, a doubly occupied p_{y_r} orbital, a surface dangling bond (surf), two O-O bond natural orbitals, two Si-O natural orbitals, two oxygen orbitals (p_{x_l} and p_{x_r}) and two oxygen π virtual orbitals ($p_{x_l}^{virt}$ and $p_{x_r}^{virt}$). All double excitations were allowed within the O-O and Si-O bonds for the configurations shown in Table XII. In this way 30 configurations are generated for the neutral and 68 for the ionic system. To these we added all single excitations from the 30 (for the neutral) and 68 (for ions) configurations described above. Thus the wavefunctions actually consisted of 646 to 1004 determinants for the cases considered here. For O_2-SiH_3 the same procedure was used to generate the configurations with the exception that there was no surface dangling bond orbital.

D. Chemisorption Models and Review of Experimental Data

The oxidation of silicon surfaces has been studied experimentally since the early sixties.^{14,15,23-33} Two basic models have been proposed; in one case the oxygen molecule is assumed to fission upon chemisorption.^{14,29} The other model proposes that initially the

Table XII Basic Configurations for Performing Double Excitations within the O-O and Si-O Orbitals
for $O_2-Si_3H_6$

	$02s_\lambda$	$02s_r$	p_{yr}	surf	O-O	O-O	Si-O	$p_{x\ell}$	p_{xr}	$p_{x\ell}^{virt}$	p_{xr}^{virt}
Neutral	2	2	2	1	2	0	2	2	1	0	0
	2	2	2	1	2	0	2	1	2	0	0
	2	2	1	1	2	0	2	2	2	0	0
	2	1	2	1	2	0	2	2	2	0	0
	1	2	2	1	2	0	2	2	2	0	0
	2	2	2	1	1	0	2	2	2	0	0
	2	2	2	1	2	0	1	2	2	0	0
	2	2	1	2	2	0	2	2	2	0	0
Ions	2	2	2	0	2	0	2	2	1	0	0
	2	2	1	0	2	0	2	2	2	0	0
	2	2	2	0	2	0	2	1	2	0	0
	2	1	2	0	2	0	2	2	2	0	0
	1	2	2	0	2	0	2	2	2	0	0
	2	2	1	1	2	0	2	2	1	0	0
	2	2	1	1	2	0	2	1	2	0	0
	2	2	2	1	1	0	2	2	1	0	0
	2	2	2	1	2	0	1	2	1	0	0
	2	1	2	1	2	0	2	2	1	0	0

Table XIII - continued

Ions	02s _ℓ	02s _r	p _y r	surf	0-0	0-0	Si-0	Si-0	p _{xℓ}	p _{xr}	virt p _{xℓ}	virt p _{xr}
1	2	2	2	1	2	0	0	2	2	1	0	0
2	2	2	2	1	2	0	0	2	2	0	0	0
2	2	2	2	1	2	0	0	2	1	1	0	0
2	2	2	0	1	2	0	0	2	2	2	0	0
2	2	2	1	1	1	0	0	2	2	2	0	0
2	2	2	1	1	2	0	0	1	2	2	0	0
2	1	1	1	1	2	0	0	2	2	2	0	0
1	2	2	1	1	2	0	0	2	2	2	0	0

molecule chemisorbs without fissioning.^{15,25} Several possibilities for the structure of the chemisorbed O_2 are possible in this case. Considerable controversy has existed in the literature concerning these two basic models.⁴

Two versions of the fissioned O_2 chemisorption have been proposed. Meyer and Vrakking²⁹ proposed a model in which the oxygen atoms are inserted into Si-Si bonds forming a complicated structure. Ludeke and Koma¹⁴ proposed a model in which the oxygen atoms form a monoxide structure with double bonds between the oxygen atoms and the surface silicons.

The nonfissioned O_2 chemisorption models propose that the O_2 molecule can still be identified as such after it has chemisorbed. Green and Maxwell²³ proposed that a peroxide bridge is formed between adjacent Si atoms by the two oxygens. Our calculations led to the peroxy radical model discussed in the previous section in which the molecule is not dissociatively chemisorbed but only one O is bonded to a surface Si.

The basic experimental features to be explained are as follows: the photoemission results (of which those presented by Ibach and Rowe¹⁵ are representative) indicate a large peak at ~ 11.9 eV with smaller peaks at 15.1 eV and 18.4 eV, also a shoulder is observed at 8.3 eV. Ibach and Rowe¹⁵ have also observed transition energies at 3.5, 5.0, 7.2, 11 and 23 eV. These are due to electronic excitations in the oxygen surface system. Ibach et al.²⁵ have observed three different vibrational frequencies with a perpendicular component due to the oxygen at

the surface. Chiaradia and Nannarone³¹ showed that the oxygen chemisorbs without greatly affecting the dangling bonds in nearby surface silicons. In addition, Rowe et al.²⁶ have showed that two geometrically inequivalent types of oxygen atoms must occur at the oxidized surface. The peroxy radical model is consistent and agrees well (where comparison is possible) with these experimental results.

The most important objection that can be raised against the fissioned O_2 models is that they cannot explain the three localized vibrational modes observed by Ibach et al.²⁵ Ludeke and Koma¹⁴ have suggested that two vibrational peaks (at 0.125 eV and 0.090 eV) can be explained by the double bond monoxide model by assuming that they are similar to those of the $^1\Sigma^+$ and $^1\Pi$ states of SiO. This suggestion is untenable on several grounds: first, only vibrational frequencies of the ground state are observed in the experiments of Ibach et al.²⁵, thus the vibrational frequencies of an excited electronic state (like the $^1\Pi$ of SiO) are irrelevant; second, bonding the SiO to the other Si atoms in the surface leads to great changes in the other orbitals (e.g., the SiO bond length increases from 1.51 Å for the SiO molecule to 1.63 Å of the chemisorbed O atom) and surely leads to large changes in the vibrational frequencies; third, the $^1\Pi$ state of SiO has the electronic configuration

$$(\sigma SiO)^2 (\pi SiO)^2 (O p_y)^2 (Si 3p_y)^1 (Si 3s)^1$$

where σSiO is an SiO bonding orbital along the axis of the molecule; πSiO is a p_x -like bonding orbital and the electrons in the $Si 3p_y$ and $Si 3s$ orbitals are singlet coupled. Hence, to excite the surface Si-O to the $^1\Pi$ configuration requires breaking all three Si-Si bonds.

E. Conclusions

We have performed calculations on clusters that model the chemisorption of single oxygen atoms as well as molecular O_2 . From them we determined that, for the initial step of the chemisorption, the optimum geometry for chemisorbed O_2 is that of a peroxy radical, with one oxygen bound to only one surface silicon and the other oxygen in such a way that the Si-O-O angle is $\sim 126^\circ$. The optimum O-O bond length is 1.366 \AA . These values fall within the range of values observed experimentally for other peroxy systems. The predicted spectrum for the peroxy radical agrees with experimental results, and the vibrational modes expected for such a system are consistent with experimental observations.

For single oxygen atoms chemisorbed to the surface we see that one of the peaks in the ionization spectrum (that one corresponding to an ionization out of the O-O bond for the peroxy radical) is not present, contrary to experimental results. In addition this system cannot account for the three vibrational modes that have a component perpendicular to the surface or with the recent observation that two inequivalent types of oxygen atoms are present in the first stage of chemisorption.

REFERENCES FOR CHAPTER 4

1. H. Ibach, K. Horn, R. Dorn and H. Luth, *Surf. Sci.* 38, 433 (1973)
2. D. R. Boyd, *J. Chem. Phys.* 23, 922 (1955).
3. M. E. Straumanis and E. Z. Aka, *J. Appl. Phys.* 23, 330 (1952).
4. See for example (a) F. Meyer and J. J. Vrakking, *Surf. Sci.* 46, 287 (1974); (b) R. Dorn, H. Luth and H. Ibach, *ibid* 46, 290 (1974).
5. W. A. Goddard III, A Redondo and T. C. McGill, *Solid State Commun.* 18, 981 (1976).
6. W. A. Goddard III, Lecture Notes for Chem. 120, California Institute of Technology, 1975 (unpublished).
7. (a) W. A. Goddard III, T. H. Dunning, Jr., W. J. Hunt and P. J. Hay, *Accts. Chem. Res.* 6, 368 (1973); (b) B. J. Moss, F. J. Bobrowicz and W. A. Goddard III, *J. Chem. Phys.* 63, 4632 (1975).
8. The Jahn-Teller theorem would remove this degeneracy but the strong Si-O bond suggests that only small distortions occur in this case.
9. The point group is that of a heteronuclear diatomic molecule, $C_{\infty v}$. The angular momentum, λ , about the axis of rotation determines the types of symmetries that the wavefunction can take. For example
$$\begin{aligned}\Sigma &\rightarrow \lambda = 0 \\ \Pi &\rightarrow \lambda = 1 \\ \Delta &\rightarrow \lambda = 2\end{aligned}$$
10. (a) Interatomic Distances, L. E. Sutton, ed., The Chemical Society (London), Special Publication No. 11 (1958); (b) Interatomic Distances, Supplement, *ibid*, Special Publication No. 18 (1965).

11. C. E. Moore, Atomic Energy Levels, Nat. Bur. Standards (U.S.) Circular No. 467 (U.S. Government Printing Office, Washington, D.C., 1949).
12. T. H. Dunning, Jr., J. Chem. Phys. 53, 2823 (1970).
13. (a) G. Herzberg, Spectra of Diatomic Molecules (Van Nostrand, N.Y., 1950); (b) D. W. Turner, Molecular Photoelectron Spectroscopy (Wiley, N.Y., 1970).
14. R. Ludeke and A. Koma, Phys. Rev. Lett. 34, 1170 (1975).
15. (a) H. Ibach and J. E. Rowe, Phys. Rev. B 9, 1951 (1974); (b) ibid 10, 710 (1974).
16. We assumed h to be 1.63\AA corresponding to the SiO bond length. r_0 was taken to be the Si-Si bond length for the bulk, 2.35\AA .
17. σ orbitals are symmetric with respect to any mirror plane that contains the molecular axis; π orbitals are anti-symmetric with respect to mirror planes containing the axis.
18. J. P. Collman, R. R. Gagne, C. A. Reed, W. T. Robinson and G. A. Rodley, Proc. Nat. Acad. Sci. USA 71, 1326 (1974).
19. (a) D. H. Liskow, H. F. Schaefer and C. F. Bender, J. Am. Chem. Soc. 93, 6734 (1971); (b) H. E. Hunziker and H. R. Wendt, VII International Conference of Photochemistry, Jerusalem, Israel, August 1973 [IBM Res. Report RJ1373 (#21044), March 28, 1974]; (c) W. A. Goddard III and T. H. Dunning, unpublished calculations.
20. (a) R. S. Gall and W. P. Schaefer, to be published; (b) A. G. Sykes and J. A. Weil, Prog. Inorg. Chem. 13, 1 (1970).
21. We assumed h to be between 1.63 and 2.43\AA corresponding to the smallest and the largest perpendicular distances to the surface

from the peroxy radical part. Taking r_0 as 2.35\AA leads to the figures quoted.

22. D. Wagman, W. H. Evans, V. B. Parker, I. Halow, S. M. Bailey and R. H. Schumm, Selected Values of Chemical Thermodynamic Properties, Nat. Bur. Standards (U.S.) Technical Note 270-3 (U.S. Government Printing Office, Washington, D.C., 1968).
23. M. Green and K. H. Maxwell, J. Phys. Chem. Solids 13, 145 (1960),
24. G. A. Bootsma, Surf. Sci. 15, 340 (1969).
25. H. Ibach, K. Horn, R. Dorn and H. Lüth, Surf. Sci. 38, 433 (1973).
26. J. E. Rowe, G. Margaritondo, H. Ibach and H. Froitzheim, Solid State Comm. 20, 277 (1976).
27. R. Dorn, H. Lüth and H. Ibach, Surf. Sci. 42, 583 (1974).
28. J. E. Rowe, H. Ibach and H. Froitzheim, Surf. Sci. 48, 44 (1975).
29. F. Meyer and J. J. Vrakking, Surf. Sci. 38, 275 (1973).
30. J. Archer and G. W. Gobeli, J. Phys. Chem. Solids 26, 343 (1965).
31. P. Chiaradia and S. Nannarone, Surf. Sci. 54, 547 (1976).
32. B. A. Joyce and J. H. Neave, Surf. Sci. 27, 499 (1971).
33. (a) R. E. Kirby and D. Lichtman, Surf. Sci. 41, 447 (1974);
(b) R. E. Kirby and J. W. Dieball, Surf. Sci. 41, 467 (1974).

APPENDIX A

The Generalized Valence Bond (GVB) Wavefunctions

In order to clarify the discussions of wavefunctions in this report we include in this appendix a brief summary of the GVB wavefunctions. For more details see Refs. 12 and 22 of Chapter 1.

Consider a two-electron system such as H_2 or the He atom. The Hartree-Fock wavefunction has the form

$$\begin{aligned}\phi^{HF}(1,2) &= \mathcal{A}[\phi(1)\phi(2)\alpha(1)\beta(2)] \\ &= \phi(1)\phi(2)[\alpha(1)\beta(2) - \alpha(1)\beta(2)]\end{aligned}\quad (A.1)$$

where \mathcal{A} is the antisymmetrizer. The optimum orbitals are obtained by solving the resulting variational equation

$$H^{HF}\phi = \epsilon\phi \quad (A.2)$$

where

$$H^{HF} = h + J_\phi,$$

h is the one-electron Hamiltonian, and J_ϕ is the Coulomb potential for an electron in orbital ϕ .

In the GVB wavefunction for two electrons one allows each electron to have its own orbital, thus

$$\begin{aligned}\phi^{GVB}(1,2) &= \mathcal{A}\{\phi_a(1)\phi_b(2)[\alpha(1)\beta(2) - \beta(1)\alpha(2)]\} \\ &= [\phi_a(1)\phi_b(2) + \phi_b(2)\phi_a(1)][\alpha(1)\beta(2) - \beta(1)\alpha(2)]\end{aligned}\quad (A.3)$$

where ϕ_a and ϕ_b are generally nonorthogonal. Applying the variational principle to the GVB wavefunction leads to the equations

$$\begin{aligned} H_a^{\text{GVB}} \phi_a &= \epsilon_a \phi_a \\ H_b^{\text{GVB}} \phi_b &= \epsilon_b \phi_b \end{aligned} \quad (\text{A.4})$$

which must be solved for the optimum orbitals. In solving for these orbitals it is generally more convenient to transform the spatial part of (A.3) to the natural orbital (NO) form

$$N[\phi_a^{(1)}\phi_b^{(2)} + \phi_b^{(1)}\phi_a^{(2)}] = C_1\phi_1(1)\phi_1(2) + C_2\phi_2(1)\phi_2(2), \quad (\text{A.5})$$

where

$$\begin{aligned} \phi_1 &= (\phi_a + \phi_b)/D_1 \\ \phi_2 &= (\phi_a - \phi_b)/D_2 \\ \frac{C_2}{C_1} &= \frac{1-S}{1+S} \\ S &= \langle \phi_a | \phi_b \rangle \\ C_1^2 + C_2^2 &= 1 \end{aligned} \quad (\text{A.6})$$

and N , D_1 , and D_2 are suitable normalization constants. Since ϕ_1 and ϕ_2 are orthogonal, the corresponding variational equations are simpler to solve.

Replacing a HF pair such as in (A.1) by a GVB pair such as in (A.3) or (A.5) accounts for the dominant electron correlation of many-body effects involving these electrons. From the form in (A.5) one can

say that in the GVB method we solve for the occupied and correlating wavefunction simultaneously and self-consistently.

For a molecular system the correlated orbitals generally localize on or around one or two atoms leading to what can aptly be interpreted as a bond pair, a core pair, a nonbonding pair, etc. It is possible to selectively correlate only certain pairs; for example, in the ab initio wavefunction for the $^1\Sigma_g^+$ state of Si_2 , we might correlate all (four) pairs involving the valence orbitals (3s and 3p) but not correlate the Si core orbitals (1s, 2s, and 2p, ten altogether). Such a wavefunction would have the form

$$\{\phi_1^2\phi_2^2\cdots\phi_{10}^2(C_{11}\phi_{11}\phi_{12} + C_{12}\phi_{12}\phi_{11})(C_{13}\phi_{13}\phi_{14} + C_{14}\phi_{14}\phi_{13})(C_{15}\phi_{15}\phi_{16} + C_{16}\phi_{16}\phi_{15})(C_{17}\phi_{17}\phi_{18} + C_{18}\phi_{18}\phi_{17})^{\alpha\beta\alpha\beta\cdots\alpha\beta}\} \quad (\text{A.7})$$

[ten doubly-occupied core orbitals and four GVB correlated pairs (expressed in the (A.3) form)]. This wavefunction would be denoted as GVB(4) indicating that four pairs are correlated.

The programs for calculating the GVB orbitals can also allow additional natural orbitals in an expansion of the form in (A.5),

$$C_1\phi_1\phi_1 + C_2\phi_2\phi_2 + C_3\phi_3\phi_3 + C_4\phi_4\phi_4 \quad (\text{A.8})$$

and occasionally there are cases where such additional correlations are important; for example, a nonbonding orbital in a negative ion (CH_3^-). Such a wavefunction for two electrons is denoted as GVB(1/4)

indicating 4 NO's for describing one electron pair. For a many-electron wavefunction the form (A.8) would just replace the doubly-occupied orbital of a HF wavefunction. Physically not more than four to five NO's in an expansion of the form (A.8) can be expected to be important, corresponding, for example, to in-out (1) and angular correlations (3) of some doubly-occupied orbital.

Appendix B - DIELECTRIC CORRECTIONS

In this appendix we describe in detail how the polarization corrections for the Si_4H_9 complex were performed. We started by assuming that we had correctly described the polarization effects in the cluster, which in this case we substituted by a hemisphere of radius r_0 (determined by the size of the complex). We also assumed that a charge of one electron was located at a height h above the center of the hemisphere on the surface. The location h is determined by the particular characteristics of the complex. In order to estimate the effect of the polarization we calculated the change in free energy for the semi-infinite (continuous) dielectric with the hemispherical cavity when the charge is placed above it. The geometry is shown in Fig. B.1.

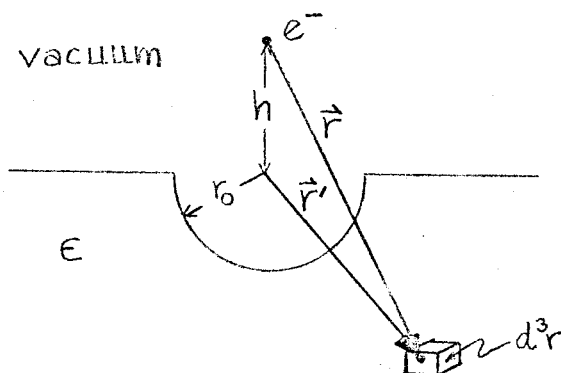


Fig. B.1. Geometry for Dielectric Corrections

The change in free energy is given by¹

$$\delta \mathcal{F} = - \frac{1}{2} \int \vec{\mathcal{P}} \cdot \vec{\mathcal{E}} d^3r \quad (\text{B1})$$

where $\vec{\mathcal{E}}$ is the electric field, given by¹

$$\vec{\mathcal{E}} = \frac{\hat{r}}{r^2} \quad , \quad (B2)$$

\hat{r} is the unit vector in the radial direction, $\vec{\mathcal{P}}$ is the polarization vector, given by¹

$$\vec{\mathcal{P}} = \frac{1}{2} \left(\frac{\epsilon-1}{\epsilon+1} \right) \frac{\hat{r}}{r^2} \quad (B3)$$

where ϵ is the dielectric constant of the semi-infinite continuum.

We now make the change $\vec{r} \rightarrow \vec{r}' - \vec{h}$, so that from Eqs. (B2) and (B3) we obtain

$$\vec{\mathcal{P}} \cdot \vec{\mathcal{E}} = \frac{1}{2\pi} \left(\frac{\epsilon-1}{\epsilon+1} \right) \frac{1}{r^4} = \frac{1}{2\pi} \left(\frac{\epsilon-1}{\epsilon+1} \right) \frac{1}{[r'^2 + h^2 - 2r'h \cos \theta]^2} \quad (B4)$$

where θ is the angle between \vec{r}' and \vec{h} . Substituting (B4) back into Eq. (B1) we get

$$\delta \mathcal{F} = - \frac{1}{4\pi} \left(\frac{\epsilon-1}{\epsilon+1} \right) \int_{\pi/2}^{\pi} \int_0^{2\pi} \int_{r_0}^{\infty} \frac{dr' d\phi d\theta r'^2 \sin \theta}{(r'^2 + h^2 - 2r'h \cos \theta)^2} \quad .$$

These integrations lead to

$$\begin{aligned} \delta \mathcal{F} = & - \frac{1}{4} \left(\frac{\epsilon-1}{\epsilon+1} \right) \frac{1}{h} \left\{ \lim_{\lambda \rightarrow \infty} \left[\frac{1}{2} \log(\lambda^2 + h^2) \right] - \frac{1}{2} \log(r_0^2 + h^2) \right. \\ & \left. + 1 - \lim_{\lambda \rightarrow \infty} [\log(\lambda + h)] - \frac{r_0}{r_0 + h} + \log(r_0 + h) \right\} \quad . \end{aligned}$$

Now

$$\lim_{\lambda \rightarrow \infty} \left\{ \frac{1}{2} \log(\lambda^2 + h^2) - \log(\lambda + h) \right\} = 0$$

leading to the final result²

$$\delta \mathcal{F} = - \frac{1}{4} \left(\frac{\epsilon - 1}{\epsilon + 1} \right) \frac{1}{h} \left\{ \frac{h}{r_0 + h} - \log \left[\frac{\sqrt{r_0^2 + h^2}}{r_0 + h} \right] \right\} .$$

REFERENCES FOR APPENDIX B

1. L. D. Landau and E. M. Lifshitz, Electrodynamics of Continuous Media (Addison-Wesley, Reading, MA, 1960), p. 52.
2. For a derivation of a similar problem in a spherical cavity see G. T. Surratt, Ph.D. Thesis, California Institute of Technology, 1975, p. 169.

Appendix C - EFFECT OF CORRELATION, d-FUNCTIONS AND LATTICE CONSTRAINTS ON THE Si_3H_6 CLUSTER MODEL FOR (100) Si SURFACES

As reported in the text, we have studied the effect of correlation (or the lack of it), the inclusion of d-functions in the basis set and the effect of the lattice constraints on the calculations for the Si_3H_6 cluster model of the Si (100) surface. Let us start with the effect of correlation; we will then examine the changes that occur when d-functions are included in the basis set. We will finally consider what happens when the constraints of the lattice are relaxed.

We have carried out calculations on the Si_3H_6 cluster for the $^1(\sigma^2)$ and $^3(\sigma\pi)$ states at the self-consistent field level. The effects of correlation are most prominent for the $^1(\sigma^2)$ state in which, for the Hartree-Fock (HF) wavefunction (no correlation), two electrons occupy the σ orbital. For $^3(\sigma\pi)$ this does not occur because the two electrons occupy two different open shell orbitals, σ and π . In order to introduce the most important effects of correlation, we have also performed calculations for the $^1(\sigma^2)$ state using a Generalized Valence Bond (GVB) wavefunction. The results are summarized in Tables C.I and C.II. For a double zeta basis (DZ) set, and keeping the constraints of the lattice at the HF level, the $^3(\sigma\pi)$ state is 0.75 eV below the $^1(\sigma^2)$ state (vertical excitation energy). When we allow for geometrical relaxation, an adiabatic excitation energy of 0.61 eV is found. If we include correlation for the same basis set and including the constraints of the lattice (i.e., letting the central Si atom move only in the [100] direction), the $^3(\sigma\pi)$ state is still the ground state,

Table C.I Summary of Results for Si_3H_6 Clusters Modelling the (100) Surface

	Optimum ^a Energy (hartree)	Optimum Angle (°)	Relaxation ^b Distance (Å)	Vertical ^c Excitation Energy(eV)	Adiabatic ^c Excitation Energy(eV)
With lattice constraints					
DZ basis set					
State: $1(\sigma^2)$ GVB	-14.555173	103.72	0.150	0.44	0.28
$1(\sigma^2)$ HF	-14.542985	104.18	0.138	0.75	0.61
$3(\sigma\pi)$	-14.565318	111.74	-0.056	0.0	0.0
DZd basis set					
State: $1(\sigma^2)$ GVB	-14.594092	105.43	0.104	0.0	0.0
$1(\sigma^2)$ HF	-14.574004	105.35	0.106	0.55	0.55
$3(\sigma\pi)$	-14.587655	111.49	-0.050	0.34	0.18
$1(\sigma\pi)$	-14.539713	111.67	-0.055	1.64	1.48
Without lattice constraints					
DZ basis set					
State: $1(\sigma^2)$ GVB	-14.553597	100.57	-	-	0.41
$1(\sigma^2)$ HF	-14.541581	101.52	-	-	0.74
$3(\sigma\pi)^d$	-14.568625	130.84	-	-	0.0
DZd basis set					
State: $1(\sigma^2)$ GVB	-14.595822	95.21	-	0.0	0.0
$1(\sigma^2)$ HF ^d	-14.575881	94.66	-	0.54	0.54
$3(\sigma\pi)$	-14.589082	119.87	-	0.49	0.18
$1(\sigma\pi)^d$	-14.542376	123.01	-	1.84	1.45

Footnotes for Table C.I

^aObtained by a cubic-splines fit to the calculated points. The values shown do not include the contribution due to the silicon core electrons, since these have been replaced by the effective potential (EP).

^bPositive values indicate motion toward the vacuum, away from the solid. Zero corresponds to the tetrahedral, unrelaxed geometry.

^cMeasured with respect to the ground state of the corresponding calculation.

^dThe minimum obtained for this state falls outside the range of calculated points and as such represents an extrapolation.

Table C.II - Potential Curves for the Si_3H_6 Cluster with the Lattice Constraints^a

	95°	105°	109°28'	115°
DZ basis set				
$^1(\sigma^2)_{\text{GVB}}$	-14.547280	-14.555010	-14.551941	-14.543080
$^1(\sigma^2)_{\text{HF}}$	-14.534341	-14.542915	-14.540308	-14.532118
$^3(\sigma\pi)$	-14.534275	-14.560361	-14.564764	-14.564172
DZd basis set				
$^1(\sigma^2)_{\text{GVB}}$	-14.579739	-14.594074	-14.592091	-14.583152
$^1(\sigma^2)_{\text{HF}}$	-14.560135	-14.573992	-14.571966	-14.563180
$^3(\sigma\pi)$	-14.552411	-14.582328	-14.587146	-14.586129
$^1(\sigma\pi)$	-14.505636	-14.534315	-14.539129	-14.538382

^aAll energies in hartree atomic units. Energies do not include the contribution of the core electrons of silicon atoms (an effective potential has been used for these).

with a vertical excitation energy for $^1(\sigma^2)$ of 0.44 eV. The adiabatic excitation energy of this state is found to be 0.28 eV. The potential curves for the double zeta basis set are shown in Fig. C.I. The effects of correlation for a basis set including d-functions are of crucial importance for $^1(\sigma^2)$. This was investigated by doing the same calculations over with the difference that to the double zeta basis set we added a set of d-functions to the central silicon atom (this basis set is called DZd in Chapter 1). In this case we found that without correlation the ground state is $^3(\sigma\pi)$ with the $^1(\sigma^2)$ state at 0.50 eV vertical excitation energy (in this case the adiabatic excitation energy is 0.37 eV for the $^1(\sigma^2)$ state). When correlation is included we find a $^1(\sigma^2)$ ground state with the $^3(\sigma\pi)$ state at 0.34 eV vertical excitation energy, as discussed in Chapter 2. Thus we see that unless both d-functions and correlation are included in the calculations we obtain the wrong ground state for the system. In terms of the potential curves (shown in Fig. C.2 and summarized in Table C.III for the DZd basis) we see that the effect of correlating the doubly-occupied pair for the $^1(\sigma^2)$ state there is a relative uniform correlation energy¹ of ~ 0.32 eV for the double zeta basis and ~ 0.54 eV for the DZd basis. The reason for this difference of ~ 0.22 eV is due to the fact that d-functions can be effectively used in correlating the $\sigma+\lambda\pi$ and $\sigma-\lambda\pi$ orbitals of $^1(\sigma^2)$; this is in spite of the fact that very small amounts of d-character are present in such orbitals. The effect is slightly more pronounced for intermediate values of the Si-Si-Si angle (between 100° and 115°). This is due to the onset of other effects that become more important at small

Table C.III Effect of d-Functions and Correlation on the Si_3H_6 Clusters Modelling the (100) Surface (with the Lattice Constraints).^a All energies are in Ev.

	$1(\sigma^2)_{\text{GVB}}$	$1(\sigma^2)_{\text{HF}}$	Correlation Energy ^b	$3(\sigma\pi)$
Central angle 95°				
DZ basis	1.27	1.63	0.35	1.63
DZd basis	0.39	0.92	0.53	1.13
Difference	0.88	0.71	-0.18	0.50
Central angle 105°				
DZ basis	1.06	1.39	0.33	0.92
DZd basis	0.0	0.55	0.55	0.32
Difference ^c	1.06	0.84	-0.22	0.60
Central angle 109°28'				
DZ basis	1.15	1.46	0.32	0.80
DZd basis	0.05	0.60	0.55	0.19
Difference ^c	1.10	0.86	-0.23	0.61
Central angle 115°				
DZ basis	1.39	1.69	0.30	0.81
DZd basis	0.30	0.84	0.54	0.22
Difference ^c	1.09	0.85	-0.24	0.59

^aAll energies are referenced with respect to the $1(\sigma^2)_{\text{GVB}}$ DZd minimum (-14.594092 hartree).

^bThe correlation energy is the difference between the $1(\sigma^2)_{\text{GVB}}$ and $1(\sigma^2)_{\text{HF}}$ energies.

^cThis is the difference produced by the inclusion of d-functions.

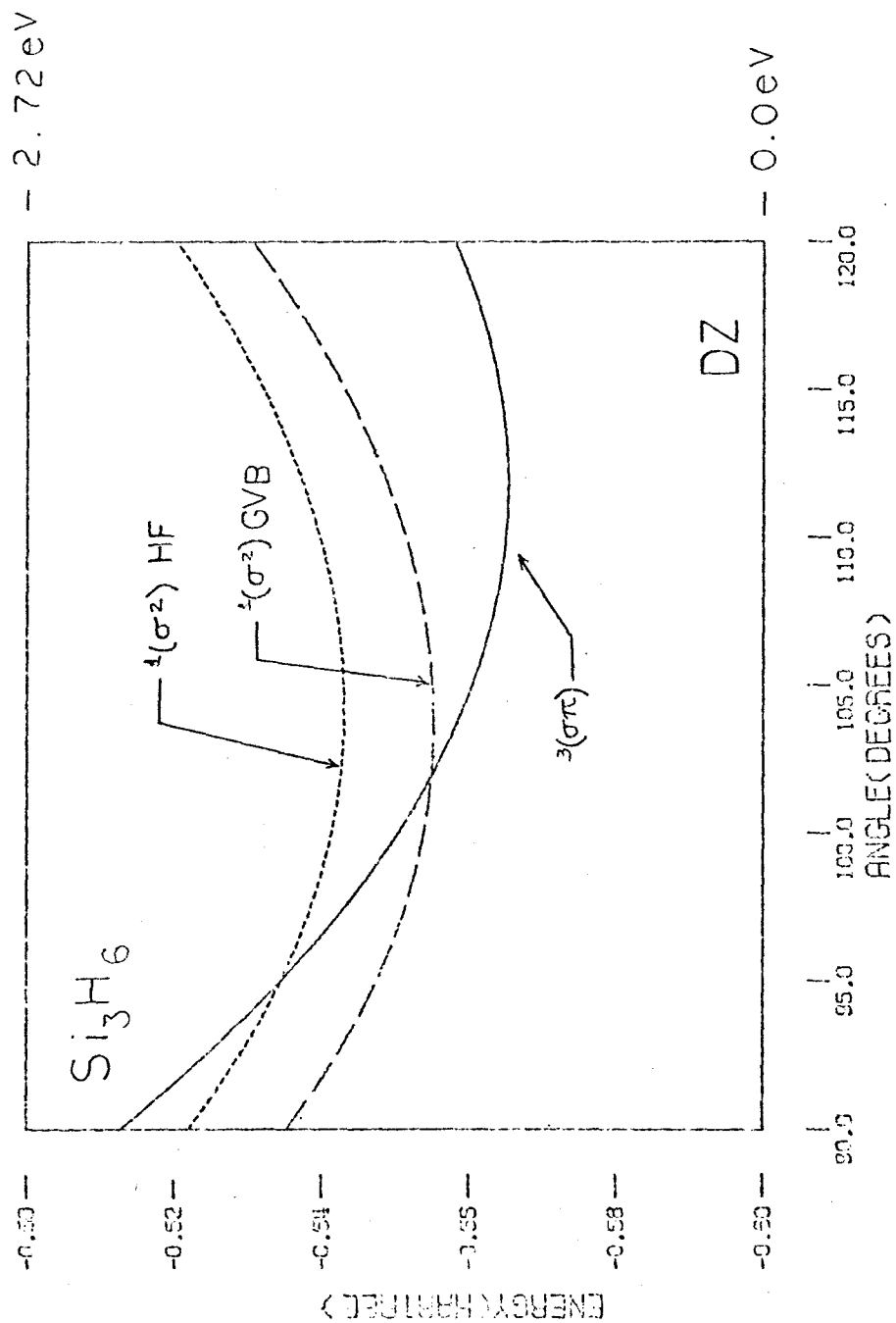


Fig. C.1 Potential Surfaces for the Si_3H_6 Cluster Using a DZ Basis
(with the constraints of the lattice). Energy is plotted as
a function of the Si-Si-Si angle.

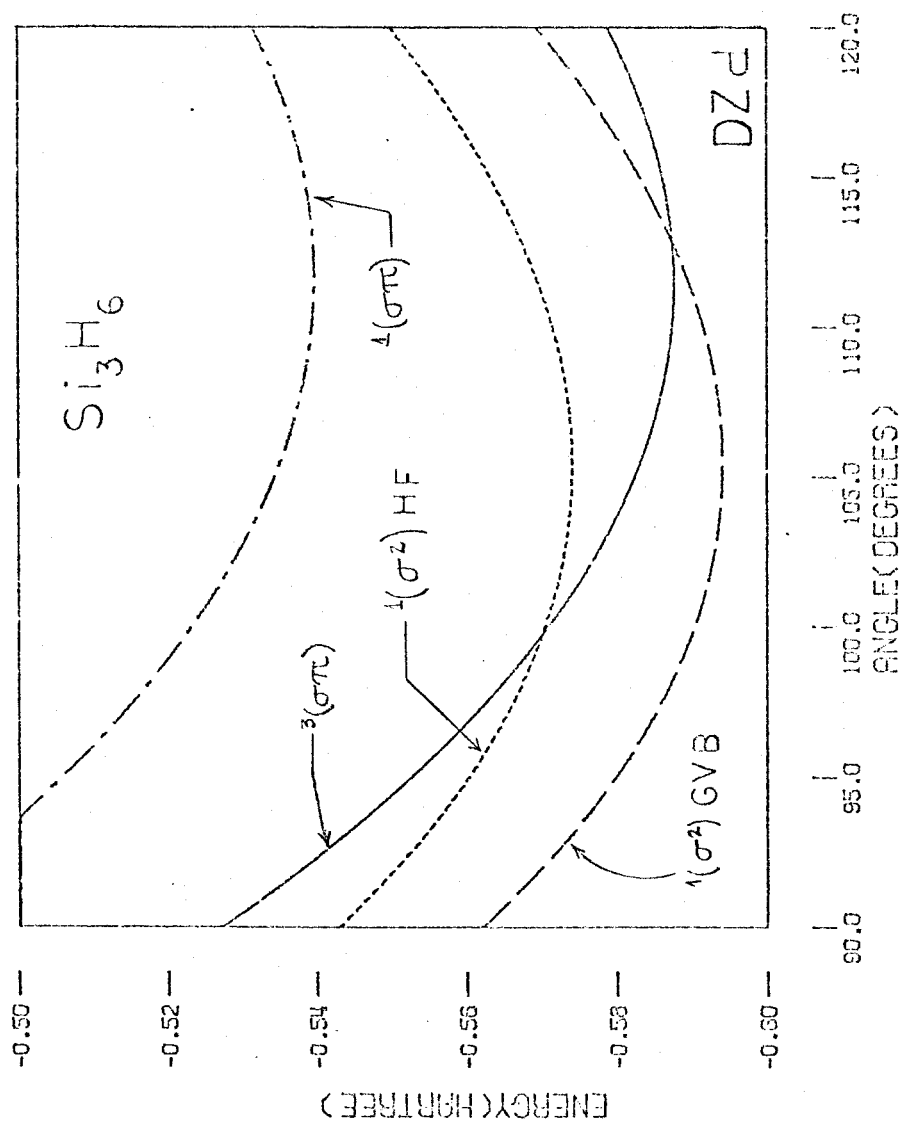


Fig. C.2 Potential Surfaces for the Si_3H_6 Cluster Using a DZD Basis
(with the constraints of the lattice).

and large angles. The most important of these other effects is Pauli principle repulsions with other pairs of electrons, which dominate over correlation when the geometry forces the σ^2 orbital to interact with the Si-Si bonds.

The effect of d-functions can be evaluated by looking at each of the states individually. This is shown in Table C.III. We see that for central angles between 105° and 115° the effect is relatively constant, with a drop in value for small angles ($\sim 95^\circ$). This is due to the fact that for 95° the geometry is such that the central atom is pulled $0.40 a_0$ (toward vacuum) with respect to the tetrahedral geometry and the electrons in the central Si make less use of d-functions. As mentioned above, the inclusion of d-functions is necessary to obtain the correct ground state. This is also true for the system in which the constraints of the lattice are not included, as we shall see below.

The above discussion concerns calculations we performed for the system which models the (100) surface. When we eliminate the constraints of the lattice (i.e., when we let the angle of the central Si vary without changing the length) the results are basically the same. The main difference occurs in the values of the Si-Si-Si angles at the optimum geometries, but this is only a consequence of the elimination of the lattice constraints. The results are summarized in Tables C.I, C.IV and C.V and the appropriate potential curves are shown in Figs. C.3 and C.4. In this case we obtain a σ^2 ground state (including d-functions and correlation) with an optimum bond angle of

Table C.IV Potential Curves for the Si_3H_6 Cluster without the Lattice Constraints^a

State	95°	100°	109°28'	120°
DZ basis set				
$1(\sigma^2)\text{GVB}$	-14.552850	-14.553585	-14.551941	-14.546634
$1(\sigma^2)\text{HF}$	-14.540590	-14.541531	-14.540308	-14.535557
$3(\sigma\pi)$	-14.554080	-14.558811	-14.564764	-14.567866
DZd basis set				
$1(\sigma^2)\text{GVB}$	-14.595821	-	-14.592091	-14.584552
$1(\sigma^2)\text{HF}$	-14.575879	-	-14.571966	-14.564420
$3(\sigma\pi)$	-14.578006	-	-14.587146	-14.589082
$1(\sigma\pi)$	-14.528481	-	-14.539129	-14.542215

^aAll energies in hartree atomic units. Energies do not include the contribution of the core electrons of silicon atoms (an effective potential has been used for these).

Table C.V Effect of d-Functions and Correlation on the Si_3H_6 Clusters
Modelling the (100) Surface (without the lattice constraints)^a.

All energies are in eV.

	$^1(\sigma^2)_{\text{GVB}}$	$^1(\sigma^2)_{\text{HF}}$	Correlation ^b Energy	$^3(\sigma\pi)$
Central angle 95°				
DZ basis	1.17	1.50	0.33	1.14
DZd basis	0.0	0.54	0.54	0.49
Difference ^c	1.17	0.96	-0.21	0.65
Central angle 100°				
DZ basis	1.15	1.48	0.33	1.01
Central angle 109°28'				
DZ basis	1.19	1.51	0.32	0.85
DZd basis	0.10	0.65	0.55	0.24
Difference ^c	1.09	0.86	-0.23	0.61
Central angle 115°				
DZ basis	1.34	1.64	0.30	0.76
DZd basis	0.31	0.85	0.55	0.18
Difference ^c	1.03	0.79	-0.25	0.58

^aAll energies are referenced with respect to the $^1(\sigma^2)_{\text{GVB}}$ DZd minimum (-14.595822 hartree).

^bThe correlation energy is the difference between the $^1(\sigma^2)_{\text{GVB}}$ and $^1(\sigma^2)_{\text{HF}}$ energies.

^cThis is the difference produced by the inclusion of d-functions.

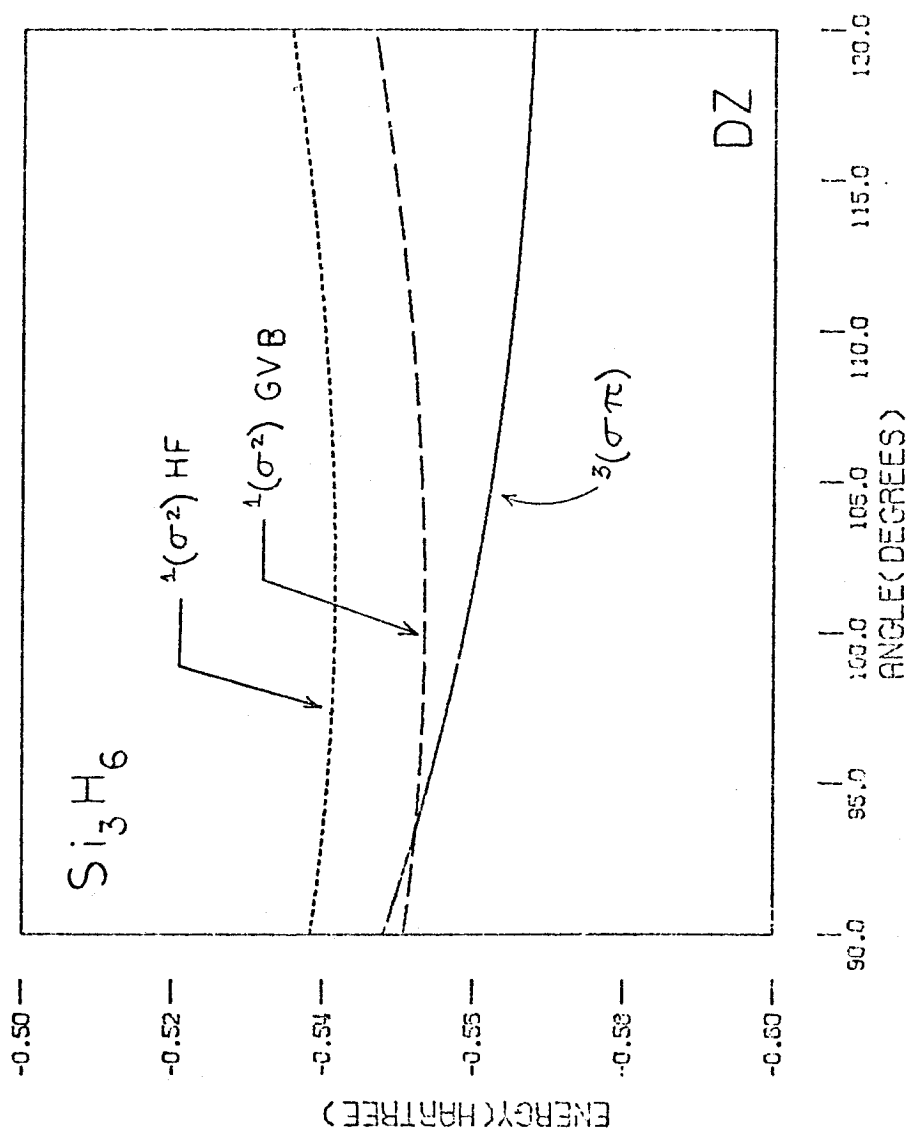


Fig. C.3 Potential Surfaces for the Si₃H₆ Cluster Using a DZ Basis (without the constraints of the lattice).

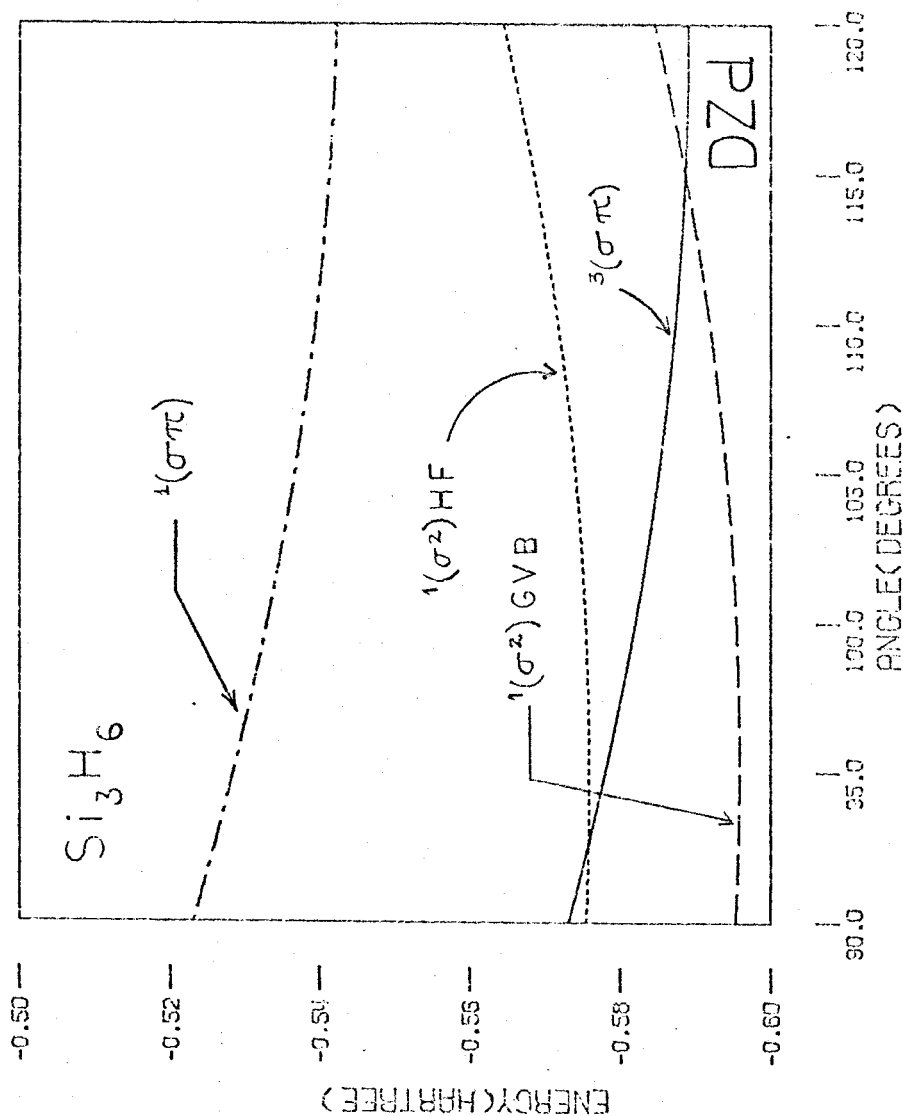


Fig. C.4. Potential Surfaces for the Si_3H_6 Cluster using a DZd Basis (without the constraints of the lattice).

95.2°. The $^3(\sigma\pi)$ state is at 0.49 eV vertical excitation energy and 0.18 eV adiabatic excitation energy (with an optimum Si-Si-Si angle of 119.9°).

REFERENCE FOR APPENDIX C

1. The correlation energy is the difference between the GVB and HF values.